

*Regulation of the
Tumour Suppressor PP2A by
Oncogenic Tyrosine Kinases*

Kathryn G. Roberts

B.BiomedSci (Hons)

**A thesis submitted in fulfilment of the requirements
for the degree of Doctor of Philosophy**

December 2009

STATEMENT OF ORIGINALITY

This thesis contains no material which has been accepted for the award of any other degree or diploma in any university or other tertiary institution and, to the best of my knowledge and belief, contains no material previously published or written by another person, except where due references has been made in the text. I give consent to this copy of my thesis, when deposited in the University Library, being made available for loan and photocopying subject to the provisions of the Copyright Act 1968.

Kathryn Roberts

TABLE OF CONTENTS

Abstract	xi
Acknowledgments	xiv
Publications	xvi
Abbreviations	xviii
CHAPTER 1 – INTRODUCTION	1
1.1 Overview	1
1.2 BCR/ABL	2
1.2.1 Clinical presentation of Chronic Myeloid Leukaemia (CML)	2
1.2.2 The Philadelphia chromosome	4
1.2.3 Overview of signalling pathways	6
1.2.3.1 Mitogen activated protein kinase (MAPK)	6
1.2.3.2 PI3K/Akt	6
1.2.3.3 Src family kinases (SFK)	9
1.2.3.4 Janus kinases (JAKs)/signal transducers and activators of transcription (STATs)	9
1.2.3.5 Wnt/ β -catenin	9
1.2.4 Transition from chronic phase to blast crisis CML	10
1.3 Receptor Tyrosine Kinase c-KIT	11
1.3.1 Structure and function	11
1.3.2 Expression of c-KIT in human malignancies	15
1.3.2.1 Gastrointestinal stromal tumours (GIST)	15
1.3.2.2 Core-binding factor Acute Myeloid Leukaemia (CBF-AML)	18
1.3.2.3 Mastocytosis	22
1.3.2.4 Melanoma	22
1.3.2.5 <i>c-KIT</i> mutations at codon 816	22
1.4 Small Molecule Inhibitors Targeting BCR/ABL and c-KIT	24
1.4.1 Imatinib	24
1.4.1.1 CML clinical trials	26
1.4.1.2 GIST clinical trials	27
1.4.1.3 AML and mastocytosis clinical trials	28

1.4.2 Second generation inhibitors	29
1.4.2.1 Nilotinib	29
1.4.2.2 Dasatinib	31
1.4.2.3 Sunitinib	33
1.4.2.4 Alternative therapeutic strategies for resistant disease	35
1.5 Protein Phosphatase 2A (PP2A)	36
1.5.1 PP2A subunits	39
1.5.1.1 The catalytic subunit (PP2Ac)	39
1.5.1.2 The structural subunit (PP2A A)	41
1.5.1.3 The regulatory subunits (PP2A B)	42
1.5.1.3.1 <i>The B55 family</i>	42
1.5.1.3.2 <i>The B56 family</i>	43
1.5.1.3.3 <i>The B" family</i>	43
1.5.1.4 PP2Ac interacting proteins	44
1.5.2 Signalling pathways regulated by PP2A	44
1.5.2.1 PP2A and MAPK signalling	45
1.5.2.2 PP2A and PI3K/Akt signalling	45
1.5.2.3 PP2A and Wnt/ β -catenin signalling	47
1.5.2.4 PP2A and p53 regulation	49
1.5.2.5 PP2A and c-Myc regulation	49
1.5.3 PP2A as a tumour suppressor	51
1.5.3.1 Okadaic acid and SV40 ST	51
1.5.3.2 Inhibition of PP2A by BCR/ABL	52
1.5.3.3 Role of PP2A regulatory subunits in transformation	54
1.5.3.4 Role of PP2A structural subunits in transformation	55
1.5.4 PP2A activators	60
1.5.4.1 Forskolin	60
1.5.4.2 Ceramide	61
1.5.4.3 FTY720	63
1.6 Aims of this Thesis	67

CHAPTER 2 – MATERIALS AND METHODS	68
2.1 Buffers and Reagents	68
2.2 Recombinant DNA Techniques	68
2.2.1 Plasmid vectors	68
2.2.1.1 cDNA constructs	68
2.2.1.2 shRNA constructs	68
2.2.2 Restriction digests	70
2.2.3 DNA electrophoresis	70
2.2.4 DNA purification from agarose gel	70
2.2.5 Nucleic acid quantification	71
2.2.6 Ligation of insert into plasmid	71
2.2.7 Expansion and purification of plasmid DNA	71
2.2.7.1 Preparation of competent bacteria	71
2.2.7.2 Transformation of competent bacteria	72
2.2.7.3 Purification of plasmid DNA from bacteria	72
2.2.8 DNA sequencing and analysis	73
2.3 Cell Culture	74
2.3.1 Media, solutions and cytokines	74
2.3.2 Cell lines and maintenance	74
2.3.3 Reviving cell lines	75
2.3.4 Cryopreservation	75
2.3.5 Retroviral infection of FDC-P1 cells	76
2.3.5.1 Generation of FDC-P1 cells expressing BCR/ABL and c-KIT	76
2.3.5.2 Generation of shRNA-expressing FDC-P1 WT BCR/ABL cells	78
2.3.6 Drug treatments	79
2.4 Polymerase Chain Reaction (PCR)	79
2.4.1 RNA extraction	79
2.4.2 Reverse transcription PCR (RT-PCR)	79
2.4.3 Quantitative real-time PCR (qRT-PCR)	80
2.5 PP2A phosphatase activity assay	82
2.6 Analytical Procedures for Proteins	82

2.6.1 Flow cytometry	82
2.6.2 Immunoblotting	83
2.6.3 Immunoprecipitation	86
2.6.4 Phosphorylation assay	86
2.7 Cellular Growth and Survival Assays	88
2.7.1 Cellular proliferation	88
2.7.2 Analysis of cellular morphology	89
2.7.3 Apoptosis assay	89
2.7.4 Cell cycle analysis	90
2.7.5 Colony-forming assay	90
2.8 Animal Procedures	90
2.8.1 Syngeneic mouse model	90
2.8.1.1 Establishing the FDC-P1 mutant c-KIT tumour model	90
2.8.1.2 Evaluating the safety of FTY720 in DBA/2J mice	91
2.8.1.3 FTY720 treatment of FDC-P1 mutant c-KIT tumours	91
2.8.1.4 Immunohistochemistry	92
2.8.1.5 TUNEL staining	93
2.9 Statistical Analysis	95
CHAPTER 3 – BCR/ABL ALTERS THE EXPRESSION OF PP2A SUBUNITS	96
3.1 Introduction	96
3.2 Results	98
3.2.1 Expression of p210 kDa BCR/ABL oncoprotein in FDC-P1 cells	98
3.2.2 Sensitivity of WT and Y253F BCR/ABL to imatinib	100
3.2.3 BCR/ABL impairs the activity of PP2A	102
3.2.4 BCR/ABL upregulates the PP2A scaffolding subunit	102
3.2.4.1. SET expression	102
3.2.4.2 PP2A catalytic subunit expression	105
3.2.4.3 PP2A scaffolding subunit expression	105
3.2.5 BCR/ABL alters the expression of PP2A regulatory subunits	109
3.2.5.1 PP2A B55 subunit family expression	109
3.2.5.2 PP2A B56 subunit family expression	109

3.2.6 PP2A mRNA levels in BCR/ABL ⁺ FDC-P1 cells	113
3.2.7 BCR/ABL disrupts PP2A assembly in FDC-P1 cells	119
3.3 Discussion	122
CHAPTER 4 – THE ROLE OF PP2A COMPLEXES IN BCR/ABL⁺ LEUKAEMOGENESIS	129
4.1 Introduction	129
4.2 Results	131
4.2.1 Subcloning of shRNA B56δ into pSR	131
4.2.2 Stable knockdown of PP2A regulatory subunits in FDC-P1 WT BCR/ABL cells	131
4.2.3 Functional effects of PP2A regulatory subunit knockdown	133
4.2.3.1 shB56α restores PP2A activity in FDC-P1 WT BCR/ABL cells	133
4.2.3.2 shB56α impairs the proliferation of FDC-P1 WT BCR/ABL cells	133
4.2.3.3 Suppression of B56α and B56δ alters the cellular morphology of FDC-P1 WT BCR/ABL cells	142
4.3 Discussion	145
CHAPTER 5 – INHIBITION OF PP2A BY ONCOGENIC C-KIT MUTATIONS	153
5.1 Introduction	153
5.2 Results	154
5.2.1 Mutant c-KIT impairs the activity of PP2A	154
5.2.2 Mutant c-KIT alters the expression of PP2A subunits	156
5.2.3 Reactivation of PP2A in mutant c-KIT FDC-P1 cells	159
5.2.4 Reactivation of PP2A inhibits the proliferation of mutant c-KIT FDC-P1 cells	159
5.2.5 Reactivation of PP2A induces apoptosis of mutant c-KIT FDC-P1 cells	162
5.2.6 Reactivation of PP2A inhibits the clonogenic potential of mutant c-KIT cells	165
5.2.7 Reactivation of PP2A dephosphorylates c-KIT in FDC-P1 cells	169
5.3 Discussion	169

CHAPTER 6 – FTY720 INHIBITS MUTANT C-KIT TUMOUR GROWTH IN VIVO	176
6.1 Introduction	176
6.2 Results	177
6.2.1 Establishing an <i>in vivo</i> model for FDC-P1 c-KIT tumour growth	177
6.2.2 Evaluating the toxicity of FTY720 in DBA/2J mice	177
6.2.3 FTY720 delays mutant c-KIT tumour growth	179
6.2.4 FTY720 improves the survival of mice bearing mutant c-KIT tumours	183
6.2.5 FTY720 prevents the infiltration of D816V c-KIT cells into secondary organs	183
6.3 Discussion	195
CHAPTER 7– CONCLUSIONS AND FUTURE DIRECTIONS	199
APPENDIX	211
REFERENCES	216

LIST OF FIGURES

Figure 1.1 Haematopoiesis and the characteristics of CML progenitors	3
Figure 1.2 The Philadelphia chromosome and functional domains of the BCR and ABL proteins	5
Figure 1.3 Oncogenic signalling by p210 kDa BCR/ABL	8
Figure 1.4 Functional domains of the c-KIT receptor	12
Figure 1.5 Signalling pathways activated by c-KIT	14
Figure 1.6 Mutations in <i>c-KIT</i> detected in human malignancies	16
Figure 1.7 Structure of BCR/ABL in complex with imatinib	25
Figure 1.8 Structure of BCR/ABL in complex with nilotinib and dasatinib	30
Figure 1.9 Mechanism of action of sunitinib	34
Figure 1.10 Structure of PP2A holoenzymes	38
Figure 1.11 Post-translational modifications of PP2Ac	40
Figure 1.12 Schematic overview of MAPK signalling regulation by PP2A	46
Figure 1.13 Schematic overview of Wnt/ β -catenin signalling regulation by PP2A	48
Figure 1.14 Schematic overview of p53 signalling regulation by PP2A	50
Figure 1.15 BCR/ABL-induced inhibition of PP2A in CML	53
Figure 1.16 Regulation of c-Myc by PP2A and CIP2A	56
Figure 1.17 Mechanisms by which mutant PP2A A α may induce transformation	58
Figure 1.18 Tumour suppressive properties of PP2A A β	59
Figure 1.19 Sphingolipid metabolic pathway and structure of FTY720	62
Figure 1.20 Mechanism of FTY720 immunomodulation	64
Figure 1.21 Reactivation of PP2A inhibits BCR/ABL-mediated leukaemogenesis	66
Figure 2.1 Schematic model for the growth of FDC-P1 mutant c-KIT tumours and FTY720 treatment	94
Figure 3.1 Expression of BCR/ABL in myeloid progenitors	99
Figure 3.2 Inhibition of BCR/ABL ⁺ myeloid progenitors with imatinib	101
Figure 3.3 Inhibition of BCR/ABL phosphorylation with imatinib	103
Figure 3.4 BCR/ABL inhibits PP2A activity in FDC-P1 myeloid progenitors	104
Figure 3.5 Expression of SET in BCR/ABL ⁺ myeloid progenitors	106

Figure 3.6 Expression of PP2Ac and PP2A A subunits in BCR/ABL ⁺ myeloid progenitors	107
Figure 3.7 Quantitation of PP2Ac and PP2A A in BCR/ABL ⁺ myeloid progenitors	108
Figure 3.8 Expression of PP2A regulatory subunits in BCR/ABL ⁺ myeloid progenitors	110
Figure 3.9 Quantitation of PP2A regulatory subunits in BCR/ABL ⁺ FDC-P1 cells	111
Figure 3.10 Quantitation of PP2A regulatory subunits in 32D and K562 cells	112
Figure 3.11 mRNA levels of PP2Ac and PP2A A in BCR /ABL ⁺ FDC-P1 cells	115
Figure 3.12 mRNA levels of PP2A B55 in BCR/ABL ⁺ FDC-P1 cells	116
Figure 3.13 mRNA levels of PP2A B56 in BCR/ABL ⁺ FDC-P1 cells	117
Figure 3.14 mRNA levels of PPP2R3A and PPP2R4 in BCR/ABL ⁺ FDC-P1 cells	118
Figure 3.15 PP2A holoenzyme composition in BCR/ABL ⁺ FDC-P1 cells	121
Figure 3.16 Proposed model of PP2A regulation by BCR/ABL in FDC-P1 cells	128
Figure 4.1 shRNA-mediated gene silencing in mammalian cells	130
Figure 4.2 Expression of GFP in shRNA-WT BCR/ABL FDC-P1 cells	132
Figure 4.3 Knockdown of PP2A regulatory subunits in WT BCR/ABL FDC-P1 cells	134
Figure 4.4 mRNA levels of PP2A regulatory subunits in shRNA-WT BCR/ABL FDC-P1 cells	135
Figure 4.5 PP2A activity in shRNA-WT BCR/ABL FDC-P1 cells	136
Figure 4.6 Growth rate of shRNA-WT BCR/ABL FDC-P1 cells	138
Figure 4.7 Clonogenic potential of shRNA-WT BCR/ABL FDC-P1 cells	139
Figure 4.8 Colonies formed by shRNA-WT BCR/ABL FDC-P1 cells	140
Figure 4.9 Colonies formed by shRNA-WT BCR/ABL FDC-P1 cells at a higher magnification	141
Figure 4.10 Cellular morphology of shRNA-WT BCR/ABL FDC-P1 cells	143
Figure 4.11 Quantitative analysis of the morphological characteristics displayed by shRNA-WT BCR/ABL FDC-P1 cells	144
Figure 4.12 Involvement of PP2A B56 δ in cell cycle regulation	149
Figure 4.13 Proposed model of PP2A regulation by BCR/ABL in FDC-P1 cells	152
Figure 5.1 Surface expression of c-KIT on FDC-P1 cells	155

Figure 5.2 Expression of PP2A regulatory subunits in c-KIT ⁺ FDC-P1 cells	157
Figure 5.3 Quantitation of PP2A subunits in c-KIT ⁺ FDC-P1 cells	158
Figure 5.4 Reactivation of PP2A in mutant c-KIT FDC-P1 cells	160
Figure 5.5 Reactivation of PP2A induces apoptosis of mutant c-KIT FDC-P1 cells	163
Figure 5.6 Reactivation of PP2A increases the sub-G ₀ population of mutant c-KIT FDC-P1 cells	164
Figure 5.7 Reactivation of PP2A impairs the clonogenic potential of mutant c-KIT FDC-P1 cells	166
Figure 5.8 Colony formation of FTY720-treated FDC-P1 cells	167
Figure 5.9 Cytotoxic effect of FTY720 on mutant c-KIT ⁺ FDC-P1 cells requires PP2A reactivation	168
Figure 5.10 Reactivation of PP2A dephosphorylates c-KIT	170
Figure 5.11 Regulation of PP2A by mutant c-KIT and reactivation with FTY720	175
Figure 6.1 Preliminary studies of FDC-P1 V560G and D816V c-KIT tumour growth	178
Figure 6.2 Safe administration of FTY720 in DBA/2J mice	180
Figure 6.3 FTY720 delays mutant c-KIT tumour growth	181
Figure 6.4 Effect of imatinib on mutant c-KIT tumour growth	182
Figure 6.5 FTY720 improves the survival of mice bearing mutant c-KIT tumours	184
Figure 6.6 Effect of imatinib on the survival of mice bearing mutant c-KIT tumours	185
Figure 6.7 FTY720 reduces mutant c-KIT tumour burden at day 14	186
Figure 6.8 FTY720 induces apoptosis in FDC-P1 V560G c-KIT tumours at day 14	187
Figure 6.9 FTY720 induces apoptosis in FDC-P1 D816V c-KIT tumours at day 14	188
Figure 6.10 FTY720 reduces the splenic weight of mice bearing FDC-P1 D816V c-KIT tumours	189
Figure 6.11 FTY720 prevents the infiltration of FDC-P1 D816V c-KIT cells into the spleen	191
Figure 6.12 FTY720 prevents the infiltration of FDC-P1 D816V c-KIT cells into the bone marrow	192
Figure 6.13 Mice bearing V560G c-KIT tumours do not develop splenomegaly	193
Figure 6.14 Absence of V560G c-KIT cells in the spleen	194

Figure 7.1 Proposed model of PP2A regulation by BCR/ABL in myeloid progenitors	203
Figure 7.2 Summary of PP2A regulation by oncogenic c-KIT in myeloid progenitors	206
Figure 7.3 Inhibition of PP2A as a general mechanism employed by oncogenic tyrosine kinases	210
Appendix Figure 1 Expression of PP2Ac-p ^{Y307} in CD34 ⁺ CML primary samples	214
Appendix Figure 2 Combined effects of FTY720 and dasatinib on D816V c-KIT FDC-P1 cell growth	215

LIST OF TABLES

Table 1.1 Signalling pathways regulated by BCR/ABL	7
Table 1.2 Signalling pathways regulated by c-KIT	13
Table 1.3 Differential activation of signalling pathways by mutant c-KIT	17
Table 1.4 Clinical significance of c-KIT mutations in t(8;21) CBF-AML	20
Table 1.5 Clinical significance of c-KIT mutations in inv(16) CBF-AML	21
Table 1.6 Nomenclature and subcellular distribution of <i>Homo sapiens</i> PP2A subunits	37
Table 2.1 shRNA constructs	69
Table 2.2 Oligonucleotides for sequencing and standard PCR	73
Table 2.3 Cell lines and maintenance	77
Table 2.4 Oligonucleotides for quantitative real-time PCR (qRT-PCR)	81
Table 2.5 Primary antibody concentrations used for immunoblotting	84
Table 2.6 Secondary antibody concentrations used for immunoblotting	85
Table 2.7 Antibodies and beads used for immunoprecipitation	87
Table 3.1 Sensitivity of BCR/ABL to imatinib	100
Table 5.1 Mutant c-KIT impairs PP2A activity	156
Table 5.2 Cytotoxicity of PP2A activators in mutant c-KIT FDC-P1 cells	161
Table 6.1 Toxicity data for FTY720 treatment of DBA/2J mice	180

ABSTRACT

Reversible protein phosphorylation plays a central role in the regulation of intracellular signalling, and is controlled by the opposing activities of protein kinases and phosphatases. Deregulation of these mechanisms can result in increased proliferation and enhanced survival, which is a hallmark feature of malignant transformation. For example, over 90% of chronic myeloid leukaemia (CML) patients express the BCR/ABL oncoprotein, which exhibits unrestrained tyrosine kinase activity. In addition, activating mutations within the receptor tyrosine kinase, c-KIT, contribute to the pathogenesis of gastrointestinal stromal tumours (GIST), systemic mastocytosis, acute myeloid leukaemia (AML), testicular seminoma and melanoma. The advent of small molecule tyrosine kinase inhibitors, such as imatinib, has revolutionised the treatment of malignancies driven by these oncogenic kinases. However, a proportion of patients are either unresponsive or develop resistance, and as such, relapse and disease progression is a major clinical problem. In order to improve the treatment outcome for these patients, a greater understanding of the signalling pathways regulated downstream of BCR/ABL and c-KIT is required.

The data presented in this thesis indicates that oncogenic BCR/ABL and mutant c-KIT both require inhibition of the tumour suppressor, protein phosphatase 2A (PP2A), to induce tumorigenesis. PP2A is a large family of serine/threonine phosphatases that provide the fine control on signalling pathways by governing the rate and duration of phosphorylation. The heterotrimeric PP2A enzyme is comprised of a structural subunit (PP2A A α and A β), a catalytic subunit (PP2A C α and C β) and a regulatory subunit, which consists of three unrelated families: B55 (α , β , γ , δ), B56 (α , β , γ , δ , ϵ) and B γ (PR72/130 / PR70/48). Binding of the regulatory subunit to the core PP2A AC dimer directs both the substrate specificity and cellular localisation of the enzyme. The combinatorial assembly of these individual components permits the formation of distinct complexes which have been implicated in numerous cellular functions such as proliferation, survival and mitosis. In particular, important roles for PP2A in various aspects of malignant transformation are beginning to emerge.

Recent work demonstrates that PP2A is functionally inactivated by BCR/ABL in myeloid progenitor cells. Using the mouse myeloid progenitor cell line, FDC-P1, these

observations were confirmed in the current study. Detailed investigation into the underlying mechanisms have demonstrated for the first time that active BCR/ABL increases the expression of the PP2A structural and certain regulatory subunits. This alters the PP2A holoenzyme composition and results in the abundance of complexes containing B55 α and B56 α . Consequently, B56 γ , a known tumour suppressive subunit, appears to be simultaneously displaced. To investigate which subunits are functionally important for BCR/ABL-mediated leukaemogenesis, individual PP2A subunits were targeted with shRNA sequences in WT BCR/ABL FDC-P1 cells. Subsequent evaluation identified B56 α as a key player which facilitates the leukaemic phenotype. In accordance with an increase in PP2A activity, knockdown of B56 α significantly inhibited the cellular growth and reduced the clonogenic potential of BCR/ABL⁺ myeloid progenitors. Furthermore, suppression of the B56 δ subunit in WT BCR/ABL FDC-P1 cells appears to delay progression through the cell cycle. Together, these findings provide new insights into the biology of PP2A and begin to define the precise mechanisms by which BCR/ABL induces leukaemogenesis via PP2A in CML.

Investigation of the regulation of PP2A was also extended to the oncogenic tyrosine kinase, c-KIT. Using FDC-P1 cells expressing imatinib-sensitive (V560G) or –resistant (D816V) mutant c-KIT, this work demonstrates for the first time that constitutive activation of c-KIT impairs the activity of PP2A, and this is essential for tumourigenesis. Pharmacological reactivation of PP2A with FTY720 significantly reduced the proliferation, impaired the clonogenic potential and induced apoptosis of oncogenic c-KIT cells, whilst having no effect on empty vector controls or WT c-KIT cells stimulated with stem cell factor (SCF). These cytotoxic effects of FTY720 are mediated, in part, by the rapid dephosphorylation, and hence inactivation, of oncogenic c-KIT receptors. These promising *in vitro* findings were translated into an *in vivo* model, where the daily administration of FTY720 significantly delayed the growth of mutant c-KIT⁺ tumours. Furthermore, FTY720 markedly prevented the infiltration of D816V c-KIT tumour cells into secondary lymphoid organs, such as the spleen and bone marrow. As a result, the survival of FTY720-treated mice was significantly prolonged compared to saline-treated controls.

Overall, this body of work greatly enhances our understanding of PP2A function and identifies the complex mechanisms of PP2A regulation by the oncogenic tyrosine kinases, BCR/ABL and c-KIT. Taken together, the data suggests that inhibition of PP2A may represent a general mechanism employed by constitutively active kinases to facilitate tumour growth. As such, this work supports the future application of PP2A-activating agents in a broad range of human malignancies.

ACKNOWLEDGEMENTS

Wow what an amazing journey I've experienced during this PhD candidature! Of course there are numerous people who have contributed along the way, and without which, the road to thesis submission would have seemed an almost impossible task. I'd like to acknowledge The University of Newcastle and The Ohio State University for providing the facilities to carry out this research. A special acknowledgement is extended to the Cancer Institute NSW for a Research Scholarship that provided project funding and also enabled me to present my work at national and international conferences. Firstly, a big thank you to my supervisor, Dr. Nikki Verrills, who has been such a fantastic mentor that I honestly could not have dreamed of a more appropriate person for guidance during the past 4 years. It continues to amaze (and scare me a little!) how much we are on the same wavelength on so many different levels. I've lost track how many times I've received an email saying "have you done/or thought about doing XYZ" when I have either just done the experiments or about to write a very similar email saying "I think it would be interesting to look at XYZ!" Being under the supervision of someone who has such a passion for research is truly inspiring and I have learnt so much from our interesting conversations. In addition to being an amazing role model, Nikki provided me with focus when required and pushed me above and beyond what I thought I was capable of. She was always there to listen and provide advice on any problems I was having, both work-related and personal. Thanks Nik!

I would like to thank Prof. Leonie Ashman for being a continual source of knowledge on a wide range of topics and helping me to think about my work in the bigger picture. Leonie has provided important guidance, particularly in the last six months, when I have had some big decisions to make. Thank you also to Prof. Alistair Sim, who is still officially my co-supervisor, although he has not worked at the University for the last two years. Despite this separation, he was always accessible and still interested in providing feedback on written work. A special thank you is extended to Prof. John Rostas, who I first met when applying for a travel grant through HMRI during the first year of my candidature. Since that time, John has showed a genuine interest in my progress and provided constructive feedback on several aspects of research such as grant writing, presentations and post-doctoral interviews. No matter what time of the

day, even if we ran into each other in the corridor, he was more than happy to stop and give advice, which is something I really appreciate.

Within the laboratory I would like to send a very big thanks to Fiona McDougall, without whose help I would still be struggling to catch mice, let alone inject and measure them on a daily basis! Fiona provided an absolute wealth of knowledge on the design of the animal experiments, helped with the daily management of the mice and established the protocols for immunohistochemical and TUNEL staining. I'd also like to thank Amanda Smith who has not only contributed to extra runs of several experiments, but on a social level is the one person who has kept me sane! Our morning coffee breaks was something I always looked forward to. Thanks to Helen Carpenter for her work in setting up our plasmid database, and always willing to help with any experiment that required an extra set of hands. Thank you also to Martin Horan for his help in setting up the real-time PCR assay.

Six months of this work was conducted at The Ohio State University and made possible by a travel award which was donated by Jennie Thomas through HMRI. Jennie is truly an inspiring person and I can not thank her enough for enabling me the amazing opportunity to study abroad. I would also like to thank my supervisor A/Prof. Danilo Perrotti for accepting me into his laboratory and continuing to maintain contact and provide feedback on my project. Thanks as well to the lab members, Anna, Paolo and Josh for making the Perrotti lab such a welcoming and fun working environment! A special thank you is extended to Anna, who started her PhD at the same time. It was very comforting to know there was someone else out there who was pulling all nighters and experiencing the same emotional and mental stress as myself!

I would like to save the biggest thanks to my wonderful parents who have always told me "the sky is the limit", and have provided me with every opportunity to achieve my very best. Their never-ending love and support is a continual source of motivation for me. Just knowing I could rely on them for anything (and that dinner would always be in the microwave when I came home late!) was extremely comforting. To my beautiful friends, especially Skye, Elizabeth, Katie and Ezz. Thank you for understanding when I couldn't make most social outings, particularly this year. You have no idea how much all your thoughtful and motivating messages helped me get through the tough times.

PUBLICATIONS

Roberts KG, Smith AM, McDougall F, Carpenter H, Neviani P, Perrotti D, Sim ATR, Ashman LK, Verrills NM (2009) Essential requirement for PP2A inhibition by c-KIT: FTY720-mediated reactivation of PP2A as a treatment strategy for c-KIT⁺ cancers. Submitted to *Cancer Research* #CAN-09-2544

Patents

International PCT Patent: Inhibition of c-KIT Cancers *Filed March 2009*

Oral Conference Presentations

Roberts KG, Ashman LK, Sim ATR, Verrills NM (2007) BCRABL regulates specific B subunits of the tumour suppressor protein phosphatase 2A (PP2A): potential targets for chronic myeloid leukaemia. *Proc. Amer. Assoc. Cancer Res.* Abstract 4154.

Roberts KG, Smith AM, Carpenter, H, Ashman LK, Santhanam R, Sim ATR, Perrotti D, Verrills NM (2008) Protein phosphatase 2A (PP2A): a novel therapeutic target for myeloid leukaemias. *New Directions for Leukaemia Research*, Sunshine Coast, Australia.

Roberts KG, Ashman LK, Sim ATR, Verrills NM (2007) BCR/ABL inactivates the tumour suppressor PP2A in chronic myeloid leukaemia. *Australian Society for Medical Research Annual Meeting*. Sydney, Australia.

Poster Conference Presentations

Roberts KG, Smith AM, Carpenter, H, Ashman LK, Santhanam R, Sim ATR, Perrotti D, Verrills NM (2009) Reactivation of PP2A as a treatment strategy for c-KIT⁺ core-binding factor acute myeloid leukemia. *Proc. Amer. Assoc. Cancer Res.* Abstract 3644.

Smith AM, **Roberts KG**, Carpenter, H, McDougall, F, Ashman LK, Sim ATR, Perrotti D, Verrills NM (2009) FTY720-mediated reactivation of PP2A as a treatment alternative for c-KIT⁺ cancers. *EMBO Europhosphatases Annual Meeting*, Egmond aan Zee, The Netherlands.

Roberts KG, Smith AM, Carpenter, H, Santhanam R, Ashman LK, Sim ATR, Perrotti D, Verrills NM (2009) Reactivation of PP2A as a treatment strategy for c-KIT⁺ cancers. *Australian Society for Medical Research Annual Meeting*. Sydney, Australia.

Awarded winner for best student poster.

Roberts KG, Smith AM, Carpenter, H, Santhanam R, Ashman LK, Sim ATR, Perrotti D, Verrills NM (2008) Inhibition of the tumour suppressor PP2A by c-KIT in acute myeloid leukaemia. *HMRI Conference on Translational Cancer Research*, Newcastle, Australia. **Awarded winner for best student poster.**

Roberts KG, Carpenter, H, Ashman LK, Sim ATR, Perrotti D, Verrills NM (2008) Altered expression of PP2A regulatory subunits in chronic myeloid leukaemia. *HMRI Conference on Translational Cancer Research*, Newcastle, Australia.

Roberts KG, Smith AM, Carpenter, H, Santhanam R, Ashman LK, Sim ATR, Perrotti D, Verrills NM (2008) c-Kit functionally inactivates the tumour suppressor PP2A in AML. *New Directions for Leukaemia Research*, Sunshine Coast, Australia.

Awarded a travel scholarship for best student abstract submission.

Roberts KG, Carpenter, H, Ashman LK, Sim ATR, Perrotti D, Verrills NM (2008) BCR/ABL alters the expression of specific PP2A regulatory subunits in CML. *New Directions for Leukaemia Research*, Sunshine Coast, Australia.

Roberts KG, Smith AM, Carpenter, H, Ashman LK, Sim ATR, Santhanam R, Neviani P, Perrotti D, Verrills NM (2008) BCR/ABL-induced inactivation of the tumour suppressor, PP2A: role of PP2A regulatory subunits and their potential as therapeutic targets in CML. *Lorne Cancer Conference*, Lorne, Australia.

Roberts KG, Ashman LK, Sim ATR, Perrotti D, Verrills NM (2007) Altered Expression of PP2A Regulatory Subunits in Chronic Myelogenous Leukemia: Identifying Targets for Improved Therapies. *Blood (American Society of Hematology Annual Meeting Abstracts)* 110: 2925.

Roberts KG, Ashman LK, Sim ATR, Verrills NM (2006) BCR/ABL expression functionally inactivates the tumour suppressor PP2A in early myeloid cells, *Australian Health & Medical Research Congress*, Melbourne, Australia.

Roberts KG, Ashman LK, Sim ATR, Verrills NM (2006) Investigating the role of protein phosphatase 2A in chronic myeloid leukaemia, *HMRI Conference on Translational Cancer Research*, Newcastle, Australia.

Awarded runner-up for best student poster.

Awards

Best Poster Presentation – *Australia Society for Medical Research Annual Meeting, Sydney, June 2009.*

GlaxoSmithKline Best Student Poster Presentation – *Hunter Medical Research Institute Conference, Newcastle, September 2008*

Leukaemia Foundation Student Travel Scholarship – *New Directions for Leukaemia Research, Sunshine Coast, April 2008.*

GlaxoSmithKline Runner-up Best Student Poster Presentation – *Hunter Medical Research Institute Conference, Newcastle, September 2008*

Hunter Medical Research Institute Travel Grant – *November 2007*

Cancer Institute NSW Research Scholar Award – *February 2006*

ABBREVIATIONS

µg	microgram
µl	microlitre
µM	micromolar
ALL	acute lymphoblastic leukaemia
AML	acute myeloid leukaemia
B-CLL	B-cell chronic lymphocytic leukaemia
bp	base pair
BSA	bovine serum albumin
CBF-AML	core-binding factor AML
CML	chronic myeloid leukaemia
cDNA	complementary DNA
CML-BC	blast crisis CML
CML-CP	chronic phase CML
Ct	cycle threshold
DAB	diaminobenzidine
DMEM	Dulbecco's modified Eagle's medium
DMSO	dimethyl sulphoxide
DNA	deoxyribose nucleic acid
ECL	enhanced chemiluminescence
ERK	extracellular signal-regulated kinase
EtOH	ethanol
FACS	fluorescence-activated cell sorter
FCS	fetal calf serum
FITC	fluorescein isothiocyanate
FLT3	fms-like tyrosine kinase 3
g	gram
<i>g</i>	gravity
GFP	green fluorescent protein
GIST	gastrointestinal stromal tumour
GM-CSF	granulocyte-macrophage colony-stimulating factor
GSK3β	glycogen synthase kinase 3β
HRP	horseradish peroxidase

HSC	haematopoietic stem cell
ID ₅₀	concentration of drug that inhibits cells by 50%
IFN	interferon
IL	interleukin
IMDM	Iscove's modified Dulbecco's medium
i.p.	intraperitoneal
JAK	Janus kinases
JMD	juxtamembrane domain
kDa	kilodalton
M	molar
mAb	monoclonal antibody
MAPK	mitogen-activated protein kinase
mg	milligram
ml	millilitre
mM	millimolar
mRNA	messenger RNA
nt	nucleotide
nm	nanometre
pAb	polyclonal antibody
PAGE	polyacrylamide gel electrophoresis
PBS	phosphate buffered saline
PBA	PBS / 0.1%BSA / 0.1% sodium azide
PCR	polymerase chain reaction
Ph ¹	Philadelphia chromosome
pH	potential of hydrogen
PI	propidium iodide
PI3K	phosphatidylinositol 3-kinase
p.o.	oral gavage
PP2A	protein phosphatase 2A
pSR	pSUPER.retro.neo+GFP
qRT-PCR	quantitative real time PCR
RIPA	radio-immunoprecipitation assay
RNA	ribonucleic acid
RT-PCR	reverse-transcriptase PCR

RTK	receptor tyrosine kinase
RTV	relative tumour volume
S1PR	sphingosine-1-phosphate receptor
s.c.	subcutaneous
SCF	stem cell factor
SDS	sodium dodecyl sulphate
SEM	standard error of the mean
SFK	Src family kinases
SMP	skim milk powder
SphK	sphingosine kinase
ST	small T antigen
STAT	signal transducer and activator of transcription
SV40	simian virus 40
TBST	tris buffered saline-Tween 0.1%
TUNEL	terminal deoxynucleotidyltransferase-mediated dUTP nick end labelling
U	units
Wnt	wingless/Int
WT	wild-type

CHAPTER 1

INTRODUCTION

1.1 Overview

A plethora of signalling pathways are utilised to govern virtually all aspects of cellular function, enabling cells to respond to extracellular signals, such as hormones and growth factors, as well as environmental and nutritional stress. The ability to balance a complex network of signal transduction pathways is important for maintaining normal cellular homeostasis. Signalling pathways are exquisitely regulated through a variety of mechanisms, one of which is reversible phosphorylation. Protein phosphorylation is the most important post-translational modification mechanism utilised by eukaryotic cells to regulate dynamic protein functions. It involves the addition or removal of a negatively charged phosphate group, which can induce a conformational change of a target protein and subsequently alter its interactions with additional proteins. This is a key component that controls numerous cellular processes including gene expression, proliferation and differentiation. The level of protein phosphorylation inside the cell is controlled by the balanced activities of protein kinases and phosphatases. As the deregulation of these enzymes has been implicated in a variety of diseases (e.g cancer, diabetes and neurodegeneration), an intense area of investigation has focused on the structure, function and regulation of these critical proteins.

During normal cellular function, signals from the microenvironment are detected by cell surface receptors and translated into the activation of protein kinases, which act by phosphorylating substrates, and induce a signal transduction cascade that directly affects the physiological response of a cell to external stimuli. Therefore, it is logical that genetic or functional alterations of these cell components can result in the aberrant activation of pathways that contribute to the development of a transformed phenotype. Some of the best known examples of oncoproteins displaying unrestrained kinase activity are BCR/ABL, which is the driving force behind chronic myeloid leukaemia (CML), and the receptor tyrosine kinase (RTK), c-KIT, which is implicated in the pathogenesis of acute myelogenous leukaemia (AML) and gastrointestinal stromal tumours (GIST).

Conversely, the reversal of protein phosphorylation by phosphatases is essential for providing the fine-tuning on signalling pathways and maintaining a balance in cellular physiology. In this light, the genetic or functional loss of these enzymes is now widely recognised as a hallmark of cancer initiation and progression. Although much is known regarding alterations in kinase function, the role of specific phosphatases in transformation remains poorly characterised. In recent years, the study of protein phosphatases and their regulation has become an expanding field of research aimed at elucidating the specific roles of these enzymes in tumourigenesis. In particular, protein phosphatase 2A (PP2A), which negatively regulates a multitude of signals targeted by oncogenic kinases, has been the subject of intense investigations that reveal its important role as a tumour suppressor protein.

1.2 BCR/ABL

1.2.1 Clinical presentation of Chronic Myeloid Leukaemia (CML)

CML accounts for 15% of adult leukaemia, and approximately 490 newly diagnosed cases are recorded every year in Australia. It can occur at any age but is more common in adults over the age of 50, who represent nearly 70% of all cases¹. CML is a proliferative disorder that typically involves the myeloid lineage of haematopoietic stem cells (HSC) and evolves in three distinct clinical phases: chronic (CP), accelerated and blast crisis (BC) (Figure 1.1). CML-CP has a relatively indolent presentation in patients and is characterised by the accumulation of mature cells in the peripheral blood, bone marrow and extramedullary sites (Savage *et al.* 1997). After 3 to 4 years, CML-CP evolves into the accelerated phase, which lasts 4 to 6 months and is characterised by an increase in the frequency of progenitor cells rather than terminally differentiated cells (Kantarjian *et al.* 1988). The disease finally progresses to CML-BC, which is associated with a severe reduction in cellular differentiation and the rapid expansion of myeloid or lymphoid precursor cells with over 30% of undifferentiated blasts present in the bone marrow and peripheral blood. Typical symptoms include anaemia, fatigue, increased bleeding, frequent infections and splenomegaly (Wong & Witte 2004). Once this end stage is reached, the survival rate is reduced to 3 to 5 months, and limited treatment is available. Therefore, the prognosis for patients presenting with CML-BC is poor (Sacchi *et al.* 1999, Kantarjian *et al.* 1987).

¹ Australian Institute of Health and Welfare (2007)

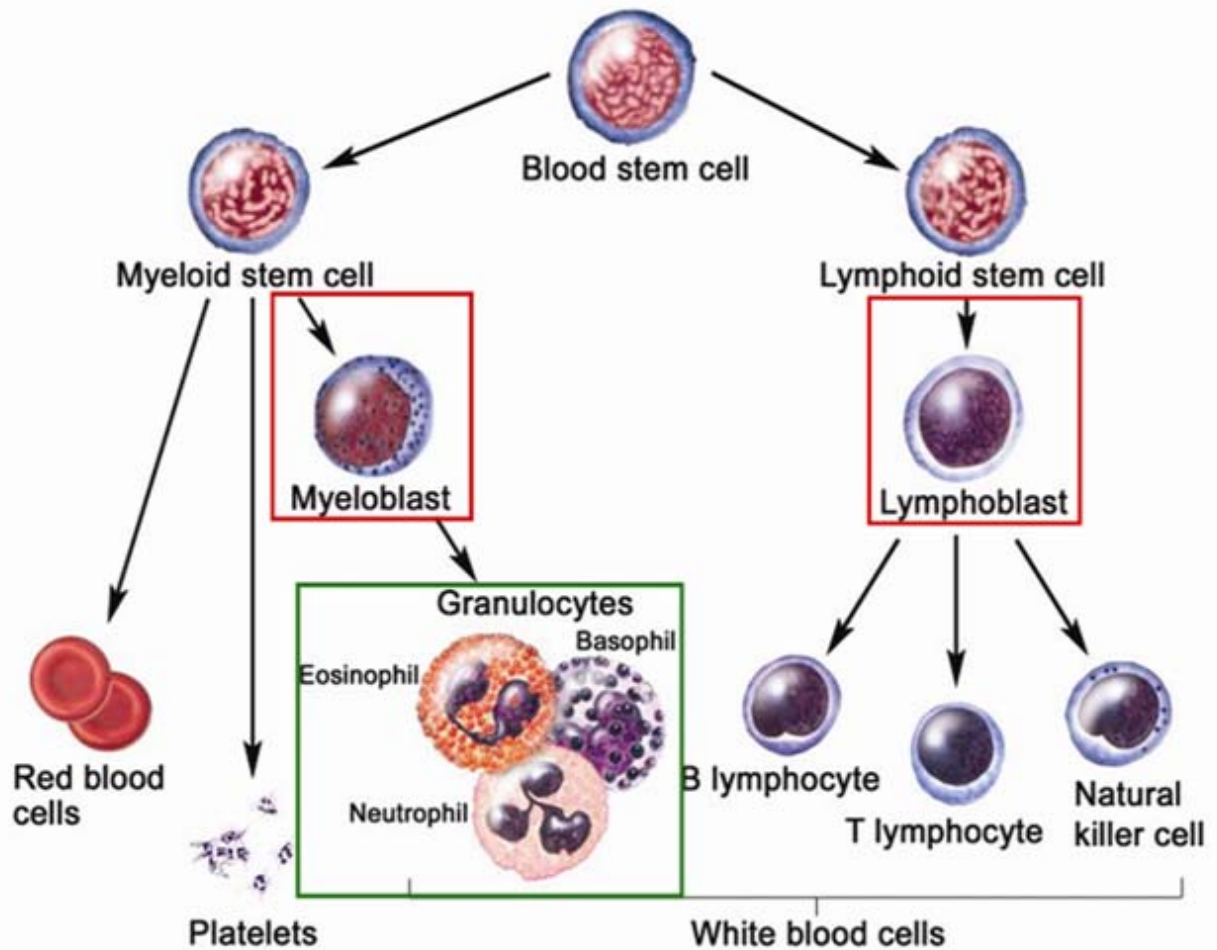


Figure 1.1 Haematopoiesis and the characteristics of CML progenitors

A multipotent haematopoietic stem cell (HSC) can differentiate into common myeloid progenitors, which are the precursors for red blood cells, platelets and granulocytes. HSCs can also differentiate into common lymphoid progenitors, which are the precursors for T- and B-cell lymphocytes. The initial phase of chronic myeloid leukaemia is characterised by the expansion of cells from the granulocyte lineage (green). Acquisition of additional molecular and genetic abnormalities causes an arrest in cell differentiation to result in the rapid expansion of common myeloid or lymphoid progenitors (red). [Adapted from *Stem Cells: Scientific Progress and Future Research Directions*. Department of Health and Human Services (2001)].

1.2.2 The Philadelphia chromosome

Over 90% of CML cases are associated with an acquired genetic abnormality known as the Philadelphia chromosome (Ph¹), which results from a reciprocal translocation between the *ABL* gene on chromosome 9 and the *BCR* gene located on chromosome 22 (Figure 1.2A) (Nowell & Hungerford 1960). The Philadelphia chromosome is also present within a smaller subset of acute lymphoblastic leukaemia (ALL) patients (Chan *et al.* 1987). The reciprocal translocation generates the *BCR/ABL* fusion oncogene that is translated into the BCR/ABL oncoprotein (Ben-Neriah *et al.* 1986).

BCR is a signalling protein that contains multiple modular domains and is highly enriched in the brain and haematopoietic cells, with its expression downregulated during myeloid maturation (Wetzler *et al.* 1993) (Figure 1.2B). ABL is a 145 kDa non-receptor tyrosine kinase that is ubiquitously expressed and exhibits a broad cellular distribution within the nucleus and cytoplasm (Figure 1.2C). The major function of ABL is the transduction of signals from cell surface growth factor and adhesion receptors that regulate cytoskeletal structure (Hernandez *et al.* 2004, Woodring *et al.* 2003). The fusion of BCR to ABL during the translocation associated with CML constitutively activates ABL and creates new regulatory motifs (Konopka & Witte 1985). Depending on the precise breakpoints during translocation and RNA splicing, three different forms of BCR/ABL proteins (p185, p210, p230) can be generated in patients, with p210 being the most common (Figure 1.3) (Ren 2005).

It is well established that the unrestrained tyrosine kinase activity of BCR/ABL is necessary for inducing and maintaining the leukaemic phenotype. Ectopic expression of p210 BCR/ABL results in factor-independent growth, increased survival and altered differentiation of immortal haematopoietic cell lines (Daley & Baltimore 1988, Lugo *et al.* 1990). The introduction of BCR/ABL-transduced bone marrow cells into lethally irradiated mice causes a myeloproliferative disorder that resembles the chronic phase of human CML (Pear *et al.* 1998, Zhang & Ren 1998). In addition, BCR/ABL fusion transcripts detected by real time quantitative polymerase chain reaction (qRT-PCR) increase with disease progression in CML patients (Elmaagacli *et al.* 2000).

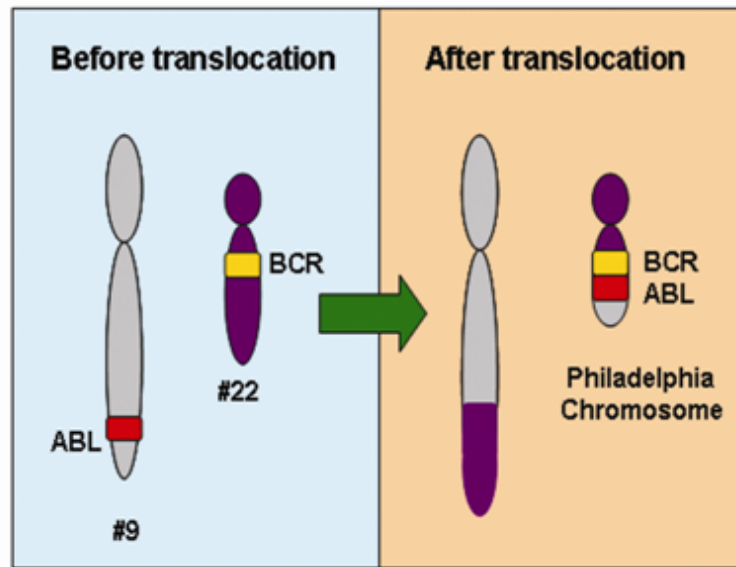
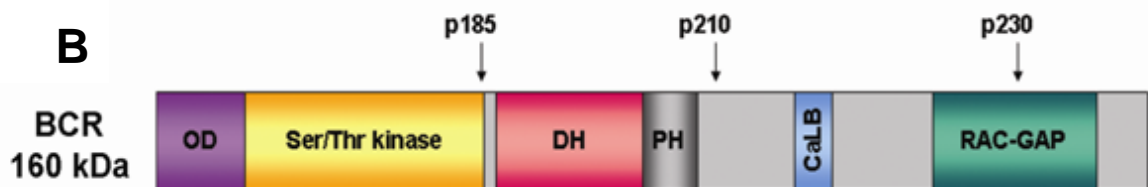
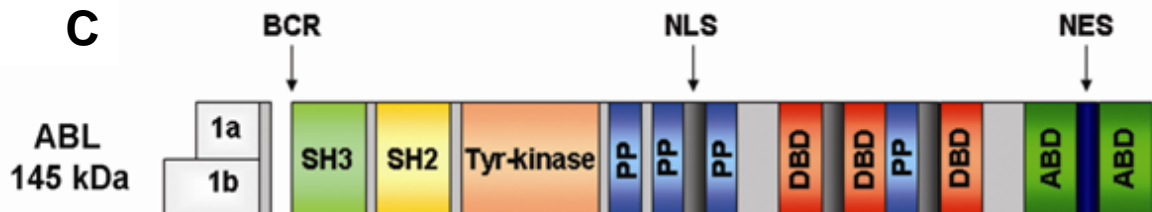
A**Philadelphia Chromosome****B****C**

Figure 1.2 The Philadelphia chromosome and functional domains of BCR and ABL proteins

A) The Philadelphia chromosome results from the reciprocal translocation between *ABL* on chromosome 9 and *BCR* on chromosome 22. Adapted from Lydon & Druker 2004. B) *BCR* contains a coil-coil oligomerisation domain (OD), serine/threonine kinase domain, Dbl/CDC24 guanine-nucleotide exchange factor homology domain (DH) and pleckstrin homology domain (PH), calcium-dependent lipid binding site (CaLB) and RAC guanosine triphosphatase-activating protein domain (RAC-GAP). Points for fusion to *ABL* are indicated at p185, p210 and p230. C) Two isoforms of *ABL* (1a and 1b) are generated by alternative splicing of the first exon. The amino terminal half contains tandem SRC homology 3 (SH3), SH2 and the tyrosine-kinase domains. In the carboxy-terminal region, *ABL* contains four proline-rich SH3 binding sites (PP); three nuclear localisation signals (NLS) and DNA binding domains (DBD); two actin binding domains (ABD); one nuclear exporting signal (NES). The point that fuses with *BCR* is indicated. Adapted from Ren 2005.

The predominant cytoplasmic location of BCR/ABL permits the assembly of phosphorylated substrates which are essential for the recruitment and activation of multiple pathways that promote proliferation and genetic instability while suppressing apoptosis (Cortez *et al.* 1995). These include, but are not limited to, RAS/mitogen activated protein kinase (MAPK) (Sawyers *et al.* 1995, Peters *et al.* 2001), phosphatidylinositol 3-kinase (PI3K)/Akt (Skorski *et al.* 1997, Skorski *et al.* 1995), CRK oncogene-like protein/focal adhesion kinase (CRKL) (ten Hoeve *et al.* 1994), signal transducer and activator of transcription 5 (STAT5) (Nieborowska-Skorska *et al.* 1999, Shuai *et al.* 1996) and the wingless/Int (Wnt)/ β -catenin pathway (Coluccia *et al.* 2007) (Figure 1.3 and Table 1.1). Together, this data indicates that BCR/ABL plays a central role in the pathogenesis of CML-CP (Ren 2005).

1.2.3 Overview of signalling pathways

1.2.3.1 Mitogen activated protein kinase (MAPK)

The MAPK pathway represents a large family of protein kinases that regulate diverse signal transduction cascades controlling cellular proliferation, differentiation, adaptation to environmental stress and apoptosis (Widmann *et al.* 1999). Thus far, five well characterised families of mammalian MAPK have been identified: extracellular signal-regulated kinase 1/2 (ERK1/2), c-Jun NH₂-terminal activated protein kinases (JNK), p38 MAPK, ERK3/4 and ERK5 (Schaeffer & Weber 1999). Activation of these pathways can be induced by a diverse range of stimuli including cytokines, growth factors, hormones and cellular stress. This results in the phosphorylation of downstream substrates including membrane and cytosolic proteins as well as transcription factors (Pearson *et al.* 2001). The most extensively studied MAPK signalling cascade in BCR/ABL-induced transformation is the Ras-Raf1-MEK1/2-ERK1/2 pathway (Calabretta & Perrotti 2004).

1.2.3.2 PI3K/Akt

PI3K are a family of lipid kinases that phosphorylate the 3'-hydroxyl group of phosphoinositides at the cellular membrane and are classified as class 1A or class 1B based on their activation by RTKs or G protein-coupled receptors, respectively. The members of class 1A exist in a heterodimeric complex composed of a 110 kDa catalytic subunit and a 85 kDa regulatory subunit (Klippel *et al.* 1994). A major downstream

Table 1.1 Signalling pathways regulated by BCR/ABL

Pathways	References
Proliferation	
RAS	(Sawyers <i>et al.</i> 1995, Skorski <i>et al.</i> 1994)
ERK1/2	(Cortez <i>et al.</i> 1997)
β -catenin	(Coluccia <i>et al.</i> 2007)
c-Myc	(Stewart <i>et al.</i> 1995)
Survival / Apoptosis	
PI3K/Akt	(Skorski <i>et al.</i> 1997, Skorski <i>et al.</i> 1995)
STAT5	(Shuai <i>et al.</i> 1996)
Bcl-xL	(Horita <i>et al.</i> 2000)
Bcl2	(Sanchez-Garcia & Grutz 1995)
BAD	(Salomoni <i>et al.</i> 2000)
Phosphatases	
PP2A	(Neviani <i>et al.</i> 2005)
SHP-1	(Bruecher-Encke <i>et al.</i> 2001)
SHIP1	(Odai <i>et al.</i> 1997)
SHIP2	(Wisniewski <i>et al.</i> 1999)
Cytoskeletal	
CrkL	(ten Hoeve <i>et al.</i> 1994)
Paxillin	(Salgia <i>et al.</i> 1995)
Cell Cycle / DNA Repair	
Cyclin D2	(Jena <i>et al.</i> 2002)
p53	(Pierce <i>et al.</i> 2000)
Mdm2	(Trotta <i>et al.</i> 2003)
Ubiquitination	
c-Cbl	(de Jong <i>et al.</i> 1995)

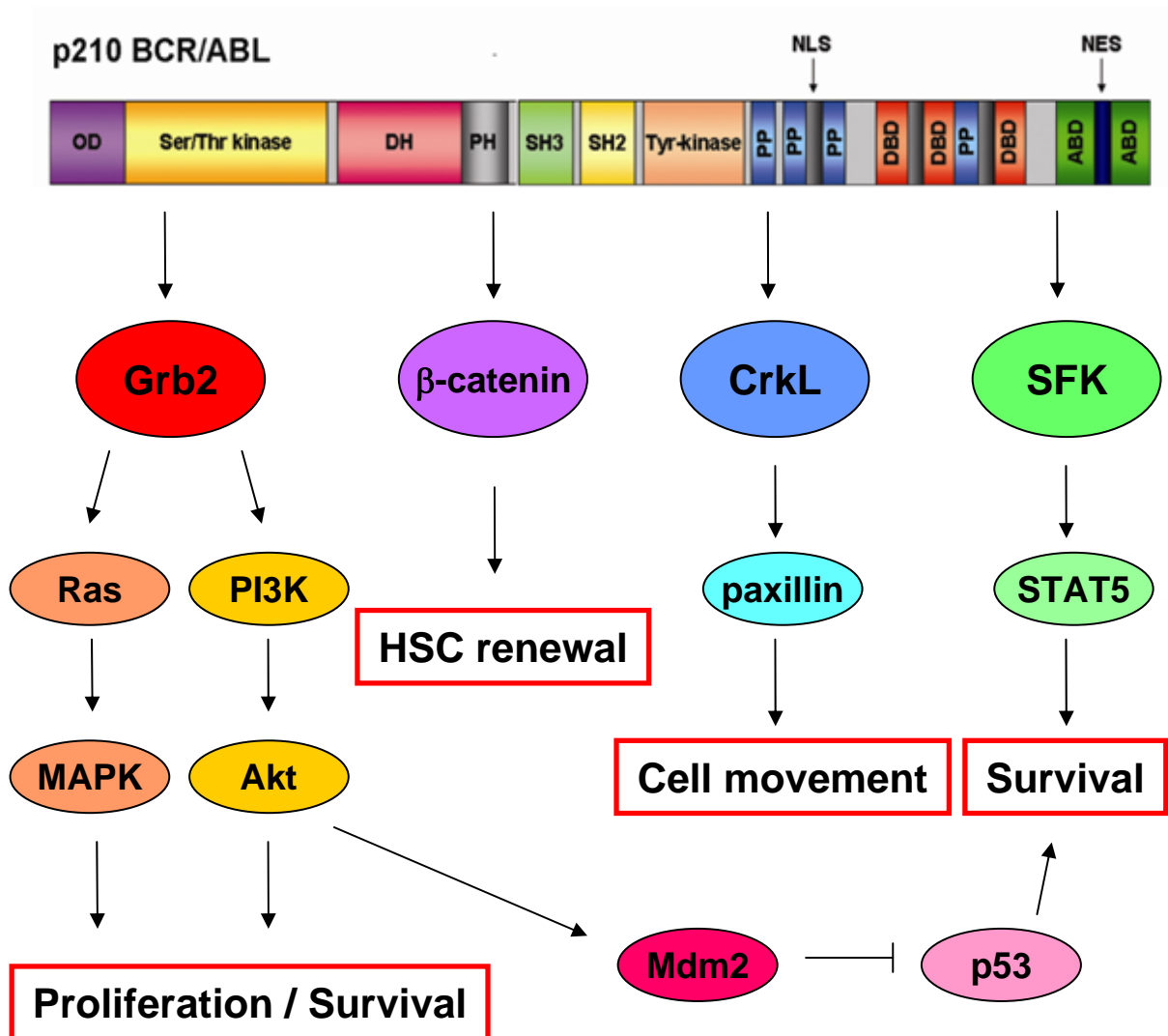


Figure 1.3 Leukaemogenic signalling by the p210 kDa BCR/ABL oncoprotein
 Schematic representation of a selection of BCR/ABL-induced pathways regulating proliferation and survival of BCR/ABL-transformed haematopoietic stem cells.

effector of the PI3K pathway is the serine/threonine kinase, Akt, which is recruited to the plasma membrane upon activation and regulates various cellular processes including survival and apoptosis (Datta *et al.* 1996). Numerous reports have demonstrated Akt is a central node in tumour-promoting pathways that contribute to cell survival and evasion of apoptosis (Manning & Cantley 2007, Cully *et al.* 2006). Like most oncogenic kinases, deregulated activity of Akt results from aberrant regulation or, less frequently, transforming mutations (Carpten *et al.* 2007, Luo *et al.* 2003).

1.2.3.3 Src family kinases (SFKs)

The proto-oncogene Src encodes a nonreceptor tyrosine kinase whose expression and activity correlates with advanced malignancy and poor prognosis in a variety of human cancers (Wheeler *et al.* 2009). Nine enzymes with homology to Src, including Lyn, Lck and Fyn have been identified and collectively are referred to as Src family kinases (SFKs). Given the large number of family members, SFKs are involved in a wide range of cellular functions including proliferation, differentiation, cell cycle progression, survival and protein trafficking (Thomas & Brugge 1997).

1.2.3.4 Janus kinases (JAKs)/signal transducers and activators of transcription (STATs)

The Janus kinases (JAKs) are cytoplasmic tyrosine kinases that are rapidly activated by ligand binding to cytokine receptors or RTKs (Rane & Reddy 2002). Important targets for activated JAKs are the cytoplasmic STAT molecules. Upon phosphorylation, STATs undergo dimerisation and subsequently translocate to the nucleus where they initiate transcription of target genes by binding to upstream promoter regions (Steelman *et al.* 2004).

1.2.3.5 Wnt/ β -catenin

The Wnt pathway is important for stem-cell maintenance and cellular proliferation during development (Reya & Clevers 2005). In the absence of Wnt factors, the modular protein axin provides a scaffold for the binding of adenomatous polyposis coli (APC), glycogen synthase kinase 3 β (GSK3 β) and β -catenin in a destruction complex (Ikeda *et al.* 1998). This facilitates serine/threonine phosphorylation of β -catenin by GSK3 β , which results in its proteasome-dependent degradation (Aberle *et al.* 1997). Binding of Wnt ligand to its cell surface receptor, Frizzled, causes activation of Dishevelled, a cytoplasmic protein that is recruited to the plasma membrane where it antagonises

GSK3 β activity (Miller *et al.* 1999). This results in β -catenin stabilisation, nuclear accumulation and interaction with T-cell factor/lymphoid enhancer factor (TCF/LEF) family members to induce transcription of numerous genes important for cell proliferation and survival (Reya & Clevers 2005). Deregulation of this pathway contributes to the pathogenesis of epithelial cancers including colon, pancreatic and skin (Eastman & Grosschedl 1999).

1.2.4 Transition from chronic phase to blast crisis CML

The evolution of CML from the chronic phase into blast crisis is associated with the accumulation of secondary chromosomal and/or molecular alterations (Kantarjian *et al.* 1987, Faderl *et al.* 1999). The precise mechanisms underlying these effects remain unclear. However, it is predicted that the unrestrained activity of BCR/ABL promotes additional abnormalities that are essential for the expansion of cell clones with increasingly malignant characteristics, such as enhanced proliferative potential and reduced apoptotic susceptibility. These events remain crucial for the leukaemic phenotype and directly promote the differentiation arrest of myeloid or lymphoid precursors, which is a distinctive feature of blast crisis (Calabretta & Perrotti 2004).

Interestingly, the vast majority of secondary changes involve 1) genes encoding nuclear-localised proteins or 2) mutation or loss of function of tumour suppressors. For example, inactivation of p53 occurs in approximately 30% of CML-BC patients (Ahuja *et al.* 1989), and loss of function impairs the response to the tyrosine kinase inhibitor, imatinib, *in vitro* and *in vivo* (Wendel *et al.* 2006). Deletion of the *INK4-ARF* tumour suppressor locus occurs in 50% of Ph¹ ALL patients (Sill *et al.* 1995). Moreover, mice injected with Arf^{-/-} BCR/ABL⁺ cells display enhanced development of leukaemia compared to Arf^{+/+} mice, and are resistant to high doses of imatinib (Williams *et al.* 2006). A recent finding demonstrates that increased expression of the leukaemia-associated SET protein functionally inactivates PP2A in blast crisis CD34⁺ progenitors, and this is essential for blastic transformation (Neviani *et al.* 2005). Together, these findings indicate that loss of tumour suppressor function may play a key role in the evolution of CML-BC. To direct the development of improved therapies that prevent the progression of CML into blast crisis, further investigation into the molecular aberrations regulated by BCR/ABL is required.

1.3 Receptor Tyrosine Kinase c-KIT

1.3.1 Structure and function

c-KIT is classified as a type III RTK and is structurally similar to platelet-derived growth factor receptor (PDGFR) and Fms-like tyrosine kinase 3 (FLT-3) (Qiu et al. 1988). The *c-KIT* gene is located at the locus 4q11-q21 (Yarden et al. 1987) and was identified at the genomic level as the cellular homologue of the *v-kit* oncogene, the transforming gene of the Hardy-Zuckerman 4 feline sarcoma virus (Besmer et al. 1986). Distinguishing features of the c-KIT receptor include an extracellular region comprised of five immunoglobulin-like loops followed by a single hydrophobic transmembrane domain that anchors the receptor to the plasma membrane. The intracellular region contains a juxtamembrane (JMD) and a tyrosine kinase domain split by an interkinase sequence into two sections, the ATP binding pocket and phosphotransferase catalytic site (Qiu et al. 1988) (Figure 1.4).

Binding of stem cell factor (SCF) to c-KIT induces homodimerisation of the receptor (Ashman 1999) and facilitates the autophosphorylation of specific tyrosine residues within the cytoplasmic domain (Mol et al. 2003). This creates a scaffold which forms docking sites for signal transduction molecules that activate pathways important for cellular proliferation, adhesion, migration, differentiation and survival (Figure 1.5 and Table 1.2) (Lennartsson *et al.* 2005, Masson & Rönnstrand 2009). These include MAPK (Hong *et al.* 2004, Lennartsson *et al.* 1999), PI3K/Akt (Lev *et al.* 1992, Blume-Jensen *et al.* 1998), JAK/STATs (Brizzi *et al.* 1999, Weiler *et al.* 1996), SFKs (Linnekin *et al.* 1997, Broudy *et al.* 1999, Voytyuk *et al.* 2003) and the Wnt/ β -catenin pathway (Kajiguchi *et al.* 2008, Tickenbrock *et al.* 2008). The c-KIT receptor also associates directly with growth factor receptor binding protein-2 (Grb2) (Thommes et al. 1999), which recruits the scaffolding protein Grb2-associated binding protein (Gab2) (Nishida *et al.* 1999) into a multiprotein complex to activate downstream pathways including MAPK and PI3K (Sun *et al.* 2008).

Negative regulation of the c-KIT receptor is mediated through multiple mechanisms, two of which include the Src homology 2 domain-containing protein tyrosine phosphatase-1 (SHP-1) (Kozlowski *et al.* 1998) and protein kinase C (PKC) (Blume-Jensen et al. 1995). SHP-1 interacts with Tyr569 in the c-KIT JMD, whilst PKC is

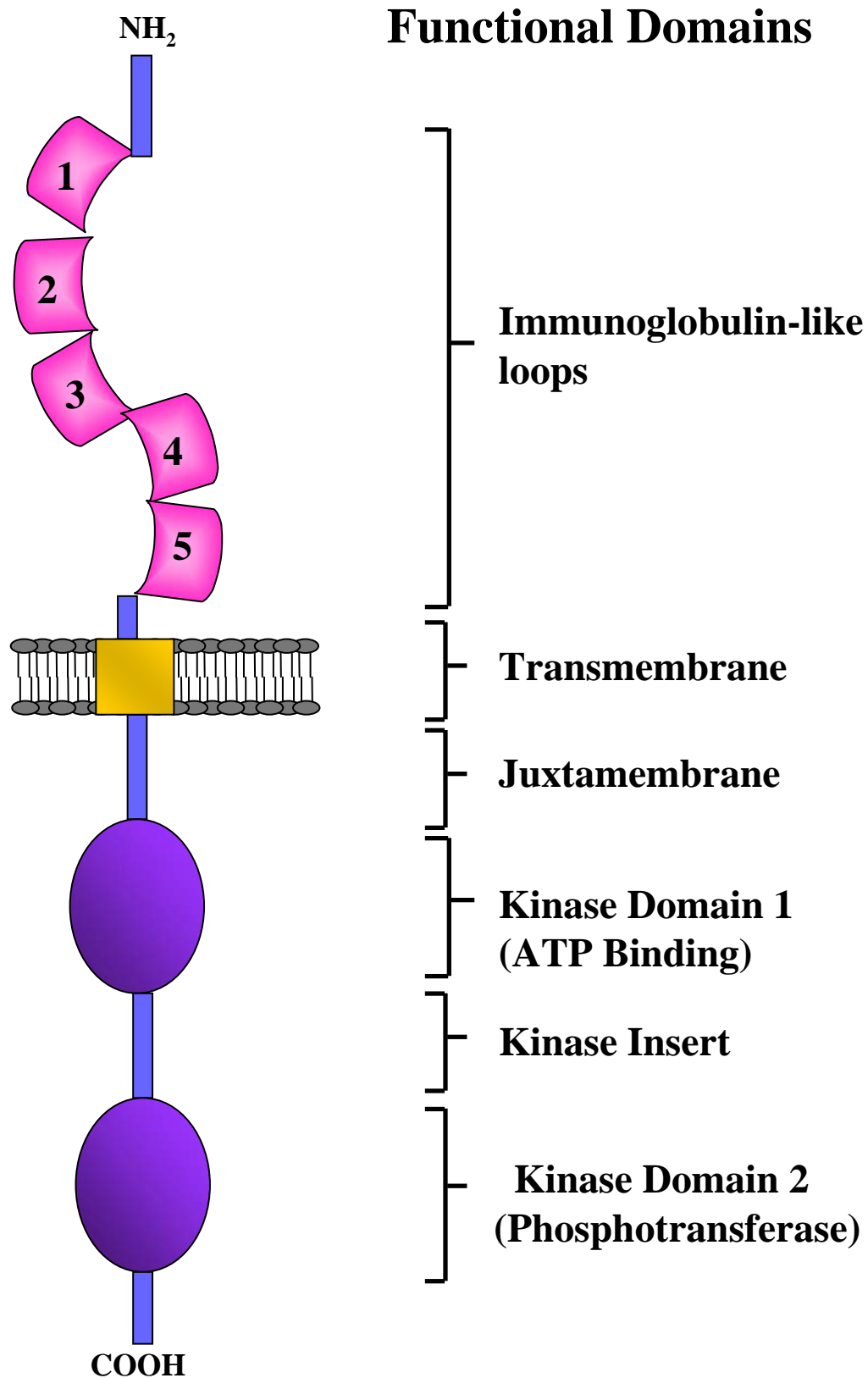


Figure 1.4 Functional domains of the c-KIT receptor

Structural features of c-KIT include an extracellular region comprised of five immunoglobulin-like loops (1-5), followed by a single hydrophobic transmembrane domain. The intracellular region contains a juxtamembrane domain and a tyrosine kinase split by the kinase insert into the ATP binding pocket and phosphotransferase catalytic site.

Table 1.2 Signalling pathways regulated by c-KIT

Pathways	References
Proliferation	
RAS	(Hong <i>et al.</i> 2004)
Shc	(Lennartsson <i>et al.</i> 1999)
SFK / Lyn	(Voytyuk <i>et al.</i> 2003, Linnekin <i>et al.</i> 1997)
β -catenin	(Kajiguchi <i>et al.</i> 2008, Tickenbrock <i>et al.</i> 2008)
c-Myc	(Kajiguchi <i>et al.</i> 2008)
Survival / Apoptosis	
PI3K	(Lev <i>et al.</i> 1992)
Akt	(Blume-Jensen <i>et al.</i> 1998)
JAK2	(Weiler <i>et al.</i> 1996)
STAT5	(Brizzi <i>et al.</i> 1999)
Ubiquitination	
SFK	(Broudy <i>et al.</i> 1999)
Cbl	(Sun <i>et al.</i> 2007)

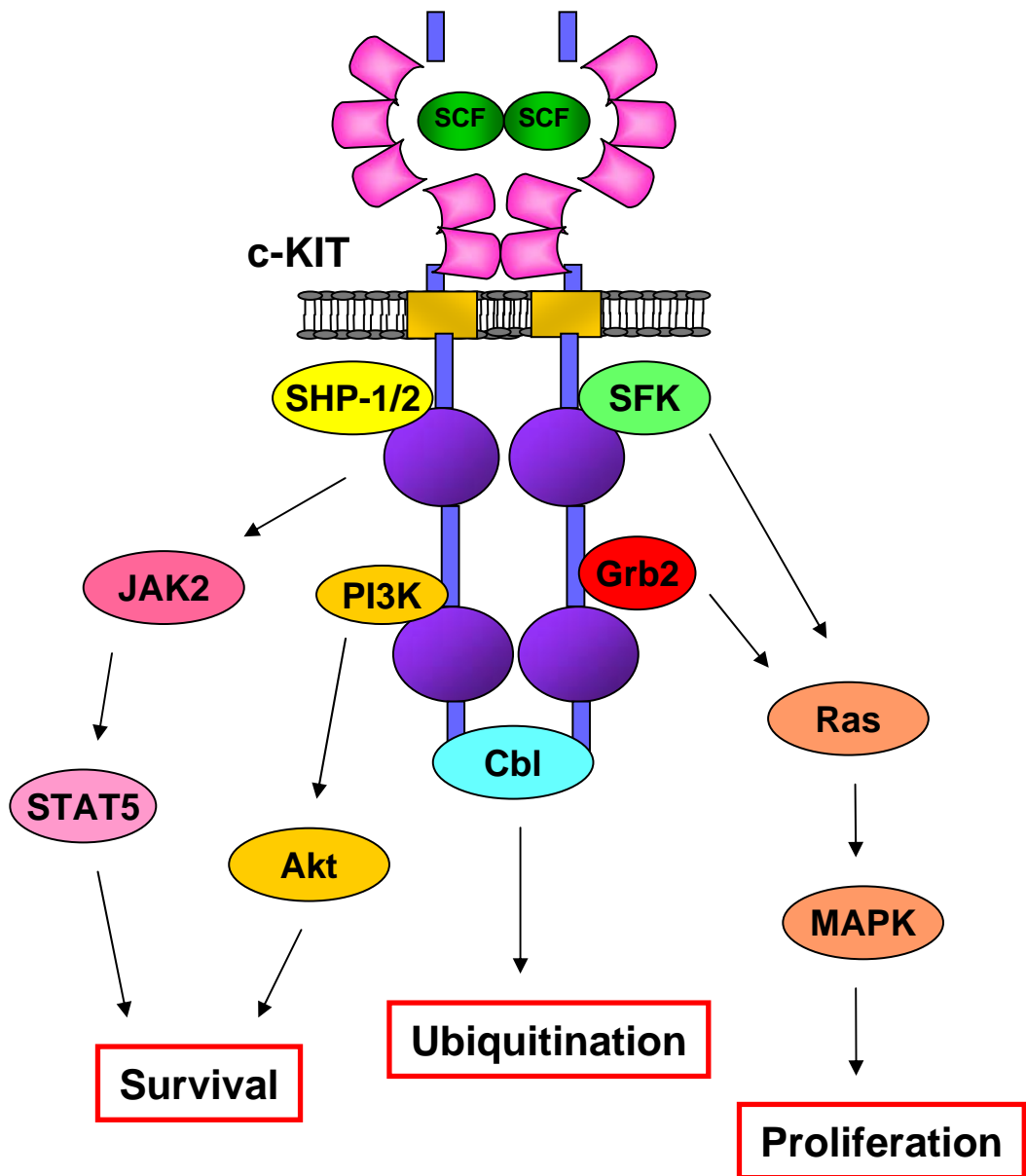


Figure 1.5 Signalling pathways activated by c-KIT

Binding of stem cell factor (SCF) to the first three immunoglobulin-like loops of c-KIT induces homodimerisation and autophosphorylation of the receptor. This leads to the activation of multiple signalling components involved in cellular proliferation and survival. SHP-1 and receptor ubiquitination by Cbl negatively regulates c-KIT signalling.

involved in a negative feedback loop following SCF stimulation and regulates c-KIT through the phosphorylation of two serine residues, 741 and 746, within the kinase insert. Another important mechanism of c-KIT modulation is through ubiquitin-mediated internalisation (Masson *et al.* 2006). This process is regulated by ubiquitin E3 ligases, such as the Cbl family, which become activated upon binding to c-KIT and attach ubiquitin molecules to the receptor, targeting it for degradation (Sun *et al.* 2007).

1.3.2 Expression of c-KIT in human malignancies

Expression of c-KIT is important for the normal development of HSCs, mast cells, germ cells, melanocytes and interstitial cells of Cajal (Ashman 1999). Consistent with this, gain-of-function *c-KIT* mutations leading to constitutive activation of the receptor have been documented in core-binding factor acute myeloid leukaemia (CBF-AML) (Mrozek *et al.* 2008), systemic mastocytosis (Worobec *et al.* 1998), GIST (Hirota *et al.* 1998), testicular seminoma (Kemmer *et al.* 2004) and a subset of melanoma patients (Figure 1.6) (Smalley *et al.* 2009). Subsequent studies have revealed that amino acid changes in the JMD are commonly detected in GIST, whilst mutations in the kinase domain, are important in the pathology of CBF-AML and mastocytosis (Lennartsson *et al.* 2005).

1.3.2.1 Gastrointestinal stromal tumours (GIST)

GIST constitutes a distinct group of stromal neoplasms that arise from the transformation of interstitial cells of Cajal, or their mesenchymal stem cell precursors (Duensing *et al.* 2004). Although GIST account for 5% of tumours located within the gastrointestinal tract, they are the most common form found within the mesenchyme (Antonescu *et al.* 2004, Fletcher *et al.* 2002). Expression of c-KIT is readily detected by immunohistochemical staining on up to 90% of patient samples (Logrono *et al.* 2004). Somatic *c-KIT* mutations detected within GIST patients are extremely heterogeneous and include in frame deletions and insertions of various sizes along with point mutations that result in amino acid substitutions (Hirota *et al.* 1998). However, the most frequent mutations are observed within exon 11, which corresponds to the JMD (e.g V560G) (Corless *et al.* 2004, Taniguchi *et al.* 1999). This region interacts with the ATP binding lobe of the kinase domain to modulate its catalytic activity (Chan *et al.* 2003). Consequently, oncogenic mutations cause structural alterations that relieve this auto-inhibitory function.

c-KIT Mutations

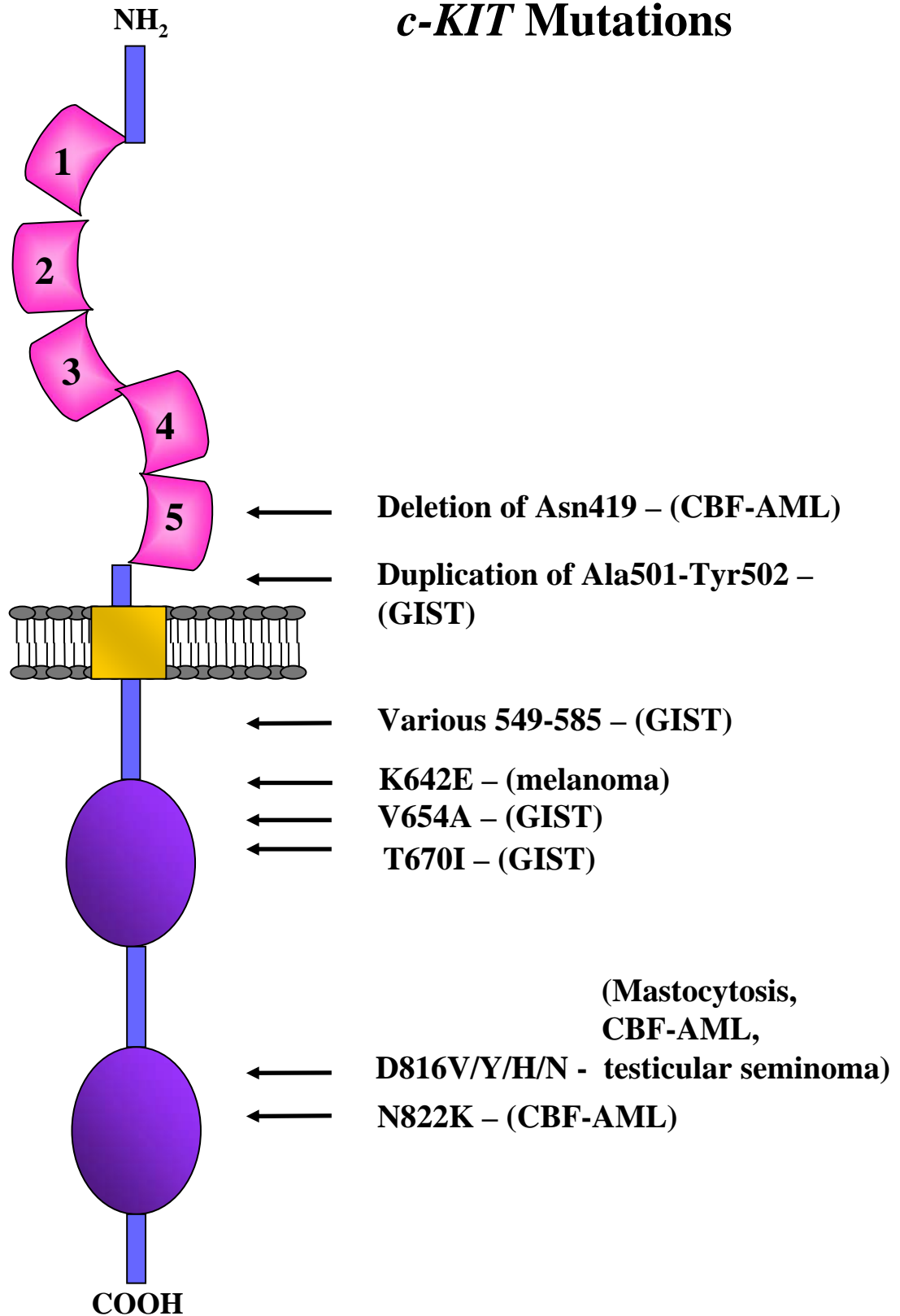


Figure 1.6 Mutations of *c-KIT* detected in human malignancies

Location of activating *c-KIT* mutations that contribute to the development of gastrointestinal stromal tumours (GIST), mastocytosis, core-binding factor acute myeloid leukaemia (CBF-AML), testicular seminoma and melanoma.

The differential activation of downstream signalling cascades from JMD mutations (V560G and del559) have been examined in cellular mouse models (Table 1.3). Notably, del559 c-KIT constitutively associates with the 85 kDa regulatory subunit of PI3K (Vanderwinden *et al.* 2006). Interestingly, there is a general consensus that JMD mutations do not activate the MAPK/ERK pathway (Casteran *et al.* 2003, Frost *et al.* 2002). With respect to other downstream signalling pathways, very low constitutive phosphorylation of Akt and STAT3/STAT5 have been reported, with a sustained response only evoked upon SCF stimulation (Chen *et al.* 2003, Frost *et al.* 2002, Casteran *et al.* 2003). The ability of these cells to activate multiple signalling pathways similar to WT c-KIT when exposed to SCF indicates that pathways driving growth factor-independent proliferation and those controlling cellular responses are distinctly regulated. SHP-1 is also regulated by oncogenic c-KIT activation, as inhibition of c-KIT with imatinib in BaF3 lymphoid cells expressing del559 c-KIT elevates the levels of SHP-1, and this effect is reversed after drug removal. In the same cellular model, the levels of alternate phosphatases including SHP-2, PTEN and the tyrosine phosphatase SH-PTP1 were comparable to WT c-KIT, indicating a specific effect on SHP-1 (Vanderwinden *et al.* 2006).

Table 1.3 Differential activation of signalling pathways by mutant c-KIT

Signalling molecule	WT c-KIT	JMD c-KIT mutant	D816V c-KIT mutant
p85 – P13K	No*	Yes	Yes
Akt	No*	No*	No*
ERK1/2	No*	No*	Yes*#
STAT3	No	Yes#	Yes
STAT5	No*	No*	NR
SFK	No*	NR	No
SHP-1	Basal	Basal	Reduced

*Induced with SCF stimulation; #Low levels
JMD, juxtamembrane domain; NR, not reported; WT, wild-type

1.3.2.2 Core-binding factor Acute Myeloid Leukaemia (CBF-AML)

AML is a heterogeneous disease that is classified based on the presence of specific cytogenetic abnormalities as well as the French-American-British classification of leukaemic cells and immunophenotype (Tefferi & Vardiman 2008). It has a prevalence of 7.4 cases per 100 000, rising to 36.7 cases in adults over 65 years of age¹. CBF-AML is among the most common cytogenetic subtype of AML, being detected in ~13% of adults with *de novo* disease (Byrd *et al.* 2002). Current therapeutic options involve multiple cycles of high-dose cytarabine (Byrd *et al.* 2004, Byrd *et al.* 1999, Bloomfield *et al.* 1998), however, only 50% of patients are cured using this treatment (Appelbaum *et al.* 2006, Marcucci *et al.* 2005, Schlenk *et al.* 2004). Thus, to direct the development of improved therapies, further investigation underlying the mechanisms of this disease is required.

CBFs are a group of heterodimeric transcriptional regulators that function in haematopoietic development. They consist of three distinct DNA-binding CBF α subunits, Runt-related transcription factor 1 (RUNX1; also known as AML1), and a common CBF β component (CBFB) (Speck & Gilliland 2002). Homozygous loss of either gene in a mouse knockout model results in lack of definitive haematopoiesis and embryonic death at day 12.5-13.5 (Downing 2003). The most common chromosomal rearrangements observed in CBF-AML are t(8;21) (Downing *et al.* 1993) and inv(16) (Liu *et al.* 1993), that result in expression of the fusion genes AML1/ETO and CBFB/MYH11, respectively.

Both *in vitro* (Peterson *et al.* 2007) and *in vivo* models (Yuan *et al.* 2001) have demonstrated that expression of AML1/ETO and CBFB/MYH11 contribute to the development of leukaemia by acting as dominant negative inhibitors of normal myeloid differentiation, thereby facilitating the expansion of a progenitor pool (Speck & Gilliland 2002). However, their expression exerts limited effect on cellular proliferation (Dayyani *et al.* 2008, Yuan *et al.* 2001), and neither fusion protein alone is sufficient for leukaemogenesis (Muller *et al.* 2008, Peterson *et al.* 2007). This is highlighted by mouse models of CBF-AML utilising either conditional knock in of AML1/ETO (Higuchi *et al.* 2002) or knock in of CBFB/MYH11 in embryonic stem cells (Castilla *et*

¹ Australian Institute of Health and Welfare (2007)

al. 1999). In both cases, the development of AML requires secondary mutations induced by chemical mutagens such as N-ethyl-N-nitrosurea (ENU) (Castilla *et al.* 1999, Yuan *et al.* 2001).

These observations support a multi-step model of leukaemogenesis involving the cooperation between activating mutations (class I) and gene rearrangements (class II) in haematopoietic progenitors. Class I mutations confer a proliferative and/or survival advantage and are best exemplified by constitutively activated tyrosine kinases. Class II mutations, such as CBF rearrangements, are associated with impaired haematopoietic differentiation (Speck & Gilliland 2002). In support of this theory, co-expression of AML1/ETO and FLT3 length mutation potently synergise to promote the development of aggressive leukaemia in a mouse bone marrow transplantation model (Schessl *et al.* 2005).

Activating mutations of c-KIT are an ideal candidate for transforming haematopoietic cells. Indeed mutations within *c-KIT* have been detected in up to 47% of patients with t(8;21) (Table 1.4) and 38% of patients with inv(16) (Table 1.5). A large proportion of activating *c-KIT* mutations in AML patients are located within the kinase domain, and particularly involve a substitution at codon 816 (e.g. D816V/H/Y) (Beghini *et al.* 1998, Beghini *et al.* 2000). In most cases, the presence of D816V is associated with a higher relapse rate and reduced overall survival compared to patients expressing the WT receptor (Paschka *et al.* 2006, Schnittger *et al.* 2006, Boissel *et al.* 2006, Shimada *et al.* 2006, Jiao *et al.* 2009). Furthermore, the Kasumi-1 cell line, which was established from the peripheral blood of a t(8;21) CBF-AML patient in relapse (Asou *et al.* 1991), expresses an N822K substitution (Beghini *et al.* 2002).

The presence of a novel *c-KIT* mutation comprising small in-frame deletions or insertions in exon 8 has also been identified in CBF-AML patients. This mutation results in the consistent loss of asparagine at codon 419, which is located in the fifth immunoglobulin-like domain of c-KIT (e.g. del D419) (Gari *et al.* 1999, Cammenga *et al.* 2005). Clinical observations demonstrate an association between exon 8 mutations and an increase in relapse rate (Care *et al.* 2003).

Table 1.4 Clinical significance of c-KIT mutations in t(8;21) CBF-AML

Cohort	Age range (median)	% mutated / total	Type of mutation (number of cases)	Prognostic outcome	Reference
UK Medical Research Council AML trials and DBHOG	16-83	13% (6/47)	D816 (5) Exon 8 (1)	NR	(Care <i>et al.</i> 2003)
Adult <i>de novo</i> CBF-AML	NR	46.8% (15/32)	D816 (NR) Exon 8 (NR)	NR	(Beghini <i>et al.</i> 2004)
CBF-AML	3-68 (27.4)	48.1% (26/54)	D816 (9) N822K (10) Exon 8 (1)	NR	(Wang <i>et al.</i> 2005)
<i>De novo</i> CBF-AML	4-48 (46)	38% (14/37)	D816 (7) N822K (3) Exon 8 (3) JMD (1)	RFS significantly lower for <i>c-KIT</i> mutations compared to WT. No impact on OS.	(Nanri <i>et al.</i> 2005)
Adult <i>de novo</i> CBF-AML. CALGB clinical trial.	18-71 (37)	22% (11/49)	D816 (4) N822 (4) Exon 8 (2)	CIR significantly higher for <i>c-KIT</i> mutations compared to WT. No impact on OS.	(Paschka <i>et al.</i> 2006)
Adult and pediatric <i>de novo</i> CBF-AML	1-75 (33)	12% (6/50)	D816 (3) Exon 8 (3)	EFS, RFS and OS significantly shorter for <i>c-KIT</i> mutations compared to WT.	(Boissel <i>et al.</i> 2006)

Table 1.4 Clinical significance of c-KIT mutations in t(8;21) CBF-AML continued

Cohort	Age range (median)	% mutated / total	Type of mutation (number of cases)	Prognostic outcome	Reference
Untreated adult CBF-AML from 6 Italian medical centres	16-76 (40.5)	47% (19/42)	D816 (12) Exon 8 (5) Exon 11 (2)	No impact on RI or OS	(Cairoli et al. 2006)
Pediatric <i>de novo</i> CBF-AML. JCACSG trial.	2-15 (7.5)	17.4% (8/46)	D816 (4) N822K (4)	RR significantly higher, EFS and OS shorter for <i>c-KIT</i> mutations compared to WT.	(Shimada et al. 2006)
Pediatric <i>de novo</i> CBF-AML.	<17	43% (12/28)	D816 (NR) N822K (NR) Exon 8 (NR)	No impact on EFS or OS	(Shih et al. 2007)
Adult and pediatric <i>de novo</i> CBF-AML	1.6-72.2 (29.3)	21% (7/34)	D816 (4) Exon 8 (1) JMD (2)	No impact on CIR or OS.	(MarkovÃ; et al. 2009)

CIR, cumulative incidence of relapse; EFS, event-free survival; NR, not reported; OS, overall survival; RFS; relapse-free survival; RR, relapse risk. DBHOG, Dutch-Belgian Haematology-Oncology Group; CALGB, Cancer and Leukemia Group B. JCACSG, Japanese Childhood AML Cooperative Study Group

Table 1.5 Clinical significance of c-KIT mutations in inv(16) CBF-AML

Cohort	Age range, (median)	% mutated / total	Type of mutation (number of cases)	Prognostic outcome	Reference
UK Medical Research Council AML trials and DBHOG	16-83	32% (20/63)	D816 (5) Exon 8 (15)	RR significantly higher for exon 8 mutations. No impact on OS.	(Care <i>et al.</i> 2003)
Adult CBF-AML	NR	45% (9/20)	D816 (NR) Exon 8 (NR)	NR	(Beghini <i>et al.</i> 2004)
Adult <i>de novo</i> CBF-AML. CALGB trial.	19-57 (40)	30% (18/61)	D816 (10) Exon 8 (8)	CIR significantly higher and OS shorter for <i>c-KIT</i> mutations compared to WT.	(Paschka <i>et al.</i> 2006)
Adult and pediatric <i>de novo</i> CBF-AML	1-75 (33)	22% (10/46)	D816 (1) Exon 8 (9)	No significant difference in 6 year EFS or OS compared to WT	(Boissel <i>et al.</i> 2006)
Untreated adult CBF-AML from 6 Italian medical centres	17-88 (51)	48% (12/25)	D816 (8) Exon 8 (3) V530I (1)	NR	(Cairoli <i>et al.</i> 2006)
Pediatric <i>de novo</i> CBF-AML.	<17	38% (5/13)	D816 (NR) N822K (NR) Exon 8 (NR)	No impact on EFS or OS	(Shih <i>et al.</i> 2007)
Adult and pediatric <i>de novo</i> CBF-AML	1.6-72.2 (29.3)	50% (13/26)	D816 (3) N822K (2) Exon 8 (9)	No impact on CIR or OS.	(Markovıj <i>et al.</i> 2009)

CIR, cumulative incidence of relapse; EFS, event-free survival; NR, not reported; OS, overall survival; RFS; relapse-free survival; RR, relapse risk. DBHOG, Dutch-Belgian Haematology-Oncology Group; CALGB, Cancer and Leukemia Group B.

1.3.2.3 Mastocytosis

Mastocytosis refers to a heterogeneous group of conditions characterised by hyperproliferation of mast cells. Cutaneous mastocytosis is limited to the skin and can be treated successfully with anti-mediator drugs that inhibit mast cell activation (Hennessy *et al.* 2004). In contrast, systemic mastocytosis involves the infiltration of mast cells into various organs such as the spleen, bone marrow, lymph nodes and the liver. The current therapy for these patients includes interferon (IFN)- α or cladribine, but their efficacy is limited and the prognosis remains poor (Valent *et al.* 2005). Systemic mastocytosis is associated with kinase domain *c-KIT* mutations and nearly all patients express the 816 codon substitutions (Longley *et al.* 1999). Clinical observations also indicate these patients are more likely to display symptoms of an associated haematological disorder (Worobec *et al.* 1998).

1.3.2.4 Melanoma

Interest in the role of c-KIT in melanoma has recently been sparked following the identification of subgroups harbouring activating *c-KIT* mutations. These particular lesions are found on sites of the body that receive very little UV exposure, such as the soles of the feet (acral) or mucosal membranes. Notably, activating mutations have been detected in up to 62% of acral and mucosal melanomas, as well as 28% of melanomas on chronic sun-induced damaged skin (Curtin *et al.* 2006, Ashida *et al.* 2009, Rivera *et al.* 2008). Within these subgroups, there are also cases in which overexpression of c-KIT leads to constitutive signalling in the absence of an activating mutation (Smalley *et al.* 2008).

1.3.2.5 *c-KIT* mutations at codon 816

Constitutive activation induced by the D816V *c-KIT* mutation occurs independently of receptor dimerisation in the extracellular domain (Tsujimura *et al.* 1999). Molecular modelling has demonstrated that aspartic acid at codon 816 forms two hydrogen bonds with the peptide backbone to stabilise the activation loop into an inactive confirmation. These bonds are disrupted when aspartate is replaced by another amino acid and results in the transition of the activation loop away from the ATP binding pocket to lock the kinase domain into a constitutively active confirmation (Foster *et al.* 2004, Mol *et al.* 2004).

Although the mechanisms of signal transduction by the WT c-KIT receptor are well characterised (Lennartsson *et al.* 2005), the mechanisms by which the oncogenic D816V mutant induces transformation have been less studied (Table 1.3). Cells expressing D816V exhibit constitutive c-Cbl phosphorylation and receptor ubiquitination, which leads to rapid receptor turnover and reduced cell surface expression (Sun *et al.* 2009). Consistent with this observation, the D816V mutant drives transformation through intracellular receptors trapped to the Golgi (Xiang *et al.* 2007), and this has the potential to alter substrate specificity (Piao *et al.* 1996). Indeed this phenomenon has been noted for FLT-3, where trapping of the internal tandem duplication (ITD) mutant to the endoplasmic reticulum leads to selective phosphorylation of STAT5 (Schmidt-Arras *et al.* 2009).

In addition to factor-independent activation of the kinase domain, the D816V mutation amplifies the intrinsic catalytic activity of c-KIT (Lam *et al.* 1999). For example, the p85 subunit of PI3K is constitutively phosphorylated and associated with D816V c-KIT in the immortalised murine progenitor cell line, MIHC. Inhibition of PI3K by wortmannin abrogates the autonomic proliferation of cells expressing D816V, indicating the importance of the PI3K pathway in transformation (Chian *et al.* 2001, Shivakrupa *et al.* 2003).

Several studies have also demonstrated aberrant phosphorylation of STAT3 by D816V c-KIT in a variety of leukaemia cell lines including HMC-1.2, FDC-P1 and MO7e (Frost *et al.* 2002, Ning *et al.* 2001a, Pan *et al.* 2007, Ning *et al.* 2001b). Suppression of STAT3 by a dominant negative molecule severely impairs the transforming capacity of D816V c-KIT *in vitro* and *in vivo*, and is accompanied by downregulation of its downstream targets Bcl-xL and c-Myc (Ning *et al.* 2001a, Ning *et al.* 2001b). The role of ERK1/2 in D816V signalling is controversial. Whilst WT c-KIT induces strong ERK1/2 activation, undetectable levels have been recorded in cells expressing the D816V mutant (Chian *et al.* 2001, Frost *et al.* 2002, Ning *et al.* 2001a). Sun *et al.*, recently reported weak activation of ERK1/2 in D816V BaF3 cells, which increased dramatically with SCF stimulation (Sun *et al.* 2009).

Differences also exist in the requirement for SFK signalling. In contrast to WT c-KIT, the D816V mutant receptor circumvents the requirement for SFK by mimicking Src kinase activity; an action which contributes to its transforming potential (Sun et al. 2009). Furthermore, mutation at the equivalent position in the murine *c-KIT* gene (D814Y) results in the ubiquitin-dependent degradation of SHP-1, a known negative regulator of c-KIT (Piao et al. 1996). This suggests that signals emanating from a tyrosine kinase can target specific proteins for proteolysis. More recently, reduced levels of the pro-apoptotic BH3-only death regulator, Bim, was detected in BaF3 cells expressing D816V c-KIT; an observation which introduces another level of complexity to this potentially transforming mutation (Aichberger *et al.* 2009).

Taken together, it is clear that the signal transduction pathways and downstream biological pathways mediated by D816V c-KIT are markedly different from those activated by the WT receptor. In particular, this mutant induces oncogenic transformation by enhancing signals that are required for growth and survival, whilst abrogating the effects of negative regulation. Further work aimed at identifying additional signal transduction molecules involved in the transformation potential of D816 substitutions could provide novel targets for selective therapy against highly oncogenic versions of c-KIT.

1.4 Small Molecule Inhibitors Targeting BCR/ABL and c-KIT

1.4.1 Imatinib

As malignant transformation in CML is dependent on the activity of BCR/ABL, the most rational approach to treating this disease was to develop a compound that inactivates the kinase domain. Imatinib mesylate, (Gleevec[®], STI571; Novartis) is a 2-phenylaminopyrimidine derivative that was among the first inhibitors developed for targeted cancer therapy (Figure 1.7A). The small molecule selectively regulates tyrosine kinase activity through competitive inhibition at the ATP binding site and interacts with the inactive conformation of the kinase domain to lock it into position (Figure 1.7B) (Buchdunger et al. 1996). Consequently, the phosphorylation of cellular substrates is prevented, and downstream signalling cascades normally generated by kinase activation are inhibited (Druker et al. 1996) (Figure 1.7C and D).

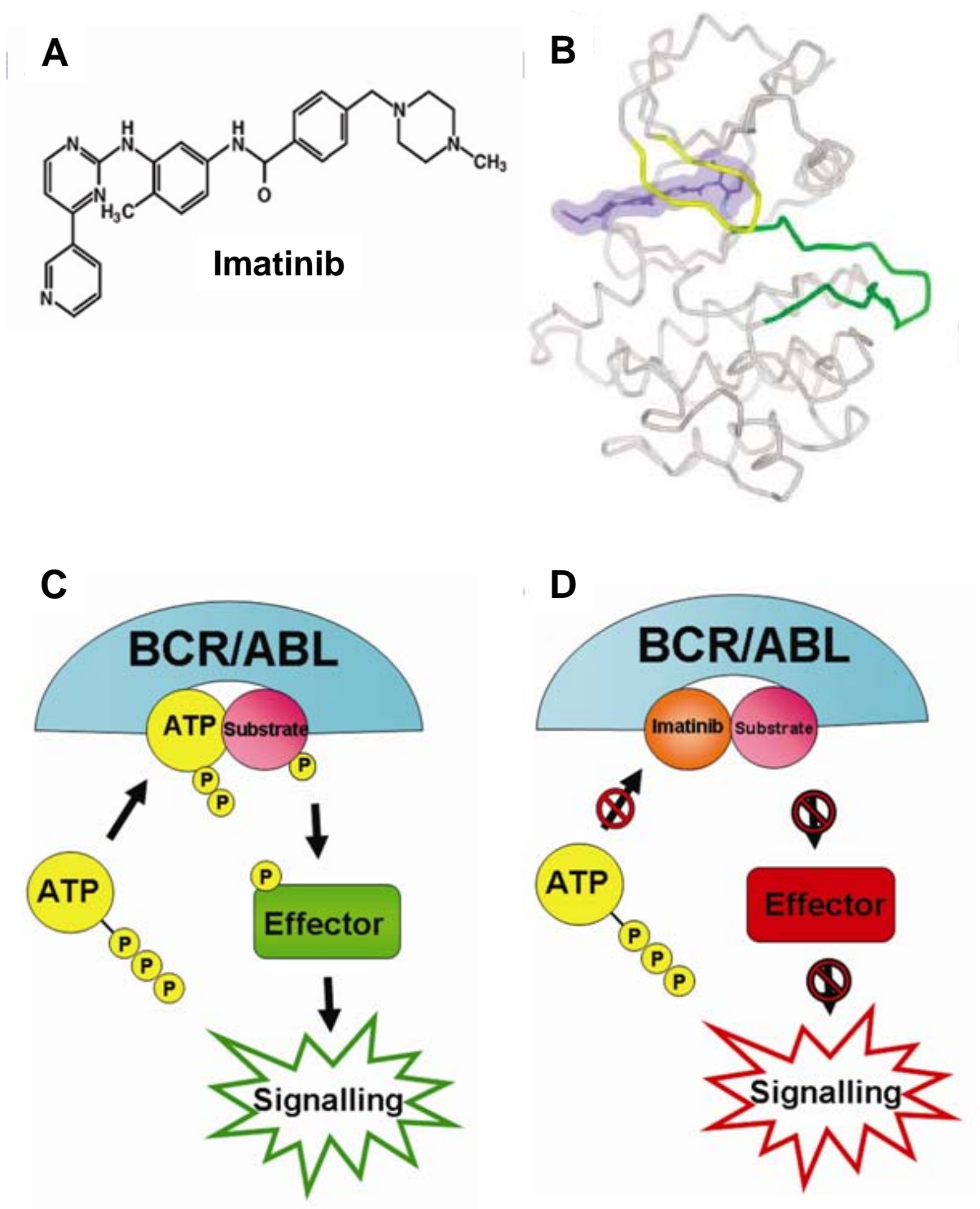


Figure 1.7 Structure of BCR/ABL in complex with imatinib

A) Molecular structure of imatinib (Kantarjian *et al.* 2007c). **B)** Binding of imatinib (purple) to the inactive conformation of the ABL kinase domain. The nucleotide-binding loop (yellow) is bent over the inhibitor and the activation loop (green) adopts an inactive conformation (Weisberg *et al.* 2007). **C)** ATP binds to the ABL kinase domain in BCR/ABL and phosphorylates substrate/effector molecules that activate oncogenic signalling pathways. **D)** Imatinib competes with ATP and inhibits downstream signalling cascades.

1.4.1.1 CML clinical trials

The first clinical trials conducted with imatinib demonstrated high cytogenetic and molecular response rates, long-term efficacy and superior tolerability over IFN-based therapy in CML-CP patients (Kantarjian *et al.* 2002a, Druker *et al.* 2001b, O'Brien *et al.* 2003). As a result, imatinib received approval by the United States Food and Drug Administration (FDA) as a standard therapy for newly diagnosed CML-CP patients, in addition to all CML patients who had failed stem cell transplant or IFN- α therapy (Talpaz *et al.* 2002). The phase III IRIS¹ trial compared 400 mg/day imatinib with IFN- α plus cytarabine in 1,106 newly diagnosed CML-CP patients (Hughes *et al.* 2003, O'Brien *et al.* 2003). With a follow up of 5 years, the major cytogenetic response rate (MCR²) was 87% and the estimated 5-year survival rate was 89% (Druker *et al.* 2006). Therefore, imatinib treatment demonstrates remarkable therapeutic effects in CML patients who present with chronic phase disease. However, the outcome for CML-BC patients treated with imatinib remains poor (Kantarjian *et al.* 2002b, Druker *et al.* 2001a). In a phase II trial, the MCR rates were 6% in patients treated with 400 mg/day (Sawyers *et al.* 2002), with a follow-up survival rate of 14% at 36 months (Silver *et al.* 2004).

In addition to the low response rates observed with imatinib in late stage disease, approximately 4% of newly diagnosed CML-CP patients develop resistance (Druker *et al.* 2006), as evidenced by the persistence of BCR/ABL transcripts (Hughes *et al.* 2003, Bhatia *et al.* 2003). The acquisition of secondary point mutations in the *BCR/ABL* gene alter the protein structure and prevent imatinib from effectively inhibiting the ABL kinase domain (Gorre *et al.* 2001, Shah & Sawyers 2003). Mutations clustered around the imatinib binding site result in the substitution of amino acids that sterically prevent the molecule from binding. This commonly involves the gatekeeper residue Thr315 (e.g. T315I) (Schindler *et al.* 2000). Mutations that cause resistance through an indirect mechanism (e.g. E255K, Y253F/H), destabilise the inactive conformation of ABL and reduce imatinib binding (Roumiantsev *et al.* 2002). Notably, mutations at Y253 and T315 elicit a higher *in vitro* and *in vivo* transforming potential than WT BCR/ABL (Griswold *et al.* 2006). Each drug-resistant mutant displays a unique substrate recognition profile that may affect disease progression through activation of altered

¹ International Randomized Study of IFN versus STI571

² MCR; 35% or less of cells positive for the Philadelphia chromosome

downstream signalling pathways (Skaggs *et al.* 2006). Accordingly, patients harbouring these mutations show reduced time to disease progression and overall survival compared to patients expressing WT BCR/ABL (Soverini *et al.* 2005).

Another contributing factor to resistance is the insensitivity of leukaemia stem cells to imatinib treatment (Graham *et al.* 2002, Roeder *et al.* 2006). Recent *in vitro* studies demonstrate 5 μM imatinib reduces BCR/ABL-mediated CRKL phosphorylation by 86% in CD34⁺ cells. However, in the more primitive CD34⁺CD38⁻ cells¹, imatinib exerts very little effect with only a 4% reduction in p-CRKL observed (Copland *et al.* 2006). Furthermore, primitive CML cells do not readily undergo apoptosis, even after prolonged *in vitro* exposure to 10 μM imatinib (Graham *et al.* 2002). It is plausible that the expansion of BCR/ABL⁺ quiescent stem cells could result in the progression of disease into blast crisis (Chu *et al.* 2005). The rapid relapses observed in some patients who have discontinued imatinib therapy after a period of PCR negativity support this theory (Cortes *et al.* 2004).

1.4.1.2 GIST clinical trials

Imatinib is also potent at inhibiting c-KIT tyrosine kinase activity in GIST models *in vitro* (Buchdunger *et al.* 2000, Heinrich *et al.* 2000) and *in vivo* (Chen *et al.* 2003). Clinical trials showed partial response or stable disease in approximately 80% of patients with advanced or metastatic GIST (Demetri *et al.* 2002, van Oosterom *et al.* 2001), with a 2 year survival rate of 70% (Verweij *et al.* 2004). Based on these results, imatinib was approved by the FDA for the treatment of malignant metastatic and/or unresectable GIST (Dagher *et al.* 2002). The location of the *c-KIT* mutation correlates with clinical efficacy of imatinib, with 83.5% of patients harbouring a JMD mutation (exon 11) achieving a partial response compared to only 47.8% of patients expressing mutations in the extracellular region (exon 9) (Heinrich *et al.* 2003).

Although many GIST patients benefit from imatinib, ~15% of patients are unresponsive, and most patients who respond or stabilise initially will develop resistance after 2 years of treatment (Van Glabbeke *et al.* 2005, Verweij *et al.* 2004). This phenomenon of acquired resistance in GIST patients recapitulates treatment failure

¹ <5% of total CD34⁺

observed in CML patients (Gorre et al. 2001), and is a major setback that must be addressed when developing targeted protein kinase inhibitors (Boyar & Taub 2007). Similar to BCR/ABL, the main mechanism underlying imatinib resistance is the acquisition of secondary *c-KIT* mutations in exon 13 (e.g. V654A) or exon 14 (T670I) (Chen *et al.* 2004a, Debiec-Rychter *et al.* 2005, Antonescu *et al.* 2005, Wardelmann *et al.* 2005, Tamborini *et al.* 2004, Heinrich *et al.* 2008). These substitutions confer resistance to imatinib by altering the structural confirmation of the ATP/drug binding pocket (Tamborini et al. 2004, Roberts *et al.* 2007). Mutations within the kinase activation loop (e.g D816V) have also been detected in imatinib-resistant GIST patients (Heinrich et al. 2008).

1.4.1.3 AML and mastocytosis clinical trials

As WT *c-KIT* expression is detected on over 70% of blast cells from AML patients (Bene *et al.* 1998, Ikeda *et al.* 1991), it seemed logical to evaluate the effectiveness of imatinib treatment in these patients. However, clinical trials administering high doses up to 800 mg/day have shown a complete lack of efficacy with very little to no responses observed (Cairolì *et al.* 2005, Chevallier *et al.*, Cortes *et al.* 2003, Heidel *et al.* 2007, Kindler *et al.* 2004, Malagola *et al.* 2005, Piccaluga *et al.* 2007). These results indicate that the expression of *c-KIT* as a sole marker for predicting sensitivity to imatinib in AML patients is insufficient. It should be noted that the mutational status of *c-KIT* was not investigated in a majority of these trials.

It has been widely demonstrated that kinase domain *c-KIT* mutations, present in systemic mastocytosis and CBF-AML, are intrinsically resistant to imatinib inhibition. This phenomenon was originally discovered in the human mast cell line, HMC-1.2, and mouse factor-dependent myeloid cell line, FDC-P1, expressing the D816V mutant *c-KIT* (Ma *et al.* 2002, Frost *et al.* 2002). The D816V substitution induces a conformational change in the protein to favour the active confirmation. As such, imatinib is unable to effectively inhibit the receptor due to the presence of an Asp-Phe-Gly motif within the ATP pocket that interferes with drug binding (Foster et al. 2004). Clinical studies investigating the effectiveness of imatinib for systemic mastocytosis and CBF-AML have confirmed that all unresponsive patients harbour D816 mutations (Pardanani *et al.* 2003, Cairolì et al. 2005, Wang *et al.* 2005, Vega-Ruiz et al. 2009). Thus, to improve therapy options for these resistant patients, a better understanding of

the signalling pathways activated downstream of imatinib-resistant c-KIT mutants is required.

1.4.2 Second generation inhibitors

The discovery of resistance mechanisms and the persistence of stem cells in response to imatinib therapy spurred the development of second generation inhibitors designed to overcome this major clinical problem. A selection of these FDA approved compounds are discussed below.

1.4.2.1 Nilotinib

Nilotinib (Tasigna®, AMN107; Novartis) was approved by the FDA in 2007 for the treatment of imatinib-resistant CML (Figure 1.8A). It exhibits superior potency to imatinib in a wide range of CML-derived cell lines and inhibits a majority of imatinib-resistant BCR/ABL mutants *in vitro*, excluding T315I (Weisberg et al. 2006, O'Hare *et al.* 2005, Weisberg et al. 2005). For the treatment of imatinib-resistant disease, phase II studies reported complete haematological response CHR¹ in 69% and CCR² in 32% of CML-CP patients. However, in a similar observation to imatinib treatment, 400 mg twice a day was not effective in treating CML-BC, with only 4% reaching CHR and 21% displaying CCR. This is attributable to the fact that nilotinib, like imatinib, is not effective against the CD34⁺ CML population (Jorgensen *et al.* 2007). In addition, an alarming fraction of patients suffered serious side effects including severe neutropaenia and thrombocytopenia (Kantarjian *et al.* 2006, Kantarjian *et al.* 2007b, le Coutre *et al.* 2008, Giles *et al.* 2006). Recent reports also indicate that patients harbouring mutations which are less sensitive to nilotinib *in vitro* (e.g. Y235H, T315I), display less favourable clinical responses (Hughes *et al.* 2009).

Nilotinib exerts little effect on HMC-1.2 and FDC-P1 cells expressing the D816V *c-KIT* mutation (Verstovsek *et al.* 2006, Roberts et al. 2007). Furthermore, primary bone marrow derived mast cells from D816V⁺ systemic mastocytosis patients are completely unresponsive to nilotinib treatment *in vitro* (Verstovsek et al. 2006). Thus in a similar manner to imatinib, the issue of drug-resistance remains a significant hurdle in treating patients harbouring *c-KIT* kinase domain mutations.

¹ CHR; achievement of a normal white blood cell count and no symptoms of CML

² CCR; absence of Ph⁺ cells

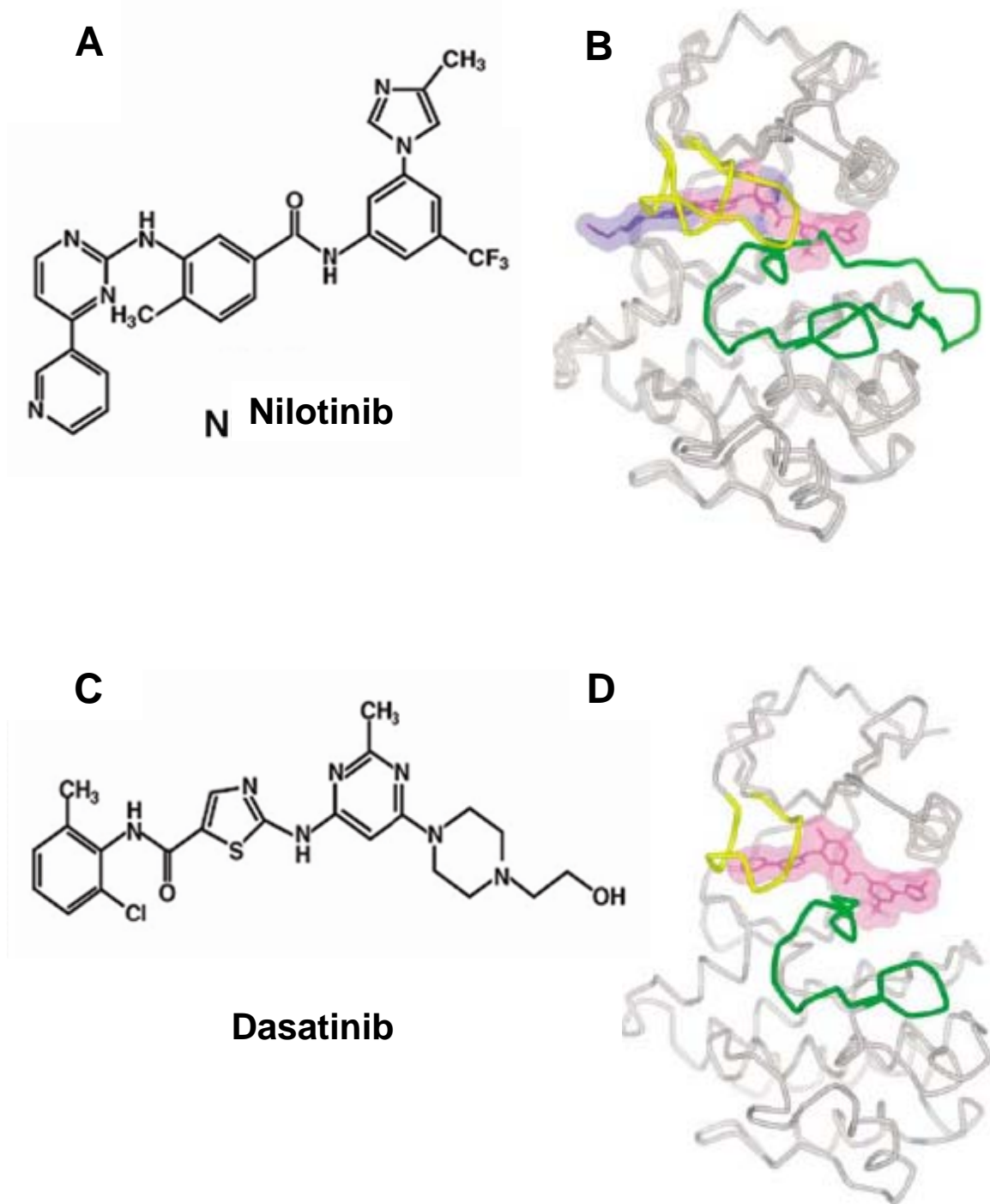


Figure 1.8. Structure of nilotinib and dasatinib in complex with the ABL kinase domain

A) Molecular structure of nilotinib (Kantarjian et al. 2007c) **B)** bound to the inactive conformation of the ABL kinase domain. The nucleotide-binding loop (yellow) is bent over the inhibitor and the activation loop (green) adopts an inactive conformation (Weisberg *et al.* 2007). **C)** Molecular structure of dasatinib (Kantarjian et al. 2007c) **D)** bound to the active conformation of the ABL kinase domain. The nucleotide-binding loop adopts an extended conformation and the activation loop is in the active position (Weisberg *et al.* 2007).

1.4.2.2 Dasatinib

Dasatinib (Sprycell®, BMS-354825; Bristol-Myers Squibb) is a highly potent orally active dual SRC/ABL inhibitor that binds to both the active and inactive conformation of the ABL kinase domain (Tokarski et al. 2006) (Figure 1.8B). It is effective against many imatinib-resistant BCR/ABL mutations *in vitro*, again excluding T315I (O'Hare et al. 2005, Shah *et al.* 2004). Dasatinib has been investigated in a series of clinical trials involving CML patients who showed resistance or intolerance to imatinib (START¹). CML-CP patients display favourable CHR and CCR with a maximum tolerated dose of 70 mg twice daily (Talpaz *et al.* 2006, Cortes *et al.* 2007, Hochhaus *et al.* 2007, Guilhot *et al.* 2007, Kantarjian *et al.* 2007a), although a recent investigation demonstrated that 140 mg daily has a similar efficacy, with an improved safety profile (Kantarjian *et al.* 2009a). In June 2006, dasatinib received accelerated approval from the US FDA and European Medicines Agency for the treatment of CML patients in all phases following imatinib failure. A follow up study of patients with accelerated phase has shown CHR and CCR rates of 45% and 32%, respectively (Apperley *et al.* 2009). As previously observed with imatinib, dasatinib exhibits lower efficacy in CML-BC patients compared to CML-CP, with only 26% achieving both CHR and CCR by 6 months. In addition, these effects are short-lived and by 8 months 69% of patients had withdrawn from the study due to either disease progression or toxic side effects (Cortes *et al.* 2007). Failure to respond is associated with expression of the T315I BCR/ABL mutation (Soverini *et al.* 2007).

Although dasatinib is moderately effective in imatinib-resistant patients (Kantarjian *et al.* 2009b), it still does not eliminate the most primitive and quiescent CML stem cell fraction (Copland *et al.* 2006). Furthermore, haematological toxicity is frequently associated with dasatinib therapy, with 72% of patients experiencing grade 2 to 4 cytopenia (Alfonso *et al.* 2009). Notably, these complications can compromise the achievement of a desirable clinical response (Sneed *et al.* 2004)

The efficacy of dasatinib in imatinib-resistant c-KIT⁺ cell lines has also been examined. (O'Hare *et al.* 2005). Preclinical studies showed it potently inhibits the growth of HMC-1.2 cells (Schittenhelm *et al.* 2006) and primary mast cells expressing the D816V

¹ SRC/ABL Tyrosine Kinase Inhibition Activity Research Trials of Dasatinib

mutation at clinically relevant concentrations (Shah et al. 2006). These results suggested that dasatinib might be effective in c-KIT⁺ AML and systemic mastocytosis patients expressing a kinase domain mutation. A recent phase II trial investigating the efficacy of dasatinib in nine patients with AML reported one complete response in an 80-year old male who expressed c-KIT on 66% of bone marrow blasts and had previously achieved a short complete response with cytarabine and daunorubicin chemotherapy (Verstovsek et al. 2008). However, the *c-KIT* mutation status of these patients was not investigated. Disappointingly, no other favourable clinical responses were observed in this trial. Out of 33 patients with systemic mastocytosis, only 2 achieved a complete response, and both tested negative for the D816V *c-KIT* mutation. Nine patients experienced symptomatic improvement with duration ranging from 3 – 18 months. In addition, 23 patients discontinued therapy due to toxicity and adverse effects, with pleural effusion being the most common (Verstovsek et al. 2008). Similar low response rates and poor tolerance to dasatinib has been observed in additional systemic mastocytosis cases (Purtill *et al.* 2008, Rondoni *et al.* 2007). Of note, these studies did not investigate the phosphorylation status of c-KIT or its downstream substrates after treatment to confirm the receptor was in fact inhibited by dasatinib.

The mechanisms underlying the reduced efficacy of dasatinib therapy in patients expressing kinase domain *c-KIT* mutations are largely unknown. One explanation is that increased toxicity precludes administration of the drug at therapeutically relevant concentrations. Indeed, in a general sense, dasatinib is associated with side effects that may prevent long-term therapeutic use of this agent even in patients who initially respond to treatment. Another possibility is the existence of unidentified molecular alterations that contribute to transformation. These would not be targeted by dasatinib and therefore continue to drive cancer cell proliferation. Data from a phase II trial evaluating the safety and efficacy of dasatinib in a larger cohort of c-KIT⁺ AML and systemic mastocytosis patients will be available in December 2009¹. In addition, a phase I study specifically focussing on dasatinib treatment in newly diagnosed CBF-AML patients has begun recruiting². The preliminary clinical trial results observed with dasatinib suggest that screening of *c-KIT* mutations prior to treatment may filter those patients who are not likely to respond, and therefore improve the outcome of the study.

¹ ClinicalTrials.gov identifier: #NCT00255346

² ClinicalTrials.gov identifier: #NCT00850382

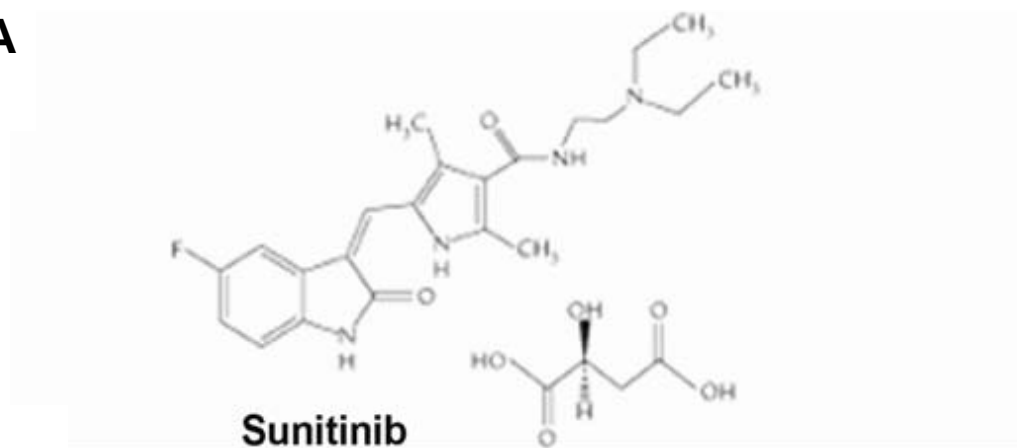
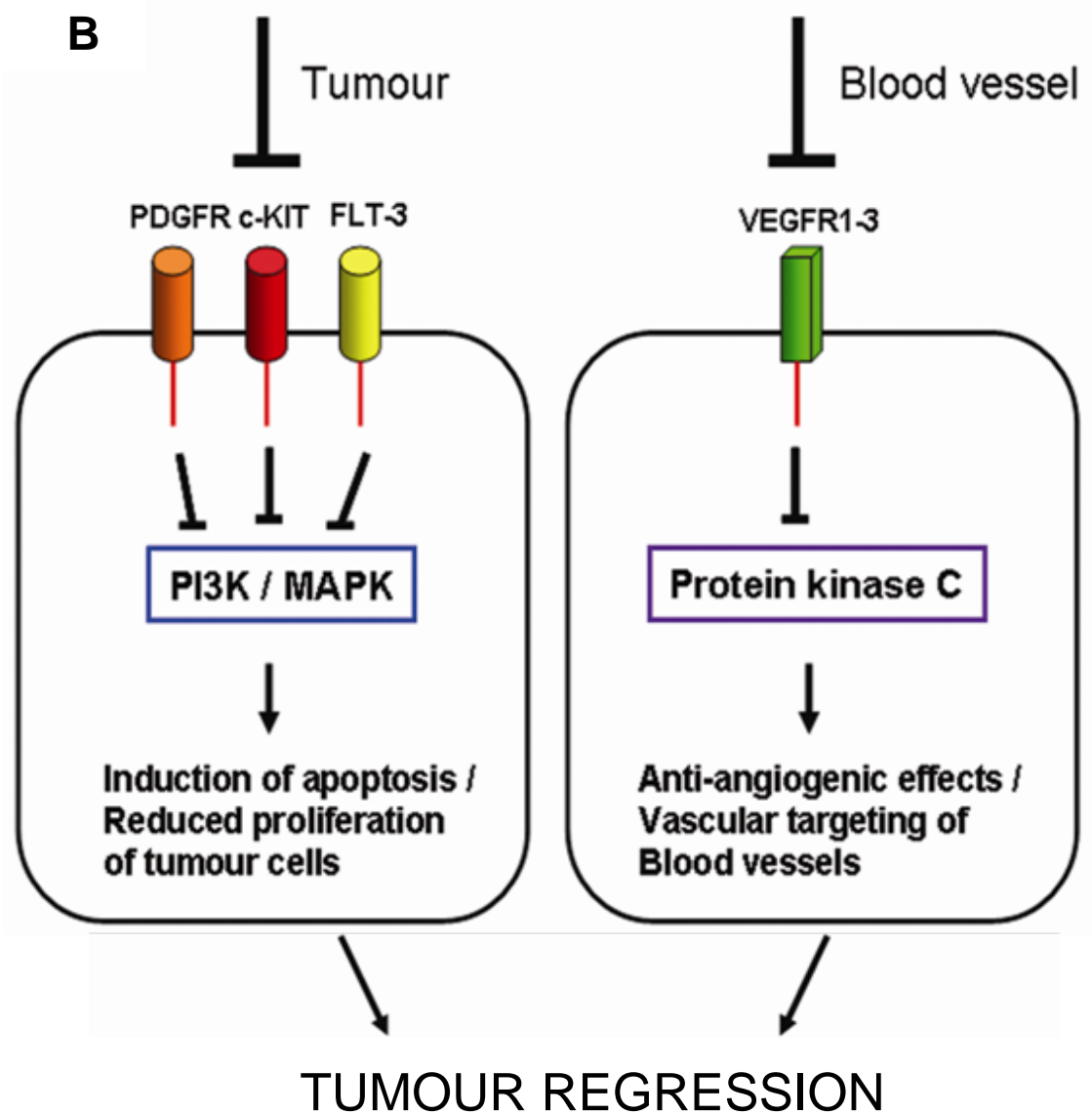
1.4.2.3 Sunitinib

Sunitinib malate (Sutent, SU11248; Pfizer) is another tyrosine kinase inhibitor currently used for imatinib-refractory GIST (Goodman et al. 2007). It is a broad spectrum indolin-2-one compound that targets multiple kinases including c-KIT (Abrams et al. 2003), vascular endothelial growth factor receptors (VEGFR), PDGFR (Sun et al. 2003) and FLT3 (O'Farrell et al. 2003) (Figure 1.9A). As such, it exerts both potent anti-tumour effects via inducing cell death, as well as anti-angiogenic effects by inhibiting the formation of new blood vessels and disrupting the existing vascular system (Figure 1.9B) (Faivre *et al.* 2007).

The FDA approval of sunitinib for GIST in January 2006 was based on a Phase III randomized, double-blinded, placebo-controlled multicenter trial including 312 patients who had documented failure or intolerance to imatinib (Demetri et al. 2006). The median time to tumour progression in patients receiving sunitinib was 27 weeks, compared to 6 weeks for placebo-treated patients (Demetri et al. 2006). Despite a significant improvement in time to tumour progression, two studies evaluating sunitinib treatment in imatinib-resistant GIST patients (Goodman et al. 2007, Demetri *et al.* 2009) have reported a partial response rate of only 7%, as defined by RECIST¹ (Therasse *et al.* 2000). Therefore, it seems to exert a cytostatic rather than a cytotoxic effect and may delay progression and/or death whilst having little effect on tumour size (Demetri et al. 2006).

In a similar mechanism to imatinib, it appears the initial *c-KIT* mutation strongly influences the response to sunitinib. Patients expressing exon 9 (e.g. insA501Y502) *c-KIT* mutants display significantly longer time to disease progression and an improvement in overall survival compared to exon 11 (e.g. V560G) patients (Maki *et al.* 2005, Heinrich et al. 2008). Interestingly, these results are in complete contrast to imatinib (Heinrich et al. 2003). The evaluation of several case studies confirms the emergence of resistance to sunitinib. One study identified different *c-KIT* mutations (V654A and D816H) within separate tumour samples obtained from the same patient during disease progression, which indicates polyclonal tumour evolution (Loughrey *et al.* 2006). In another study, the acquisition of mutations within the kinase domain

¹ Response Evaluation Criteria in Solid Tumours; at least a 30% decrease in the sum of the longest diameter of target lesions, taking as reference the baseline sum

A**B****Figure 1.9 Mechanism of action of sunitinib**

A) Molecular structure of sunitinib (Faivre et al. 2007) **B)** Sunitinib interacts with the ATP-binding sites of receptor tyrosine kinases (c-KIT, FLT3 and PDGFR) within the tumour cell. Sunitinib also targets VEGFRs on blood vessels. Receptor inhibition exerts both anti-tumour and anti-angiogenic effects that contribute to tumour regression.

(D816V) conferred resistance to both imatinib and sunitinib (Heinrich *et al.* 2007). These studies demonstrate the urgent need for the development of treatment options for GIST patients that combat this major clinical problem of resistance to targeted therapies (Hopkins *et al.* 2008).

1.4.2.4 Alternative therapeutic strategies for resistant disease

Although research efforts are focussing on the development of a global compound that inhibits the full spectrum of identified BCR/ABL and c-KIT drug-resistant mutants, the issue of new mutations at crucial points that compromise drug binding continues to exist. Preclinical results from ENU-induced mutagenesis screens in BaF3 lymphoid progenitors have uncovered additional BCR/ABL mutations that are resistant to nilotinib and dasatinib (von Bubnoff *et al.* 2006, Bradeen *et al.* 2006). Imatinib-resistant patients are more likely to develop new mutations that confer resistance to second generation inhibitors compared with patients who do not express imatinib-resistant mutations (45% vs 18%, respectively) (Soverini *et al.* 2009). Furthermore, patients who demonstrate treatment failure with two tyrosine kinase inhibitors are unlikely to respond to third line therapy with an alternate second generation compound (Garg *et al.* 2009). This challenge warrants the development of new therapeutics that will decrease the rate of relapse and overcome tyrosine kinase resistance.

The investigation of signalling pathways that are aberrantly regulated by BCR/ABL and mutant c-KIT is required to identify molecular networks that, if appropriately modified, will simultaneously affect the function of these oncogenic tyrosine kinases and their downstream effectors. Recent studies have reported the loss of PP2A phosphatase activity plays a central role in the development of several haematological malignancies including CML and Ph¹ ALL, as well as B-cell chronic lymphocytic leukaemia (B-CLL) (Neviani *et al.* 2005, Liu *et al.* 2008, Neviani *et al.* 2007). Importantly, restoration of PP2A activity significantly impairs the *in vitro* and *in vivo* growth of imatinib-resistant BCR/ABL⁺ myeloid and lymphoid progenitors (Neviani *et al.* 2007). Thus PP2A has emerged as a potential candidate which can be targeted in BCR/ABL-mediated leukaemogenesis. Furthermore, as BCR/ABL and mutant c-KIT activate similar oncogenic pathways, the inhibition of PP2A may also be important for c-KIT-driven cancers.

1.5 Protein Phosphatase 2A (PP2A)

Reversible phosphorylation is one of the most important mechanisms for regulating protein function in eukaryotic cells. Coordination of protein kinases and phosphatases controls the intracellular signalling response to changing physiological demands within the cell, and dysregulation of this process contributes to many disease states. Phosphatases regulate the rate and duration of phosphorylation, thereby providing the fine control on signalling pathways. Although much is known regarding alterations in kinase function, the role of specific phosphatases in cancer remains poorly characterised.

PP2A refers to a large family of heterotrimeric serine/threonine phosphatases that act to dephosphorylate proteins. It makes up 1% of total cellular proteins and along with PP1, accounts for over 90% of serine/threonine phosphatase activity in the cell (Eichhorn *et al.* 2009). The PP2A core enzyme consists of a structural subunit (PP2A A/PR65) and a catalytic subunit (PP2Ac). In mammals, two distinct genes (α and β) encode closely related versions of the A (Hemmings *et al.* 1990) and C subunits (Arino *et al.* 1988). A third regulatory subunit (PP2A B) binds to the AC heterodimer, and determines both the substrate specificity and cellular localisation of PP2A complexes. Three B subunit families have been identified to date: B/B55/PR55 (Strack *et al.* 1999, Zolnierowicz *et al.* 1994, Mayer *et al.* 1991), B'/B56/PR61 (McCright *et al.* 1996, McCright & Virshup 1995), B''/PR72/130/PR70/48 (Yan *et al.* 2000, Stevens *et al.* 2003, Hendrix *et al.* 1993) (Table 1.6 and Figure 1.10A).

The combinatorial assembly of these various A, B and C subunits permits the formation of over 70 distinct PP2A complexes that are involved in the regulation of cellular processes including development, proliferation, apoptosis, adhesion and cytoskeletal dynamics (Janssens & Goris 2001, Sontag 2001, Virshup 2000). In particular, recent work has implicated PP2A in various aspects of malignant transformation, and thus PP2A has emerged as an important tumour suppressor. Understanding how PP2A is regulated, and in turn how this complex enzyme modulates signalling pathways in both normal and BCR/ABL or c-KIT-transformed cells may provide novel targets for improved therapeutic strategies.

Table 1.6 Nomenclature and subcellular distribution of *Homo sapiens* PP2A subunits

Subunit Family	Gene Name	Isoforms	Protein Names	Subcellular localisation	Reference	
Catalytic	PPP2CA	C α	PP2A _{cα}		(Arino <i>et al.</i> 1988)	
	PPP2CB	C β	PP2A _{cβ}			
Structural	PPP2R1A	A α	PP2A A α PR65 α		(Hemmings <i>et al.</i> 1990)	
	PPP2R1B	A β	PP2A A β PR65 β			
Regulatory	PPP2R2A	B55 α	B α PR55 α	Cytoskeleton, cytoplasm, nucleus, plasma membrane, Golgi and endoplasmic reticulum	(Mayer <i>et al.</i> 1991)	
	B55	PPP2R2B	B55 β	B β PR55 β	Enriched in brain, located in cytosol	(Mayer <i>et al.</i> 1991)
		PPP2R2C	B55 γ	B γ PR55 γ	Enriched in brain, mainly cytoskeleton	(Zolnierowicz <i>et al.</i> 1994)
		PPP2R2D	B55 δ	B δ PR55 δ	Cytosol	(Strack <i>et al.</i> 1999)
B56	PPP2R5A	B56 α	B' α PR61 α	Cytoplasm	(McCright & Virshup 1995)	
	PPP2R5B	B56 β	B' β PR61 β	Cytoplasm	(McCright & Virshup 1995)	
	PPP2R5C	B56 γ 1-3	B' γ 1-3 PR61 γ 1-3	Nucleus	(McCright & Virshup 1995)	
	PPP2R5D	B56 δ 1-4	B' δ 1-4 PR61 δ	Nucleus, cytosol, mitochondria, microsome	(McCright <i>et al.</i> 1996)	
	PPP2R5E	B56 ϵ	B' ϵ PR61 ϵ	Cytoplasm	(McCright <i>et al.</i> 1996)	
PR72	PPP2R3A	PR130	B'' α 1	Centrosome and Golgi	(Hendrix <i>et al.</i> 1993)	
		PR72	B'' α 2	Cytosol, nucleus	(Hendrix <i>et al.</i> 1993)	
	PPP2R3B	PR70	B'' β	Unknown	(Stevens <i>et al.</i> 2003)	
		PR48		Nucleus	(Stevens <i>et al.</i> 2003)	
Interacting	PPP2R4	PR53	PTPA		(Janssens <i>et al.</i> 2000)	
	STRN	PR110	Striatin	Post-synaptic densities of neurons	(Moreno <i>et al.</i> 2000)	
	STRN3	PR93	SG2NA	Nucleus	(Moreno <i>et al.</i> 2000)	

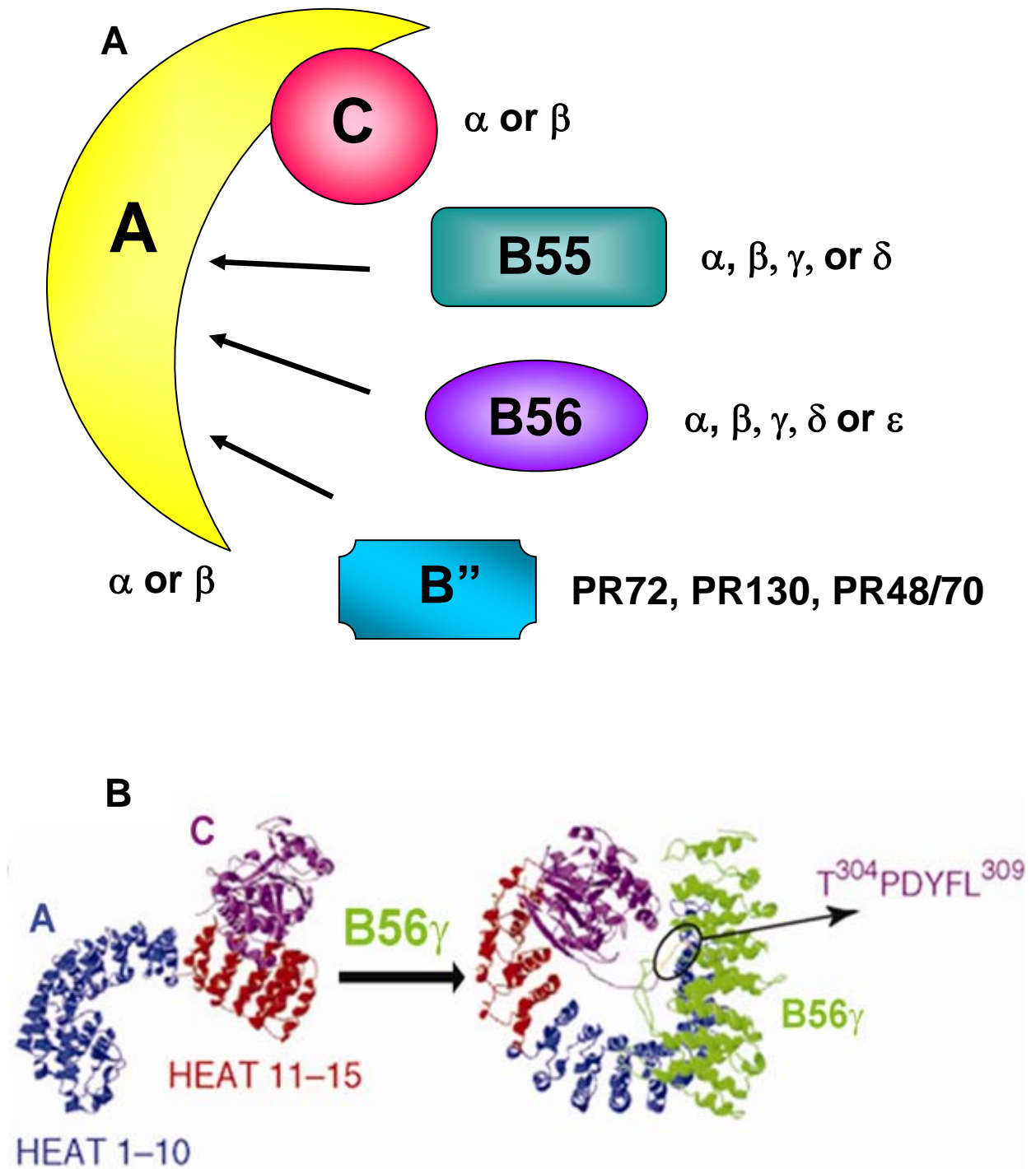


Figure 1.10 Structure of PP2A holoenzymes

A) PP2A is a heterotrimeric complex composed of a structural subunit (A), a catalytic subunit (C) and one of several regulatory subunits (B55, B56, B''), each with specified isoforms. **B)** Ribbon diagrams based on the crystal structure of the PP2A AC dimer and A-C-B56 γ holoenzyme. PP2Ac (purple) binds to HEAT repeats 11-15 of PP2A A (red). The regulatory subunits (B56 γ ; green) associate via HEAT repeats 1-10 of PP2A A (blue). The C-terminal tail of PP2Ac (circled; T³⁰⁴PDYFL³⁰⁹) is subject to post-translational modifications that determine dynamic B subunit interactions and locks the complex into a fully functional enzyme (Janssens et al. 2008).

1.5.1 PP2A subunits

1.5.1.1 The catalytic subunit (PP2Ac)

PP2Ac is a 37 kDa protein encoded by two distinct genes, α and β , with the former being expressed approximately 10 fold higher due to a stronger promoter (Khew-Goodall & Hemmings 1988). The two isoforms share 97% sequence homology and are localised to human chromosome 5q23-31 and 8p12, respectively (Arino et al. 1988). As the catalytically active component of the enzyme, it has a large conserved domain that forms a bimetallic active site for phospho-ester hydrolysis and targets phosphate groups on either serine or threonine residues. Due to the promiscuous nature of PP2A, the consensus motifs required for PP2Ac/substrate interaction are not well characterised (Guergnon *et al.* 2006).

The levels of PP2Ac are tightly regulated in the cell by a potent autoregulatory mechanism that inhibits the efficiency of PP2A translation when there is an abundance of mRNA. This ensures PP2A protein levels remain constant and makes ectopic expression of this protein in cellular models extremely difficult (Baharians & Schonthal 1998). A fundamental role for PP2Ac in development is evidenced by the fact that C α knockout mice are embryonically lethal (Gotz et al. 1998). Although both subunits are highly conserved, they are not redundant, as the expression of C β is unable to rescue this phenotype. C α and C β exhibit similar subunit interaction properties and holoenzyme phosphatase activities *in vitro* (Zhou *et al.* 2003b). Thus, the functional differences may be explained by distinct subcellular patterns of these subunits within the developing embryo. PP2A-C α complexes are found predominantly in the plasma membrane, whilst PP2A-C β holoenzymes localise to the cytoplasm and nucleus (Gotz et al. 1998).

The PP2A holoenzyme crystal structure revealed that the highly conserved C-terminal tail of PP2Ac (residues 304-309; TPDYFL), resides at a critical interface between the scaffolding subunit and regulatory subunits (Figure 1.10B) (Cho & Xu 2007, Xing *et al.* 2006). As such, the recruitment of B subunits to the core enzyme is tightly regulated by post-translational modifications including methylation and phosphorylation (Figure 1.11) (Janssens et al. 2008). Methylation on carboxyl Leu309 is catalysed by the S-adenosylmethionine-dependent leucine carboxyl transferase 1 (LCMT1)

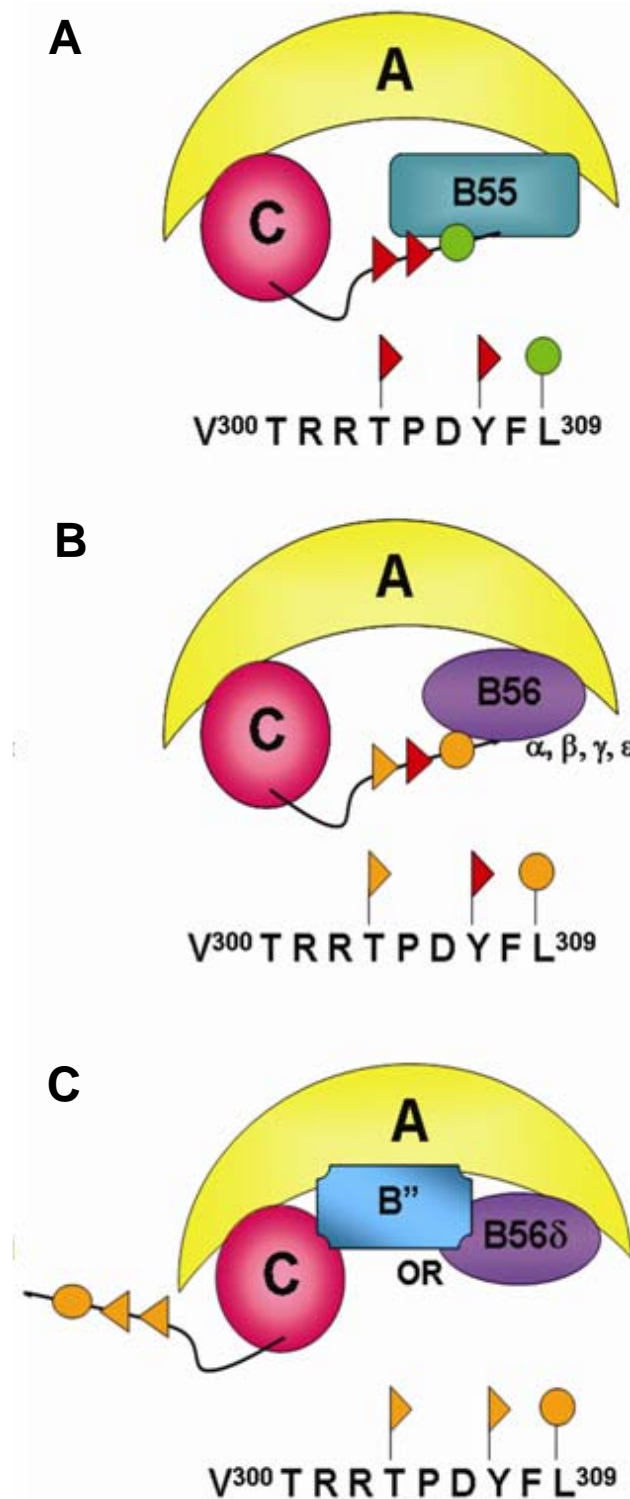


Figure 1.11 Post-translational modifications of PP2Ac

Schematic overview of PP2A regulatory subunits and associated post-translational modifications on the PP2Ac C-terminal tail (T³⁰⁴PDYFL³⁰⁹). Flags; phosphorylation, circles; methylation. Colour coding: red; inhibitory, green; required, orange; no preference. **A)** The B55 subunits strictly require Leu³⁰⁹ methylation, whereas Tyr³⁰⁷ or Thr³⁰⁴ phosphorylation inhibits binding. **B)** For B56 α , β , γ and ϵ subunit binding, methylation is not required and p-Tyr³⁰⁷ is unfavourable for holoenzyme assembly. **C)** B56 δ and B'' binding are not affected by either methylation or phosphorylation.

(Leulliot *et al.* 2004) and is reversed by the specific phosphatase methyltransferase (PME-1) (Ogris *et al.* 1999). RNAi-mediated knockdown of LCMT1 results in the specific degradation of B55 family members, as they can not form stable complexes with unmethylated PP2Ac (Longin *et al.* 2007). Furthermore, deletion of Leu309 or a L309A substitution in PP2Ac abolishes B55 binding, whereas binding of B56 and B'' is not affected (Longin *et al.* 2007, Nunbhakdi-Craig *et al.* 2007).

Another important post-translational modification that regulates PP2A activity is phosphorylation of Tyr307 (Chen *et al.* 1992), or the newly identified Thr304 residue (Longin *et al.* 2007). Specifically, p-Tyr307 inhibits recruitment of the B55 and B56 α , β , ϵ family members to the core enzyme (Chen *et al.* 1994). Mutational studies indicate that phosphorylation of Tyr307 limits the methylation status of Leu309, possibly explaining the defect in B55 binding (Longin *et al.* 2007). Interestingly, p-Tyr307 does not effect B56 δ or B'' holoenzyme assembly (Longin *et al.* 2007). As many tyrosine kinases (e.g. Src) are able to phosphorylate Tyr307, this may temporarily inactivate PP2A and allow signalling cascades to efficiently proceed from receptors through to nuclear effectors (Lechward *et al.* 2001). Although the role of p-Tyr304 is currently unclear, several studies using phospho-mimetic mutants suggest it might be a mechanism for preventing the recruitment of B55 or even facilitate the dissociation of B55 from an existing PP2A trimer (Longin *et al.* 2007).

1.5.1.2 The structural subunit (PP2A A)

The 65 kDa PP2A structural subunit is composed of 15 Huntington/elongation/A subunit/TOR (target of rapamycin) (HEAT) repeats and primarily acts as a scaffolding protein to assemble the individual subunits into one holoenzyme complex (Groves *et al.* 1999). Upon binding of PP2Ac to HEAT repeats 11-15, the protein folds into a horseshoe shape structure. This enables unimpeded access to the PP2A substrate that is recruited by the regulatory subunit (Xu *et al.* 2006, Cho & Xu 2007). Although PP2A A is encoded by two ubiquitously expressed genes, α and β , which share 87% sequence identity (Hemmings *et al.* 1990), a majority of PP2A complexes (~90%) contain the A α isoform (Zhou *et al.* 2003a). While the A α scaffold can interact with all B subunits, A β is unable to interact with the B55 family members and shows a preference for binding to B'' (Zhou *et al.* 2003a). Downregulation of A α by inducible RNAi in

neuronal cells leads to proteasomal degradation of the catalytic and B family regulatory subunits, with a concomitant loss of total PP2A activity that results in apoptotic cell death. This indicates the importance of PP2A A in maintaining mammalian cell viability (Strack *et al.* 2004).

1.5.1.3 The regulatory subunits (PP2A B)

To date, 11 genes have been identified in the human genome which encode at least 24 alternate transcripts and splice forms that constitute the *bona fide* PP2A regulatory subunits. They are subdivided into distinct families, which share no sequence homology, apart from a few conserved amino acids that allow interaction with the N-terminal HEAT domains 1-10 of PP2A A (Li & Virshup 2002). Binding of the B subunit to the core AC dimer directs the enzyme to various intracellular localisations and provides distinct substrate specificity (Janssens *et al.* 2008). It is believed the B subunit provides a docking platform upon which a substrate can bind in the correct orientation such that its serine/threonine residue is positioned within the active site. This prevents access of non-specific substrates and facilitates dephosphorylation by the otherwise promiscuous catalytic subunit (Janssens *et al.* 2008). The exact mechanisms determining this specificity are largely unknown.

1.5.1.3.1 The B55 family

The B55 family of regulatory subunits contains 4 identified members that are transcribed from different genes (α , β , γ , δ) into a 50/55 kDa protein (Mayer *et al.* 1991). They exhibit distinct temporal and spatial expression patterns, with B55 α and B55 δ displaying a widespread tissue distribution, whereas B55 β and B55 γ are highly enriched in the brain (Mayer *et al.* 1991, Strack *et al.* 1999, Zolnierowicz *et al.* 1994). Substrate binding is mediated by a stretch of 5 degenerate WD40 repeats; these are conserved amino acid sequences that end with tryptophan-aspartate (WD) and modulate protein-protein interactions. Loss of the PP2Ac C-terminal tail abolishes both carboxyl methylation (Ogris *et al.* 1997) and phosphorylation, and prevents binding of B55 to the core enzyme (Figure 1.11) (Bryant *et al.* 1999, Longin *et al.* 2007).

1.5.1.3.2 The B56 family

The B56 family consists of at least 9 members represented by 5 alternative genes (α , β , γ , δ , ϵ). They show specific spatial patterns within the cell, with the B56 α , B56 β and B56 ϵ subunits expressed in the cytoplasm, whilst B56 γ is expressed in the nucleus and B56 δ (72 kDa) is found in both (McCright & Virshup 1995, McCright et al. 1996). The PP2A B56 γ locus resides at 14q32.2 and encodes three differentially spliced variants B56 γ 1, B56 γ 2 and B56 γ 3, which share the first 12 exons (Muneer *et al.* 2002). The full-length 61 kDa B56 γ 3 contains all 14 exons, whereas exon 13 is absent in the intermediate 57 kDa B56 γ 2. The B56 γ 1 variant terminates at an alternatively spliced exon 12a, resulting in a smaller protein of 52 kDa. Non-complexed B56 γ consists exclusively of two anti-parallel helices similar to HEAT repeats, although they share no sequence homology (Magnusdottir et al. 2009). It is believed that B56 γ initially interacts with PP2A A, which induces a conformational change in the scaffolding subunit that enables subsequent binding to PP2Ac. This interaction in turn, leads to the formation of a binding pocket for the invariant C-terminus of PP2Ac that functions as a barrel bolt lock for the holoenzyme (Figure 1.10B) (Magnusdottir et al. 2009).

1.5.1.3.3 The B'' family

PR130 (B'' α 1) and PR72 (B'' α 2) are variants of the same gene (PPP3R3A) transcribed from different promoters (Hendrix et al. 1993). The difference in size arises from PR130 containing a specific stretch of 665 amino acids at the N-terminus that is functionally replaced by 44 amino acids in PR72. This results in specific subcellular distribution where PR130 is associated with the centrosome and golgi apparatus, whilst PR72 is found more generally within the cytosol and nucleus. PR72 contains two EF-hand domains that bind calcium and induce a conformational change that is required for binding to the PP2A AC core dimer (Janssens *et al.* 2003). A third member of the B'' family, PR70 (B'' β ; PPP2R3B) has recently been shown to interact with the tumour suppressor retinoblastoma and mediate its dephosphorylation (Magenta *et al.* 2008). The final member of the B'' family, PR48, is a truncated form of PR70 that localises to the nucleus in mammalian cells (Yan et al. 2000, Stevens et al. 2003).

1.5.1.4 PP2Ac interacting proteins

In addition to the regulatory subunits, several PP2Ac interacting proteins have been identified. The phosphotyrosol phosphatase activator of PP2A (PTPA/PR53; PPP2R4) binds to PP2A A and exerts ATP-Mg²⁺-stimulated peptidyl prolyl *cis/trans* isomerase activity that targets Pro190 of PP2Ac, which is essential for enzyme activation (Longin *et al.* 2004, Jordens *et al.* 2006, Leulliot *et al.* 2006). Striatin (PR110; STRN) and S/G(2) nuclear autoantigen (SG2NA/PR93; STRN3) are calmodulin-binding proteins that modulate PP2A by localising the AC dimer with components of Ca²⁺ dependent signalling pathways (Moreno *et al.* 2000, Goris & Merlevede 1988).

A distinct population (5-10%) of PP2Ac associates directly with the $\alpha 4$ protein (Inui *et al.* 1998, Murata *et al.* 1997, Chen *et al.* 1998), which results in enhanced PP2A activity and altered substrate specificity (Inui *et al.* 1998). The distinguishing feature of $\alpha 4$ is that it displaces both the structural and regulatory subunits (Murata *et al.* 1997, Prickett & Brautigan 2004). Based on these observations, it is believed that $\alpha 4$ acts as a scaffolding protein, where the interaction of PP2Ac at its N-terminal helical domain promotes the dephosphorylation of PP2A substrates recruited to the C-terminal region (Kong *et al.* 2004). Because $\alpha 4^{-/-}$ mice are embryonically lethal, to determine the role of $\alpha 4$ in cell survival, Kong *et al.*, examined the phenotype of immortalised mouse embryonic fibroblasts from these mice compared to $\alpha 4^{+/+}$ littermates (Kong *et al.* 2004). Subsequent studies revealed that $\alpha 4$ functions as an essential inhibitor of apoptosis via its ability to promote the dephosphorylation and hence destabilisation of the transcription factors, p53 and c-Jun (Kong *et al.* 2004).

1.5.2 Signalling pathways regulated by PP2A

In contrast to the plethora of kinases that activate signalling pathways, there exist a limited number of serine/threonine phosphatase catalytic subunits. Since PP2A is one of the most abundant cellular phosphatases, it is reasonable to expect that PP2A may exert phosphatase function on similar pathways at different levels. Recent work investigating the diverse function of PP2A indicates substrate specificity is mediated by distinct PP2A complexes.

1.5.2.1 PP2A and MAPK signalling

A major function of PP2A is regulation of the Ras-Raf-1-MEK1/2-ERK1/2 signalling pathway. Interestingly, PP2A can exert both inhibitory and activating effects in a context-dependent manner (Figure 1.12). For example, knockdown of the single *Drosophila melanogaster* B family subunit results in ERK1/2 activation (Silverstein *et al.* 2002), whereas the *Caenorhabditis elegans* B55 α homolog (SUR-6) has been identified as a positive regulator of Raf-1 and MPK-1 (ERK homolog) (Kao *et al.* 2004). PP2A negatively regulates the MAPK pathway via the dephosphorylation of MEK (Heriche *et al.* 1997, Sontag *et al.* 1993) and ERK both *in vitro* and in mammalian cells (Alessi *et al.* 1995, Wang *et al.* 2003, Zhou *et al.* 2002). Specific knockdown of B56 β and B56 γ , but not B55 family subunits in NIH3T3 mouse fibroblasts increases basal ERK activation and prolongs ERK signal during stimulation in the absence of pMEK (Figure 1.12A) (Letourneux *et al.* 2006).

More recent evidence indicates that PP2A activates Ras-dependent MAPK signalling at the level of Raf-1 and its scaffolding protein Kinase Suppressor of Ras-1 (KSR1) (Abraham *et al.* 2000, Ory *et al.* 2003, Jaumot & Hancock 2001, Kubicek *et al.* 2002). Dephosphorylation of KSR1 (Ser329) and Raf-1 (Ser259) by B55 α -containing PP2A complexes induces membrane translocation and increases the kinase activity of both proteins in several mammalian cell models, including NIH3T3, COS and HEK293 cells (Figure 1.12B) (Abraham *et al.* 2000, Ory *et al.* 2003, Adams *et al.* 2005, Dougherty *et al.* 2005). Taken together, these studies provide biochemical mechanisms for how PP2A functions as a negative and positive regulator of MAPK signalling, depending on the specific regulatory subunit and substrate involved.

1.5.2.2 PP2A and PI3K/Akt signalling

The normal function of Akt is tightly modulated by phosphorylation events on Thr308 or Ser473 (Vanhaesebroeck & Alessi 2000, Sarbassov *et al.* 2005), and PP2A is the major phosphatase targeting these residues *in vitro* (Borgatti *et al.* 2003, Ivaska *et al.* 2002, Resjo *et al.* 2002). Over-expression of B55 α -containing PP2A holoenzymes in the pro-lymphoid FL5.12 cell line substantially dephosphorylates Akt at Thr308 and results in subsequent growth suppression (Kuo *et al.* 2008). Conversely, A α downregulation impairs Akt phosphorylation in neuronal cells, implicating PP2A as a positive regulator of the PI3K/Akt survival signalling cascade (Strack *et al.* 2004). An intriguing study by

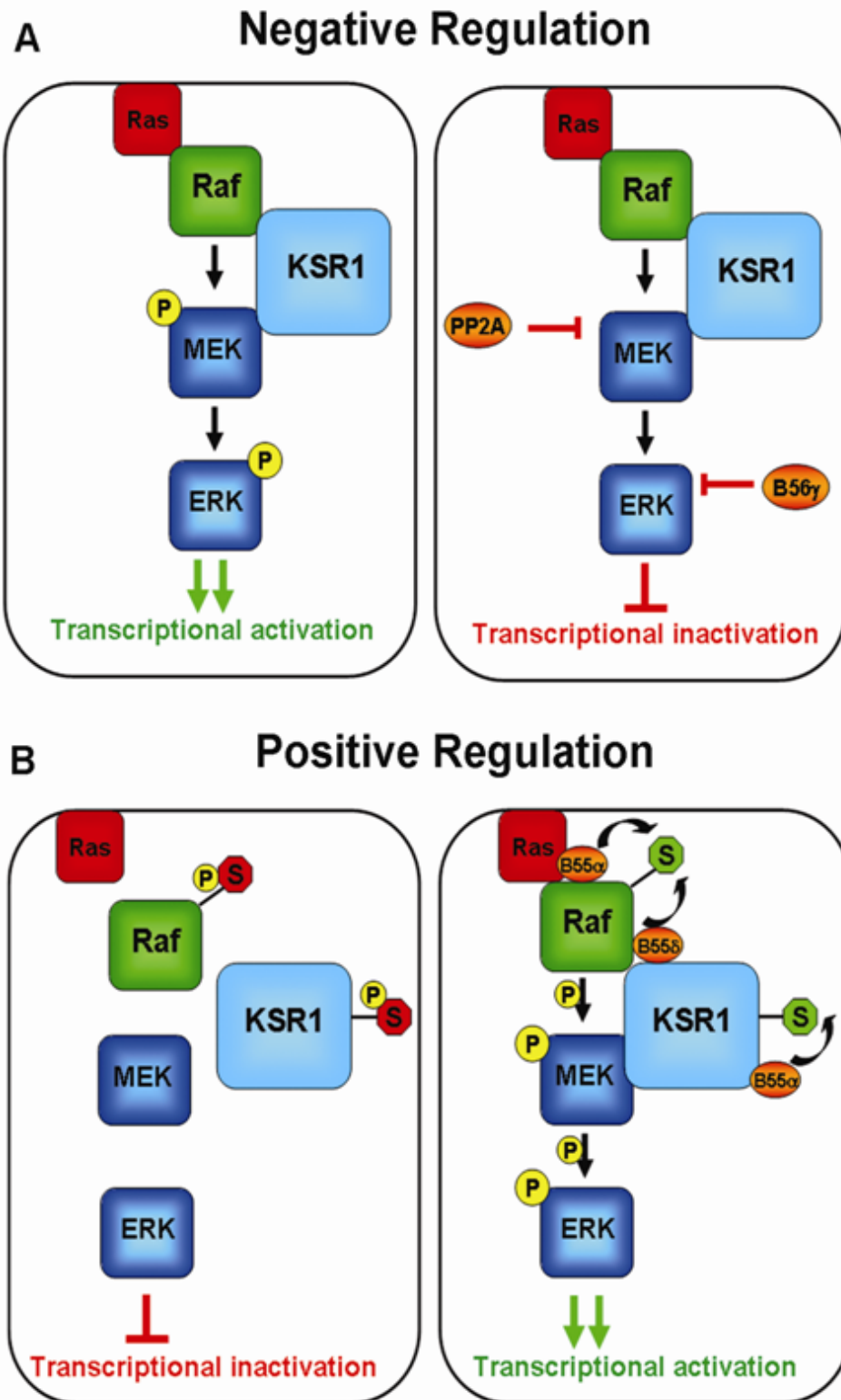


Figure 1.12 Schematic overview of MAPK signalling regulation by PP2A

A) PP2A holoenzymes containing B56 family members negatively regulate MAPK signalling by inactivating MEK and ERK. **B)** In the inactive state, Raf and KSR1 are phosphorylated on Ser259 and Ser329, respectively, and are located within the cytoplasm. Upon stimulation, B55 α -containing PP2A complexes dephosphorylate these residues, which results in protein activation and translocation to the plasma membrane. This facilitates the Ras/Raf interaction and induces transcriptional activation.

Andrabi *et al.*, demonstrated that Akt can act as a pro- or anti-apoptotic protein depending on environmental stimuli, and this is governed by PP2A (Andrabi *et al.* 2007). The specific PP2A regulatory subunits controlling this apparent switch remain undefined; however, this study reinforces the importance of understanding PP2A regulated cell signalling in a context dependent manner.

1.5.2.3 PP2A and Wnt/ β -catenin signalling

The function of PP2A in Wnt/ β -catenin signalling is similar to its role in the MAPK pathway, with individual PP2A subunits exerting either **positive** or negative effects (Figure 1.13). B56 family members associate with APC (Seeling *et al.* 1999, Yamamoto *et al.* 2001) and axin (Li *et al.* 2001, Hsu *et al.* 1999) to impair Wnt signalling; a function that is critical for normal dorsal/ventral axis formation in *Xenopus* development (Li *et al.* 2001). Further studies demonstrate that association of the PP2A PR72 subunit with Naked cuticle is critical for the inhibitory function of this protein on the Wnt pathway (Figure 1.13A) (Creyghton *et al.* 2005).

PP2A is also an important positive regulator of Wnt signalling (Bajpai *et al.* 2004, Gotz *et al.* 2000, Ratcliffe *et al.* 2000, Willert *et al.* 1999). Loss of function analysis suggests that B56 ϵ is required for Wnt-mediated development in *Xenopus* embryogenesis (Yang *et al.* 2003). Purified B55 α -containing PP2A holoenzymes directly dephosphorylate β -catenin *in vitro*. Accordingly, specific knockdown of B55 α in SW480 colon cancer cells significantly elevates β -catenin phosphorylation, which induces protein degradation and inhibits the Wnt pathway (Zhang *et al.* 2009). Surprisingly, PR130 opposes the action of PR72 and modulates Wnt signal transduction by restricting the ability of Naked to function as a Wnt inhibitor (Figure 1.13B) (Creyghton *et al.* 2006). The identification of PR130 as a positive modulator of the Wnt cascade adds another level of complexity to this pathway. It illustrates an excellent example whereby specific PP2A regulatory subunits determine holoenzyme function and provide the fine control on important cellular processes.

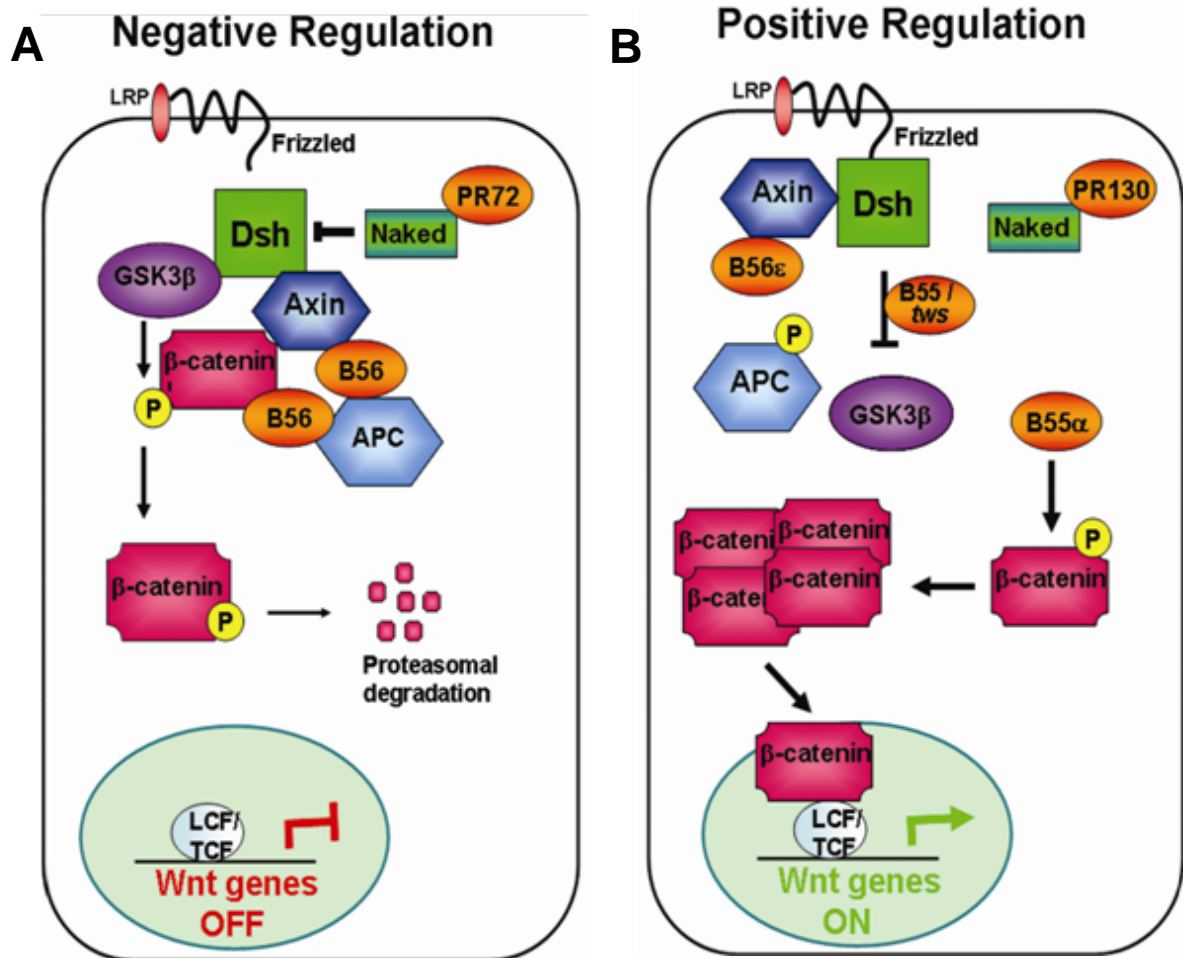


Figure 1.13 Schematic overview of Wnt regulation by PP2A

A) In the absence of Wnt signal β -catenin is complexed with axin, APC and GSK-3 β in the destruction complex. GSK-3 β phosphorylates β -catenin, which undergoes ubiquitination and is targeted for proteasome degradation. The PP2A B56 subunits interact with axin and APC to result in decreased levels of β -catenin. PR72 is required for the inhibitory function of Naked. **B)** Upon Wnt binding, the destruction complex is degraded. Dishevelled (Dsh) antagonises GSK-3 β through B55-containing PP2A complexes and B56 ϵ interacts with axin at the plasma membrane. In addition, PP2A B55 α directly dephosphorylates β -catenin and PR130 restricts the ability of Naked to function as a Wnt inhibitor. Consequently, β -catenin accumulates and translocates to the nucleus where it engages with LCF/TCF factors to induce transcription of numerous target genes.

1.5.2.4 PP2A and p53 regulation

The tumour suppressor, p53, plays a critical role in mediating cellular responses to various types of stress, such as DNA damage, by inducing growth arrest or programmed cell death. The stability and activity of p53 is regulated by phosphorylation which, under normal cellular growth conditions, targets the protein for proteasome-mediated degradation (Vogelstein *et al.* 2000). **PP2A B56 γ holoenzymes dephosphorylate p53 on Ser37 (Dohoney *et al.* 2004) and Thr55 (Li *et al.* 2007) following γ radiation;** an event which stabilises p53 in response to DNA damage and contributes to apoptosis in mammalian cells (Figure 1.14A). Conversely, RNAi knockdown of B56 γ reduces p53 stability and inhibits cell death (Li *et al.* 2007).

Other findings implicate an important role for B56 α -containing PP2A complexes in p53 degradation (Figure 1.14B). One target of p53, cyclin G, recruits B56 α into a quarternary complex with the E3 ubiquitin ligase, mouse double minute 2 (Mdm2) (Okamoto *et al.* 2002, Okamoto *et al.* 1996). The subsequent dephosphorylation and activation of Mdm2 leads to ubiquitination and degradation of p53 (Haupt *et al.* 1997), thus allowing the cell to proliferate. In this context, PP2A serves as a negative regulator.

1.5.2.5 PP2A and c-Myc regulation

PP2A also plays a prominent role in controlling the accumulation of the proto-oncoprotein, c-Myc (Yeh *et al.* 2004). Aberrant regulation of c-Myc has been linked to transformation in up to 70% of human tumours; therefore tight control of this protein is crucial for maintaining cellular homeostasis (Nesbit *et al.* 1999). c-Myc stability is regulated, in part, through phosphorylation at two residues, Ser62 and Thr58 (Sears *et al.* 2000). Whilst ERK-mediated phosphorylation at Ser62 stabilises c-Myc, specific B56 α -containing PP2A complexes reverse these effects, leading to destabilisation and ubiquitin-mediated degradation (Arnold & Sears 2006).

Collectively, these results illustrate the dynamic interaction of the PP2A holoenzyme with signalling cascades involved in fundamental cellular processes such as proliferation, survival and development. The fact that PP2A is involved in both the negative and positive regulation of these pathways highlights the exquisite nature of

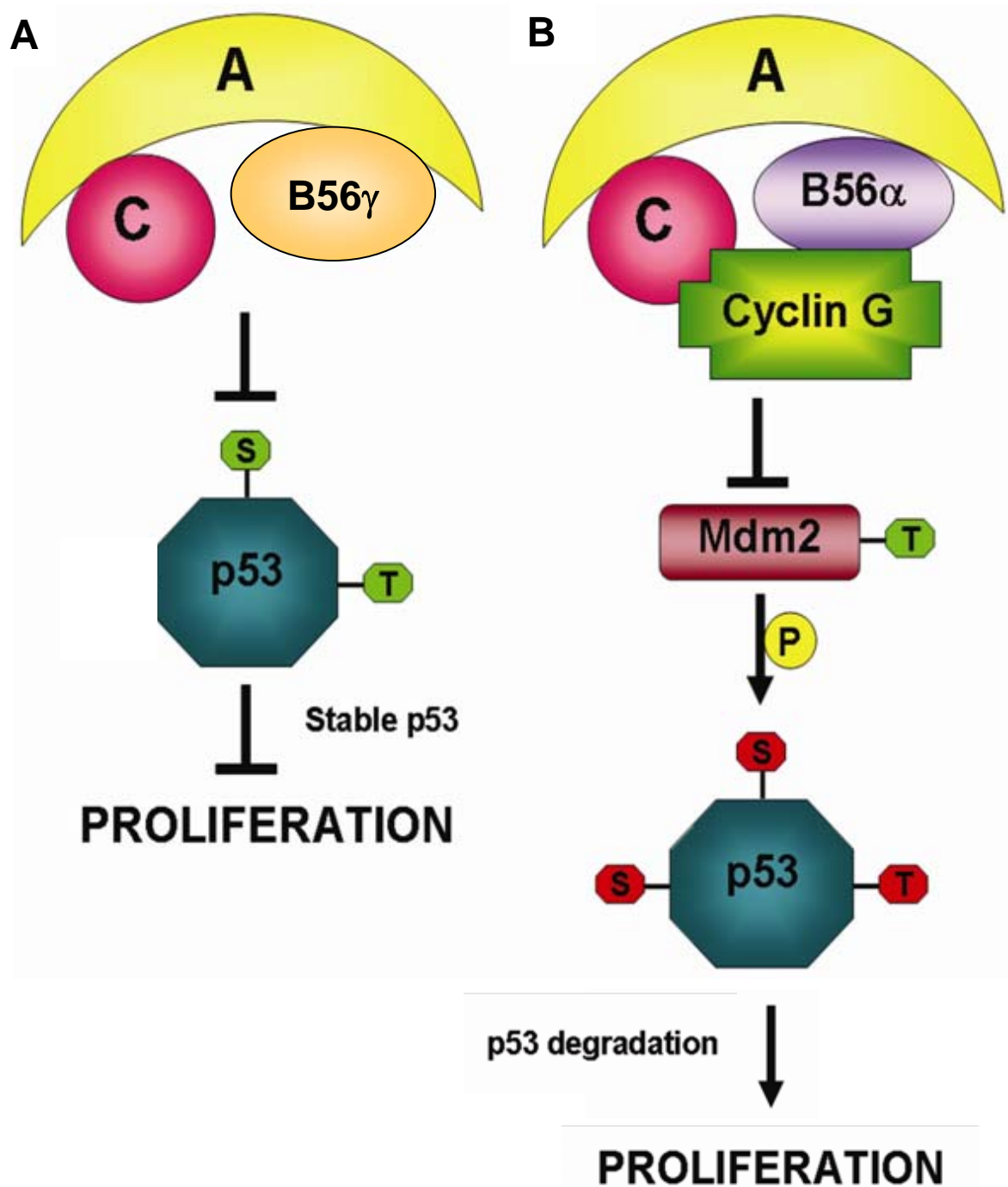


Figure 1.14 Schematic overview of p53 regulation by PP2A

A) PP2A-B56 γ complexes dephosphorylate Ser37 and Thr55 residues of p53 (green circles), which stabilises the protein and inhibits proliferation. **B)** The PP2A B56 α holoenzyme is recruited by cyclin G to dephosphorylate Mdm2 at Thr216 (green circle). The activation of Mdm2 results in p53 phosphorylation (red circles), which targets it for ubiquitination and degradation. The cell then continues to proliferate.

PP2A modulation and underscores the importance of investigating specific complexes when determining PP2A function. Furthermore, as PP2A regulation differs between species and even cell-types, one must take into account the specific model when characterising the individual role of these subunits. Elucidating the importance of these components in normal signalling will aid in the identification of critical subunits that are aberrantly regulated during transformation, and may ultimately lead to the development of novel treatments for cancer patients.

1.5.3 PP2A as a tumour suppressor

1.5.3.1 Okadaic acid and SV40 ST

The fundamental evidence that implicated PP2A as a tumour suppressor was the discovery that okadaic acid, a tumour promoter (Fujiki & Suganuma 2009, Suganuma *et al.* 1988), potently inhibits the phosphatase activity of PP2A (Bialojan & Takai 1988, Haystead *et al.* 1989). In addition, the oncogenic polyomavirus middle and small tumour (ST) antigens, along with the simian virus 40 (SV40) ST antigen, transforms mammalian cells by inhibiting PP2A (Pallas *et al.* 1990). A very elegant experimental model established by Hahn *et al.*, demonstrated that transformation of the normal human fibroblast kidney epithelial cell line, HEK293, required several key genetic elements; human telomerase catalytic subunit, an oncogenic allele of H-Ras, and the SV40 large T (LT) and ST antigens (HEK-TER) (Hahn *et al.* 1999). Whilst expression of LT enables the cells to bypass senescence by simultaneously disabling the retinoblastoma and p53 pathways, complete tumour formation requires the addition of ST and thus inhibition of PP2A (Yu *et al.* 2001). Accordingly, ST mutants lacking the PP2A binding domain fail to induce tumourigenic transformation of HEK-TER cells (Hahn *et al.* 2002). Structural insights reveal that ST interacts with HEAT repeats 3-7 of A α , which overlaps the binding site for the B56 subunit and results in its displacement from the core enzyme. In addition, the first zinc-binding motif of ST interacts directly with PP2Ac (Cho *et al.* 2007, Chen *et al.* 2007) to reduce its phosphatase activity towards downstream substrates (Rodriguez-Viciano *et al.* 2006). Functionally, expression of ST activates Akt signalling in immortalised human keratinocytes (Yuan *et al.* 2002, Rodriguez-Viciano *et al.* 2006) and mammary epithelial cells (Zhao *et al.* 2003). Taken together, these observations indicate that complete transformation of human cells requires the perturbation of PP2A, for example by ST.

1.5.3.2 Inhibition of PP2A by BCR/ABL

Functional inactivation of PP2A by BCR/ABL is essential for the development of CML-BC and Ph¹ ALL, and is thought to result from upregulation of the SET (I₂PP2A or TAF-1 β) protein in CD34⁺ BC progenitors and CD34⁺CD19⁺ Ph¹ ALL samples (Neviani et al. 2005, Neviani et al. 2007). SET is an established endogenous inhibitor of PP2A (Li *et al.* 1995), and although its physiological function remains incompletely understood, abnormal expression of SET mRNA has been documented in solid tumours and haematological disorders (Carlson *et al.* 1998, Fornerod *et al.* 1995, Li *et al.* 1996). Notably, SET was described as part of a fusion gene with the nucleopore complex protein CAN in a patient with t(6;9)(p23;q34) AML (Adachi *et al.* 1994, von Lindern *et al.* 1992), and it associates with the oncoprotein MLL in leukaemic cell lines (Adler *et al.* 1997). Forced expression of BCR/ABL in 32Dcl3 (32D) mouse myeloid precursor cells stimulates SET expression and correlates with a loss of PP2A activity (Neviani *et al.* 2005). Conversely, inhibition of BCR/ABL with imatinib treatment dramatically reduces SET expression, which results in the restoration of PP2A activity back to untransfected levels. Interestingly, BCR/ABL-induced overexpression of SET enhances its stability, as knockdown of SET leads to BCR/ABL proteolytic degradation (Neviani *et al.* 2005). Reactivation of PP2A by SET depletion, overexpression of PP2Ac or inhibition of BCR/ABL with imatinib, results in the dephosphorylation of several substrates which are shared by BCR/ABL and PP2A (Neviani et al. 2005). These include STAT5, ERK1/2, Akt, BAD and JAK2 (Calabretta & Perrotti 2004, Janssens & Goris 2001). A reduction in the stability and protein expression of c-Myc is also observed (Neviani et al. 2005). Importantly, restoration of PP2A activity reduces proliferation, impairs clonogenic potential, induces apoptosis and restores differentiation of patient derived CML-BC progenitors and imatinib-resistant BCR/ABL⁺ cell lines. Taken together, these results suggest that SET-dependent inhibition of PP2A is required for the transduction of aberrant mitogenic, survival and anti-differentiation signals that contribute to the development of CML from the chronic phase into blast crisis (Figure 1.15) (Neviani et al. 2005).

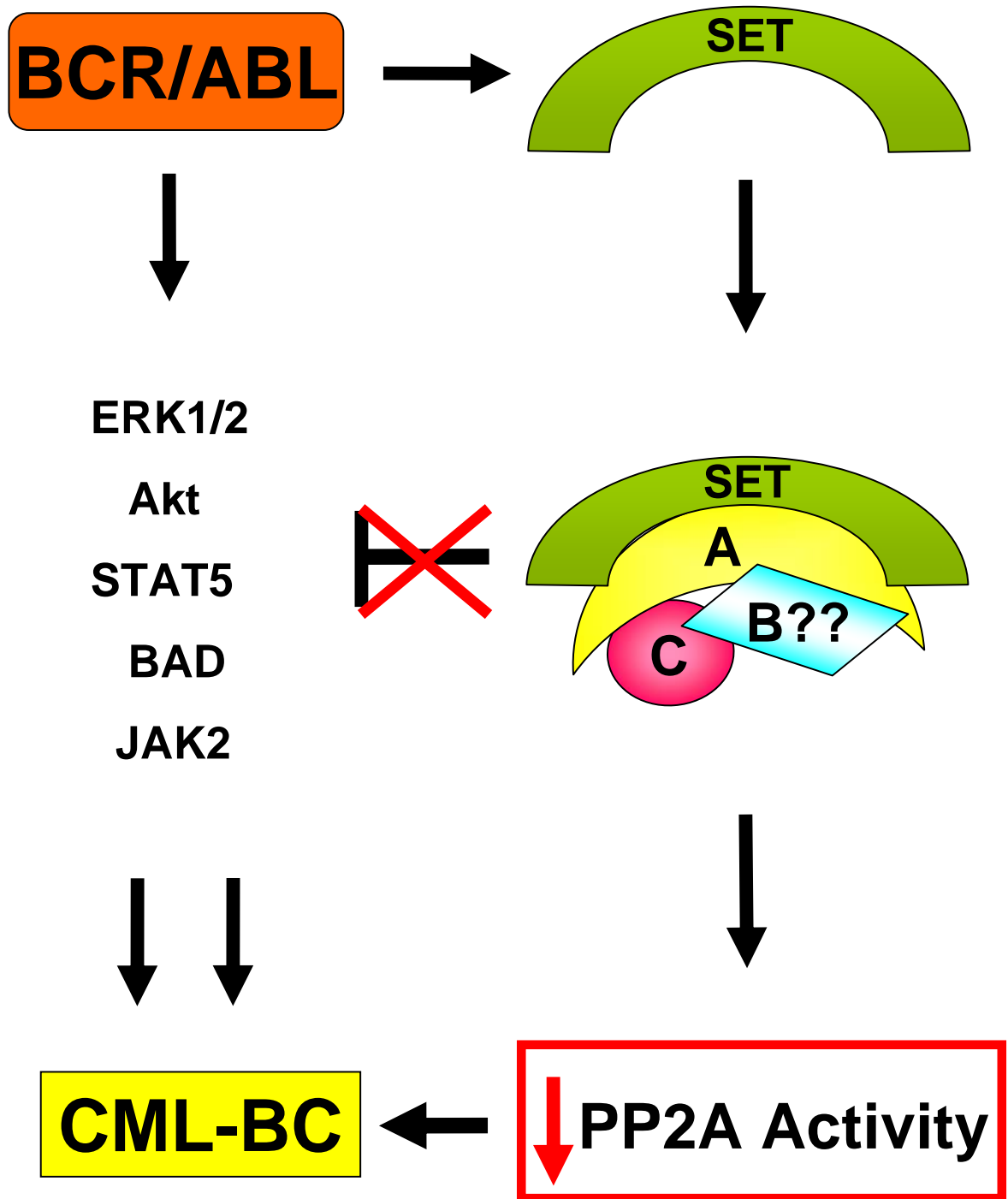


Figure 1.15 BCR/ABL-induced inhibition of PP2A in CML

A) The oncogenic tyrosine kinase BCR/ABL stimulates downstream signalling pathways (e.g. ERK1/2 and Akt) that induce transformation. Increased BCR/ABL activity also upregulates the endogenous PP2A inhibitor, SET, which inactivates PP2A via an unknown mechanism to result in increased signalling through downstream pathways.

1.5.3.3 Role of PP2A regulatory subunits in transformation

A somewhat confusing aspect of PP2A function in cancer arises because PP2A plays important roles in promoting cell cycle progression and cell survival (Li *et al.* 2002, Lin *et al.* 1998, Mayer-Jaekel *et al.* 1993), which are functions usually associated with tumour initiation and progression rather than suppression. Therefore, cellular transformation will most likely occur through the disruption of PP2A holoenzymes that normally exert negative regulation on oncogenic pathways.

Pivotal studies using the HEK-TER transformation model demonstrated that suppression of B56 γ , but not B55 α , [functionally mimicked the introduction of ST and resulted in partial tumourigenic transformation](#) (Chen *et al.* 2004b, Moreno *et al.* 2004). Moreover, depletion of B56 γ containing complexes leads to activation of the anti-apoptotic Akt pathway (Chen *et al.* 2005). These observations were the first to demonstrate that PP2A complexes containing B56 γ modulate the phosphorylation of substrates associated with transformation. In addition, expression of a dominant negative truncated protein, Δ B56 γ 1, contributes to the enhanced cellular motility and metastatic potential of the mouse melanoma cell line, BL6 (Ito *et al.* 2000, Ito *et al.* 2003, Koma *et al.* 2004).

Despite these observations, it remains unclear whether loss of B56 γ occurs in human cancers. While one group reported higher expression levels of B56 γ mRNA in human melanoma cell lines compared to normal melanocytes (Francia *et al.* 1999), a second group observed decreased expression in primary human melanoma samples compared to melanocytic nevi (Deichmann *et al.* 2001). In support of the latter observation, a number of lung cancer cell lines lack B56 γ , and overexpression partially reverses the tumourigenic phenotype (Chen *et al.* 2004b). Furthermore, reduced transcript levels of B56 γ have been documented in patients with aggressive B-CLL compared to those with stable disease (Falt *et al.* 2005). While these findings suggest that loss of B56 γ contributes to cancer development, further work is necessary to determine whether it is a *bona fide* tumour suppressor gene.

It is well established that PP2A complexes containing B56 α induce the destabilisation and ubiquitin-mediated degradation of c-Myc (Figure 1.16) (Arnold & Sears 2006). More recently, a novel PP2A-interacting protein displaying c-Myc stabilisation activity in human transformed fibrosarcoma cells was identified through an affinity purification approach (Junttila *et al.* 2007). This 90 kDa protein, designated cancerous inhibitor of PP2A (CIP2A), selectively targets the catalytic activity of PP2A-B56 α associated with c-Myc, and protects c-Myc from Ser62 dephosphorylation. Accordingly, depletion of CIP2A results in significantly increased PP2A activity measured from c-Myc immunoprecipitates and correlates with c-Myc destabilisation (Figure 1.16) (Junttila *et al.* 2007). Consistent with these experiments, overexpression of CIP2A in the HEK-TER model can replace ST in inducing transformation (Junttila *et al.* 2007), and increased CIP2A has been detected in gastric and colon cancer samples (Soo Hoo *et al.* 2002, Li *et al.* 2008, Khanna *et al.* 2009).

1.5.3.4 Role of PP2A structural subunits in transformation

Whilst some contradiction exists as to the importance of PP2A scaffolding subunits in cancer development (Marsh *et al.* 2006, Yeh *et al.* 2007), several mutations have been identified in spontaneously arising human cancers. Notably, somatic alterations of the gene encoding A β (PPP2R1B) have been detected in up to 8-15% of colon, 15% of lung and 13% of breast cancers (Calin *et al.* 2000, Takagi *et al.* 2000, Tamaki *et al.* 2004, Wang *et al.* 1998). Mutations of the more abundant A α subunit have been observed, albeit at a lower frequency (Calin *et al.* 2000). Biochemical investigations confirm that cancer-associated A α and A β mutants exhibit differential defects in binding to the B and C subunits, which correlates with impaired PP2A activity (Chen *et al.* 2005, Ruediger *et al.* 2001a, Ruediger *et al.* 2001b, Sablina *et al.* 2007).

Analyses of tumour samples show that PP2A A α mutations generally involve only one allele. Although overexpression of cancer-derived A α mutants fails to induce cell transformation in the HEK-TER model, reduction of WT PP2A A α by ~50% confers a tumourigenic phenotype (Chen *et al.* 2005). Rescue of expression with RNAi-resistant WT PP2A A α reverses cell transformation, whereas introduction of PP2A A α cancer mutants does not (Chen *et al.* 2005). These observations suggest that A α mutations contribute to human cell transformation by creating a state of haploinsufficiency. Thus,

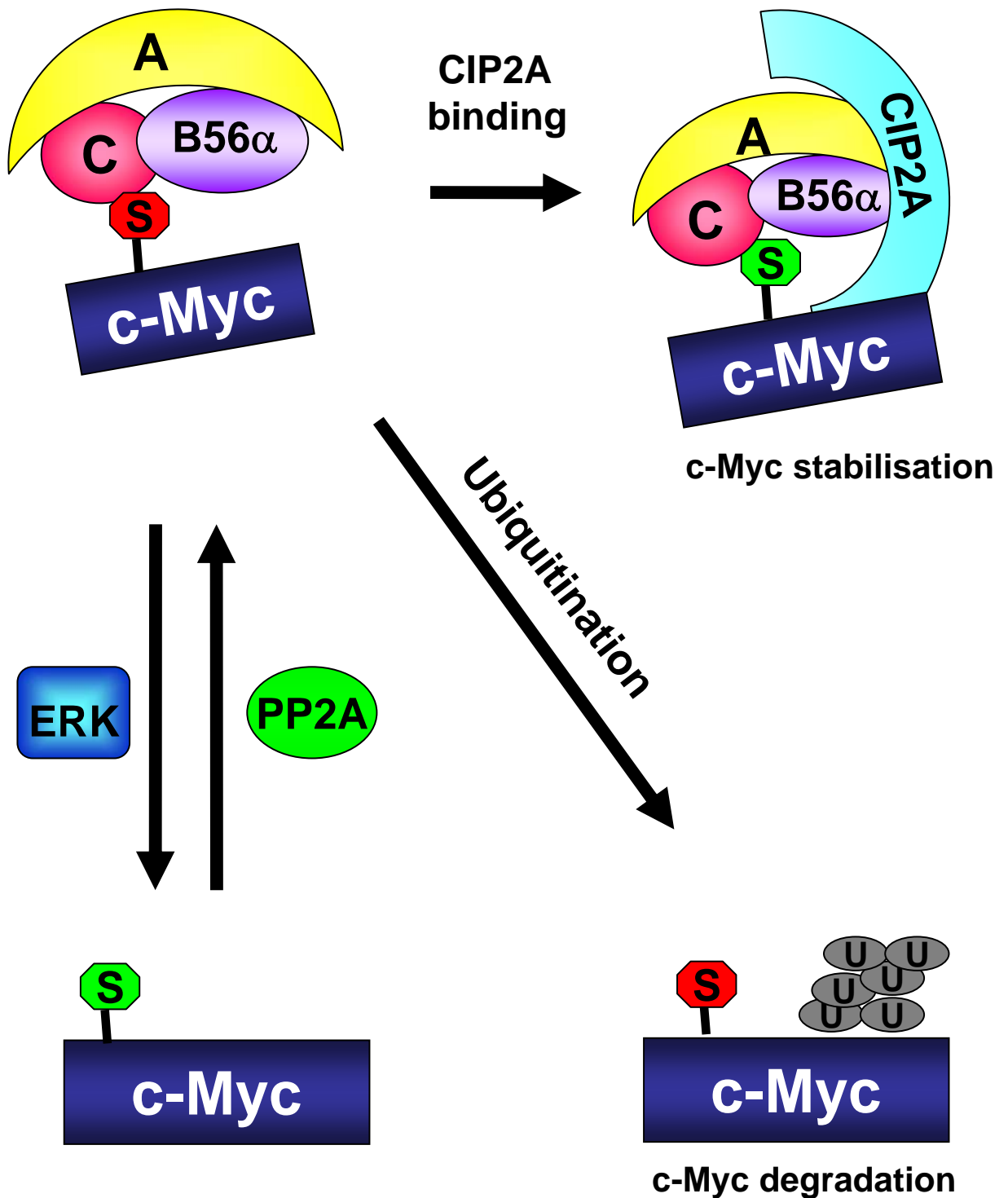


Figure 1.16 Regulation of c-Myc by PP2A and CIP2A

A) The oncogenic c-Myc protein is phosphorylated on Ser62 by ERK (green) and dephosphorylated by PP2A B56α (red). CIP2A directly interacts with c-Myc and inhibits PP2A-mediated Ser62 dephosphorylation to result in c-Myc stabilisation (green). In the absence of CIP2A, c-Myc becomes ubiquitinated (red) and is targeted for proteolytic degradation

a mutation in one A α allele effectively decreases by half the amount of A α available for B subunit binding (Figure 1.17). At present, the signalling molecules affected by these changes are not fully defined, although preliminary studies reveal the PI3K/Akt and Wnt pathways, along with p53, are potential candidates (Westermarck & Hahn 2008).

Somatic alterations of PP2A A β are commonly accompanied by deletion or mutation of the second allele, implicating A β as a *bona fide* tumour suppressor gene (Sablina et al. 2007). Functionally, suppression of A β induces transformation of HEK-TER cells, and the introduction of WT PP2A A β into lung carcinoma cells expressing biallelic A β mutations partially reverses the tumourigenic phenotype (Sablina et al. 2007). Recent work has shown that A β -containing PP2A complexes dephosphorylate and downregulate the activity of the small GTPase RalA (Figure 1.18). Accordingly, lung cancer cell lines that harbour inactivating mutations of A β exhibit constitutive RalA phosphorylation (Sablina et al. 2007).

Even in the absence of mutations, reduced protein expression of A α has been found in 25 out of 58 brain tumours (Colella *et al.* 2001). Decreased levels of A β have also been observed in 16 of 32 cancer cell lines derived from human lung, colon and breast cancer, as well as primary glioblastoma and B-CLL patient samples compared to normal tissue (Zhou et al. 2003a, Takagi et al. 2000, Suzuki & Takahashi 2003, Kalla et al. 2007).

While it is becoming increasingly clear that PP2A exerts its tumour suppressive function via a distinct subset of regulatory subunits, no study to date has investigated which PP2A subunits are altered in myeloid blast crisis. To significantly improve our understanding of PP2A function in BCR/ABL-induced leukaemogenesis, it is important to identify the role of specific PP2A holoenzymes in transformation. This will highlight potential downstream substrates and aberrant protein interactions that may provide new targets to develop improved therapies for CML patients.

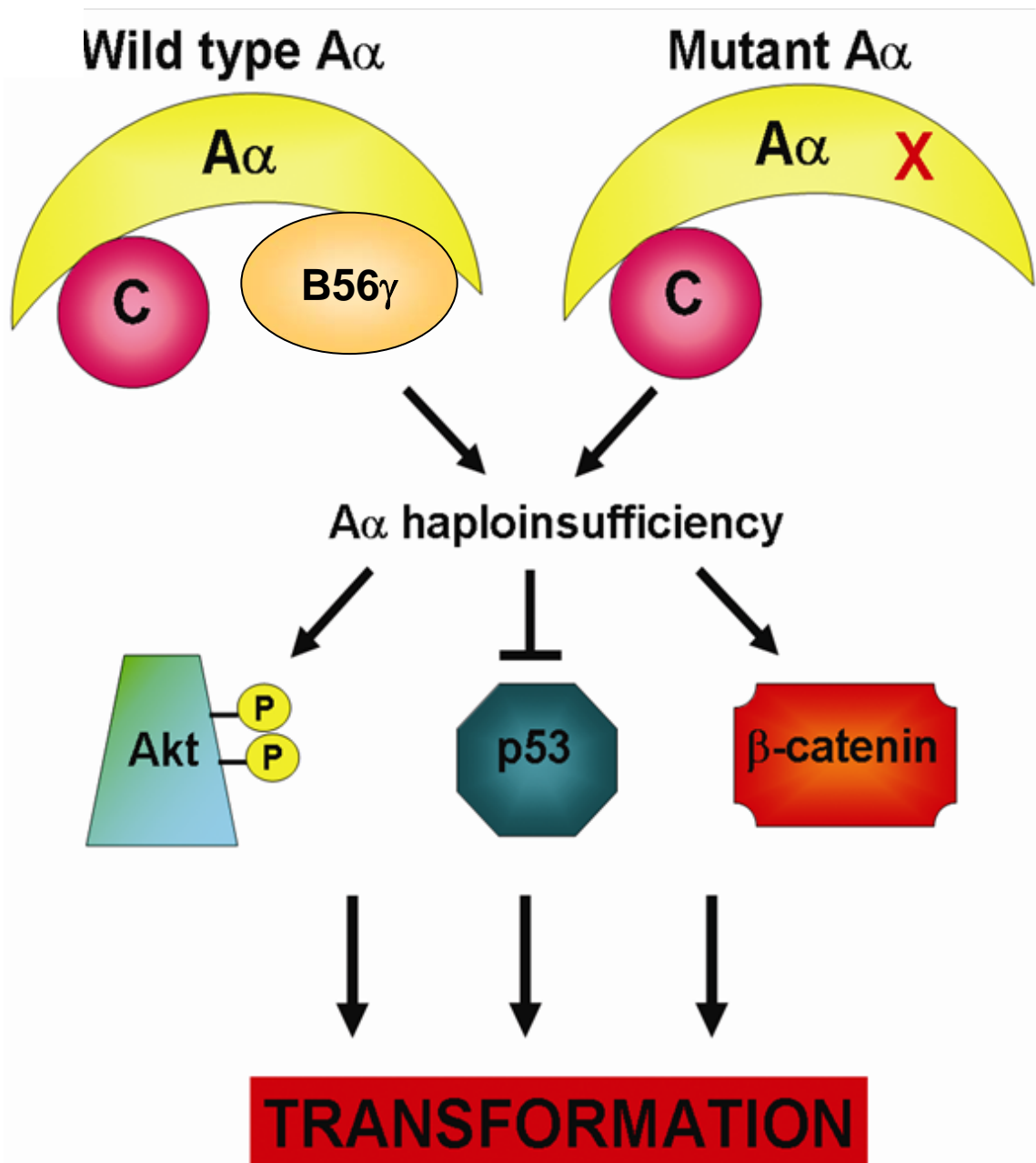


Figure 1.17 Mechanisms by which mutant PP2A Aα may induce transformation
 Cancer-associated PP2A Aα mutations (X) result in Aα haploinsufficiency, which may induce human cell transformation by selectively eliminating PP2A B56γ containing complexes. Loss of B56γ-containing complexes has been linked to constitutive AKT phosphorylation, accumulation of β-catenin, and p53 degradation.

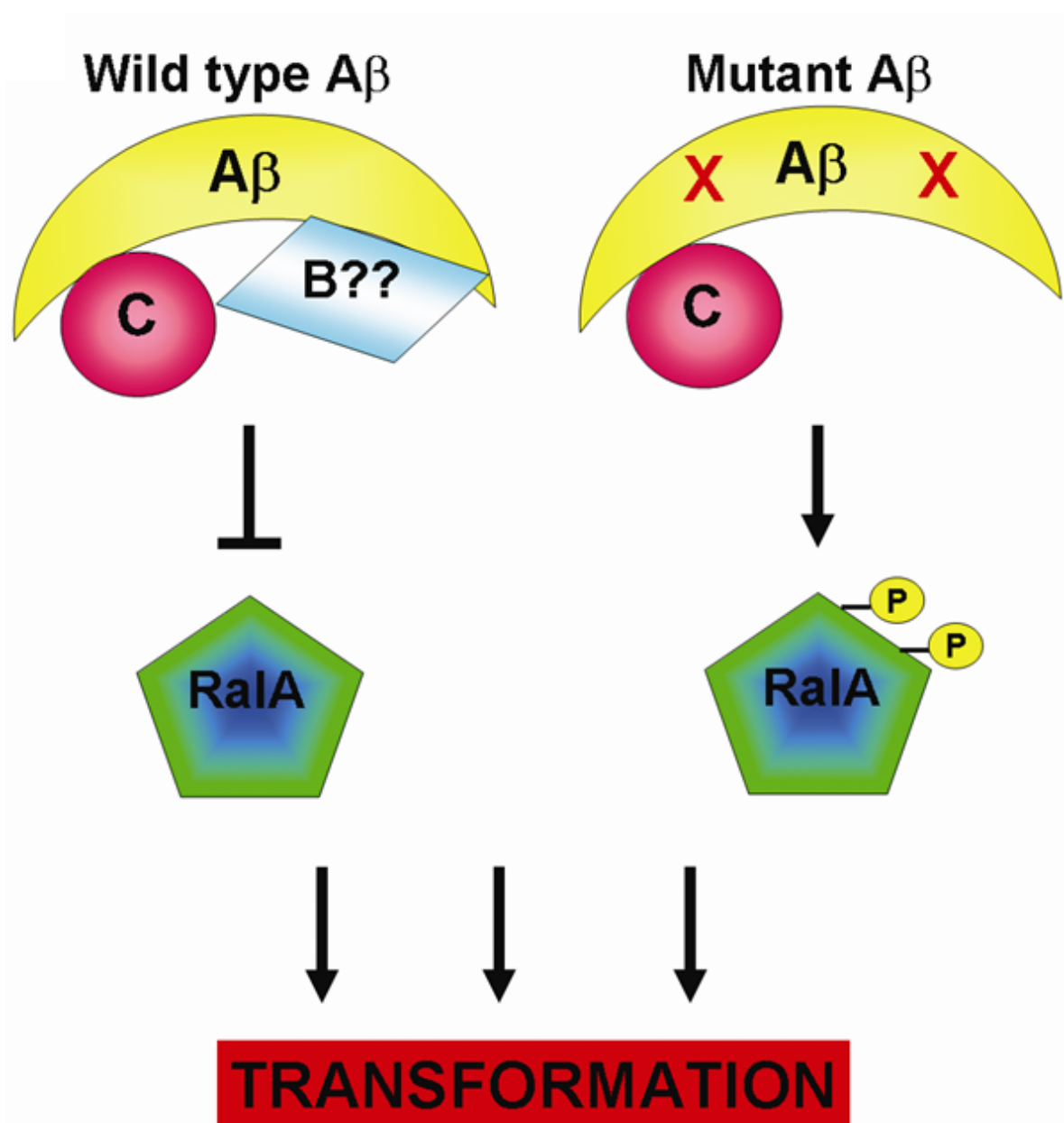


Figure 1.18 Tumour suppressive properties of PP2A Aβ

Cancer-associated PP2A Aβ mutations usually involve both alleles and leads to complete loss-of-function of PP2A, which permits the accumulation of activated RalA.

1.5.4 PP2A activators

PP2A plays a central role in the regulation of cell growth, survival and differentiation, and its functional inactivation or downregulation has been demonstrated in a variety of human malignancies (Westermarck & Hahn 2008) including CML and Ph¹ ALL (Neviani et al. 2007). In this scenario, the BCR/ABL example of kinase-driven cancers may serve as a paradigm for those cancers characterised by exacerbated oncogenic kinase activity and loss of PP2A tumour suppressive function. Within these cancers, PP2A appears to play the role of a gatekeeper by controlling the expression or activity of the oncogene itself (Neviani et al. 2005). Furthermore, inhibition of PP2A permits the activation of oncogenic pathways which promote disease progression by enhancing cellular proliferation and survival. Therefore, rescuing PP2A tumour suppressive activity is an attractive therapeutic strategy for these cancers (Perrotti & Neviani 2008).

Several studies have demonstrated the antiproliferative agents, forskolin and ceramide, both mediate cell death through the activation of PP2A (Dobrowsky *et al.* 1993, Feschenko *et al.* 2002, Hannun & Obeid 2002). In a recent example of innovative pharmacology, activation of PP2A was discovered as an underlying mechanism by which the small molecule immunomodulator, FTY720 (Fingolimod; Novartis, Basel, Switzerland) induces apoptosis (Matsuoka *et al.* 2003). This section provides an overview of the major PP2A activators and describes in detail the recent studies conducted with FTY720 in BCR/ABL⁺ CML and ALL.

1.5.4.1 Forskolin

Forskolin, a diterpene isolated from the roots of *Coleus forskohlii*, is primarily known to stimulate the adenylate cyclase system, which results in elevated levels of cyclic AMP (cAMP) and subsequent activation of protein kinase A (PKA) (Seamon & Daly 1981, Seamon *et al.* 1981). The anticancer properties of this compound were initially demonstrated through potent inhibition of growth and tumour colonisation of the highly metastatic BL6 melanoma cell line (Agarwal & Parks 1983). Further studies indicated its potential use against ALL (Gutzkow *et al.* 2002) and CML cell lines (Taetle & Li-en 1984). However, more recent findings demonstrate that forskolin also activates PP2A (Feschenko *et al.* 2002); a mechanism which contributes to induction of apoptosis in B-CLL and CML-BC patient samples (Moon & Lerner 2003, Neviani et al. 2005).

Treatment with 1,9-dideoxy-forskolin, which lacks adenylate cyclase activity, significantly impairs the clonogenic potential of 32D BCR/ABL⁺ cells to a similar degree as forskolin. These findings suggest that the anti-leukaemic effects of forskolin and its derivative depends on the induction of PP2A activity rather than cAMP, and was the first to highlight the therapeutic relevance of using PP2A-activators to specifically target leukaemia cells (Neviani et al. 2005).

1.5.4.2 Ceramide

Ceramide is a central component of the sphingolipid metabolic pathway and is produced by hydrolysis of the membrane-associated sphingomyelin (Okazaki *et al.* 1989). Within the cytoplasm, ceramide is converted to sphingosine via ceramidases (el Bawab *et al.* 2002), which in turn become phosphorylated by sphingosine kinases (SphK) to produce sphingosine-1-phosphate (S1P) (Figure 1.19A). Increased levels of ceramide induce apoptosis in response to a variety of stress-related stimuli including chemotherapeutic agents, ultraviolet light and γ -irradiation (Hannun & Obeid 2002). One mechanism by which ceramide regulates cell death is via the activation of heterotrimeric PP2A complexes (Dobrowsky et al. 1993, Galadari *et al.* 1998, Chalfant *et al.* 1999, Leoni *et al.* 1998). The structural requirements governing this interaction are mediated by a ceramide binding site within PP2Ac (Law & Rossie 1995). A high degree of specificity exists between the two molecules, with molecular studies showing that even slight modifications to the sphingoid backbone greatly reduces the association (Chalfant et al. 2004). Functionally, ceramide promotes the translocation of B56 α -containing PP2A complexes to the mitochondrial membrane. This leads to rapid dephosphorylation and inactivation of the anti-apoptotic protein, Bcl2, contributing to cell death (Ruvolo et al. 2002, Ruvolo et al. 1999). More recently in the human lung adenocarcinoma A549 cell line, ceramide has been shown to interact with the SET protein and restrict its inhibitory function on PP2A, resulting in PP2A activation. In addition, this association regulates the dephosphorylation and degradation of c-Myc, thus defining a novel mechanism for the antiproliferative role of PP2A-induced activation by ceramide (Mukhopadhyay *et al.* 2009).

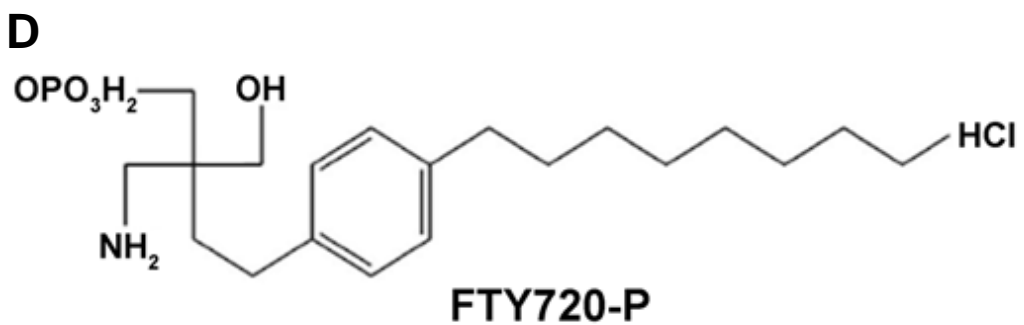
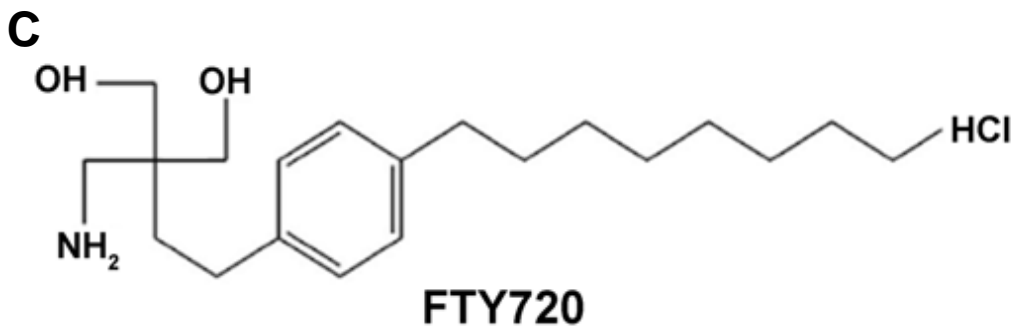
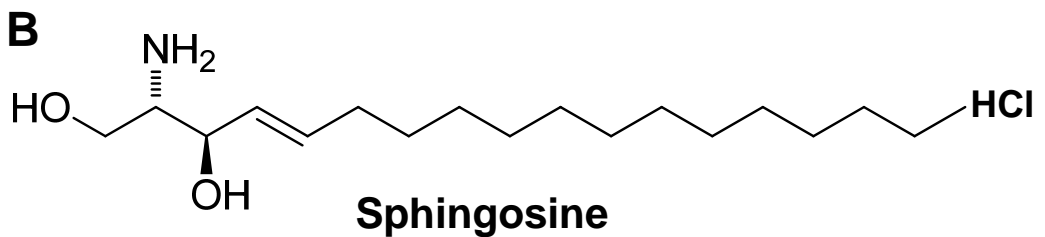
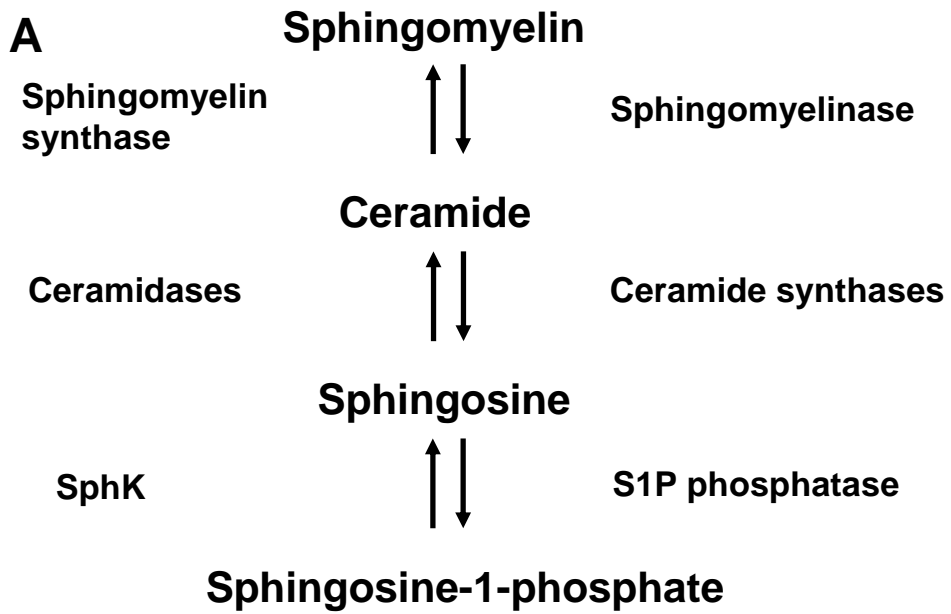


Figure 1.19 Sphingolipid metabolic pathway and structure of FTY720

A) Sphingolipid metabolic pathway. Sphingosine kinase (SphK); Sphingosine-1-phosphate (S1P). **B)** Structure of sphingosine **C)** FTY720, and **D)** FTY720-P.

1.5.4.3 FTY720

FTY720 was first synthesised by structural modifications of myriocin (ISP-1), a fungal metabolite isolated from *Isaria sinclairii* culture broth (Fujita *et al.* 1994), and is structurally similar to sphingosine (Figure 1.19B and C) (Albert *et al.* 2005, Kiuchi *et al.* 2005). It is effectively phosphorylated *in vivo* by SphK2 to yield the biologically active FTY720-phosphate (FTY720-P; Figure 1.19D) (Brinkmann *et al.* 2002, Zemmann *et al.* 2006). Interestingly, the (S)-configured FTY720-P, but not the (R)-FTY720-P or parent FTY720, binds with high-affinity to four of the five known S1P receptors (S1PR), excluding S1PR₂ (Brinkmann *et al.* 2002, Albert *et al.* 2005). Interaction of FTY720-P with S1PR induces receptor internalisation and degradation (Figure 1.20) (Matloubian *et al.* 2004, Graler & Goetzl 2004). S1P signal is required for the migration of lymphocytes from secondary lymphoid tissues back into the efferent lymphatics and systemic circulation (Matloubian *et al.* 2004, Cyster 2005). Consequently, prolonged S1PR downregulation by FTY720-P effectively inhibits the immune response by sequestering functional lymphocytes within secondary lymphoid organs (Brinkmann *et al.* 2002, Mandala *et al.* 2002). The use of FTY720 as an immunomodulator is currently being evaluated in Phase III trials for multiple sclerosis (Takabe *et al.* 2008, Cohen *et al.* 2009).

In addition to the antagonism of S1PR signalling, a more recent mechanism of action identified for FTY720 is that it activates purified PP2A ABC trimers *in vitro* (Matsuoka *et al.* 2003). Loss of PP2A phosphatase activity contributes to the pathophysiology of BCR/ABL-driven leukaemias (Neviani *et al.* 2007); therefore, a logical prediction would be that restoration of PP2A levels reverses the leukaemic phenotype. Indeed, an extensive study has shown that pharmacological reactivation of PP2A with FTY720 or forskolin inhibits the proliferation, enhances apoptosis, restores differentiation and impairs colony formation of imatinib-sensitive and -resistant (T315I) myeloid 32D BCR/ABL⁺ cells and primary CML-BC progenitors. This effect is also observed with lymphoid BaF3 BCR/ABL⁺ cells and patient Ph¹ ALL progenitors (Neviani *et al.* 2007). FTY720 had no effect on parental 32D and BaF3 cells or normal bone marrow CD34⁺ control samples, indicating specificity for leukaemia cells (Neviani *et al.* 2005, Neviani *et al.* 2007). In addition, the reactivation of PP2A has been shown to play a role in IFN- α -2b induced apoptosis of K562 cells, confirming its potential as an important therapeutic target in BCR/ABL⁺ leukaemia (Saydam *et al.* 2003).

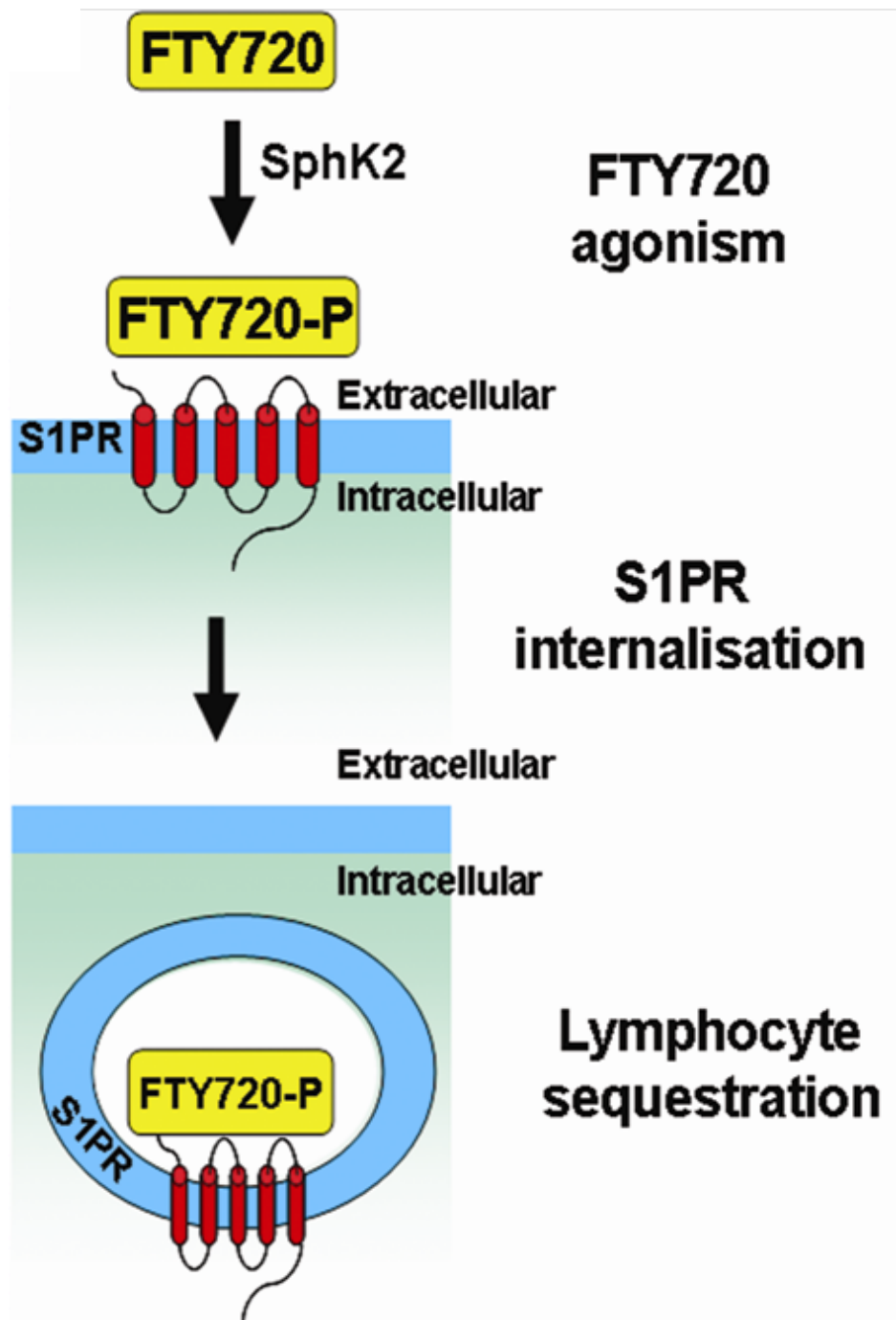


Figure 1.20 Mechanism of FTY720 immunomodulation

FTY720 is phosphorylated by sphingosine kinase 2 (SphK2) into FTY720-P, which binds to sphingosine-1-phosphate receptors (S1PR) on lymphocytes. This results in sustained S1PR internalisation and lymphocyte sequestration.

Notably, FTY720 promotes BCR/ABL tyrosine dephosphorylation and proteolytic degradation, together with reduced phosphorylation of the PP2A targets Akt, ERK1/2 and STAT5 (Neviani et al. 2007). Co-treatment with okadaic acid reverses the enhancement of PP2A activity and restores substrate phosphorylation, strongly indicating that FTY720 functions through a PP2A-dependent mechanism. Furthermore, inhibition of S1PRs did not counteract the effects of FTY720 on BCR/ABL expression and activity, suggesting that reactivation of PP2A is not mediated by S1PR-induced signalling cascades (Neviani et al. 2007). These results demonstrate that the therapeutic potential of PP2A reactivation in myeloid and lymphoid progenitors is based on its ability to abolish BCR/ABL kinase activity, whilst simultaneously inhibiting downstream signalling pathways that contribute to BCR/ABL leukaemogenesis (Figure 1.21).

Importantly, the *in vitro* efficacy of FTY720 translated into an *in vivo* model, with the administration of 10 mg/Kg/day markedly suppressing both imatinib-sensitive (WT) and –resistant (T315I) 32D BCR/ABL⁺ leukaemogenesis (Neviani et al. 2007). After 4 weeks of treatment, saline-treated mice contained a large number of undifferentiated myeloid cells within the peripheral circulation, representing an overt AML phenotype. These mice also developed massive splenomegaly, which correlated with extensive infiltration of blast cells into the spleen and other secondary organs including the bone marrow and liver. In contrast, FTY720-treated mice displayed undetectable levels of BCR/ABL⁺ cells in the systemic circulation and secondary organs. Accordingly, these effects were sustained long term with 80% and 50% of WT and T315I BCR/ABL⁺ FTY720-treated mice, respectively, still alive at 27 weeks and showing no signs of leukaemia. In contrast, all saline-treated mice were sacrificed 5 weeks post-tumour cell injection (Neviani et al. 2007).

In addition, FTY720 treatment significantly prolongs animal survival in a xenograft severe combined immunodeficient mouse model of disseminated B-cell lymphoma/leukaemia (Liu et al. 2008). In both studies no toxic side effects were observed with daily administration of FTY720, highlighting the safety and therapeutic relevance of utilising PP2A-activating drugs in leukaemia patients (Liu et al. 2008, Neviani et al. 2007). Further investigation into the use of FTY720, or other means of

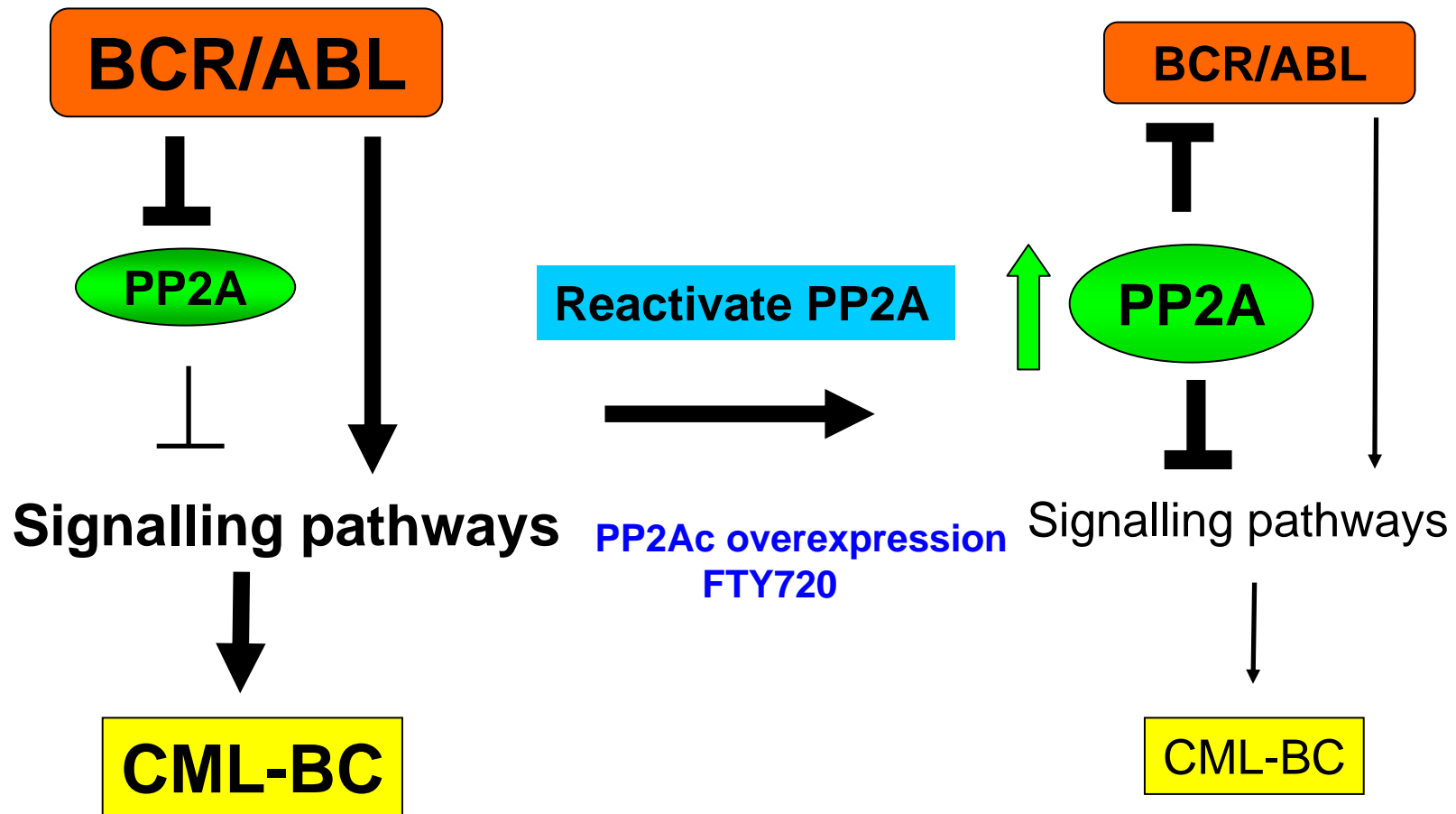


Figure 1.21 Reactivation of PP2A inhibits BCR/ABL-mediated leukaemogenesis

The combined stimulation of downstream signalling pathways and inactivation of PP2A by BCR/ABL results in enhanced leukaemogenesis and the development of blast crisis CML. Reactivation of PP2A not only inhibits signalling pathways but also inhibits the oncogenic activity of BCR/ABL itself, leading to impaired leukaemia growth.

PP2A reactivation, may prove beneficial in the treatment of cancers in which transformation is characterised by the loss of PP2A tumour suppressive function.

1.6 Aims of this Thesis

Given that BCR/ABL and c-KIT induce malignancy via activation of similar signalling pathways, the overall objective of this thesis was to test the hypothesis that PP2A inhibition is essential for BCR/ABL and mutant c-KIT-induced tumourigenesis, and that reactivation of PP2A is a valid treatment strategy for these cancers. In testing this hypothesis I have investigated the molecular mechanisms by which oncogenic BCR/ABL and mutant c-KIT regulate PP2A activity. The major aims were to:

1. Identify the individual PP2A components that are altered by BCR/ABL expression.
2. Elucidate the specific PP2A holoenzyme complexes that are involved in BCR/ABL-mediated leukaemogenesis.
3. Investigate whether PP2A is functionally inactivated by mutant c-KIT, and determine if this is essential for c-KIT-induced tumourigenesis.
4. Demonstrate that reactivating PP2A is a potential therapeutic strategy for mutant c-KIT⁺ malignancies using an *in vitro* and *in vivo* model.

Together, this project has the unifying theme that perturbation of a tumour suppressor represents a critical step in the induction and maintenance of human malignancies characterised by the aberrant activation of oncogenic tyrosine kinases. Furthermore, it identifies the broad application of PP2A as a novel therapeutic target for the development of improved treatment strategies.

CHAPTER 2

MATERIALS AND METHODS

2.1 Buffers and Reagents

All reagents and chemicals were purchased from Sigma Chemical Co. (St Louis, MO) or Merck Pty Ltd. (Kilsyth, VIC) unless otherwise stated, and were of molecular biology or research grade. Buffers and stock solutions are listed in Appendix 1.

2.2 Recombinant DNA Techniques

2.2.1 Plasmid vectors

2.2.1.1 cDNA constructs

The 6.7 kb cDNA encoding p210 kDa WT *BCR/ABL* was obtained from Prof. Timothy Hughes (Institute of Medical and Veterinary Science (IMVS), Adelaide, SA) and cloned as a blunt ended fragment into the Hpa I site of the retroviral expression vector pRUFneo (Rayner & Gonda 1994). The p210 kDa Y253F *BCR/ABL* substitution was created using site-directed mutagenesis (QuikChange®; Stratagene, La Jolla, CA). The primers were designed to change nucleotide (nt) 4057 from A to T: 5'-GGGCGGGGGCCAGTTCGGGGAGGTG-3' and 5'-CACCTCCCCGAACTGGCCC CCGCCC-3' (Sigma Genosys, Sydney, NSW). This was performed by Dr. Michelle Frost (Ashman laboratory, IMVS).

pBluescript containing human WT *c-KIT* cDNA was obtained from Dr. D. Williams (Immunex; Seattle, WA) and subcloned into the Hpa I site of pRUFneo (Dr. Gina Caruana; Ashman laboratory, IMVS). The cDNAs encoding V560G and D816V *c-KIT* point mutations were isolated from the HMC-1.2 cell line and directionally cloned into WT *c-KIT* pRUFneo (Ferrao *et al.* 1997, Chian *et al.* 2001).

2.2.1.2 shRNA constructs

The shRNA retroviral vectors targeting the PP2A subunits B55 α , B56 α and B56 δ are described in Table 2.1. The pMKO.1 vectors (Addgene Inc., Cambridge, MA) were deposited by Prof. William Hahn (Dana Faber Cancer Institute, Boston, MA) and have been described previously (Chen *et al.* 2004). The B56 δ -specific shRNA (shB56 δ)

Table 2.1 shRNA constructs

Vector	PP2A subunit	shRNA sequence 5' → 3'	Nucleotides	Supplier	Reference
pMKO.1-GFP	Empty vector	N/A		Addgene Inc. ID# 10676	(Chen <i>et al.</i> 2004)
pMKO.1-GFP	B55 α	CTCCTCTATTTTCGGATGTA	1156-1175	Addgene Inc. ID# 10679	(Chen <i>et al.</i> 2004)
pMKO.1-GFP	B56 α	AATGATCAGTGCTAACATCTT	374-394	Addgene Inc. ID# 10680	(Chen <i>et al.</i> 2004)
pSUPER.retro.neo+GFP (pSR)	Empty vector	N/A		A/Prof. Danilo Perrotti	(Neviani <i>et al.</i> 2005)
pSUPER.retro.neo+GFP (pSR)	B56 δ	AAGACCATTTTGCATCGCATC	774-795	shB56 δ supplied by Prof. Stefan Strack and cloned into pSR by Kathryn Roberts	

construct in pSUPER.basic (obtained from Prof. Stefan Strack, University of Iowa, IA), was originally generated by cloning nucleotides AAGACCATTTTGCATCGCATC of B56 δ in both the sense and antisense orientations separated by a 9 nt spacer (Oligoengine Inc., Seattle, WA). To subclone the shB56 δ sequence into a retroviral vector for transduction into the FDC-P1 cells, pSUPER.basic was digested with HindIII/EcoR1 and ligated into the retroviral vector pSUPER.retro.neo+GFP (pSR; obtained from A/Prof. Danilo Perrotti, The Ohio State University, Columbus, OH).

2.2.2 Restriction digests

For all restriction digests 3 Units (U) of enzyme (Promega, Madison, WI) was added to 1 μ g of plasmid DNA with 1x restriction enzyme buffer (supplied) diluted with water to a total volume of 10-50 μ l. The reaction was incubated at 37°C for 1-3 hours and subsequently analysed on a 1.5% (w/v) agarose gel by electrophoresis (Section 2.2.3).

2.2.3 DNA electrophoresis

For analysis of plasmid DNA, fragments were separated according to size by agarose gel electrophoresis. DNA samples were mixed with loading buffer and loaded onto 1-1.5% (w/v) agarose gels (Progen, Darra, QLD) made in 1x TAE buffer with 1 μ g/ml ethidium bromide. The samples were electrophoresed in a horizontal gel apparatus (Biorad, Hercules, CA) in 1x TAE at 100 V for 45-60 minutes. DNA fragments were visualised using a TyphoonTM 9410 Variable Mode Imager (GE Healthcare, Buckinghamshire, UK), and the relative band sizes were determined by comparison to 1 kb DNA molecular weight markers (Fermentas, Burlington, ON, Canada).

2.2.4 DNA purification from agarose gel

DNA fragments separated by agarose gel electrophoresis were purified using the Wizard[®] SV Gel Clean-Up System according to manufacturer's instructions (Promega). Firstly, the agarose gel was visualised on a Mini Transilluminator (Biorad) and the DNA bands were excised using a scalpel blade. The agarose slices were weighed in eppendorf tubes, an equal volume of membrane binding solution (w/v) was added and the gel was dissolved by heating at 65°C for 10 minutes with periodic mixing. The solution was transferred to an SV Minicolumn assembly, incubated for 1 minute at room temperature to facilitate DNA binding and centrifuged at 16,000 x g for 1 minute.

The column was washed with 700 µl of membrane wash solution and centrifuged for 1 minute. This was repeated with 500 µl of wash solution and the column was spun for a further 5 minutes. To remove all traces of wash buffer, the column was centrifuged again for a further minute. DNA was eluted from the column with 25 µl of nuclease free water. Purified DNA was quantified on a spectrophotometer to determine concentration and purity (Section 2.2.5).

2.2.5 Nucleic acid quantification

DNA or RNA samples were measured at an absorbance of 260 nm using a spectrophotometer (DU640, Beckman Coulter, Fullerton, CA). The following equation was used to calculate DNA concentration:

$$O.D. @ 260nm \times dilution\ factor(DF) \times conversion\ factor = \mu g\ DNA\ or\ RNA / ml$$

O.D. = optical density

Conversion factor for DNA = 50 (50 µg/ml of DNA is equivalent to O.D₂₆₀ of 1)

Conversion factor for RNA = 40 (40 µg/ml of RNA is equivalent to O.D₂₆₀ of 1)

For each sample the absorbance ratio O.D₂₆₀/O.D₂₈₀ was determined to indicate purity. Values ranging from 1.6-1.8 were acceptable, and values less than 1.6 indicated protein contamination.

2.2.6 Ligation of insert into plasmid

Each ligation reaction contained 50 ng of vector DNA with a 3 fold excess of insert DNA in 1x ligation buffer (supplied) and 1 µl T4 DNA ligase (3 Weiss units/µl) (Promega). The reaction was left overnight at 4°C and subsequently transformed into competent *Escherichia coli* cells.

2.2.7 Expansion and purification of plasmid DNA

2.2.7.1 Preparation of competent bacteria

Competent cells (*E. coli*, DH5α strain) were streaked onto an LB agar plate (without ampicillin) and grown overnight at 37°C. A single colony was used to inoculate 5 ml of LB medium and incubated overnight with shaking at 37°C. 1 ml of this culture was

aliquoted into 50 ml of fresh LB medium and grown until the optical density at 600 nm was between 0.5 and 0.6. The culture was chilled on ice for 10 minutes and subsequently centrifuged at 3,220 x g for 10 minutes at 4°C. The pellet was resuspended in 20 ml of Inoue transformation buffer and centrifuged for 10 minutes at 4°C. The pellet was then resuspended in 4ml Inoue transformation buffer and 300 µl dimethyl sulphoxide (DMSO) was added drop-wise. Cells were aliquoted into sterile eppendorf tubes, snap frozen in liquid nitrogen and stored at -80°C.

2.2.7.2 Transformation of competent bacteria

Aliquots of chemically competent *E. coli* cells were thawed on ice for 10 minutes and 50-150 ng of plasmid DNA was added to 50 µl of cells. The suspension was incubated on ice for 30 minutes and cells were heat shocked at 42°C for 60 seconds, then placed immediately on ice for a further 3 minutes. 150 µl of pre-warmed LB medium was added and the tubes were incubated with shaking at 37°C for 1 hour. 100 µl of cell suspension was spread onto LB agar plates containing the selective antibiotic ampicillin (100 µg/ml). The plates were incubated overnight at 37°C and stored at 4°C until further use.

2.2.7.3 Purification of plasmid DNA from bacteria

Small scale purification of plasmid DNA was performed using the Fast Plasmid Mini Isolation kit according to manufacturer's instructions (Eppendorf, Hamburg, Germany). A single colony was inoculated into 5 ml LB medium containing 100 µg/ml ampicillin and incubated overnight at 37°C on a shaking rotator. 2 ml of bacterial culture was then centrifuged at 16,000 x g for 1 minute. The bacterial pellet was resuspended in 400 µl of ice-cold lysis solution, vortexed to ensure thorough resuspension and incubated for 3 minutes at room temperature. The lysate was transferred to a spin column assembly and centrifuged for 1 minute. Columns were washed in 400 µl of wash buffer and centrifuged for a further minute. The flow through was discarded and the columns spun for another minute to dry. Purified plasmid DNA was eluted in 50 µl of water and quantified on a spectrophotometer (Section 2.2.5).

Large scale plasmid DNA isolations were performed using the PureYield™ Plasmid Midiprep System, as per manufacturer's instructions (Promega). A single colony was

inoculated into 5 ml LB medium with ampicillin (100 µg/ml) and incubated for 8 hours with shaking at 250 rpm. 200 µl of this starter culture was added to 100 ml fresh LB medium and incubated overnight with shaking. The bacterial culture was centrifuged at 3,220 x g for 10 minutes and the pellet was resuspended in 3 ml resuspension solution. 3 ml lysis buffer was then added and the mixture was incubated at room temperature for 3 minutes to facilitate efficient cell lysis. Following this, 5 ml neutralisation solution was added and the tube was incubated for another 3 minutes to ensure thorough lysate clearing. The lysate was then poured into a clearing column and the cell debris was allowed to rise to the top for complete lysate filtration. The column was centrifuged at 1,500 x g for 5 minutes and the filtrate transferred to a binding column. This was spun for 3 minutes and 5 ml of endotoxin removal wash was subsequently added. The column was spun for 3 minutes and the flow through discarded. 20 ml of column wash was added and the tube was centrifuged for 7 minutes until the membranes appeared dry. The plasmid DNA was eluted in 400 µl of water by centrifugation for 5 minutes and quantified on a spectrophotometer (Section 2.2.5).

2.2.8 DNA sequencing and analysis

Automated sequencing of plasmid DNA (800 ng) was performed by the Australian Genome Research Facility (AGRF, University of QLD, Brisbane, QLD). Sequencing primers directed against either side of the shB56δ insert were used at a concentration of 6.4 pM (Table 2.2). The chromatograms were visually inspected to ensure correct sequencing and the sequences were analysed using the ANGIS/BioManager service (www.angis.org.au).

Table 2.2 Sequencing and standard PCR primers

Primer	Gene Accession	Oligonucleotide Sequence 5' → 3'
BCR	NM 004327	Fwd - CGGGAGCAGCAGAAGAAGTGT
ABL	M14752	Rev - AAAGGTTGGGGTCATTTTCAC
β-actin	NM 007393	Fwd - CAGCCTTCCTTCTTGGGTAT Rev - CTCAGGAGGAGCAATGATCTT
Sequencing	Directed to pSR	Fwd - GTCAAGCCCTTTGTACAC
pSR shRNA	vector sequence	Rev - GTGTTCCCGCCTAGTGAC

2.3 Cell Culture

2.3.1 Media, solutions and cytokines

All cell culture reagents were supplied by Gibco (Grand Island, NY) unless otherwise specified. Dulbecco's Modified Eagle's Medium (DMEM) and Iscove's Modified Dulbecco's Medium (IMDM) was supplemented with 15 mM HEPES, 2 mM glutamine and 10% heat inactivated fetal calf serum (FCS) (JRH Biosciences Inc., Lenexa, KN). Phosphate buffered saline (PBS) was used to wash cells. A solution of 0.125% trypsin and 0.125 mM Ethylenediaminetetra-acetic acid (EDTA) in PBS was used to remove adherent cells from tissue culture dishes or flasks.

Cytokine units are defined such that 50 U results in 50% of the maximum number of colonies in soft agar cultures containing 5×10^4 mouse bone marrow cells. Mouse granulocyte-macrophage colony stimulating factor (GM-CSF) was synthesized by yeast expressing a GM-CSF expression vector and was a gift from Dr T. Wilson and Dr. N. Gough (Walter and Eliza Hall Institute, Melbourne, VIC). Recombinant human stem cell factor (SCF) was purchased from Peprotech (Rocky Hill, NJ). Interleukin-3 (IL-3) was obtained from WEHI-3 conditioned medium. WEHI-3 is a myelomonocytic cell line that produces constitutively high levels of IL-3 (Lee *et al.* 1982).

2.3.2 Cell lines and maintenance

All cell lines were maintained in tissue culture flasks (Corning Inc. Life Sciences, Lowell, MA) and incubated at 37°C in a humidified atmosphere containing 5% CO₂ (v/v) in air. To determine cell density, a 50 µl aliquot of cells was diluted with an equal volume of 0.4% trypan blue in PBS and loaded onto a haemocytometer. Cell viability was measured using the following formula:

$$\text{mean of 4 large haemocytometer squares} \times 2 \text{ (DF)} \times 10^4/\text{ml} = \text{cells} \times 10^6/\text{ml}$$

The mouse factor-dependent myeloid progenitor cell line, FDC-P1 (Dexter *et al.* 1980), was cultured in DMEM/10% FCS supplemented with 20 U/ml mouse GM-CSF. The mouse IL3-dependent myeloid progenitor cell line, 32Dcl3 (Greenberger *et al.* 1983), expressing the pMIG empty vector or p210 kDa WT BCR/ABL were obtained from A/Prof. Danilo Perrotti (Perrotti *et al.* 2002). 32Dcl3 cells and the Ph¹ human suspension CML cell line, K562 (Lozzio & Lozzio 1975), were cultured in IMDM/10%

FCS and the 32Dcl3 empty vector cells were supplemented with 10% WEHI-3 conditioned medium. Cell densities were maintained in the log phase to preserve viability, with cultures seeded at $1-5 \times 10^4$ cells/ml and grown to a maximum of 1×10^6 cells/ml.

The adherent retroviral packaging cell lines Ψ 2 (Mann *et al.* 1983) and PhoenixTM (Pear *et al.* 1993) were maintained in DMEM/10% FCS. PhoenixTM cells were originally created by introducing constructs capable of generating retroviral particles into human embryonic kidney 293T cells (Orbigen, San Diego, CA). Upon confluency, the cells were washed in PBS and incubated with trypsin for 2 minutes to facilitate removal from the tissue culture flask. The trypsin was inactivated by the addition of DMEM/10% FCS, after which the cells were centrifuged ($220 \times g$) for 5 minutes, resuspended in fresh DMEM/10% FCS and re-seeded at $2-5 \times 10^5$ cells/ml.

2.3.3 Reviving cell lines

Cryopreserved cells were retrieved from liquid nitrogen and thawed rapidly in a water bath at 37°C. The cells were transferred to a 10 ml tube and 6 ml of cell culture medium was added drop-wise with gentle swirling. The cell suspension was centrifuged at $220 \times g$ for 5 minutes, resuspended in 12 ml cell culture medium and placed in the incubator at 37°C in 5% CO₂.

2.3.4 Cryopreservation

Cells were harvested during log phase, centrifuged at $220 \times g$ for 5 minutes and resuspended in fresh culture medium to a density of 1×10^7 cells/ml. An equal volume of freezing mix was added drop wise with mixing. 1ml of this cell suspension was aliquoted into cryotubes (Thermo Fisher Scientific, Roskilde, Denmark), which were wrapped in cotton wool and placed in a -80°C freezer. After 3 to 5 days, the cryotubes were transferred to liquid nitrogen for long term storage.

2.3.5 Retroviral infection of FDC-P1 cells

2.3.5.1 Generation of FDC-P1 cells expressing BCR/ABL and c-KIT

The generation of FDC-P1 cells expressing the pRUFneo empty vector, WT BCR/ABL and Y253F BCR/ABL were established by a previous member of the Ashman laboratory (Dr. Michelle Frost, *unpublished data*). FDC-P1 cells expressing WT c-KIT, V560G c-KIT and D816V c-KIT have been previously described (Frost *et al.* 2002). For all established cell lines, the stable Ψ 2 retroviral packaging system was used. Briefly, Ψ 2 cells were seeded 24 hours prior to transfection at a density of 3×10^5 cells/60mm dish in 4 ml DMEM/10% FCS without antibiotics, as the presence of antibiotics reduces transfection efficiency. 6 μ l of FuGENE (Roche, Basel, Switzerland) was added to 94 μ l of DMEM and incubated for 5 minutes at room temperature. This mixture was then added drop-wise to 2 μ g of pRUFneo vector DNA and incubated for a further 30 minutes at room temperature. The FuGENE:DNA complex was added drop-wise to the Ψ 2 cells, which were incubated for 48 hours at 37°C. To select for transfected Ψ 2 packaging cells, the media was removed and cells were cultured in fresh DMEM/10% FCS containing Geneticin (G418, Gibco), at a concentration of 400 μ g/ml. A control dish that contained Ψ 2 parent cells was also cultured in 400 μ g/ml of G418 and the selection process was concluded when all the control cells were dead.

FDC-P1 parent cells were infected with retroviral particles by co-cultivation with G418-selected Ψ 2 transfectants. Firstly, Ψ 2 cells were γ -irradiated by a linear accelerator at 30 Gray to inhibit proliferation. 2.8×10^6 cells were then seeded in a T₇₅ cm² tissue culture flask and 1.2×10^6 FDC-P1 parent cells were added. The co-culture was maintained in DMEM/10% FCS, supplemented with 20 U/ml GM-CSF and 8 μ g/ml polybrene (Chemicon, Temecula, CA). After 48 hours of co-cultivation, FDC-P1 cells were harvested and selected in medium containing 20 U/ml GM-CSF and 1 mg/ml G418 until the parent control cells were dead. After selection, FDC-P1 pRUFneo empty vector cells were maintained in 20 U/ml GM-CSF. FDC-P1 WT c-KIT cells were maintained in 100 ng/ml SCF (Peprotech). FDC-P1 WT and Y253F BCR/ABL, V560G and D816V c-KIT cells were cultured in the absence of factor (Table 2.3).

Table 2.3 Cell lines and maintenance

Cell Line	Species	Media	Growth Factors	Reference
FDC-P1				(Dexter <i>et al.</i> 1980)
pRUFneo EV	Mouse	DMEM / 10% FCS	20 U/ml GM-CSF	(Frost <i>et al.</i> 2002)
WT BCR/ABL			Factor-independent	
Y253F BCR/ABL			Factor-independent	
WT c-KIT			100 ng /ml human SCF	(Frost <i>et al.</i> 2002)
V560G c-KIT			Factor- independent	(Frost <i>et al.</i> 2002)
D816V c-KIT			Factor-independent	(Frost <i>et al.</i> 2002)
32Dcl3				(Greenberger <i>et al.</i> 1983)
pMIG EV	Mouse	IMDM / 10% FCS	10% WEHI-medium (IL-3)	(Perrotti <i>et al.</i> 2002)
WT BCR/ABL			Factor-independent	(Perrotti <i>et al.</i> 2002)
K562	Human	IMDM / 10% FCS	Factor-independent	(Lozzio & Lozzio 1975)
Ψ2	Mouse	DMEM / 10% FCS	Factor-independent	(Mann <i>et al.</i> 1983)
PhoenixTM	Human	DMEM / 10% FCS	Factor-independent	(Pear <i>et al.</i> 1993) (Orbigen, San Diego, CA)

2.3.5.2 Generation of shRNA-expressing FDC-P1 WT BCR/ABL cells

The retroviral expression vectors pMKO.1-shB55 α , pMKO.1-shB56 α , pMKO.1-shB56 γ , pSR-shB56 δ and the corresponding control vectors pMKO.1-GFP-EV and pSR-EV were introduced into FDC-P1 WT BCR/ABL cells using the transient PhoenixTM retroviral packaging system and Profection Calcium Phosphate Transfection kit according to manufacturer's instructions (Promega). Phoenix cells were seeded 24 hours prior to transfection at a density of 3.5×10^6 cells/T₇₅ cm² in 20 ml DMEM/10% FCS. For each flask, 20 μ g of plasmid DNA was diluted in 1 ml of 0.25 mM CaCl₂. This mixture was added drop-wise to hanks buffered solution (HBS) and incubated for 30 minutes at room temperature. The DNA solution was then added drop-wise to the flask of cells and incubated for 14 hours, after which time the media was replaced with fresh DMEM/10% FCS. The viral supernatant was collected 24 hours later and filtered through a 0.45 μ m filter (Millipore, Billerica, MA).

For retroviral infection, 8×10^5 FDC-P1 WT BCR/ABL cells were resuspended in 4 ml viral supernatant with 8 μ g/ml polybrene (Chemicon). The cell mixture was split into two wells of a 6 well plate, spun at 650 x g for 45 minutes then incubated at 32°C for 2 hours. The medium was replaced with 2 ml fresh viral supernatant, the plate spun again and incubated for 4 hours at 32°C. The cells were cultured in fresh DMEM/10% FCS overnight at 37°C and the viral supernatant was left at 4°C. A final spin followed by a 5 hour incubation with viral supernatant at 32°C was performed. The cells were left to recover for two days in fresh DMEM/10% FCS at 37°C and selected for GFP expression using a fluorescent-activated cell sorter (FACSAria) and FACSDiva software (BD Biosciences, San Jose, CA).

For cell sorting, 5×10^6 cells were resuspended in 5 ml ice-cold DMEM/10% FCS and the top 5-10% GFP-expressing cells were collected into 1 ml ice-cold DMEM/20% FCS. The cells were then transferred with an additional 4 ml medium into a T₂₅ cm² flask and allowed to recover at 37°C. To monitor GFP expression, 5×10^5 cells were washed 3 x in PBA (define first time) and resuspended in 500 μ l FACS fixative. Fluorescence (488 nm) was detected using a FACSCalibur flow cytometer (BD Biosciences) and the data was analysed with CellQuest software (BD Biosciences).

2.3.6 Drug treatments

Imatinib was resuspended in milli-Q water at 10 mM from capsules that were originally obtained from Novartis and provided by Prof. Bruce Lyons (IMVS). Where indicated, cells were treated with 0.1 μ M for 24 hours, with a half dose (0.05 μ M) added at 18 hours. For animal administration, imatinib was made up fresh each day in milli-Q water at 5 mg/ml. FTY720 (Cayman Chemicals, Ann Arbor, MI) and FTY720-P(S) (Echelon Biosciences Inc., Salt Lake City, UT) were dissolved in DMSO at a stock concentration of 50 mM. For animal treatments, FTY720 was made up fresh at 0.5 or 1 mg/ml in 0.9% saline (St John Ambulance, Sydney, NSW). Okadaic acid (Sigma) was dissolved in DMSO at a stock concentration of 1 mM. All drugs were stored at -20°C.

2.4 Polymerase Chain Reaction (PCR)

2.4.1 RNA extraction

Total RNA was extracted from FDC-P1 cells using an RNeasy Mini kit, as per manufacturer's instructions (QIAGEN Pty Ltd., Valencia, CA). Briefly, 5 x 10⁶ cells were washed in PBS and lysed in 600 μ l Buffer RLT. The lysate was homogenised by centrifugation at 16,000 x g for 2 minutes in a QIAshredder spin column and 600 μ l of 70% ethanol (EtOH) was added to the lysate. The mixture was then transferred to an RNeasy spin column which was centrifuged for 15 seconds at 16,000 x g. The column was washed in 350 μ l Buffer RW1 and the membrane incubated for 15 minutes in DNase I to remove contaminating DNA. The column was washed again in 350 μ l Buffer RW1, then 2x with 500 μ l Buffer RPE. The RNA was eluted in 50 μ l RNase free water and quantified on a spectrophotometer (Section 2.2.5).

2.4.2 Reverse transcription PCR (RT-PCR)

To make cDNA, 10 μ g of RNA in 20 μ l DEPC-water was incubated with 0.5 μ g/ml oligo dT (Sigma Genosys) at 65°C for 10 minutes to allow for primer annealing. For reverse transcription the RNA was divided into two tubes and incubated at 42°C for 1.5 hours with 10 μ l master mix including 10 U RNase inhibitor, 0.5 mM dNTPs and either 1 U M-MLV reverse transcriptase (Promega) or 1 μ l water for the negative control. The enzyme was inactivated at 70°C for 10 minutes, after which time the samples were diluted with 180 μ l DEPC-water and stored at -20°C. Oligonucleotide primers (Sigma Genosys) are presented in Table 2.2. To detect the presence of BCR/ABL transcripts in

the FDC-P1 cells each PCR reaction contained 5 μ l cDNA, 100 ng primer, 0.2 mM dNTPs, 2 mM MgCl₂, 1x reaction buffer (supplied) and 1 U GoTaq polymerase (Promega) made up to 50 μ l in nuclease-free water. The denaturing stage was performed at 95 °C for 2 minutes and amplification carried out with 35 cycles of 95 °C for 40 seconds, 60 °C for 30 seconds and an extension period of 72 °C for 40 seconds. The final reaction was held at 72 °C for 2 minutes to ensure complete extension of the PCR product. β -actin levels were monitored in a separate reaction as a control for equal cDNA loading.

2.4.3 Quantitative real-time PCR (qRT-PCR)

Total RNA was extracted from cells using an RNeasy Mini kit as per manufacturer's instructions (Section 2.4.1). Reverse transcription was performed with 10 μ g of RNA in 20 μ l of master mix as described above (Section 2.4.2). Oligonucleotide primers that detect individual PP2A subunit isoforms (Sigma Genosys) are presented in Table 2.4. Each 12.5 μ l qRT-PCR reaction was prepared using the Power SYBR® Green PCR Master Mix (Applied Biosystems, Foster City, CA) and contained 1 μ l cDNA with 4 pM primer. All qRT-PCR experiments were performed using the 7500 Real Time PCR System (Applied Biosystems). Triplicate reactions were performed for each run on four repeats from two RNA isolations. Thermal cycling conditions consisted of 50°C for 2 minutes, initial heating at 95 °C for 10 minutes, followed by 40 cycles of 95 °C for 15 seconds and 60 °C for 1 minute. Ribosomal protein S18 (RPS18), a component of the 40S ribosome subunit, was chosen as the reference gene based on preliminary experiments which confirmed its expression remained constant between the FDC-P1 cell lines. In addition, a standard curve of 10-fold serial cDNA dilutions was routinely included to monitor the reaction efficiency between plates. For analysis of fold changes in PP2A gene expression compared to FDC-P1 empty vector cells, comparative quantification algorithms were used (Applied Biosystems). The first step was to subtract the average RPS18 cycle threshold (Ct) from the Ct of the specific gene of interest to give the normalised Avg Δ Ct value for each cell line (1). The $\Delta\Delta$ Ct for each gene of interest was calculated by subtracting the Avg Δ Ct for the FDC-P1 empty vector cell line from the FDC-P1 test cell line (either WT or Y253F BCR/ABL) (2). To determine relative gene expression compared to the empty

Table 2.4 Quantitative real-time PCR Primers

Primer	Gene Accession	Oligonucleotide Sequence 5' → 3'
RPS18	NM 022331	Fwd - TAGCCTTTGCCATCACTGCC Rev - CATGAGCATATCTTCGGCCC
PPP2CA	NM 002715	Fwd -CTTGTAGCTCTTAAGGTTCG Rev - TCTGCTCTCATGATTCCCTC
PPP2CB	NM 004156	Fwd -TTCTTGTAGCATTAAGGTGCG Rev - TCCATACTTTCGCAGACAT
PPP2R1A	NM 014225	Fwd -GCTCTTCTGCATCAATGTGCT Rev - ATGCGCAGAACCGTGGGTA
PPP2R1B	NM 002716	Fwd -ACTTTATTCTGCATTAATGCACT Rev - TGGGCAGCATTTGCTTAGTA
PPP2R2A	NM 002717	Fwd -CTGTGGAAACATAACCAGGTG Rev - AACACTGTCAGATCCATTCC
PPP2R2D	NM 018461	Fwd -AACGGTTCGGATAGCGCCA Rev - GCGTGTCTCTATCAAACATC
PPP2R5A	NM 006243	Fwd -TTGTTTCATGCTCAGCTAGC Rev - GGCTCTGTTAGTGTTGTATC
PPP2R5B	NM 006244	Fwd -ACTCTGACAGAGCACGTGAT Rev - GAAACATCACCTCCTTCTGG
PPP2R5C	NM 002719	Fwd -TGGCCTCATCTACAGCTTGT Rev - GGTTGGAAATCTGGAGACTCT
PPP2R5D	NM 006245	Fwd -ACTGAGGCTGTTTCAGATGCT Rev - CGCAGCAGCACTTTCTCCT
PPP2R5E	NM 006246	Fwd -TCAGATCGTCAGCGTGAGA Rev - CTCTTTAACTCCAGATCCTC
PPP2R3A	NM 002718	Fwd -TTGCGGTCCAGAAGGATGT Rev - ACAAGCGTCTCATACTCCTC
PPP2R4	NM 178001	Fwd -ATGTATAAGGCCGAGTGCCT Rev - TCCCGAACTTGAAGTGCTG

vector cell line, the number 2 was raised to the power of $(-\Delta\Delta Ct)$ (3). This is because one cycle difference indicates twice as much starting template.

1. $Ct_{Gene\ of\ interest} - Ct_{RPS18} = Avg\ \Delta CT$
2. $Avg\ \Delta CT_{test\ cell\ line} - Avg\ \Delta CT_{empty\ vector\ cell\ line} = \Delta\Delta CT$
3. $Fold\ difference\ (relative\ to\ FDC-P1\ empty\ vector\ cell\ line) = 2^{-\Delta\Delta CT}$

2.5 PP2A phosphatase activity assay

Cellular PP2A activity was determined using the PP2Ac immunoprecipitation phosphatase assay kit according to manufacturer's instructions (Millipore). Briefly, cells were set up at 2.5×10^5 /ml in 50 ml and treated with or without the final concentration of indicated drugs for 12 hours. Approximately 2×10^7 cells were washed in HEPES and lysed in PP2A activity assay buffer for 1 hour on ice. Protein concentration was determined using a BCATM Protein Assay Kit (Pierce, Rockford, IL). Lysates (250 μ g) were mixed with 4 μ g anti-PP2Ac 1D6 (Millipore) and 40 μ l protein-A Sepharose beads (GE Healthcare) in pNPP Ser/Thr assay buffer for 2 hours at 4°C. PP2Ac complexes were washed 3x in tris-buffered saline (TBS) and 1x in pNPP assay buffer. 20 μ l of assay buffer and 60 μ l of a PP2A specific phospho-threonine peptide (750 μ M; K-R-pT-I-R-R) was added to the beads, which were then incubated at 30°C for 10 minutes. The amount of free phosphate (PO_4) was measured colourimetrically with addition of malachite green (20 μ l) at an absorbance of 620 nm. A standard PO_4 curve ranging from 200 pM to 2000 pM was included on each plate and the phosphate release per sample was determined by linear regression. The percentage of phosphatase activity was calculated by the following formula:

$$\% PP2A\ activity = \frac{\text{free phosphate of the test cells}}{\text{untreated empty vector cells}} \times 100.$$

2.6 Analytical Procedures for Proteins

2.6.1 Flow cytometry

Flow cytometric analysis was used to monitor c-KIT expression on the surface of FDC-P1 derived cell lines. 1×10^6 cells were harvested and washed in PBA (PBS/0.1% BSA/0.1% sodium azide) then resuspended in 400 μ l PBA containing 10% normal rabbit serum in PBA. Cells were incubated on ice for 10 minutes and 100 μ l was

aliquoted into each tube. The primary antibody, mouse IgG_{2A} mAb 1DC3, used to detect human c-KIT was produced in the Ashman lab (Aylett et al. 1995). An anti-Giardia antibody, IB5 (Prof. George Mayhofer, The University of Adelaide, Adelaide, SA), was incorporated as an isotype-matched negative control. For staining, 2 µl of either antibody was added to the cells and incubated on ice for 1 hour. The cell suspension was washed three times in PBA to remove unbound antibody and incubated in the dark on ice for 45 minutes with a 1/50 dilution of the secondary antibody; fluorescein isothiocyanate (FITC) conjugated sheep anti-mouse Ig (Chemicon). Cells were washed another three times in PBA, resuspended in 500 µl FACS fixative and left in the dark at 4°C overnight. Immunofluorescence (488 nm) was detected using a FACSCalibur flow cytometer (BD Biosciences) and the data was analysed with CellQuest software (BD Biosciences).

2.6.2 Immunoblotting

Cells (1×10^7) were washed in PBS and lysed for 30 minutes on ice in radio-immunoprecipitation assay (RIPA) buffer. Lysates were clarified by centrifugation (15,000 x g for 15 minutes at 4°C). Protein concentration was determined using a BCA Assay (Pierce). Whole cell lysates (50 µg) were mixed with 5x SDS loading buffer, boiled for 10 minutes, then separated by 12% SDS-polyacrylamide gel electrophoresis (PAGE) and transferred onto Hybond ECL nitrocellulose membranes (GE Healthcare).

The membranes were stained with Ponceau S in 0.1% acetic acid to determine successful transfer and equal loading before being blocked for 1 hour in either 5% skim milk powder (SMP) or 3% bovine serum albumin (BSA) in Tris-buffered saline/0.1% Tween-20 (TBST) (Table 2.5) and washed 3x 10 minutes in TBST before incubation with primary antibodies in either 0.5% SMP or 1% BSA in TBST for 1 hour at room temperature (Table 2.5). The membranes were washed again for 3x 10 minutes in TBST and incubated with horseradish peroxidase (HRP)-conjugated secondary antibodies in TBST for 1 hour at room temperature (Table 2.6). Protein-antibody complexes were visualised by enhanced chemiluminescence (ECL; GE Healthcare). Images were captured on a TyphoonTM 9410 Variable Mode Imager (GE Healthcare) and protein bands were analysed by densitometric volume quantification using Image Quant v5.1 (GE Healthcare). To obtain relative protein expression, the volume for each

Table 2.5 Primary antibodies used for immunoblotting

Antibody	Immunogen	Supplier	Block	Concentration
Rabbit pAb anti-PP2A A	MAAADGDDSLY	Millipore, #07-250	5% SMP	1:250 in 0.5% SMP
Rabbit pAb anti-PP2A B55 α	CFSQVKGAVDDDDV	Peptide made by Auspep, Parkville, VIC Serum produced at IMVS (Chen <i>et al.</i> 2004)	3 % BSA	1:500 in 1% BSA
Goat pAb anti-PP2A B56 α	AYNMHSILSNTSAE	Novus Biologicals, Littleton, CO, #NB100-847	5% SMP	1:500 in 0.5% SMP
Goat pAb anti-PP2A B56 β	QRLTPQVAASGGQS	Novus Biologicals, #NB100-66290	5% SMP	1:500 in 0.5% SMP
Mouse mAb anti-PP2A B56 γ 3 clone TQ11-1G6	C-terminus	Novus Biologicals, #NB100-501	5% SMP	1:500 in 0.5% SMP
Goat pAb anti-PP2A B56 δ	KRAEEFLTASQEAL	Novus Biologicals, #NB100-66292	5% SMP	1:500 in 0.5% SMP
Goat pAb anti-PP2A B56 ϵ	LKRGLRRDGIPT	Novus Biologicals, #NB100-66293	5% SMP	1:500 in 0.5% SMP
Rabbit pAb anti-PP2Ac	PHVTRRTPDYFL	Supplied by Alistair Sim (Sim <i>et al.</i> 1998)	5% SMP	1:5000 in 0.5% SMP
Rabbit mAb anti-PP2Ac- p ^{Y307}	Phospho-peptide corresponding to residues surrounding Try307	Epitomics, Burlingame, CA	3% BSA	1:500 in 1% BSA

Table 2.5 Primary antibodies used for immunoblotting continued

Antibody	Immunogen	Supplier	Block	Concentration
Rabbit pAb anti-I2PP2A (SET) (H-120)	Amino acids 1-120 at N-terminus	Santa Cruz Biotechnology, Santa Cruz, CA; #sc-25564	5% SMP	1:500 in 0.5% SMP
Rabbit pAb anti-actin	SGPSIVHRKC	Sigma, #A2066	5% SMP	1:1000 in 0.5% SMP
Mouse mAb anti-phosphotyrosine clone 4G10	N/A	Millipore, #05-321	3% BSA	1:1000 in 1% BSA
Goat pAb anti-c-KIT (M-14)	C-terminus	Santa Cruz Biotechnology, #sc-1494	5% SMP	1:500 in 0.5% SMP
Mouse mAb Anti-c-Abl (Ab-3) clone 24-21	C-terminus	EMD Chemicals Inc., Gibbstown, NJ, #OP20	5% SMP	1:250 in 0.5% SMP

Table 2.6 Secondary antibody concentrations used for immunoblotting

Antibody	Company	Concentration
Anti-rabbit IgG HRP-conjugated	GE Healthcare #NA934	1:5000 in TBST
Anti-mouse IgG HRP-conjugated	GE Healthcare #NXA931	1:5000 in TBST
Anti-goat IgG HRP-conjugated	Sigma #A9452-1VL	1:5000 in TBST
Anti-rabbit IgG TruBlot™ HRP-conjugated	eBioscience #18-8816	1:5000 in TBST
Anti-mouse IgG TruBlot™ HRP-conjugated	eBioscience #18-8877	1:5000 in TBST
Anti-goat IgG TruBlot™ HRP-conjugated	eBioscience #18-8814	1:5000 in TBST

protein of interest was divided by the corresponding volume for the actin band for each cell line. These values were then normalised to empty vector controls.

1. $\text{volume protein of interest} / \text{volume of actin} = \text{relative protein to actin}$
2. $\text{relative actin value of test cell line} / \text{relative actin value of empty vector}$
 $= \text{relative protein expression}$

2.6.3 Immunoprecipitation

For immunoprecipitation of PP2Ac or PP2A A, FDC-P1 cells (1×10^7) were lysed in IP buffer for 30 minutes on ice and clarified by centrifugation ($15,000 \times g$ for 15 min at 4°C). Total protein content was determined by a BCA Assay (Pierce). For immunoprecipitations, primary antibody was pre-incubated with $50 \mu\text{l}$ of beads for 2 hours at 4°C (Table 2.7). The antibody-coated beads or microcystin-conjugated sepharose beads (supplied by Greg Moorhead, University of Calgary, AB, Canada) (Moorhead *et al.* 2007) were washed and incubated with 1 mg lysate overnight at 4°C . Complexes were washed again 3x in IP lysis buffer, boiled and eluted in 2x SDS loading buffer then subjected to 12% SDS-PAGE before being transferred onto Hybond ECL nitrocellulose membranes (GE Healthcare). The membranes were probed as described above (Section 2.6.2); however, TrueBlot™ HRP-conjugated secondary reagents were used (eBioscience, San Diego, CA) (Table 2.5).

2.6.4 Phosphorylation assay

Immunoprecipitation of c-KIT has been described previously (Roberts *et al.* 2007). Briefly, FDC-P1 cells expressing BCR/ABL or c-KIT were set up at $2.5 \times 10^5/\text{ml}$ in 300 ml with or without indicated concentration of drugs, and harvested at the designated time points. For FTY720 treatment, a half-dose ($1.25 \mu\text{M}$) was added every 12 hours. Cells were lysed in modified RIPA buffer for 30 minutes on ice. Lysates were clarified by centrifugation ($15,000 \times g$ for 15 minutes at 4°C) and total protein content was determined using a BCA Assay (Pierce). For immunoprecipitation, lysates (1mg) were incubated with $4 \mu\text{g}$ of primary antibody (Table 2.7) and $40 \mu\text{l}$ protein-A agarose beads (GE Healthcare) for 2 hours at 4°C . The immunoprecipitated complexes were washed 3x in lysis buffer, eluted in 2x SDS loading buffer then subjected to SDS-PAGE on 4-15% Tris HCl gradient gels (Biorad). Gels were transferred onto Hybond ECL nitrocellulose membranes (GE Healthcare), blocked in 1% BSA/TBST for 1 hour and

Table 2.7 Antibodies and beads used for immunoprecipitation

Antibody	Immunogen	Supplier	Concentration	Beads
Mouse mAb anti-PP2Ac clone 1D6	RGEPHVTRRTPDYFL	Millipore, #05-421	4 µg / IP	Trueblot™ anti-Mouse Ig beads (eBioscience)
Rat mAb anti-PP2A Aα (6F9)	MAAADGDDSLY	Covance, Berkeley, CA; #MRT-204R	10 ul / IP	rec-Protein G-Sepharose® 4B Conjugate (Zymed, San Francisco, CA)
Mouse mAb anti-c-Abl (Ab-3) clone 24-21	C-terminus of Abl	Calbiochem	4 µg / IP	Protein-A agarose (GE Healthcare)
Mouse mAb anti-c-KIT clone Kit4	C-terminus of c-KIT	Leonie Ashman (Aylett <i>et al.</i> 1995)	4 µg / IP	Protein-A agarose (GE Healthcare)

probed with anti-phosphotyrosine 4G10 (Millipore). After incubation with HRP-conjugated secondary antibody for 1 hour (Table 2.6), immunoblots were visualised with ECL (GE Healthcare) and captured on a Typhoon™ 9410 Variable Mode Imager (GE Healthcare). To detect total protein, the blots were incubated in stripping buffer at 55°C for 3x 20 minutes and re-probed with anti-c-ABL or anti-c-KIT (Table 2.5). After incubation with HRP-conjugated secondary antibody for 1 hour (Table 2.6), immunoblots were visualised with ECL (GE Healthcare) and captured on a Typhoon™ 9410 Variable Mode Imager (GE Healthcare). Protein bands were analysed by densitometric volume quantification using Image Quant v5.1 (GE Healthcare). To obtain relative pY / total c-KIT levels for each cell line, the volume for pY c-KIT was divided by the corresponding total c-KIT at each time point (1). These values were then normalised and data points are presented as a percentage of untreated controls for each time point (2).

1. $\text{volume pY} / \text{volume of total c-KIT} = \text{relative ratio at any given time point}$
2. $\text{relative ratio at any time point} / \text{relative ratio of untreated levels} \times 100$
 $= \% \text{ pY} / \text{total c-KIT for each time point}$

2.7 Cellular Growth and Survival Assays

2.7.1 Cellular proliferation

To evaluate the growth of shRNA-expressing FDC-P1 WT BCR/ABL cells, cells were seeded at 5×10^4 /ml and a trypan blue cell count (Section 2.3.2) was performed every 12 hours until confluency was reached. Three independent experiments were performed in duplicate.

The CellTiter-Blue™ Cell Viability Assay was used according to manufacturer's instructions (Promega). Briefly, FDC-P1 cells were seeded at 4×10^4 /well (200 μ l) in a 96-well plate in DMEM/10% FCS containing appropriate factors and the indicated concentrations of drugs. After 48 hours, 20 μ L CellTiter-Blue™ Reagent was added to each well and the plates were incubated for an additional 5 hours. Fluorescence was measured at $560_{\text{Ex}} / 590_{\text{Em}}$ on a FLOUstar OPTIMA plate reader (BMG Labtechnologies, Offenburg, Germany). The concentration of drug that inhibits 50% of the cell population (ID₅₀) was analysed using fit-spline lowess regression (Verrills *et al.*

2006). The relative sensitivity was determined by dividing the ID₅₀ of the test cells by that of empty vector controls. Assays were plated in quadruplicate and repeated at least 4 times.

2.7.2 Analysis of cellular morphology

The cellular morphology of FDC-P1 derived cell lines was examined by May-Grunwald/Giemsa staining on cytopspin cells. To prepare cytopspins, FDC-P1 WT BCR/ABL derived cell lines were harvested from culture and resuspended in ice-cold 5% FCS/PBS at 2.5×10^5 cells/ml. The cell suspension (100µl) was deposited onto microscope slides by centrifugation (500 rpm for 5 minutes) in a Cytospin centrifuge (Shandon Scientific Ltd., England). Slides were allowed to dry and fixed for 1 minute in 100% methanol before staining with May-Grunwald (Sigma) for 5 minutes. The slides were rinsed briefly in distilled water and placed in 1:20 dilution of Giemsa for 20 minutes. The slides were dipped in water again, allowed to dry and mounted in Vectamount (Vector Laboratories, Inc., Burlingame, CA). Cells were evaluated under 200x or 400x magnification on a light microscope (BH2, Olympus, Japan). Photographs were taken with a ColorView II camera and analySIS software (Olympus Soft Imaging Systems GmbH, Munster, Germany). To determine the percentage of cells with altered morphology, a total of 400 cells were examined for the presence of differentiation characteristics such as an [enlarged vacuolated cytoplasm](#).

2.7.3 Apoptosis assay

The induction of apoptosis by FTY720 was measured using the annexin V-FITC apoptosis detection kit following manufacturer's instructions (BD Biosciences). Briefly, untreated and 2.5 µM FTY720-treated cells were set up at 2.5×10^5 /ml in 10 ml and 1.25 µM FTY720 was added at 12 hours. For analysis, 5×10^5 cells were harvested 24 hours post-treatment and resuspended in 500 µl binding buffer. The cells were stained with 4 µl annexin V-FITC and 200 ng/ml propidium iodide (PI) for 15 minutes at room temperature in the dark. Samples were run on a FACSCalibur flow cytometer (BD Biosciences), and the data was analysed using CellQuest software (BD Biosciences). Four independent assays were averaged to determine the percentage of annexin-V positive cells.

2.7.4 Cell cycle analysis

To determine the percentage of cells at each stage of the cell cycle, 1×10^6 cells were treated with or without 2.5 μM FTY720. A half dose (1.25 μM) was added every 12 hours until the 36 hour time point when the cells were washed in PBS containing 0.1% glucose and fixed with ice-cold 70% EtOH for 1 hour. Cells were washed again in PBS, resuspended in 200 μl 50 $\mu\text{g}/\text{mL}$ PI (BD Biosciences) with 20 μl of 10mg/ml RNase (Fermentas) and incubated at 37°C for 30 minutes. 1×10^5 cells were analysed for DNA content on a FACSAria flow cytometer (BD Biosciences). Histograms were fit for cell-cycle ratios using ModFit LT version 3.2 (Verity Software House, Topsham, ME). Four independent assays were averaged to determine the percent of cells in sub-G₀, G₀/G₁, S, and G₂/M phase at each time point.

2.7.5 Colony-forming assay

To assess the growth of myeloid progenitors, 5×10^2 FDC-P1 cells were diluted in IMDM/2% FCS and seeded in 1% methylcellulose medium (MethoCult[®]; Stem Cell Technologies, Vancouver, BC, Canada). Where indicated, cells were plated in the presence of appropriate factors and concentration of drugs. Colonies (>50 cells) were counted after 7 days and viewed under 100x with a CK40 microscope (Olympus). Photographs were taken with a ColorView II camera and analySIS software (Olympus Soft Imaging Systems GmbH).

2.8 Animal Procedures

2.8.1 Syngeneic mouse model

2.8.1.1 Establishing the FDC-P1 mutant c-KIT tumour model

To determine the optimal cell number and growth kinetics of tumours formed by FDC-P1 cells expressing V560G or D816V oncogenic c-KIT, a preliminary tumour growth study with 4 mice per group was conducted. On day 0, 8- to 10-week-old female DBA/2J mice (Animal Resources Centre, Canning Vale, WA) were subcutaneously (s.c.) injected on both flanks with either 2.5 or 5×10^6 FDC-P1 V560G or D816V c-KIT cells in 200 μl 1:1 PBS/Matrigel (Trevigen, Gaithersburg, MD). The mice were weighed every second day. Tumours were visibly inspected and palpated until day 18, when tumour volume was accurately measured with callipers based on the formula:

$$\text{tumour volume} = 0.5 \times \text{length (mm)} \times \text{width}^2 \text{ (mm)}$$

Mice were culled when the combined tumour volumes reached 10% of the body weight (~2100 mm³).

2.8.1.2 Evaluating the safety of FTY720 in DBA/2J mice

There were no previous studies which had reported the administration of FTY720 to DBA/2J mice. Therefore, a preliminary toxicity study with 4 mice per group was conducted to determine the maximal tolerable dose. The mice received daily 200 µl intraperitoneal (i.p.) injections of either 0.9% saline as an untreated control (St John Ambulance), or 5 or 10 mg/Kg FTY720 made up daily in 0.9% saline. The mice were weighed every day to monitor toxic side effects and culled at day 23. Peripheral blood was harvested via heart puncture into an EDTA collection tube (BD Biosciences) and used to evaluate red blood cell (RBC) and white blood cell (WBC) numbers. The organs were weighed and snap-frozen in liquid nitrogen. To count the RBC, 5 µl of whole blood was added to 4995 µl of PBS and mixed by inversion. 10 µl of this mixture was placed on a haemocytometer and the number of RBC was determined by the following formula:

$$\text{Average count per small square} \times 16 \times 1000 \text{ (dilution factor)} = \text{RBC} \times 10^{12}/\text{dL blood}$$

For WBC, 10 µl of whole blood was added to 190 µl room temperature RBC lysis buffer and mixed by inversion. 10 µl was placed on a haemocytometer and the number of WBC was determined by the following formula:

$$\text{Average count per large square} \times 0.2 = \text{WBC} \times 10^8/\text{dL blood}$$

2.8.1.3 FTY720 treatment of FDC-P1 mutant c-KIT tumours

Eight- to 10-week-old female DBA/2J mice (Animal Resources Centre) were s.c. injected on both flanks with either 5×10^6 FDC-P1 V560G or D816V c-KIT cells in 200 µl 1:1 PBS/Matrigel (Trevigen). Relative tumour volume (RTV) was calculated by:

$$\text{RTV} = \text{tumour volume on any given day} / \text{tumour volume at start of treatment (day 5)}$$

Once the tumours reached a volume of ~200 mm³ (day 5), mice were randomised into groups that received daily treatments of either 0.9% saline (i.p. or p.o.), 50 mg/Kg imatinib p.o. or 10 mg/Kg FTY720 (i.p. or p.o.). The mice were weighed daily to

monitor toxic side effects and tumour volume was measured with callipers every second day. On day 14, three mice from FDC-P1 V560G c-KIT and six mice from FDC-P1 D816V c-KIT tumour groups were sacrificed. The remaining mice were used for survival studies and culled when tumour volumes reached $\sim 2100 \text{ mm}^3$ (Figure 2.1).

The tumours and organs were weighed and fixed immediately in 10% neutral buffered formalin (NBF) solution for 48 hours, then transferred into 70% EtOH and stored at 4°C until processing. Bone marrow samples obtained from the femur were subjected to an extra decalcification step in 10% formic acid/NBF for 48 hours prior to storage in 70% EtOH at 4°C. Peripheral blood was harvested via heart puncture and used to evaluate RBC and WBC numbers as described previously (Section 2.8.1.2). All tissue samples were taken through a series of dehydration steps and paraffin-embedded in a Lynx II tissue processor (Advanced Biotechnologies Inc., Columbia, MD). This involved 1x 70% EtOH for 20 minutes, 3x 95% EtOH for 20 minutes, 3x 100% EtOH for 20 minutes, 1x xylene for 20 minutes, 1x xylene for 60 minutes, 1x paraffin at 65°C for 60 minutes and 1x paraffin at 65°C for 20 minutes. The paraffin molds were cooled on ice for 30 minutes and tissue blocks were stored at room temperature. Animal studies were performed with approval of The University of Newcastle Animal Care and Ethics Committee (#A-2008-117).

2.8.1.4 Immunohistochemistry

Immunohistochemical staining was carried out on 4 μm tissue sections from formalin-fixed, paraffin-embedded specimens. To section the tissue, blocks were placed face down on ice for 10 minutes and inserted into the microtome. The sliced sections were placed onto clean glass slides and subsequently incubated at 65°C for 20 minutes to melt the wax and bond the tissue to the glass. Prior to staining, slides were heated at 55°C for 2 minutes then deparaffinised in 2x xylene for 5 minutes before being rehydrated through a series of gradually decreasing concentrations of EtOH including 1x 100% EtOH for 5 minutes and 1x 80% EtOH for 5 minutes. Slides were washed 2x in PBS for 5 minutes and endogenous peroxidase activity was blocked by incubation in PBS containing 1% H_2O_2 for 5 minutes at room temperature. For antigen retrieval, slides were treated in a microwave with 10 mM citrate buffer, pH 6.0, for 2 minutes on high and 10 minutes on medium power.

All antibody dilutions and solutions were made up in PBS containing 1% BSA and 0.1% Tween-20 (PBT). Non-specific binding was blocked by 30 minutes incubation in normal goat serum provided in the Vectastain Elite ABC kit (ABC; Avidin Biotinylated Complex; Vector Laboratories, Inc.). The sections were incubated for 1 hour with a 1:400 dilution of either rabbit polyclonal anti-human c-KIT (CD117; Dako, Glostrup, Denmark), or normal rabbit serum (Sigma), followed by a 1 hour incubation in biotinylated goat anti-rabbit IgG (Vector Laboratories, Inc.). Tissue obtained from age-matched non-tumour bearing mice served as a negative control for antibody cross-reactivity. Positive staining was detected using the ABC solution, with diaminobenzidine (DAB) as the chromogen (Vector Laboratories, Inc.). The sections were then counterstained with Gills double strength haematoxylin (Pro Sci Tech, Thuringowa, QLD) for 30 seconds and washed in tap water until clear. Slides were gradually dehydrated by placing in 1x 80% EtOH for 5 minutes and 1x 100% EtOH for 5 minutes and 2x xylene for 5 minutes prior to mounting in Vectamount (Vector Laboratories, Inc.). Positive staining was evaluated under 100x or 400x magnification on an inverted light microscope (BH2, Olympus). Pictures were taken with a ColorView II camera and analySIS software (Olympus).

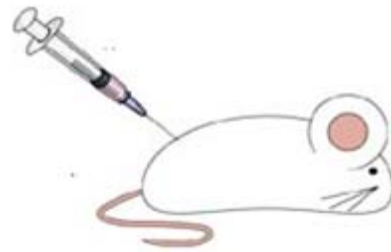
2.8.1.5 TUNEL staining

Apoptotic death within the tumour tissue of saline and FTY720-treated mice expressing V560G and D816V c-KIT⁺ tumours was assessed by terminal deoxynucleotidyltransferase-mediated dUTP nick end labelling (TUNEL) staining using an In Situ Cell Death Detection Kit, according to manufacturer's instructions (Roche Diagnostics). Slides were deparaffinised and rehydrated as described above (Section 2.8.1.4), then permeabilised by treatment with 20 µg/ml Proteinase K (10 mM Tris-HCl, pH7.4-7.8) at 37°C for 15 minutes. The sections were incubated in TUNEL reaction mixture for 60 minutes at 37°C in the dark and counterstained for 5 minutes with a 1:2000 dilution of DAPI in PBS. The slides were washed briefly in PBS before being dehydrated as previously described (Section 2.8.1.4) A coverslip was mounted using the anti-fade Vectashield (Vector Laboratories Inc.), and sealed with toluene free nail-polish. For the negative control, a slide was incubated in Label Solution only. For the positive control, another slide was treated with 0.5 mg/ml DNase (Promega) for 10 minutes at room temperature prior to labelling procedures. Images were acquired

1. Culture FDC-P1 V560G and D816V c-KIT cells



2. Inject cells into flanks of DBA/2J mice



Day 0

3. Begin treatment - Measure tumour volume daily



Saline i.p/day

Day 5



**10 mg/Kg/day
FTY720 i.p.**

5. Rest for survival study: Cull when tumours reach 2100 mm³



4. Day 14: Cull 6 mice / group
- Record tumour and organ mass
- Harvest spleen, liver, kidneys bone marrow and tumour

Figure 2.1 Schematic model for the growth of FDC-P1 tumours and FTY720 treatment

100x or 400x on DAPI and FITC channels with an Axioplan 2 imaging system and merged with Axio Vision v4.7 software (Carl Zeiss, Oberkochen, Germany).

2.9 Statistical Analysis

Statistical significance between different cell lines or comparing untreated and drug treated samples was assessed using an unpaired two-tailed Student's t-test. Survival probabilities between animal groups were determined by the Kaplan-Meier method and differences in survival distributions were evaluated by the log-rank test. All values shown are the mean \pm standard error of the mean (SEM) and statistical analysis was performed using GraphPad Prism v4.02 (GraphPad Software Inc., La Jolla, CA).

CHAPTER 3

BCR/ABL ALTERS THE EXPRESSION OF PP2A SUBUNITS

3.1 Introduction

CML is a clonal proliferative disorder that arises from the neoplastic transformation of a HSC and is clinically characterised by three distinct stages: chronic phase (CP), accelerated phase and blast crisis (BC). It accounts for ~15% of adult leukaemia, with approximately 490 newly diagnosed cases recorded every year in Australia¹. The hallmark genetic abnormality associated with CML is a t(9;22)(q34;q11) translocation which results in the shortened Philadelphia chromosome (Ph¹) (Nowell & Hungerford 1960). This generates the *BCR/ABL* fusion gene that is translated into the p210 kDa BCR/ABL oncoprotein in over 90% of CML patients (Ben-Neriah et al. 1986). The unrestrained tyrosine kinase activity of BCR/ABL facilitates the assembly of components essential for the activation of oncogenic cascades that promote factor-independent growth, reduced differentiation and inhibition of apoptosis (Cortez et al. 1995). These include the MAPK, PI3K/Akt and JAK/STAT pathways (Calabretta & Perrotti 2004).

The small molecule tyrosine kinase inhibitor, imatinib, has demonstrated remarkable therapeutic success in CML-CP patients (Deininger et al. 2005). While most patients initially achieve clinical remission with imatinib therapy, a small proportion will develop resistance (Gorre *et al.* 2001). This is due to the acquisition of mutations within BCR/ABL that impair drug binding (e.g. T315I, Y253F/H) (Shah & Sawyers 2003). Furthermore, leukaemia stem cells are insensitive to imatinib (Graham *et al.* 2002, Roeder *et al.* 2006), and as such, a majority of CML-BC patients do not respond to treatment (Silver *et al.* 2004, Druker *et al.* 2001a). Second generation inhibitors, such as nilotinib and dasatinib, have recently been approved for the treatment of imatinib-resistant disease (Kantarjian *et al.* 2007). However, neither compound is effective in a) treating CML-BC patients (le Coutre *et al.* 2008, Cortes *et al.* 2007, Talpaz *et al.* 2006) or b) inducing apoptosis of cells expressing the common imatinib-resistant T315I *BCR/ABL* mutation (O'Hare *et al.* 2005, Soverini *et al.* 2007). In addition, neither

¹ Australian Institute of Health and Welfare (2007)

inhibitor eliminates the most primitive CML stem cell fraction (Copland *et al.* 2006, Jorgensen *et al.* 2007).

Thus, understanding the precise molecular circuitry directing the transition of CML from the chronic phase into blast crisis is required for generating new therapies that simultaneously target BCR/ABL and its downstream oncogenic pathways. Recent work in 32Dcl3 myeloid precursors and CD34⁺ CML patient samples has shown that functional inactivation of PP2A by BCR/ABL contributes to the development of CML-BC (Neviani *et al.* 2005). Restoration of PP2A activity via PP2Ac overexpression, or pharmacological activation (e.g. FTY720), inhibits the proliferation and restores the differentiation of imatinib-resistant BCR/ABL⁺ cell lines and patient-derived blast crisis progenitors (Neviani *et al.* 2005, Neviani *et al.* 2007, Hu *et al.* 2009). Notably, treatment of BCR/ABL⁺ leukaemic mice with FTY720 remarkably prolongs the lifespan and decreases the leukaemia burden compared to saline-treated controls (Neviani *et al.* 2007). These findings identify PP2A as a potential candidate which can be targeted for novel therapeutic strategies in CML.

PP2A is a heterotrimeric enzyme composed of a structural subunit (A α and A β) (Hemmings *et al.* 1990), a catalytic subunit (C α and C β) (Arino *et al.* 1988), and a variable regulatory B subunit categorised under three unrelated families: B55 (α , β , γ , δ) (Strack *et al.* 1999, Zolnierowicz *et al.* 1994, Mayer *et al.* 1991), B56 (α , β , γ , δ , ϵ) (McCright *et al.* 1996, McCright & Virshup 1995) and B'' (PR72/130 / PR70/48) (Yan *et al.* 2000, Stevens *et al.* 2003, Hendrix *et al.* 1993). Regulatory subunits bind to the AC dimer in a mutually exclusive manner to form individual PP2A holoenzymes that exert substrate specificity and direct the enzyme to distinct subcellular localisations. Consequently, the wide array of physiological functions attributed to PP2A is governed by the association of a particular PP2A B subunit to the core enzyme (Janssens *et al.* 2008).

Although increased levels of the endogenous inhibitor, SET, have been shown to contribute to PP2A inactivation in CML-BC (Neviani *et al.* 2005), the direct effect of BCR/ABL on PP2A subunit expression has not been determined. To improve the understanding of PP2A function in the development of CML-BC, the aim of this

chapter was to investigate the expression of individual PP2A subunits in BCR/ABL⁺ myeloid progenitors.

3.2 Results

3.2.1 Expression of p210 kDa BCR/ABL oncoprotein in FDC-P1 cells

The factor-dependent myeloid progenitor cell line, FDC-P1, was originally derived from long-term normal mouse bone marrow cultures maintained in WEHI-3B-conditioned medium (Dexter *et al.* 1980). These cells have a normal diploid karyotype, are nontumorigenic and grow only in the presence of IL-3 or GM-CSF (Hapel *et al.* 1984). FDC-P1 cells represent a powerful *in vitro* model for studying the regulation of cell growth and transformation by various oncogenic tyrosine kinases. The FDC-P1 BCR/ABL⁺ cell model used in this study was established by a previous member of the Ashman laboratory (Dr. Michelle Frost, *unpublished data*). Briefly, the pRUFneo retroviral vector containing no cDNA (pRUFneo empty vector; EV), or cDNA encoding the imatinib-sensitive WT BCR/ABL or -resistant Y253F BCR/ABL mutant (Roumiantsev *et al.* 2002) were introduced into the FDC-P1 cell line by retroviral infection using the Ψ2 stable packaging system (Mann *et al.* 1983). Successfully infected cells were initially selected in G418. Expression of the p210 kDa BCR/ABL oncoprotein induces factor-independence (Hariharan *et al.* 1988), and accordingly, the FDC-P1 WT and Y253F BCR/ABL cells grow in the absence of factor at a similar rate to empty vector control cells cultured in GM-CSF.

Expression of BCR/ABL in the FDC-P1 cells was confirmed by performing qualitative PCR on cDNA using a forward primer that recognises the terminal portion of the human *BCR* gene, and a reverse primer that detects human *ABL* (Figure 3.1). The absence of a band in the FDC-P1 EV control cells indicates primer specificity for the human *BCR/ABL* transcript and confirms the absence of BCR/ABL in these cells (Figure 3.1). Two previously established BCR/ABL⁺ myeloid cell lines were also used in this study. These included the mouse IL3-dependent myeloid precursor, 32Dcl3 (Greenberger *et al.* 1983), expressing either the pMIG empty vector (EV) or the p210 kDa WT BCR/ABL oncoprotein (32D-BCR/ABL) (Perrotti *et al.* 2002), and the K562 human Ph¹ CML cell line (Lozzio & Lozzio 1975). Similar to FDC-P1 cells, the expression of BCR/ABL in 32Dcl3 cells confers factor-independent growth (Perrotti *et al.* 2002). Qualitative

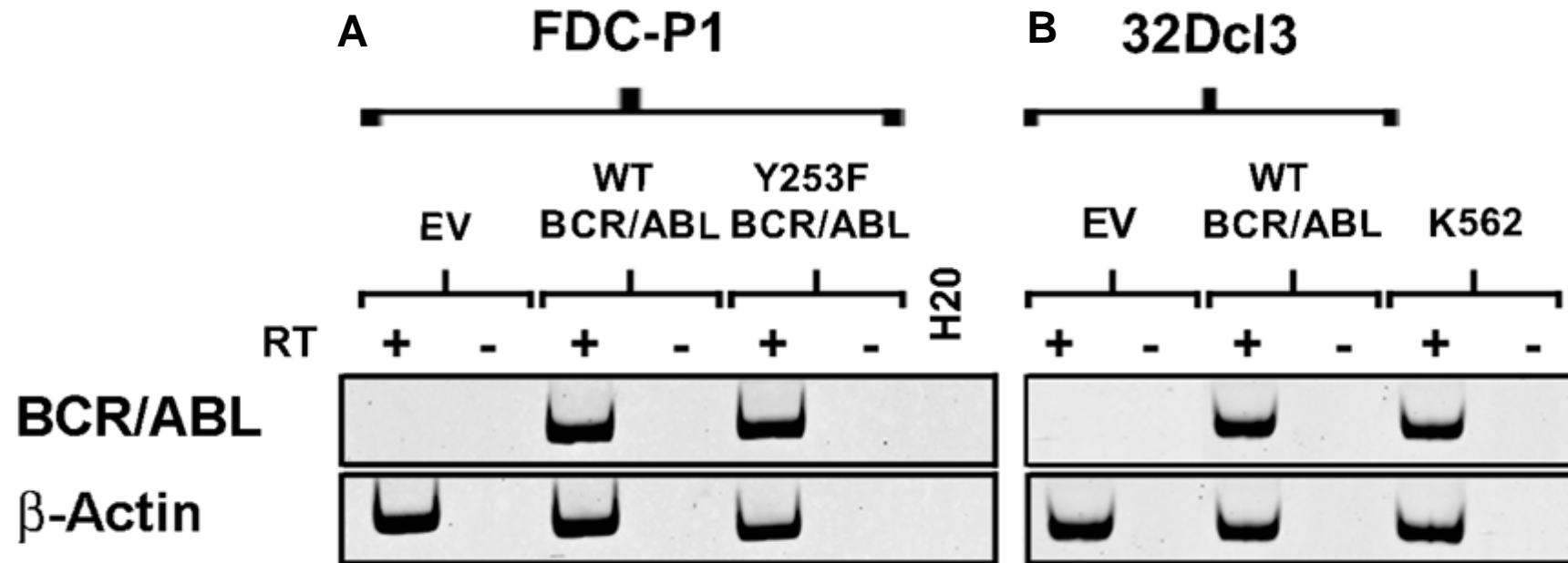


Figure 3.1 Expression of BCR/ABL in myeloid progenitors

Total RNA was extracted from **A**) FDC-P1 cells expressing either the pRUFneo empty vector (EV) or **B**) WT and Y253F BCR/ABL; 32Dcl3 cells expressing the pMIG empty vector (EV) or WT BCR/ABL and Ph¹ K562 cells. cDNA was generated by reverse transcription with reverse transcriptase (+RT), or water as a control for genomic DNA contamination (-RT). PCR was performed using primers that amplify the human *BCR* and *ABL* genes (Table 2.2). β -actin was used as a loading control in a separate reaction.

RT-PCR performed on these cell lines confirmed the expression of BCR/ABL in 32D-BCR/ABL and K562 cells, while it was absent in the empty vector 32Dcl3 cells (Figure 3.1).

3.2.2 Sensitivity of WT and Y253F BCR/ABL to imatinib

Imatinib is an effective therapeutic option for CML-CP patients expressing WT BCR/ABL (Druker *et al.* 2001b); however, patients harbouring Y253F BCR/ABL do not respond to treatment (Roumiantsev *et al.* 2002). The inclusion of FDC-P1 cells expressing either imatinib-sensitive (WT) or –resistant (Y253F) BCR/ABL provides an important control which can highlight and compare the direct effect of BCR/ABL on downstream molecules. Specifically, if BCR/ABL regulates certain signalling pathways, these effects should be reversed with imatinib treatment in the presence of WT BCR/ABL but not the Y253F mutant.

To confirm the differential effects of imatinib in the FDC-P1 BCR/ABL cell model, the proliferation of cells was evaluated using a cell viability assay (Figure 3.2). Importantly, FDC-P1 EV cells cultured in mouse GM-CSF were insensitive to imatinib treatment, confirming the absence of non-specific effects (Figure 3.2). As expected, FDC-P1 cells expressing WT BCR/ABL were sensitive to imatinib inhibition and displayed an ID₅₀ of 53 nM (Table 3.1). Conversely, FDC-P1 Y253F BCR/ABL cells were 8-fold resistant to imatinib with an ID₅₀ of 412 nM (Table 3.1). K562 cells displayed an intermediate response with an ID₅₀ of 192 nM (Table 3.1).

Table 3.1 Sensitivity of BCR/ABL to imatinib

Cell Line	ID₅₀ (nM)¹
FDC-P1	
EV	> 1000
WT BCR/ABL	52.6 ± 4.5
Y253F BCR/ABL	412 ± 29.8**
K562	192.2 ± 18.1**

¹ID₅₀ is the concentration of drug (nM) that kills 50% of the cell population and was calculated using fit-spline lowess regression (Verrills *et al.* 2006). Data is presented as the mean of three independent experiments ± SEM. **p<0.01, Student's t-test compared to WT BCR/ABL.

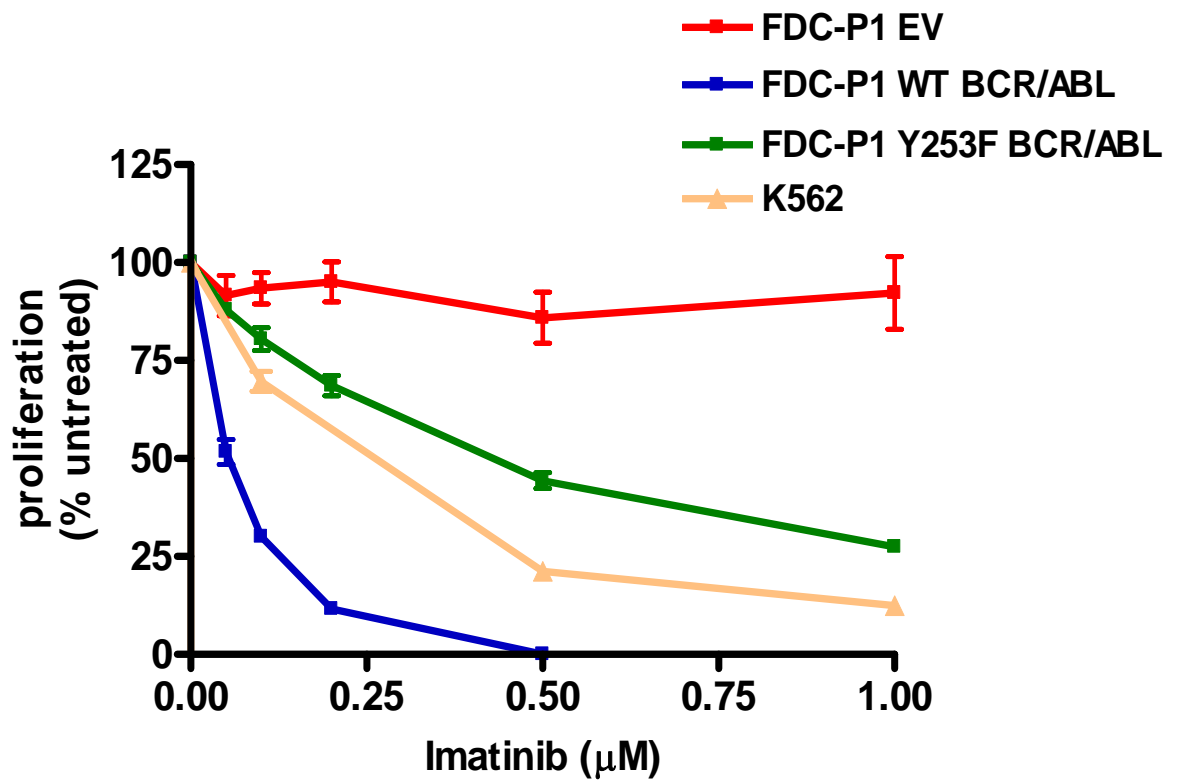


Figure 3.2 Inhibition of BCR/ABL⁺ myeloid progenitors with imatinib

FDC-P1 and K562 cell lines were incubated in increasing concentrations of imatinib (0-1 μM) for 48 hours. Proliferation was measured using a CellTiter-Blue™ Cell Viability Assay and is expressed as a percentage of untreated controls. *Points*, mean of four independent experiments performed in quadruplicate; *bars*, standard error of the mean (SEM).

Accordingly, imatinib treatment (0.1 μ M; 24 hours) inhibited the activity of WT BCR/ABL in FDC-P1 cells, as indicated by reduced tyrosine phosphorylation of immunoprecipitated BCR/ABL (Figure 3.3). The presence of imatinib at the same concentration had no effect on Y253F BCR/ABL phosphorylation (Figure 3.3). The ID₅₀ for imatinib in 32D-BCR/ABL cells is reportedly 250 nM (Druker *et al.* 1996), and accordingly, inhibition of WT BCR/ABL in 32Dcl3 and K562 cells was confirmed (1 μ M; 24 hours) (Figure 3.3). These results demonstrate that WT BCR/ABL expressed in three different myeloid cell lines (FDC-P1, 32Dcl3 and K562) is sensitive to imatinib, whereas Y253F BCR/ABL is resistant.

3.2.3 BCR/ABL impairs the activity of PP2A

Previous studies have demonstrated that BCR/ABL expression in mouse 32Dcl3 and human K562 cells impairs PP2A activity (Neviani *et al.* 2005, Neviani *et al.* 2007). Indeed, the phosphatase activity of PP2A was significantly reduced to 53% and 69% in FDC-P1 cells expressing WT and Y253F BCR/ABL, respectively, compared to empty vector controls (Figure 3.4). Inhibition of BCR/ABL with imatinib (0.1 μ M; 24 hours) in FDC-P1 WT BCR/ABL cells augmented PP2A activity slightly higher than empty vector untreated control levels (Figure 3.4). By contrast, imatinib treatment had little effect on the activation of PP2A in FDC-P1 cells expressing the Y253F BCR/ABL mutant (Figure 3.4). Importantly, the presence of imatinib did not affect PP2A activity in FDC-P1 EV cells grown in mouse GM-CSF (Figure 3.4). This data confirms that PP2A is a specific target of BCR/ABL in the FDC-P1 cell model, and that restoration of its activity is a direct consequence of BCR/ABL inhibition.

3.2.4 BCR/ABL upregulates the PP2A scaffolding subunit

3.2.4.1. SET expression

To define the underlying mechanisms that lead to PP2A inhibition in BCR/ABL⁺ myeloid progenitors, a number of candidates were examined by immunoblotting. In all experiments, the cells were treated with or without imatinib to compare the direct effect of BCR/ABL activity on protein expression. As functional inactivation of PP2A in 32D-BCR/ABL and K562 cells has been shown to be associated with increased expression of SET (Neviani *et al.* 2005), it was important to investigate whether this protein was also regulated by BCR/ABL in the FDC-P1 cell lines. Two splice variants of the SET protein

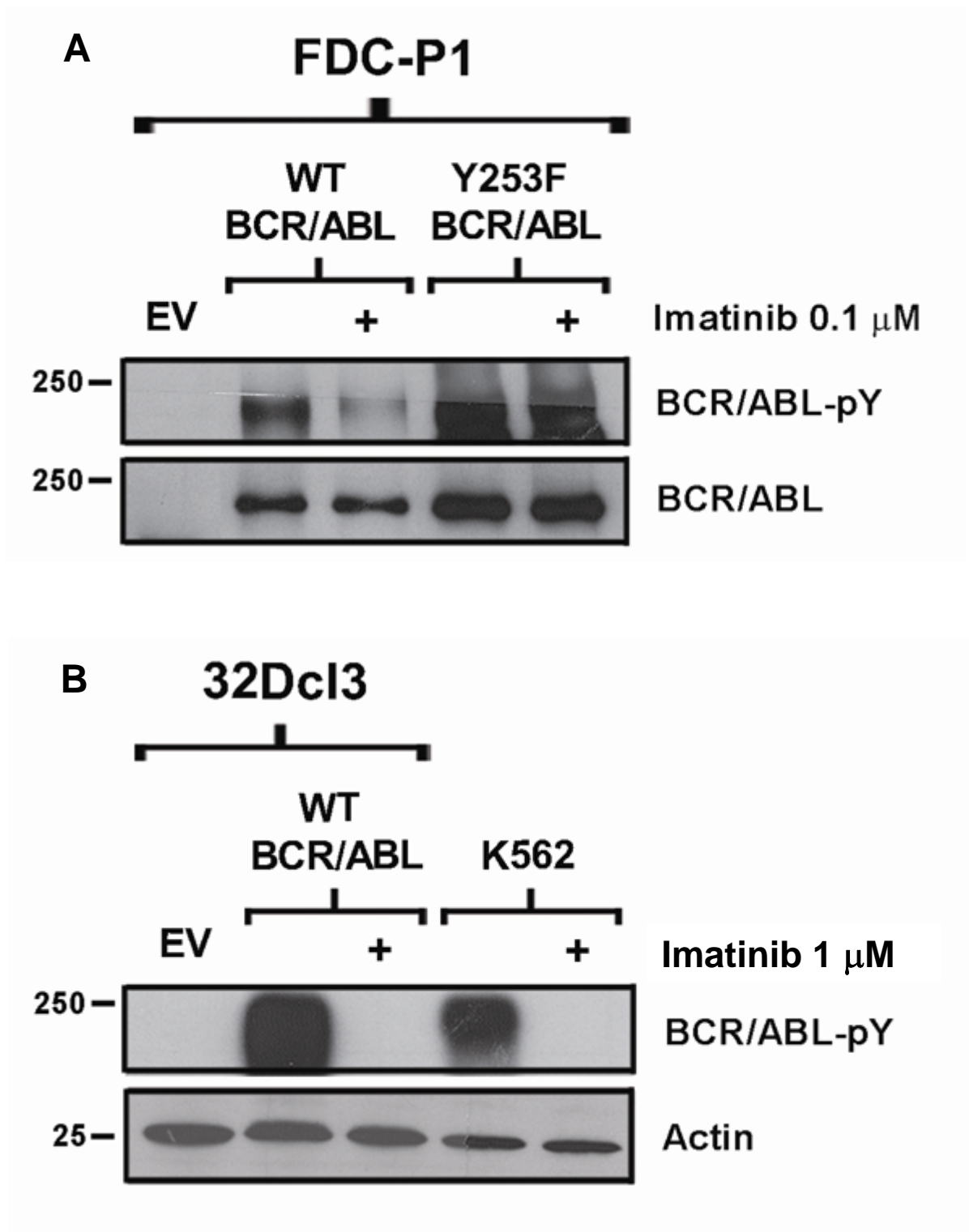


Figure 3.3 Inhibition of BCR/ABL phosphorylation with imatinib

A) FDC-P1 cells were treated without or with imatinib (0.1 μ M, 24 hours) and BCR/ABL was immunoprecipitated from whole cell lysates. The complexes were subjected to SDS-PAGE and probed by Western blotting with a phosphotyrosine (pY) or c-ABL antibody. **B)** 32Dcl3 and K562 cells were treated without or with imatinib (1 μ M, 24 hours). Whole cell lysates were subjected to SDS-PAGE and probed with a pY antibody. Actin was used a loading control. Blots are representative of two independent experiments.

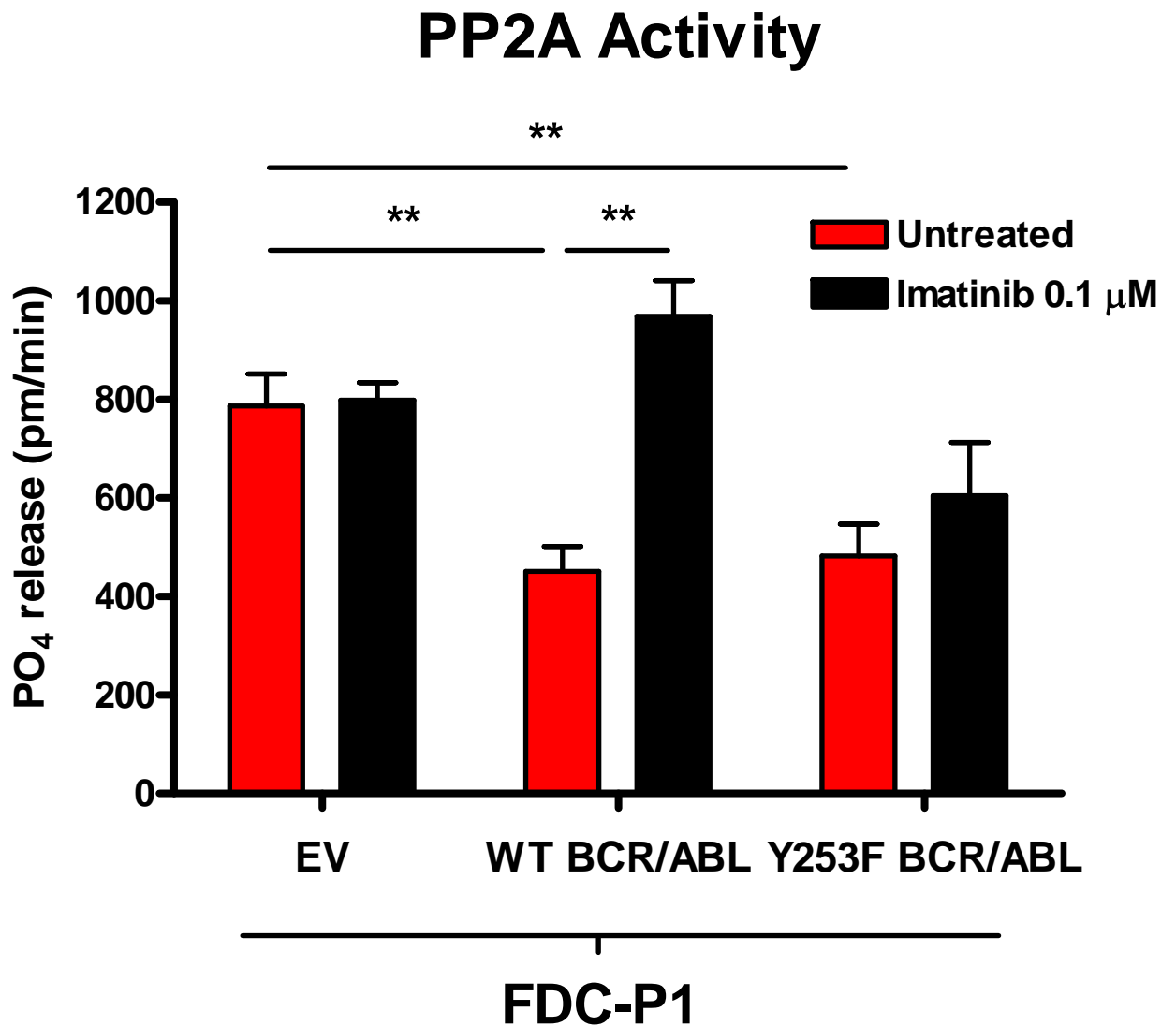


Figure 3.4 BCR/ABL inhibits PP2A activity in FDC-P1 myeloid progenitors

FDC-P1 cells were treated without (red) or with imatinib (0.1 μ M, 24 hours; black) and PP2Ac was immunoprecipitated from whole cell lysates. PP2A activity was determined by incubating the complex with a PP2A-specific phospho-peptide and measuring free phosphate (PO_4) release at an absorbance of 620 nm. *Columns*, mean PO_4 release (pm/min) from four independent experiments performed in duplicate; *bars*, SEM. ** $p < 0.01$, Student's t-test.

were detected in all cell lines. It is believed the additional band above the 41 kDa isoform in the FDC-P1 cells is a phosphorylated version of the protein. As previously reported, enhanced levels of SET correlated with BCR/ABL expression in the 32D-BCR/ABL cells (Figure 3.5) (Neviani et al. 2005). Inhibition of BCR/ABL kinase activity with imatinib (1 μ M, 24 hours) reduced SET expression in the 32Dcl3 cells back to control levels, and also resulted in the appearance of a lower molecular weight band (Figure 3.5). While total SET expression was not reduced in the K562 cells, there was a shift to expression of the lower molecular weight isoform with imatinib treatment (Figure 3.5). Surprisingly, the presence of BCR/ABL did not effect SET levels in the FDC-P1 cells (Figure 3.5), suggesting that additional molecular alterations are responsible for reducing PP2A activity in this cell line.

3.2.4.2 PP2A catalytic subunit expression

Next, a systematic analysis of PP2A subunit expression was conducted. In all four BCR/ABL⁺ myeloid progenitor cell lines, there was no change in the total expression of the catalytic subunit (PP2Ac) compared to their respective controls (Figure 3.6 and 3.7). PP2Ac is subject to post-translational modifications that can influence holoenzyme composition and activity. For example, phosphorylation at amino acid Tyr307 (p^{Y307}) can induce transient deactivation (Chen et al. 1992). To evaluate whether this is a mechanism contributing to impaired PP2A activity in BCR/ABL⁺ myeloid progenitors, the levels of PP2Ac-p^{Y307} were investigated. No significant differences were observed with BCR/ABL expression in the FDC-P1 or 32Dcl3 cell lines (Figure 3.6 and 3.7). Similarly, imatinib treatment had no effect on PP2Ac-p^{Y307} in the K562 cell line.

3.2.4.3 PP2A scaffolding subunit expression

Reduced expression of the PP2A structural subunit (PP2A A) has been observed in primary brain tumours compared to normal tissue (Colella *et al.* 2001), and is also associated with PP2A inhibition in B-CLL patient samples (Kalla *et al.* 2007). Unexpectedly, compared to empty vector controls, the levels of PP2A A were significantly enhanced 2-fold in FDC-P1 cells expressing both the WT and Y253F BCR/ABL oncoprotein (Figure 3.6 and 3.7). Inhibition of WT BCR/ABL with imatinib reduced this back to normal levels, whilst PP2A A expression remained elevated in the FDC-P1 Y253F BCR/ABL cells (Figure 3.6 and 3.7). Similarly, the structural subunit

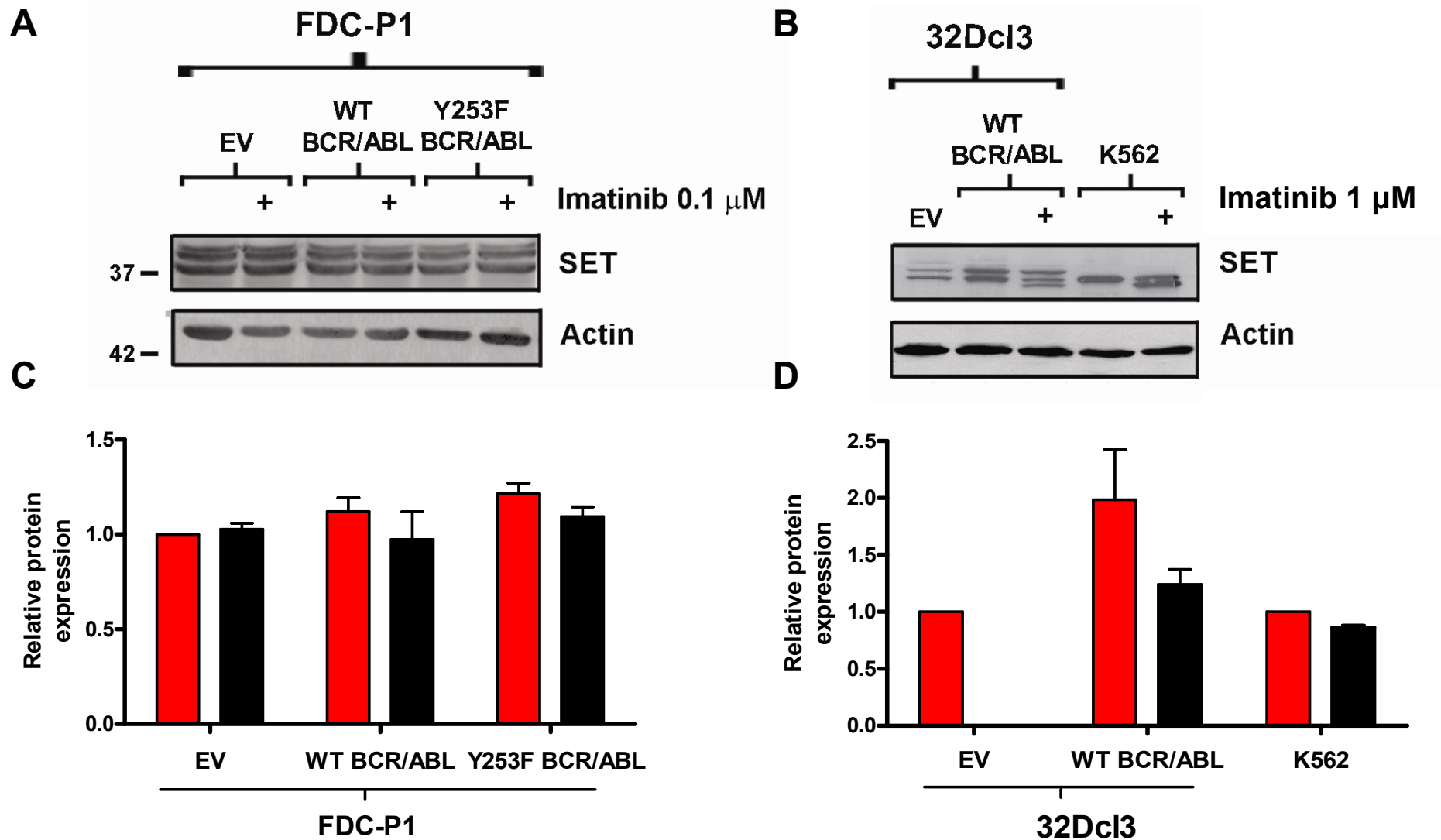


Figure 3.5 Expression of SET in BCR/ABL⁺ myeloid progenitors

A) FDC-P1 or **B)** 32Dcl3 and K562 cells were incubated without (red) or with imatinib (0.1 μ M or 1 μ M, 24 hours; black). Lysates were subjected to SDS-PAGE and probed for SET. Actin was used as a loading control. **C)** Quantitation of SET protein bands normalised to actin and relative to EV for FDC-P1 or **D)** 32Dcl3 and K562 cells. *Columns*, mean densitometry; *bars*, SEM; n=3.

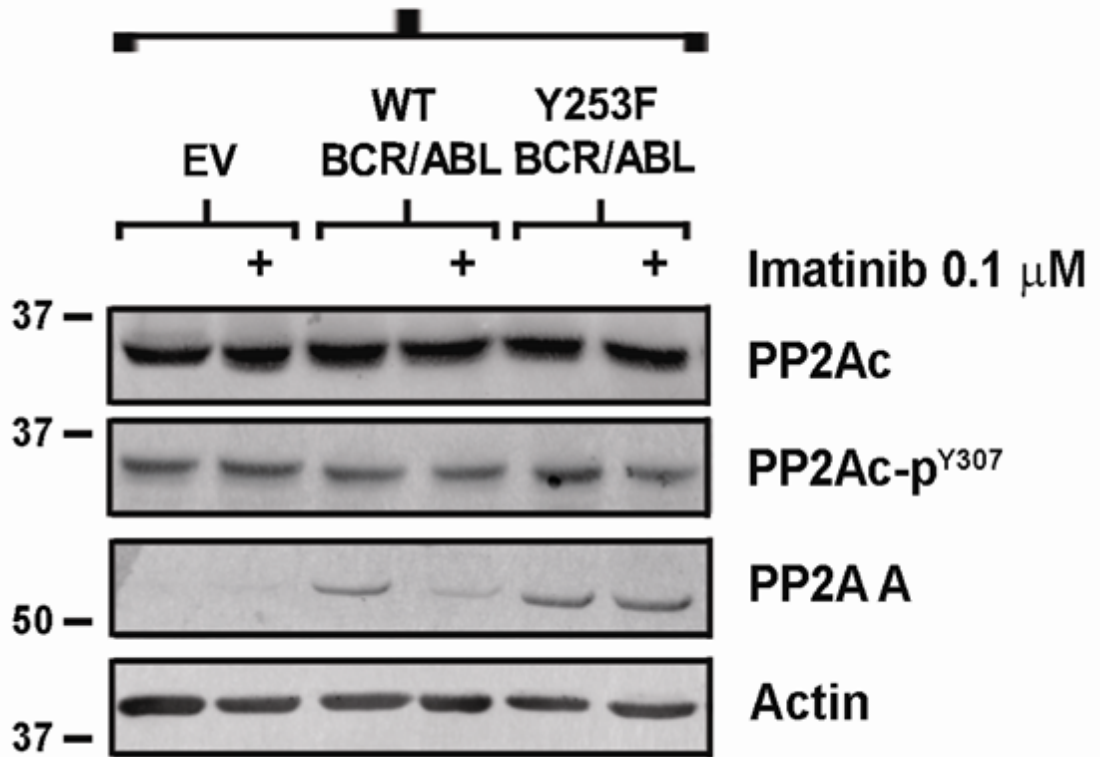
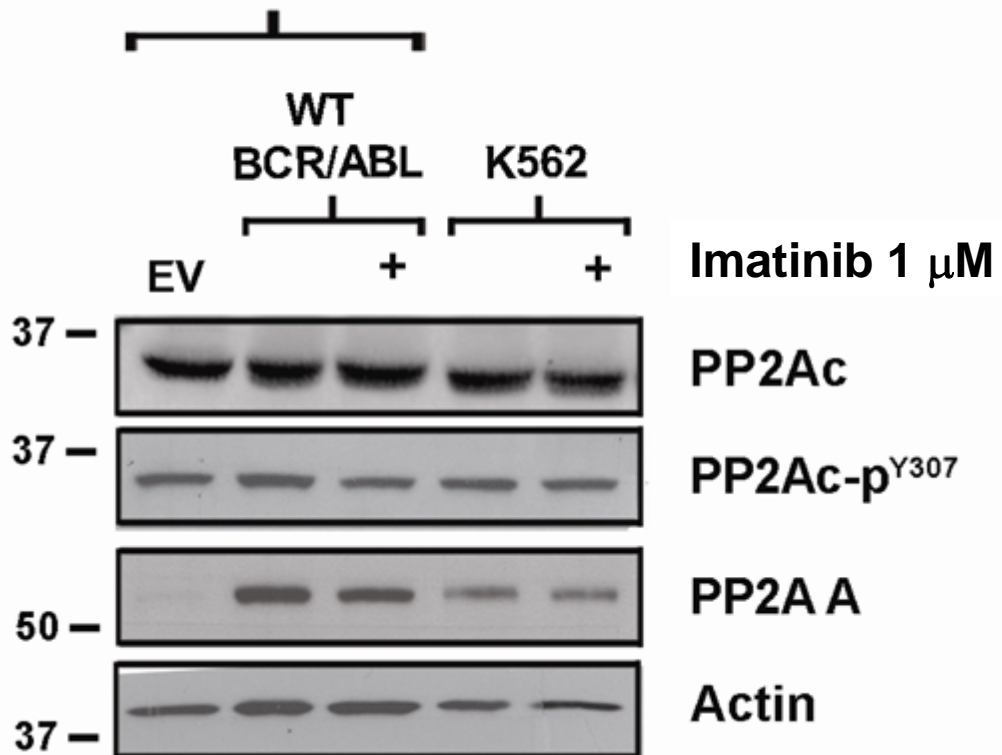
A**FDC-P1****B****32Dcl3**

Figure 3.6 Expression of PP2Ac and PP2A A in BCR/ABL⁺ myeloid progenitors
A) FDC-P1 or **B)** 32Dcl3 and K562 cells were incubated with or without imatinib (0.1 μ M or 1 μ M, 24 hours). Lysates were subjected to SDS-PAGE and probed for PP2Ac, PP2Ac-p^{Y307} and PP2A A. Actin was used as a loading control. Blots are a representative of four independent experiments.

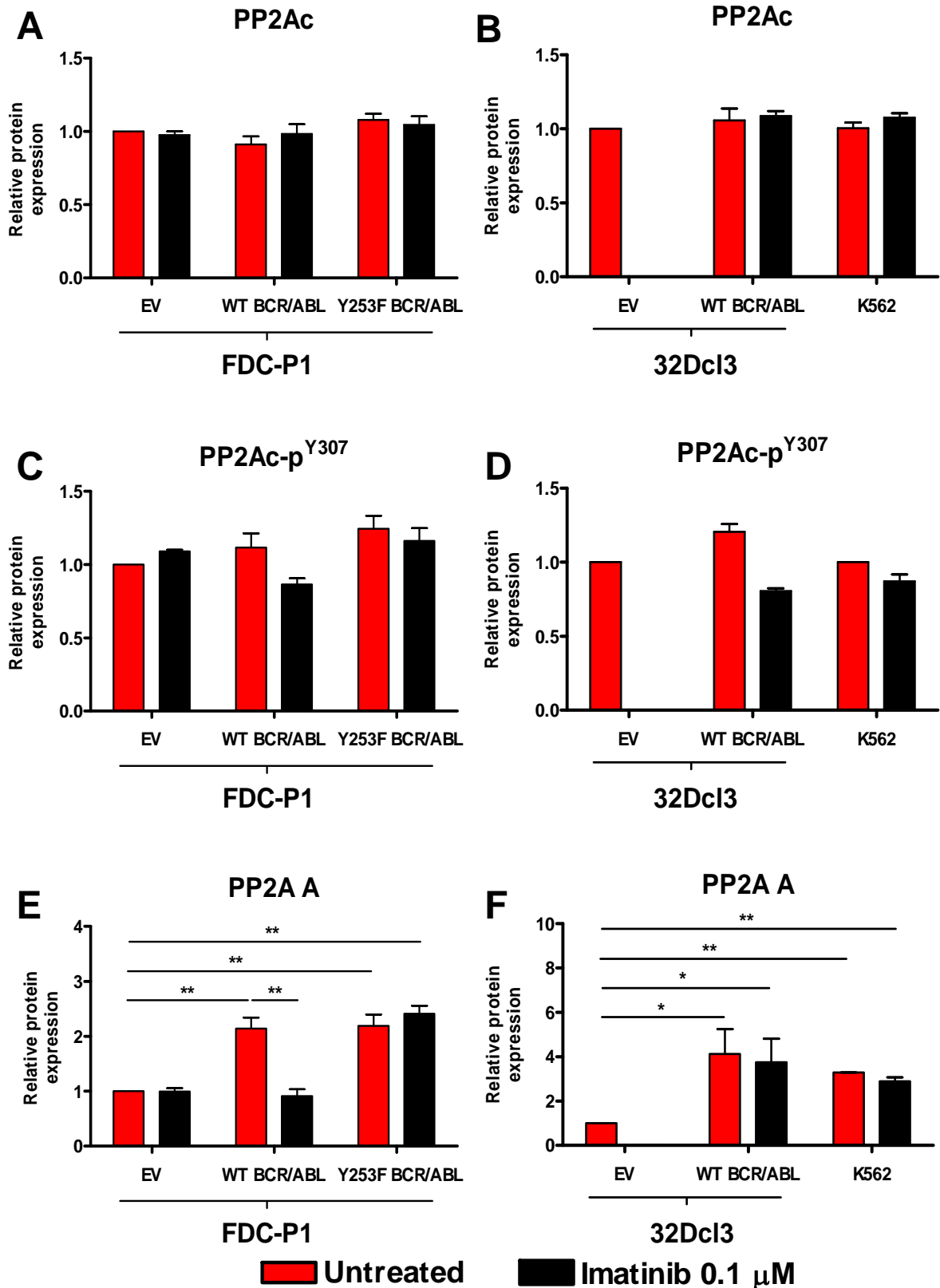


Figure 3.7 Quantitation of PP2Ac and PP2A A in BCR/ABL⁺ myeloid progenitors

Quantitation of PP2Ac, PP2Ac-p^{Y307} and PP2A A protein bands in FDC-P1 cells (A, C, E) or 32Dcl3 and K562 cells (B, D, F) treated without (red) or with imatinib (0.1 μM or 1 μM, 24 hours; black). *Columns*, mean densitometry normalised to actin, relative to EV; *bars*, SEM, n=4. *p<0.05, **p<0.01, Student's t-test.

was dramatically increased in 32D-BCR/ABL cells compared to the empty vector control; however, imatinib treatment did not appear to reduce PP2A A expression in this cell line or the K562 cells (Figure 3.6 and 3.7). In summary, these results demonstrate that BCR/ABL activity upregulates the PP2A scaffolding subunit in myeloid precursors, but its regulation by BCR/ABL inhibition is dependent on the cell line studied.

3.2.5 BCR/ABL alters the expression of PP2A regulatory subunits

It is widely accepted that PP2A substrate specificity and cellular distribution is determined by the binding of regulatory subunits (B) to the core AC dimer. As such, it is logical to predict that tumour suppressive function will be achieved through a distinct subset of PP2A complexes. To identify the specific components important for BCR/ABL-mediated inactivation of PP2A, the expression of individual B subunits was examined by immunoblotting

3.2.5.1 PP2A B55 subunit family expression

Depending on the cell-type and signalling pathway involved, the B55 α subunit can exert either a positive or negative effect on cellular proliferation and survival (Ory *et al.* 2003, Kuo *et al.* 2008, Zhang *et al.* 2009). Interestingly, BCR/ABL significantly enhanced the expression of B55 α nearly 2-fold in FDC-P1 and 32Dcl3 cells (Figure 3.8, 3.9 and 3.10). Treatment of all three WT BCR/ABL⁺ cell lines (FDC-P1, 32Dcl3 and K562) with imatinib resulted in a marked reduction of B55 α , highlighting a direct effect of BCR/ABL expression (Figure 3.8, 3.9 and 3.10). The B55 β and B55 γ isoforms are neuronal specific and were not detected in the FDC-P1, 32Dcl3 or K562 cell lines (data not shown) (Mayer *et al.* 1991, Zolnierowicz *et al.* 1994). The levels of B55 δ were not investigated by immunoblotting due to the lack of a suitable antibody.

3.2.5.2 PP2A B56 subunit family expression

The B56 family members have recently received much attention as key players in the tumour suppressive function of PP2A. In a similar observation to B55 α , the oncogenic kinase activity of BCR/ABL increased the expression of B56 α and B56 δ in FDC-P1 cells compared to empty vector controls (Figure 3.8 and 3.9). Imatinib treatment of FDC-P1 WT BCR/ABL cells reduced this back to normal levels, whilst Y253F BCR/ABL cells showed enhanced expression that was unaffected by imatinib (Figure

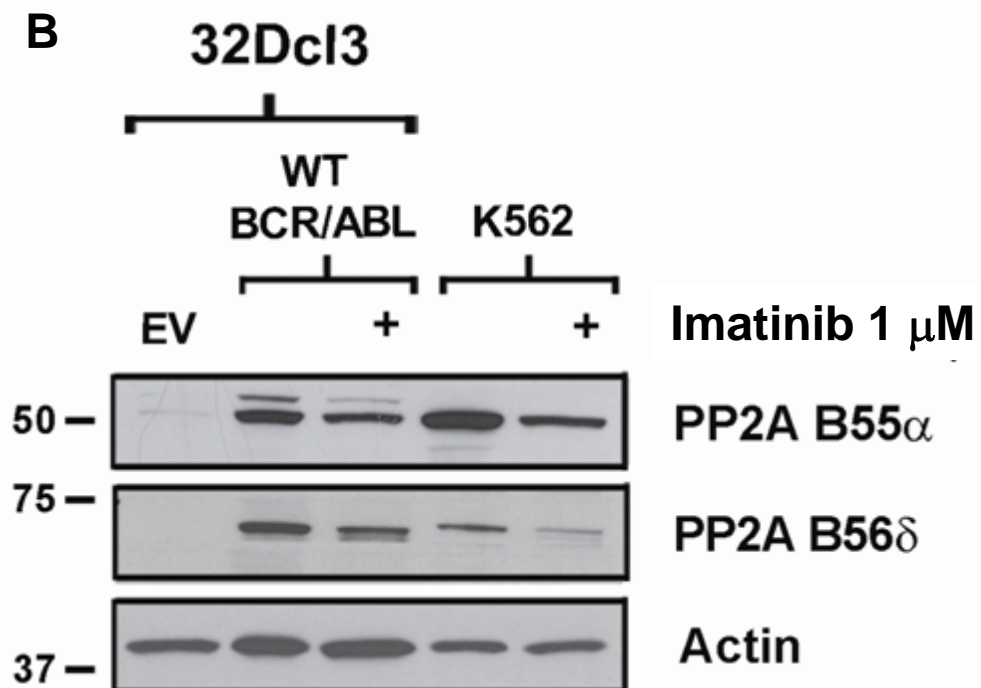
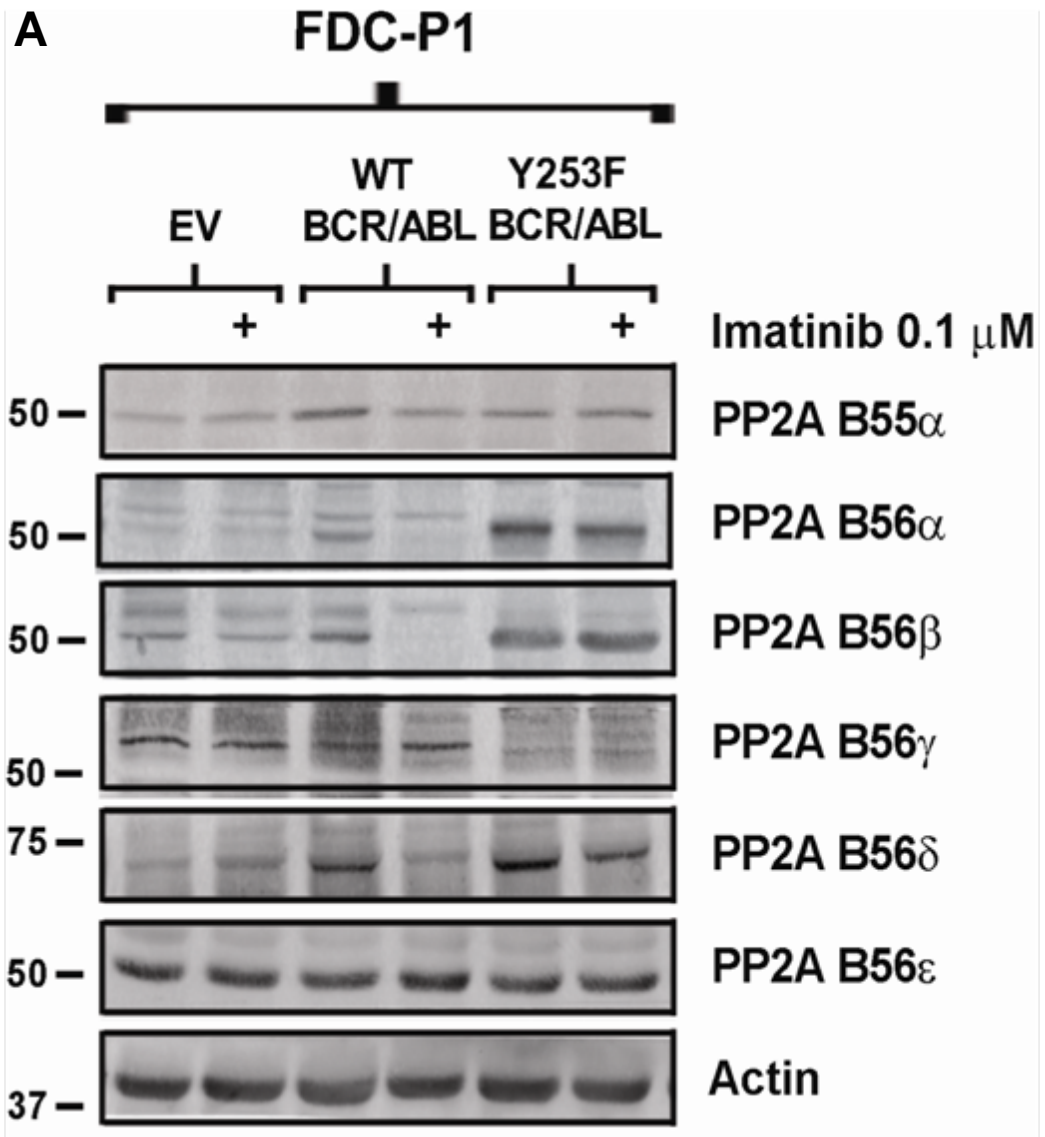


Figure 3.8 Expression of PP2A regulatory subunits in BCR/ABL⁺ myeloid progenitors

A) FDC-P1 or **B)** 32Dcl3 and K562 cells were incubated with or without imatinib (0.1 μ M or 1 μ M, 24 hours). Lysates were subjected to SDS-PAGE and probed for PP2A B55 α , B56 α , B56 β , B56 γ , B56 δ and B56 ϵ . Actin was used as a loading control. Blots are a representative of three independent experiments.

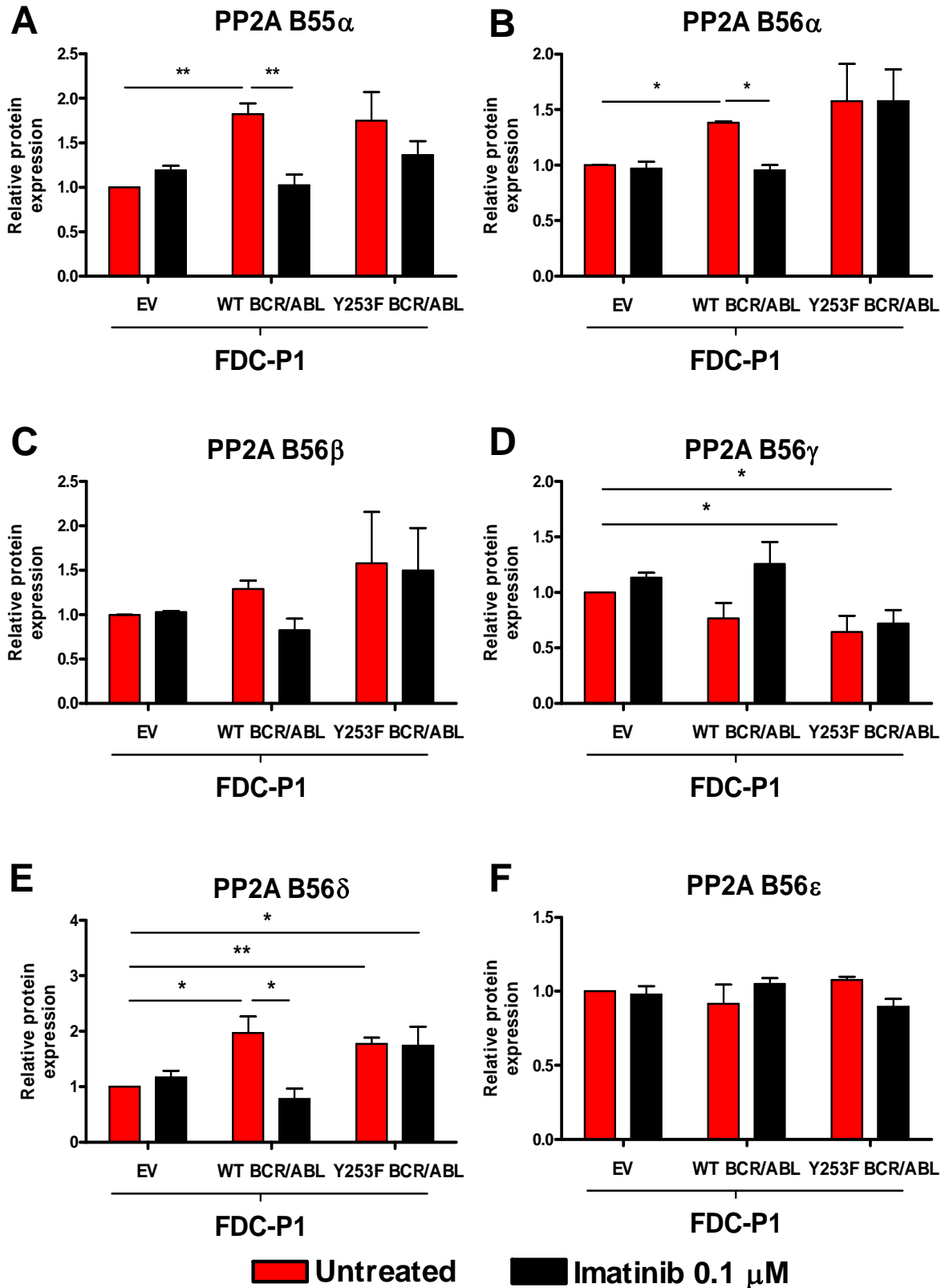


Figure 3.9 Quantitation of PP2A regulatory subunits in BCR/ABL⁺ FDC-P1 cells
 Quantitation of A) PP2A B55 α B) B56 α C) B56 β D) B56 γ E) B56 δ F) B56 ϵ protein bands in FDC-P1 cells treated without (red) or with imatinib (0.1 μ M, 24 hours; black). *Columns*, mean densitometry normalised to actin, relative to EV; *bars*, SEM, n=3. * p<0.05, ** p<0.01, Student's t-test.

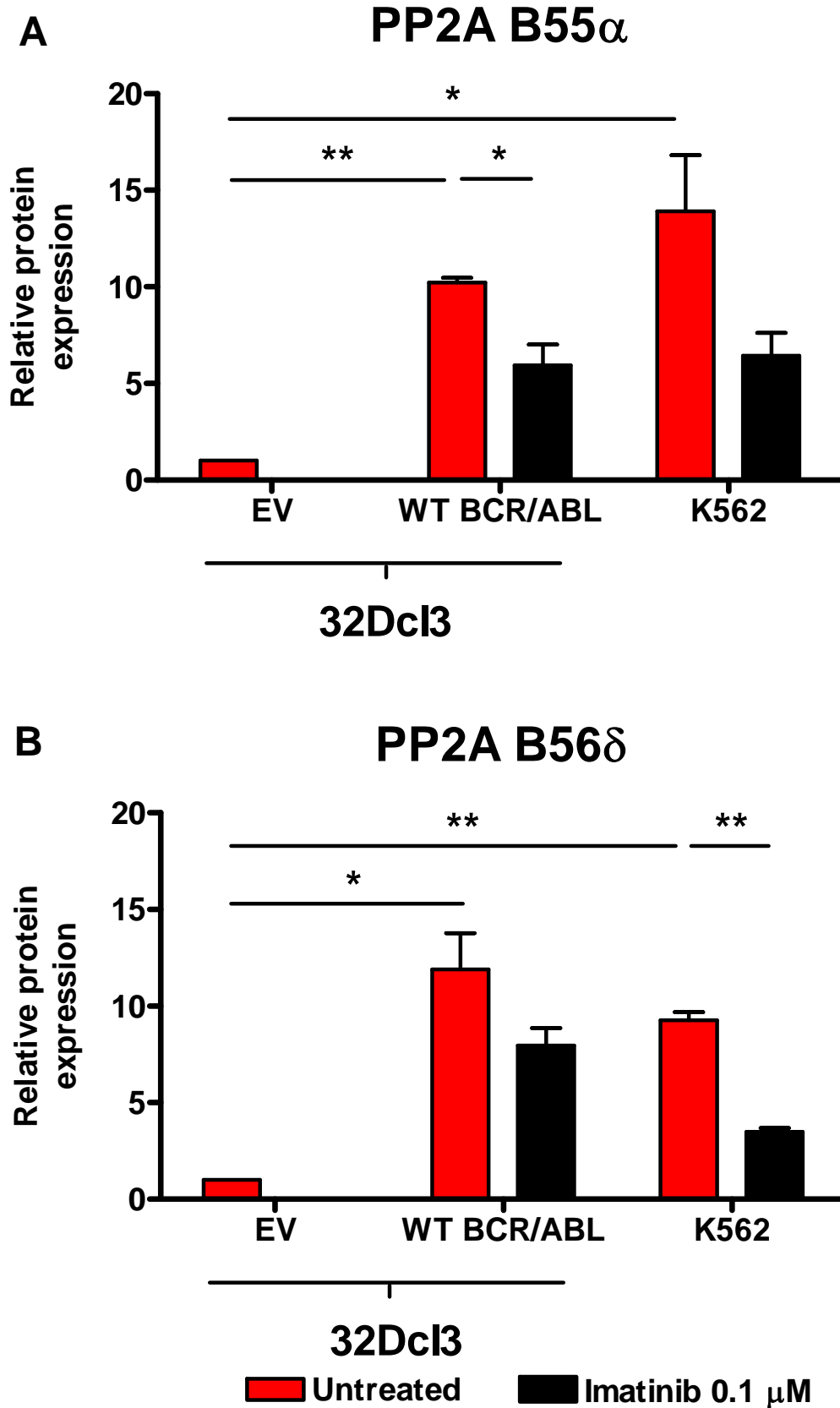


Figure 3.10 Quantitation of PP2A regulatory subunits in 32Dcl3 and K562 cells
 Quantitation of **A**) PP2A B55 α and **B**) B56 δ protein bands in 32Dcl3 and K562 cells treated without (red) or with (1 μ M, 24 hours; black). *Columns*, mean densitometry normalised to actin, relative to EV; *bars*, SEM, n=3. * p<0.05, ** p<0.01, Student's t-test.

3.8 and 3.9). These observations were confirmed for the B56 δ subunit in the 32Dcl3 and K562 cell lines (Figure 3.8 and 3.10). PP2A B56 β also showed a trend toward increased protein expression in FDC-P1 cells expressing BCR/ABL (Figure 3.8 and 3.9).

The B56 γ subunit contains at least 4 transcript variants with B56 γ 1, B56 γ 2 and B56 γ 3 being the most studied (Muneer *et al.* 2002, Martens *et al.* 2004). Based on the peptide sequence, the antibody used in this study is directed against the full-length 61 kDa isoform, B56 γ 3, and the slightly smaller B56 γ 2. According to the molecular weight (~61 kDa), the band detected in the FDC-P1 cells corresponds to B56 γ 3. Compared to empty vector controls, a decrease in B56 γ 3 expression was observed with active BCR/ABL, which reached significance in the Y253F mutant cells (Figure 3.8 and 3.9). Treatment with imatinib increased this back to normal levels in the WT BCR/ABL cells but had no effect on Y253F BCR/ABL, indicating that BCR/ABL kinase activity may also regulate B56 γ 3 (Figure 3.8 and 3.9). The final subunit evaluated in the FDC-P1 cell lines was B56 ϵ , which did not change with active BCR/ABL (Figure 3.8 and 3.9). In summary, these results highlight a common mechanism for PP2A regulation whereby the expression of B subunits is modulated by the BCR/ABL oncoprotein in myeloid progenitors.

3.2.6 PP2A mRNA levels in BCR/ABL⁺ FDC-P1 cells

The persistent expression of BCR/ABL in CML-CP promotes genetic instability and the accumulation of chromosomal abnormalities that contribute to the development of blast crisis (Calabretta & Perrotti 2004). As such, it is reasonable to predict that the aberrant expression of PP2A in BCR/ABL⁺ myeloid precursors may arise from altered gene transcription. To investigate this possibility, the mRNA levels of all PP2A subunits in the FDC-P1 cells were measured by quantitative real-time PCR (qRT-PCR), using primers that specifically detect each individual isoform (Table 2.4). The FDC-P1 empty vector controls were used as a calibrator to compare the expression of PP2A subunits in untreated FDC-P1 cells expressing WT and Y253F BCR/ABL.

Consistent with the western blotting data (Figure 3.6 and 3.7), BCR/ABL had no effect on the levels of either PP2A C α (PPP2CA) or PP2A C β (PPP2CB) in the FDC-P1 cells (Figure 3.11). Enhanced protein expression of PP2A A in BCR/ABL⁺ FDC-P1 cells was

not associated with a change in either PP2A A α (PPP2R1A) or PP2A A β (PPP2R1B) mRNA levels (Figure 3.11). No appreciable difference was observed with PP2A B55 α , B55 δ , B56 β , B56 γ , B56 δ or B56 ϵ (Figure 3.12 and 3.13). The only significant difference in gene expression was observed with PP2A B56 α (PPP2R5A), with transcripts in FDC-P1 cell lines expressing WT and Y253F BCR/ABL reduced to ~70% of empty vector control cells (Figure 3.13). Interestingly, this is opposite to the increased expression observed at the protein level. As with the immunoblotting, levels of the neuronal specific B55 β and B55 γ isoforms were undetectable (data not shown) (Mayer et al. 1991, Zolnierowicz et al. 1994). **Furthermore, no difference was observed with imatinib treatment (data not shown).** Thus, post-transcriptional aberrations most likely contribute to the enhanced protein expression of PP2A scaffolding and regulatory subunits observed in BCR/ABL⁺ myeloid progenitors.

In addition to the B55 and B56 family of PP2A subunits, the transcript of a third family member, PR72/PR130 (PPP2R3A), was investigated by qRT-PCR. Interestingly, mRNA levels of this gene were much less abundant in FDC-P1 cells expressing WT and Y253F BCR/ABL compared to negative controls (Figure 3.14). This observation highlights another potentially interesting subunit which may contribute to BCR/ABL-induced leukaemogenesis. A specific antibody was not available at the time to assess the corresponding protein levels. Lastly, examination of the PP2Ac binding partner, PTPA (PPP2R4), revealed no significant changes in the FDC-P1 WT and Y253F BCR/ABL cells compared to the empty vector (Figure 3.14).

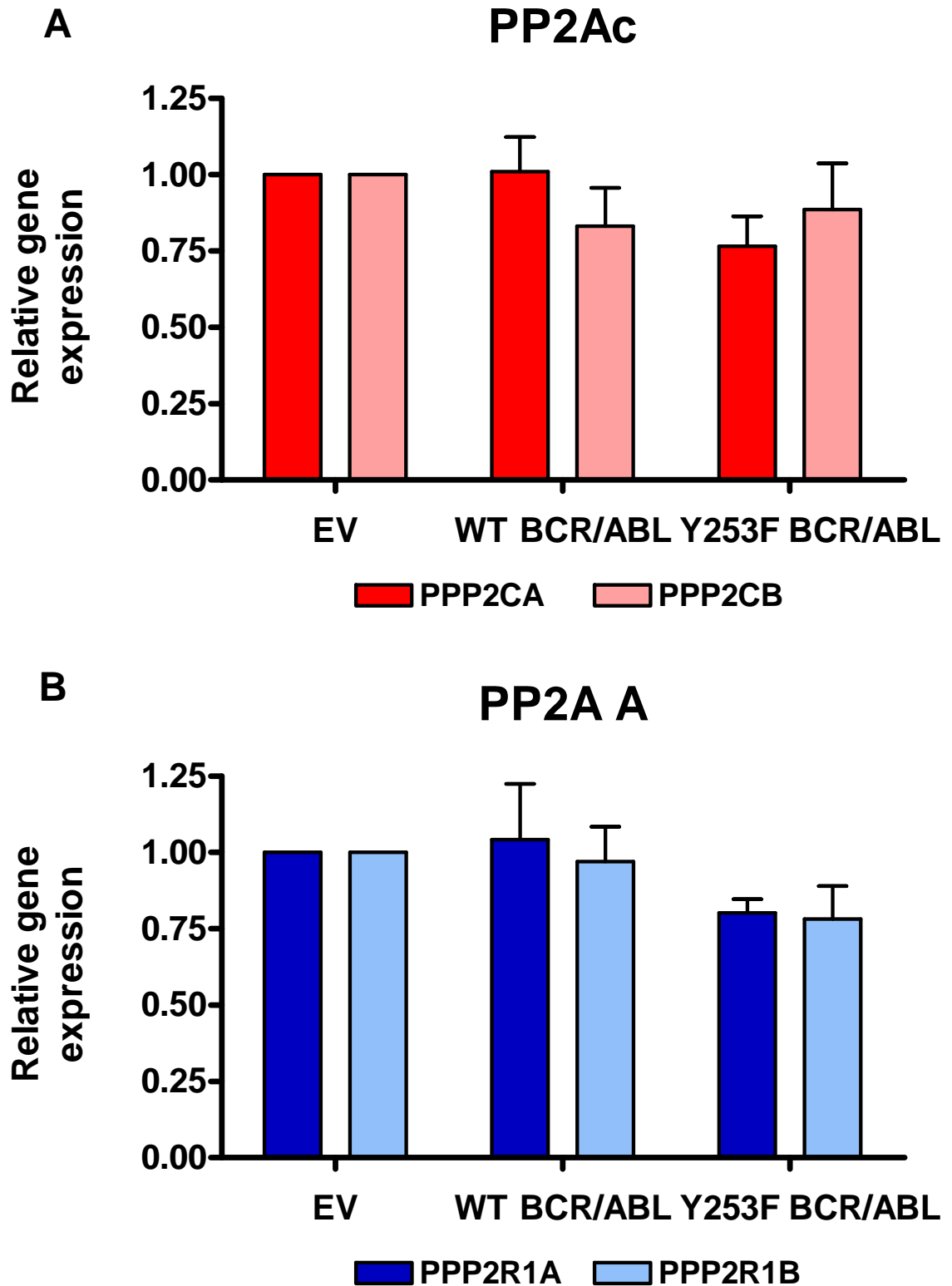


Figure 3.11 mRNA levels of PP2Ac and PP2A A in BCR/ABL⁺ FDC-P1 cells

Total RNA was extracted from untreated FDC-P1 cells and cDNA was generated by reverse transcription. Quantitative real-time PCR analysis detecting **A**) PP2A C α (PPP2CA) and C β (PPP2CB) or **B**) PP2A A α (PPP2R1A) and A β (PPP2R1B) was performed. Gene expression is relative to EV controls. *Columns*, mean of four independent experiments performed in triplicate; *bars*, SEM.

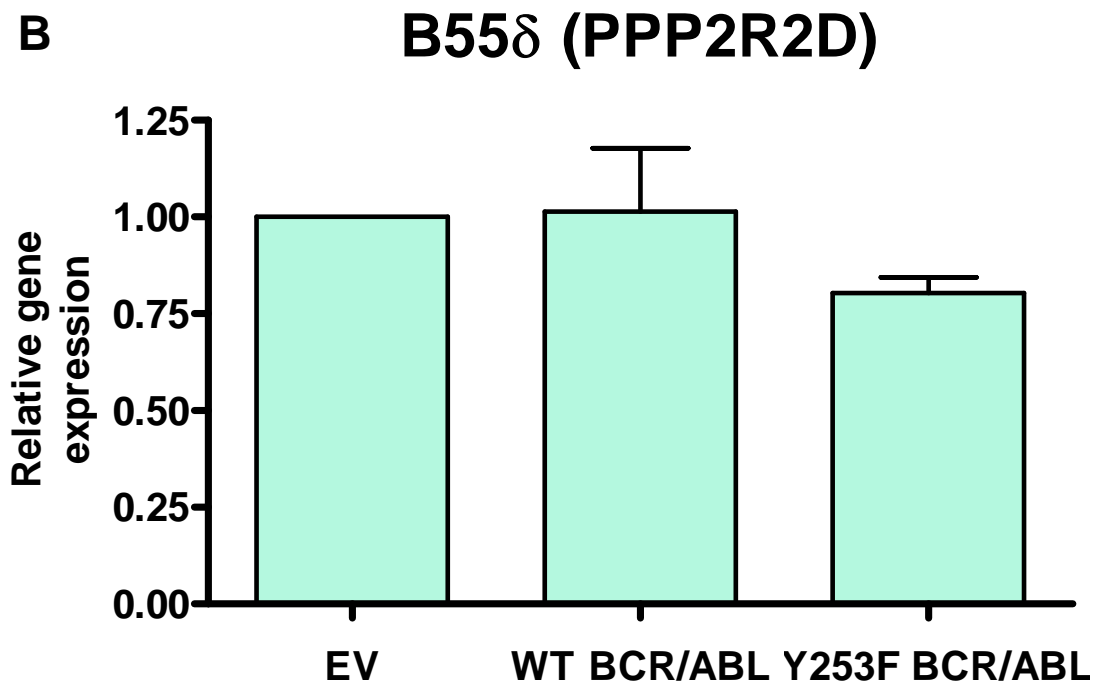
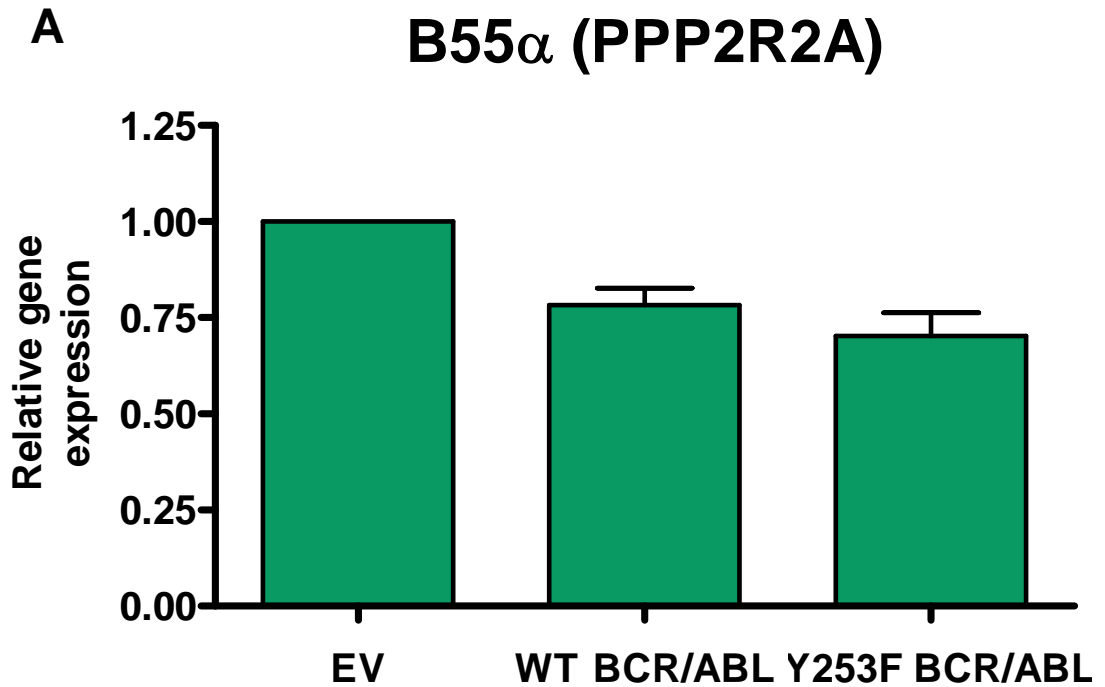


Figure 3.12 mRNA levels of PP2A B55 in BCR/ABL⁺ FDC-P1 cells

Total RNA was extracted from untreated FDC-P1 cells and cDNA was generated by reverse transcription. Quantitative real-time PCR analysis detecting **A**) PP2A B55 α (PPP2R2A) or **B**) B55 δ (PPP2R2D). Gene expression is relative to EV controls. *Columns*, mean of four independent experiments performed in triplicate; *bars*, SEM.

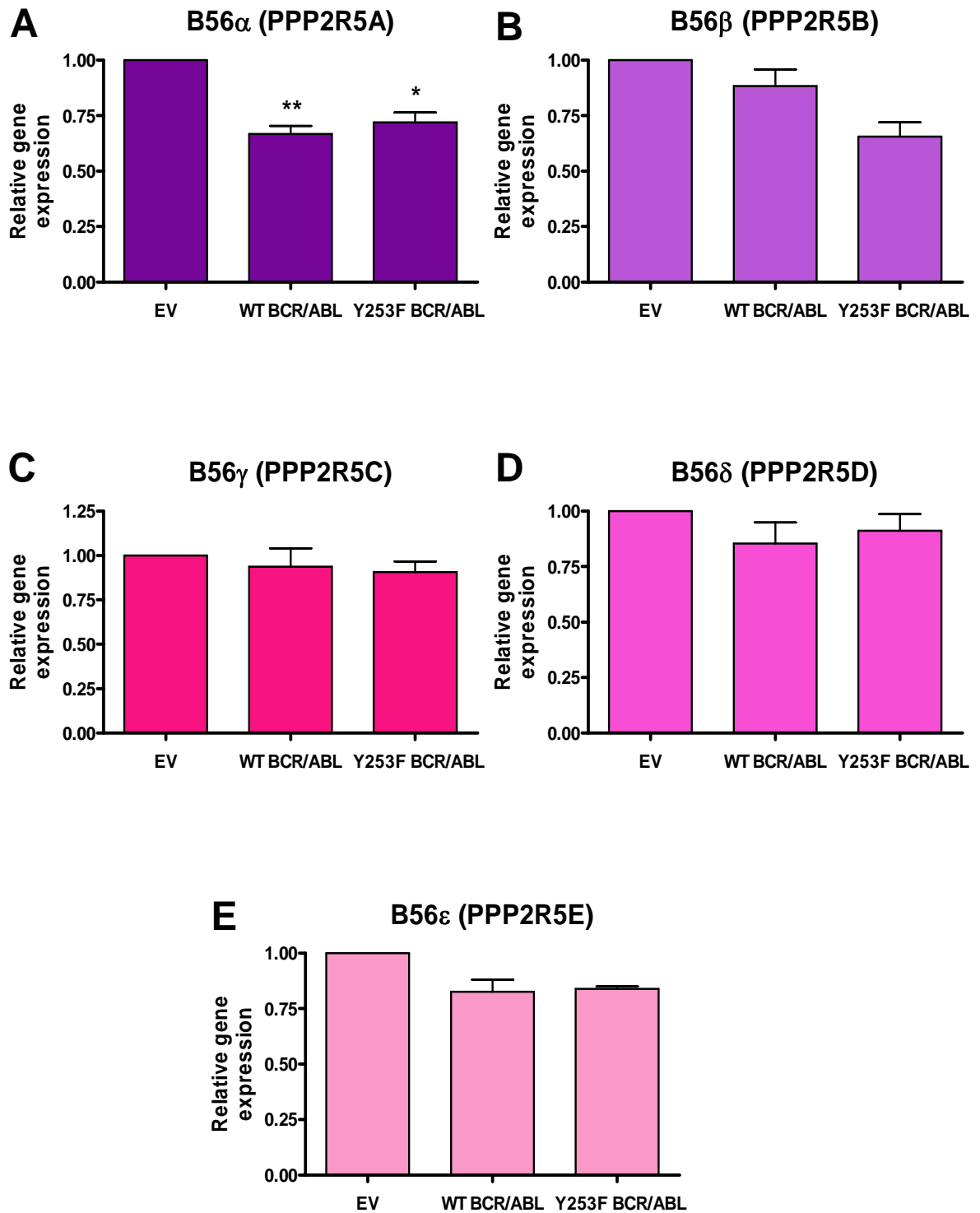


Figure 3.13 mRNA levels of PP2A B56 in BCR/ABL⁺ FDC-P1 cells

Total RNA was extracted from untreated FDC-P1 cells and cDNA was generated by reverse transcription. Quantitative real-time PCR analysis detecting **A)** PP2A B56 α (PPP2R5A) **B)** B56 β (PPP2R5B) **C)** B56 γ (PPP2R5C) **D)** B56 δ (PPP2R5D) or **E)** B56 ϵ (PPP2R5E). Gene expression is relative to EV controls. *Columns*, mean of four independent experiments performed in triplicate; *bars*, SEM. * $p < 0.05$, ** $p < 0.01$, Student's t-test compared to EV.

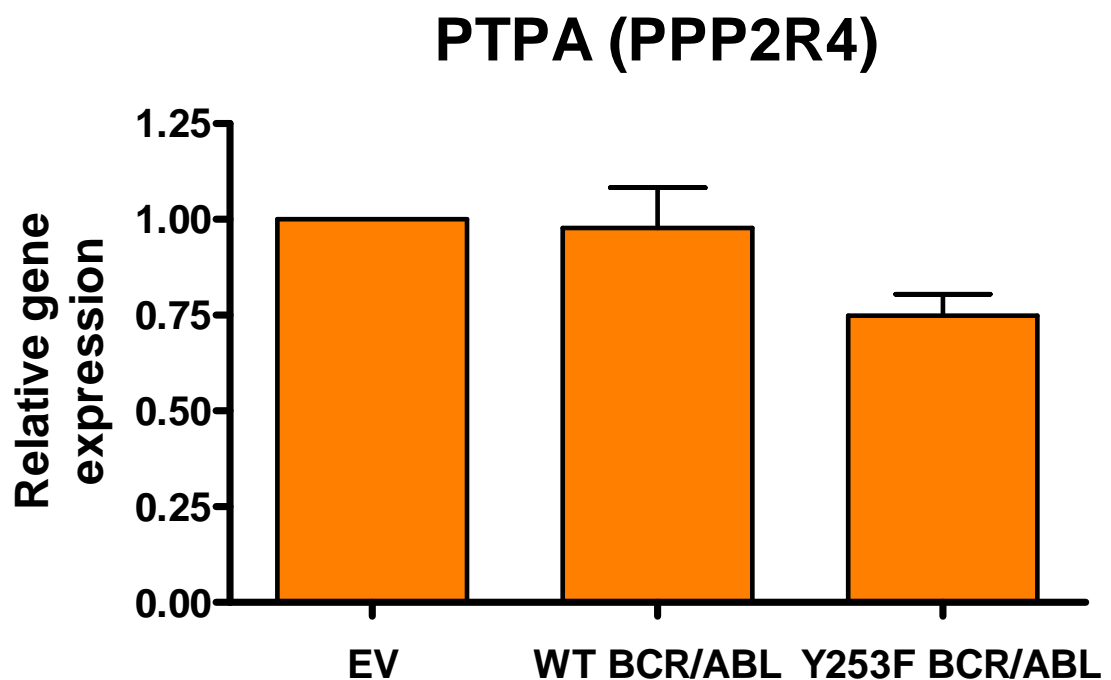
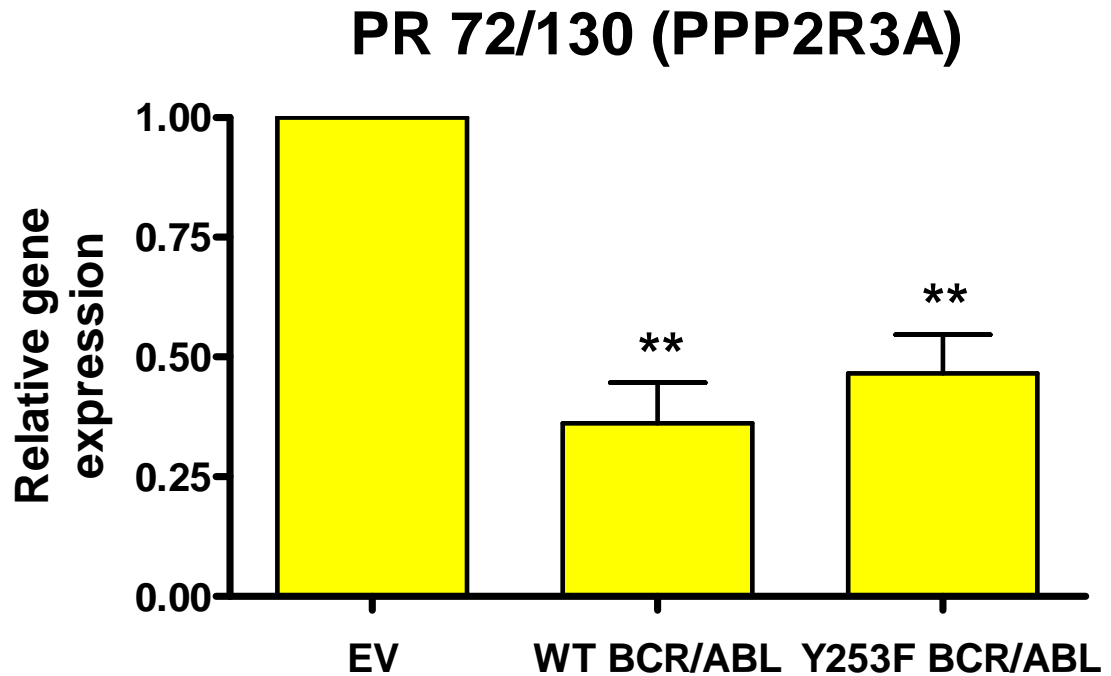


Figure 3.14 mRNA levels of PPP2R3A and PPP2R4 in BCR/ABL⁺ FDC-P1 cells
 Total RNA was extracted from untreated FDC-P1 cells and cDNA was generated by reverse transcription. Quantitative real-time PCR analysis detecting **A)** PP2A PR72/130 (PPP2R3A) or **B)** PTPA (PPP2R4). Gene expression is relative to EV controls. *Columns*, mean of four independent experiments performed in triplicate; *bars*, SEM. ** p<0.01, Student's t-test compared to EV.

3.2.7 BCR/ABL disrupts PP2A assembly in FDC-P1 cells

The results obtained thus far demonstrate that BCR/ABL modulates PP2A activity by upregulating specific enzyme components. This may appear counter-intuitive, but a likely scenario is that an abundance of certain subunits could disrupt normal binding dynamics and switch the global PP2A holoenzyme composition towards complexes which facilitate oncogenic signals. To address this issue, PP2A complexes were isolated from FDC-P1 cell extracts by immunoprecipitation with an anti-PP2Ac antibody. The complexes were separated by SDS-PAGE and immunoblotting was performed to detect the individual PP2A subunits bound to PP2Ac. The location of the heavy immunoglobulin chains at 55 kDa makes it difficult to identify the PP2A regulatory subunits B55 α , B56 α and B56 γ , which are approximately this size. To improve the visualisation of these subunits, the TrueBlotTM detection system was included in the experimental protocol. This unique secondary antibody preferentially binds to the non-reduced form of IgG over the reduced, SDS-denatured form, thus enabling detection of immunoblotted target bands without interference by the immunoprecipitating heavy chains.

In all experiments performed, the levels of isolated PP2Ac were similar between the FDC-P1 cell lines, serving as a normalisation control for protein recovery and gel loading. As PP2A A levels were increased in whole cell lysates (Figure 3.6), it was important to determine whether the enhanced availability of this subunit altered PP2A binding dynamics in the BCR/ABL⁺ FDC-P1 cells. As shown in Figure 3.15A, the affinity of PP2A A for PP2Ac remained unchanged in the BCR/ABL⁺ FDC-P1 cells compared to the empty vector controls. Next, the PP2A holoenzyme composition was determined by probing for the individual regulatory subunits. Despite the use of the TrueBlotTM reagent, the PP2A B55 α subunit was not detected in PP2Ac complexes isolated from the FDC-P1 cell lines (data not shown). This may also be a result of the experimental conditions used as the antibody does not detect methylated PP2Ac, which is required for PP2A B55 binding (Longin *et al.* 2007). However, increased association of the B56 α subunit to PP2Ac was observed with WT BCR/ABL expression (Figure 3.15A). The abundance of B56 β -containing holoenzymes remained the same for FDC-P1 cell lines expressing either the empty vector or WT BCR/ABL (data not shown).

Strikingly, the binding of B56 γ was depleted in FDC-P1 cells expressing BCR/ABL compared to the empty vector controls (Figure 3.15A). This is a very interesting result, as suppression of B56 γ has been shown to enhance tumourigenesis in other model systems (Chen *et al.* 2004). For an unknown technical reason, the 72 kDa B56 δ subunit was not detected in PP2Ac complexes isolated from all FDC-P1 cell lines (data not shown). To enable its evaluation, immunoprecipitation with an anti-PP2A A antibody was performed. Equal levels of the A subunit were isolated from all cell lines, with no appreciable differences observed in B56 δ subunit binding between FDC-P1 BCR/ABL⁺ and empty vector control cells (Figure 3.15B).

To improve the detection of PP2A B55 α , protein extracts from FDC-P1 cells were subjected to microcystin-affinity purification (Moorhead *et al.* 2007). Microcystin binds with nanomolar affinity to a specific pocket located above the active site in the catalytic subunit (Xing *et al.* 2006) and inhibits PP2A (MacKintosh *et al.* 1990). This strong interaction was exploited in the present study to isolate PP2Ac complexes from protein lysates by incubating them with microcystin-conjugated sepharose beads. A major advantage of this technique is the lack of interfering immunoglobulin heavy chains, which normally preclude protein visualisation at 50-55 kDa.

The levels of PP2Ac were similar between all FDC-P1 cell lines, indicating consistent pull down of PP2A complexes and gel loading (Figure 3.15C). As seen with the PP2Ac antibody immunoprecipitations (Figure 3.15A), no significant differences were noted in the affinity of PP2A A to PP2Ac in the BCR/ABL⁺ FDC-P1 cells compared to the empty vector controls (Figure 3.15C). Interestingly, FDC-P1 cells expressing either WT or Y253F BCR/ABL showed enhanced binding of the B55 α subunit to the core PP2A AC dimer, suggesting that an abundance of this subunit alters the exchange dynamics of PP2A complexes in BCR/ABL⁺ myeloid progenitors (Figure 3.15C). Based on the biochemical requirements for B55 α binding (Longin *et al.* 2007), it is predicted that the PP2Ac present in these immunoprecipitated complexes is associated with higher levels of methylation; however, this was not investigated due to the lack of a specific antibody. Taken together, these novel findings suggest that the BCR/ABL oncoprotein may regulate PP2A in FDC-P1 cells by inducing aberrant B subunit exchange and altering the normal holoenzyme composition. Specifically, an increase in B55 α and B56 α subunits appears to be associated with a decrease in B56 γ complexes.

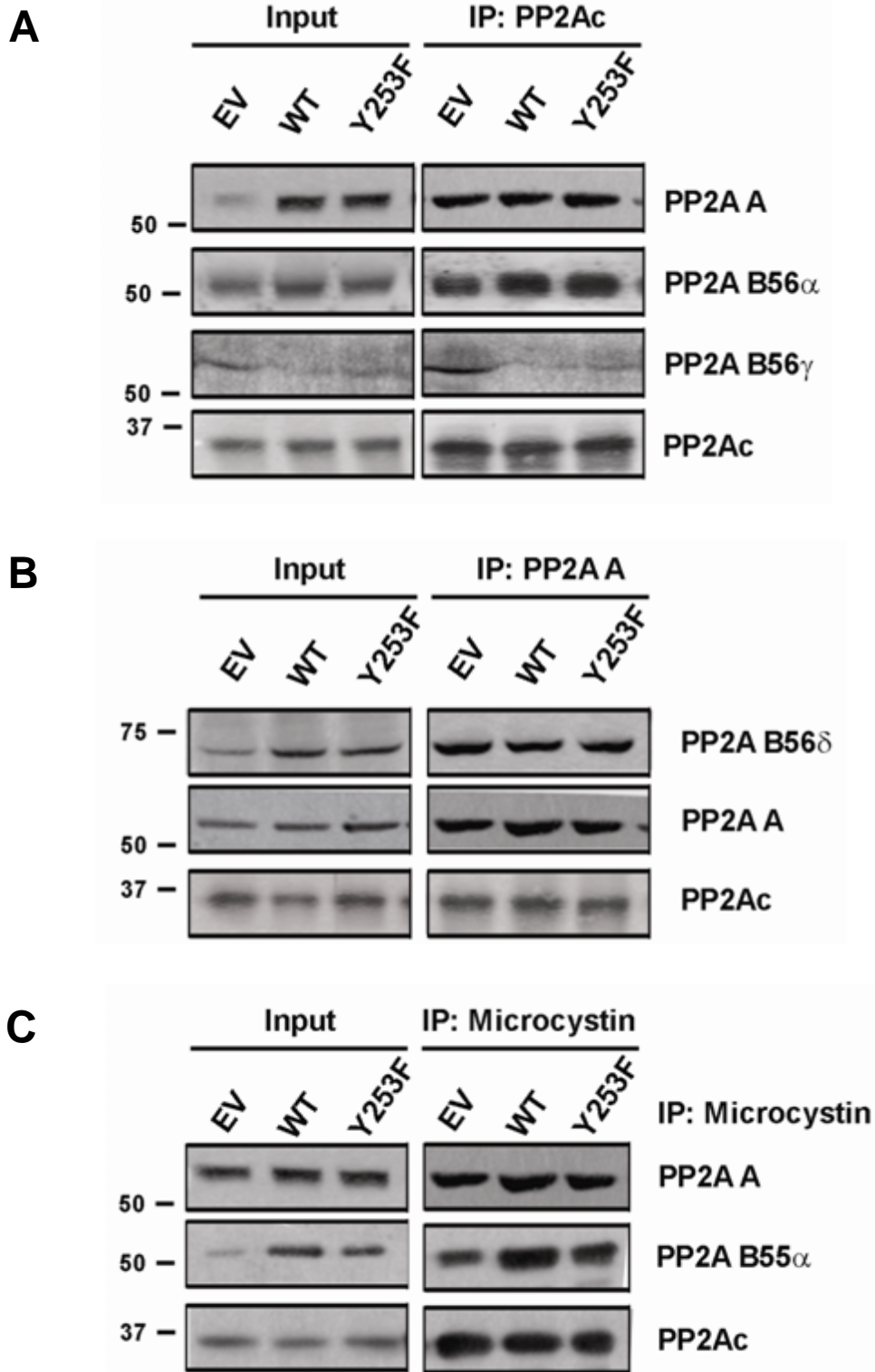


Figure 3.15 PP2A holoenzyme composition in BCR/ABL⁺ FDC-P1 cells

A) The PP2Ac subunit was immunoprecipitated from untreated FDC-P1 cell lysates. Complexes were separated by SDS-PAGE and probed for PP2Ac, PP2A A, and B56 α or B56 γ . **B)** The PP2A A subunit was immunoprecipitated from untreated FDC-P1 cell lysates. Complexes were separated by SDS-PAGE and probed for PP2Ac, PP2A A and B56 δ . **C)** PP2Ac complexes were isolated by microcystin-affinity purification. Complexes were separated by SDS-PAGE and probed for PP2Ac, PP2A A and B55 α .

3.3 Discussion

Although the mechanisms responsible for CML disease progression remain largely undefined, it is accepted that the unrestrained activity of BCR/ABL induces secondary alterations which contribute to the blast crisis phenotype (Calabretta & Perrotti 2004). Previous studies show that BCR/ABL functionally inactivates the tumour suppressor, PP2A (Neviani et al. 2005, Neviani *et al.* 2007). The major aim of this project was to identify the PP2A-associated mechanisms by which expression of BCR/ABL induces leukaemogenesis. Utilising mouse myeloid cell lines (FDC-P1 and 32Dcl3) and the human Ph¹ CML cell line, K562, this study confirms that constitutive activation of BCR/ABL inhibits the activity of PP2A. A detailed analysis at the mRNA and protein levels indicate that BCR/ABL augments the protein expression of several PP2A components, which alters the subunit binding dynamics and results in the formation of different PP2A holoenzymes.

Initial experiments confirmed that expression of WT or Y253F mutant BCR/ABL attenuates the activity of PP2A in FDC-P1 myeloid cells (Figure 3.4). The ability of the BCR/ABL kinase inhibitor imatinib to restore PP2A activity in FDC-P1 WT BCR/ABL cells indicates that BCR/ABL induces alterations which lead to functional inactivation of PP2A. This observation was previously found to be associated with increased expression of the endogenous PP2A inhibitor, SET, in 32D-BCR/ABL cells and CD34⁺ blast crisis progenitors (Neviani et al. 2005). The current study confirms the increased expression of SET in the 32D-BCR/ABL and K562 cell lines; however, this protein was unaffected by BCR/ABL in the FDC-P1 myeloid progenitors (Figure 3.5). The reason for this discrepancy remains unclear. Interestingly, a lower molecular weight SET band was detected in imatinib-treated 32D-BCR/ABL and K562 cells. The mechanisms underlying this observation are also not known. However, one possibility is that inactivation of BCR/ABL could result in reduced phosphorylation of SET and the subsequent removal of its inhibitory effect on PP2A.

Given that the PP2A heterotrimer is composed of multiple components, it was important to investigate the effect that BCR/ABL exerts on each individual subunit. No change was observed in the total expression of PP2Ac in WT or Y253F BCR/ABL FDC-P1 cells at the protein (Figure 3.6) or mRNA level (Figure 3.11). This result was not

surprising considering the levels of PP2Ac are tightly regulated at the transcriptional level (Baharians & Schonthal 1998), and minor fluctuations have a drastic effect on cell survival (Gotz et al. 1998). Post-translational modifications such as phosphorylation of PP2Ac are known to alter B subunit binding and reduce enzyme activity (Chen et al. 1992, Longin et al. 2007). The levels of PP2Ac phosphorylation were comparable between BCR/ABL⁺ FDC-P1 and 32Dcl3 cell lines and the empty vector controls, suggesting that alternate mechanisms are responsible for the reduction in PP2A activity (Figure 3.6).

While previous reports have shown that reduced PP2A activity and/or cell transformation is associated with mutated or decreased PP2A A subunit expression (Colella et al. 2001, Zhou *et al.* 2003, Wang *et al.* 1998), the results presented in this study clearly indicate that the levels of PP2A A are significantly increased in all four BCR/ABL⁺ myeloid cell lines compared to respective controls (Figure 3.6). Importantly, treatment with imatinib restored this expression back to normal in the imatinib-sensitive WT BCR/ABL cells, but had no effect on the imatinib-resistant Y253F BCR/ABL mutant. This identifies a molecular event which is unique to the transforming ability of the p210 kDa BCR/ABL oncoprotein. The mechanisms underlying this observation are currently unknown. However, no changes in mRNA expression were observed in the BCR/ABL⁺ FDC-P1 cells, suggesting regulation is most likely exerted at the post-transcriptional level (Figure 3.11). Furthermore, immunoprecipitation experiments showed no change in the levels of PP2A A associated with PP2Ac in FDC-P1 cells expressing BCR/ABL (Figure 3.15).

Mammalian cells utilise distinct translational mechanisms that tightly monitor the expression of PP2Ac (Baharians & Schonthal 1998). One important aspect of translational control that regulates PP2A A expression is mediated by the 5' UTR, which acts as a translational repressor due to an upstream AUG and stable stem-loop structure. Release of this translational inhibition leads to overexpression of PP2A A in COS-1 cells (Wera *et al.* 1995). In BCR/ABL⁺ myeloid progenitors, autoregulatory machinery may relieve this translational repression on PP2A A in an attempt to compensate for reduced PP2A activity. Alternatively, genomic instability induced by BCR/ABL itself may contribute to enhanced PP2A A levels. Investigating the activity of PP2A and expression of PP2A A in an inducible BCR/ABL model may aid in

determining the specific order of events. It is also possible that PP2A A interacts with substrates independently of PP2Ac; however, no studies to date have reported cellular functions for non-complexed PP2A A. Immunoprecipitating the PP2A A subunit and identifying additional binding partners in the BCR/ABL⁺ cells compared to the empty vector controls will provide insight into the functional role of increased PP2A A.

A detailed analysis of PP2A regulatory subunit expression also revealed several changes that were associated with BCR/ABL kinase activity. Specifically, active BCR/ABL augments the levels of PP2A B55 α , B56 α and B56 δ (Figure 3.8). Although a BCR/ABL⁻ control is not available for the K562 cell line, imatinib-treated cells showed reduced B55 α and B56 δ expression compared to untreated K562 cells. All together, this data indicates for the first time that constitutive activation of BCR/ABL in myeloid cells directly affects the expression of several PP2A components. [It should be noted that the use of cell lines does not accurately represent the clinical setting. Therefore, the investigation of PP2A activity and subunit expression in patient samples would confirm the relevance of these findings.](#)

In addition to altering the translational machinery, BCR/ABL kinase activity may also prevent the ubiquitination of PP2A subunits to result in enhanced protein stability. Proteasome-dependent degradation of the nucleocytoplasmic shuttling protein, FUS, is blocked in 32D-BCR/ABL cells and contributes to the leukaemic phenotype (Perrotti *et al.* 2000). Aberrant regulation of the ubiquitination process results in PP2Ac accumulation in Opitz G/BBB Syndrome (OS) (Schweiger & Schneider 2003). In this disease, patients express a mutated form of the E3 ubiquitin ligase, MID-1, which under normal circumstances interacts with $\alpha 4$ to facilitate the ubiquitin-mediated degradation of PP2Ac. The non-functional MID-1 present in OS patients is unable to bind with $\alpha 4$ and results in defective PP2Ac ubiquitination. An abundance of PP2Ac causes hypophosphorylation of microtubule associated proteins and contributes to the pathogenesis of OS (Trockenbacher *et al.* 2001). Whether BCR/ABL induces PP2A scaffolding and regulatory subunit expression by effectively blocking their ubiquitin-mediated degradation is unknown. However, it is an attractive theory considering enhanced [expression](#) of PP2A proteins, without a concomitant increase in mRNA expression, is a common observation in this study.

An obvious question arising from these results is how does the overexpression of certain PP2A components contribute to BCR/ABL-mediated leukaemogenesis? A possible explanation is that enhanced subunit levels alter the stoichiometry of PP2A assembly and disrupt an important complex that exerts tumour suppressive function. Indeed, loss of PP2A holoenzyme integrity is the mechanism by which ST induces tumourigenesis in mammalian cells (Chen *et al.* 2007). Subunit exchange *in vivo* most likely requires recruitable pools and the existence of mechanisms that regulate the stability and synthesis of appropriate subunits, which can be readily adapted according to demand. The aberrant expression of certain PP2A subunits by BCR/ABL could augment the formation of complexes which exert positive regulation on oncogenic pathways, thereby switching the cellular equilibrium towards pro-survival signals and enhancing transformation. In a study by Guo *et al.*, dissociation of B55 α from the PP2A AC dimer was observed in response to cellular stress and leads to activation of important cell cycle checkpoints in the Jurkat human T-cell lymphoma cell line (Guo *et al.* 2002). Although not proven, it is believed that the core dimer forms new complexes which direct PP2A activity towards substrates that exert negative regulation on cell cycle progression. This study demonstrates the importance of B subunit exchange in controlling normal cellular function.

To determine the effect of enhanced regulatory subunit availability on PP2A binding dynamics in BCR/ABL⁺ FDC-P1 cells, PP2A complexes were isolated and the individual holoenzyme compositions were assessed. In the FDC-P1 cell model, the association of B55 α and B56 α with PP2Ac was augmented by the expression of BCR/ABL (Figure 3.15). Several reports implicate B55 α as a positive regulator of the MAPK (Abraham *et al.* 2000, Ory *et al.* 2003, Adams *et al.* 2005, Dougherty *et al.* 2005) and Wnt/ β -catenin pathways (Zhang *et al.* 2009), whilst B56 α induces the ubiquitination and subsequent degradation of p53 (Okamoto *et al.* 2002). Extensive studies have shown the aberrant activation of these pathways is essential for BCR/ABL-mediated transformation (Steelman *et al.* 2004, Zhao *et al.* 2007, Wendel *et al.* 2006). Therefore, the enhanced recruitment of B55 α and B56 α -containing PP2A complexes may contribute to the leukaemic phenotype by facilitating the transmission of signals that confer proliferative and survival advantages.

A likely consequence of increased B55 α and B56 α binding to PP2Ac is the simultaneous dissociation of alternate subunits which are involved in the negative regulation of oncogenic pathways. In the current study, slightly reduced levels of B56 γ were observed in both BCR/ABL⁺ FDC-P1 cell lines (Figure 3.8), whilst mRNA expression remained unchanged (Figure 3.13). Interestingly, immunoprecipitation of PP2Ac showed decreased association of B56 γ in complexes isolated from BCR/ABL⁺ FDC-P1 cells compared to empty vector controls (Figure 3.15B). These observations suggest that depletion of B56 γ -containing PP2A holoenzymes in BCR/ABL⁺ myeloid progenitors may contribute to the leukaemic phenotype. In support of these findings, recent evidence implicates B56 γ as an important component directing the tumour suppressive function of PP2A. Specific suppression of B56 γ can substitute for ST in inducing tumourigenic transformation in the HEK-TER model (Chen et al. 2004, Moreno *et al.* 2004), and reduced B56 γ transcript levels have been reported in patients with aggressive B-CLL (Falt *et al.* 2005). Several lung cancer cell lines have undetectable B56 γ , and its overexpression partially reverses the tumourigenic phenotype (Chen et al. 2004). Furthermore, expression of a truncated B56 γ protein, Δ B56 γ 1, is associated with enhanced metastatic potential of the melanoma cell line, BL6 (Ito *et al.* 2000, Ito *et al.* 2003).

At present the specific substrates of PP2A B56 γ are unknown, with possible targets including p53 and the PI3K/Akt or Wnt/ β -catenin pathways (Westermarck & Hahn 2008). For example, B56 γ reportedly interacts with APC and axin to facilitate the formation of the β -catenin destruction complex, leading to destabilisation of β -catenin and inhibition of Wnt signalling in *Xenopus* embryos (Li et al. 2001). PP2A B56 γ holoenzymes have also been implicated in the stabilisation of p53 in response to DNA damage (Shouse *et al.* 2008). Depletion of B56 γ leads to activation of the anti-apoptotic Akt pathway in HEK-TER cells (Chen et al. 2005). In addition, expression of the Δ B56 γ 1 isoform results in impaired cell cycle checkpoint integrity and the acquisition of chromosomal aberrations, indicating that B56 γ also plays an important role in guarding genome integrity (Ito *et al.* 2003). As the constitutive activation of these pathways has been implicated in the development of CML (Coluccia et al. 2007, Honda et al. 2000, Skorski *et al.* 1995), the removal of negative regulation normally displayed by PP2A B56 γ is a possible contributing factor to BCR/ABL⁺ leukaemia growth.

The most striking difference arising from the gene expression analysis was the marked depletion of PPP2R3A (PR72/130) transcripts in FDC-P1 WT and Y253F BCR/ABL cells compared to empty vector controls (Figure 3.14). This finding is consistent with a recent study that reported depletion of PPP2R3A in several leukaemia cell lines and childhood ALL primary samples compared to normal blood or bone marrow (Dunwell *et al.* 2009). Interestingly, gene suppression was associated with hypermethylation of 5' CpG islands within the promoter region (Dunwell *et al.* 2009). An interesting follow on from the current project would be to investigate the methylation status of PPP2R3A in BCR/ABL⁺ FDC-P1 cells and CD34⁺ blast crisis progenitors. Further examination is also required to determine if the changes in PPP2R3A are reflected at the protein level, and to evaluate the functional consequences of this effect.

In this study, a systematic investigation of PP2A subunits was performed to elucidate the PP2A-associated mechanisms underlying BCR/ABL-driven transformation of myeloid progenitors. A unifying, and somewhat surprising, theme emerging from this body of work indicates that BCR/ABL upregulates the expression of several PP2A holoenzyme components. The functional consequence may be disruption of B subunit exchange which could facilitate the leukaemic phenotype by:

- 1) augmenting the formation of PP2A complexes that direct positive regulation of oncogenic pathways (e.g. B55 α and B56 α) (Figure 3.16A) and
- 2) displacing PP2A subunits which provide negative regulation on these signalling cascades (e.g. B56 γ) (Figure 3.16B).

Taken together, these findings provide new insight into the regulation of PP2A and begin to dissect the precise mechanisms by which BCR/ABL induces transformation via PP2A in CML. Importantly, the perturbed PP2A subunits, and their downstream substrates, may provide useful targets for the development of improved therapies for CML patients.

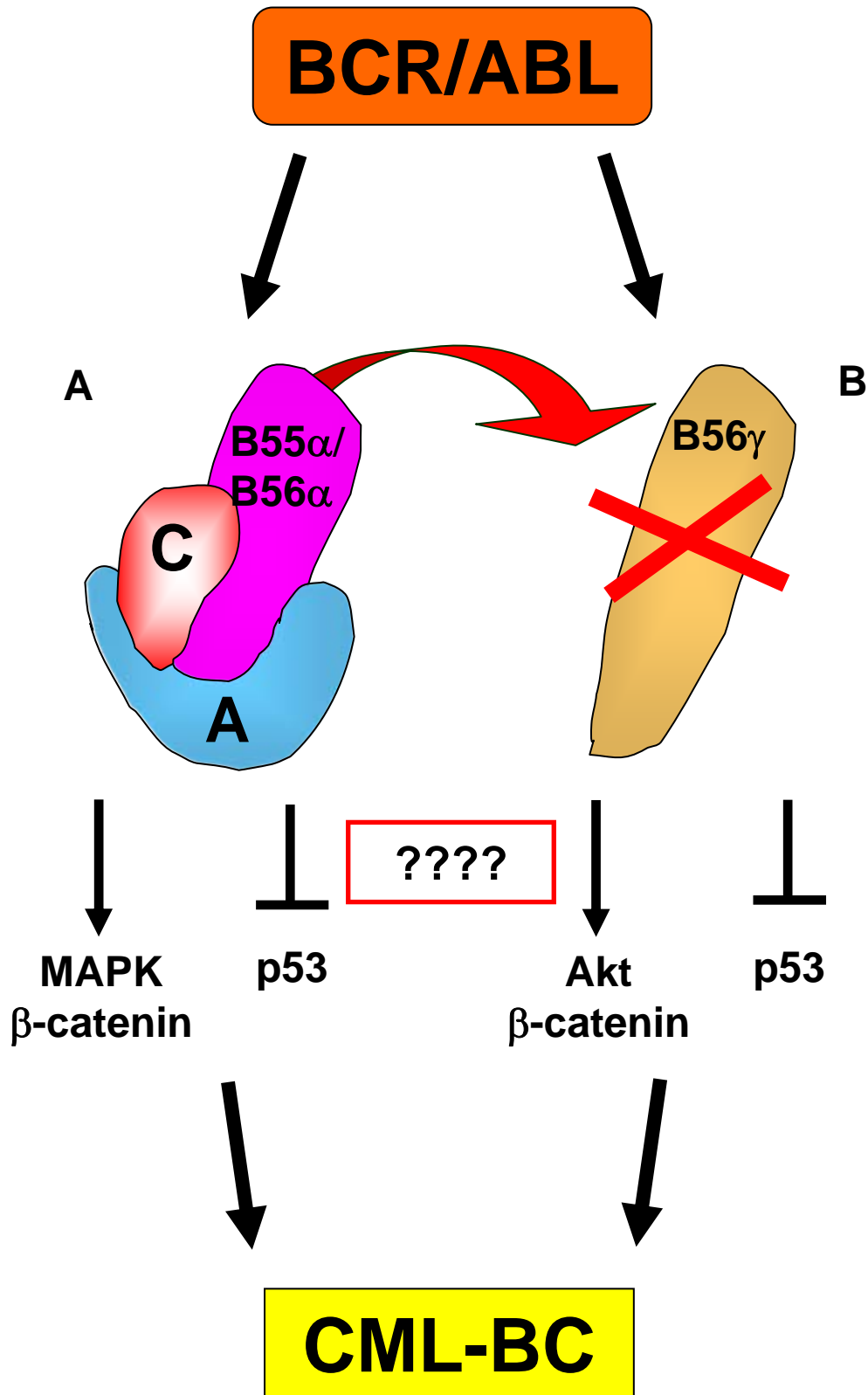


Figure 3.16 Proposed model for PP2A regulation by BCR/ABL in FDC-P1 cells

A) Enhanced formation of PP2A complexes containing B55α by BCR/ABL may activate certain pathways such as MAPK and Wnt/β-catenin. An abundance of PP2A complexes containing B56α in BCR/ABL⁺ cells could also inhibit p53. **B)** Simultaneous displacement of B56γ in BCR/ABL⁺ cells may result in aberrant regulation of Akt, β-catenin and p53.

CHAPTER 4

THE ROLE OF PP2A COMPLEXES IN BCR/ABL⁺ LEUKAEMOGENESIS

4.1 Introduction

The development of CML from the indolent chronic phase to the aggressively fatal blast crisis is associated with inhibition of the tumour suppressor, PP2A (Neviani *et al.* 2005, Neviani *et al.* 2007). Recent evidence indicates the tumour suppressive function of PP2A is dependent on regulatory subunit binding and the formation of distinct holoenzymes that govern substrate specificity (Westermarck & Hahn 2008). Prior to this study, no investigations had been undertaken to determine which particular PP2A subunits are involved in BCR/ABL-mediated leukaemogenesis.

The results presented in Chapter 3 identify a mechanism whereby overexpression, or increased association, of PP2A B55 α , B56 α and B56 δ may contribute to BCR/ABL-induced transformation of mouse myeloid progenitors (FDC-P1 and 32Dcl3) and the Ph¹ human K562 cell line. Immunoprecipitation findings suggest that an abundance of B55 α and B56 α may disrupt normal B subunit binding dynamics and facilitate the formation of PP2A holoenzymes that could contribute to increased proliferation and survival. Understanding the relative functional importance of these complexes in CML progression will provide critical insight into the biology of PP2A.

The major aim of this Chapter was to investigate the functional role of PP2A holoenzymes in BCR/ABL⁺ leukaemia growth. To address this issue, the individual PP2A subunits B55 α , B56 α and B56 δ were targeted with specific shRNA in FDC-P1 WT BCR/ABL cell lines. In this procedure, the shRNA sequences were cloned into a retroviral vector and delivered into the cell via retroviral infection. An RNA polymerase III promoter upstream of the shRNA is utilised to express the specific sequence within the nucleus (Figure 4.1). The shRNA is then actively exported to the cytoplasm, where it is recognised and cleaved by the RNase III enzyme Dicer to produce a double-stranded short interfering RNA (siRNA). One strand of each siRNA molecule is incorporated into a cytoplasmic, multi-protein RNA-Induced Silencing Complex (RISC) and serves as a guide for locating complementary target mRNAs.

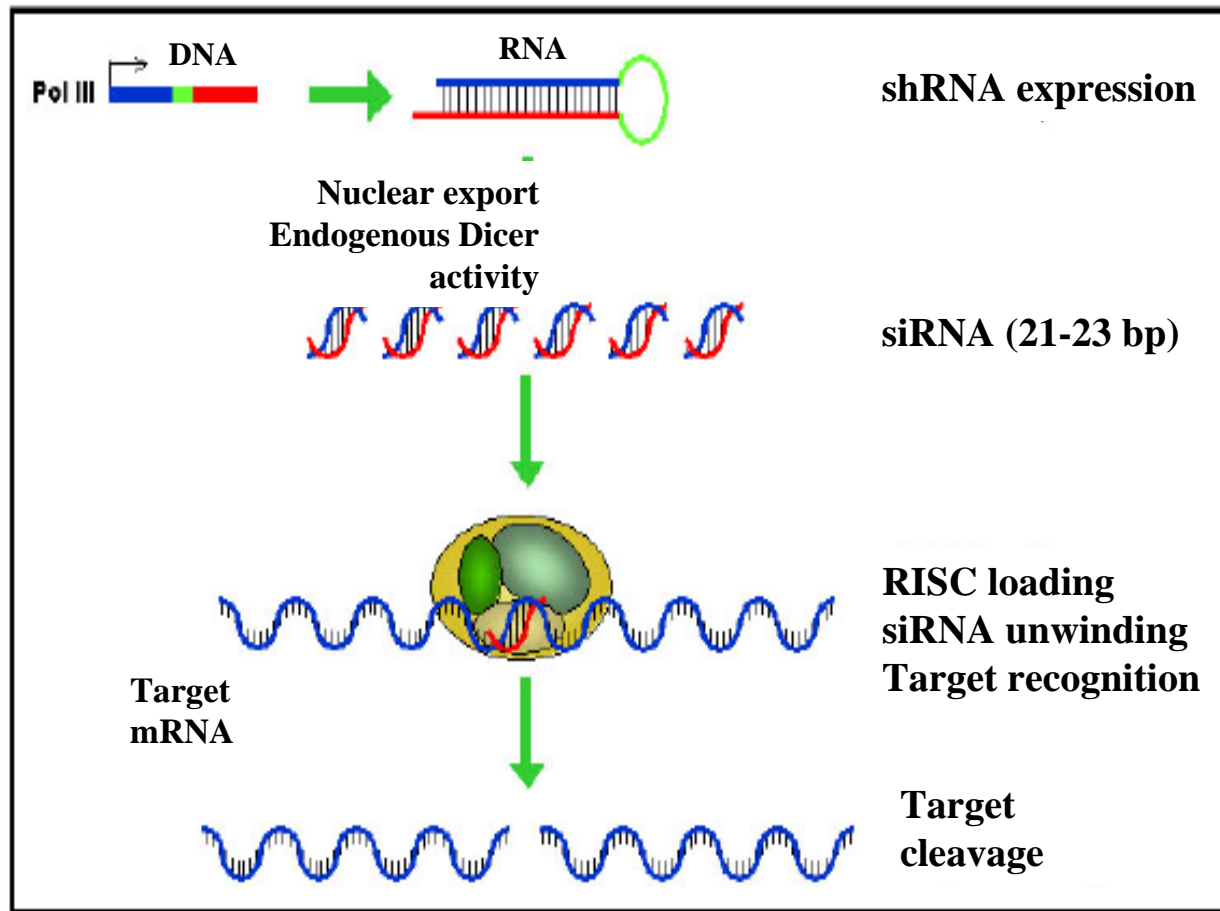


Figure 4.1 shRNA-mediated gene silencing in mammalian cells

Within the nucleus, shRNA sequences are transcribed by RNA polymerase III (Pol III). These are exported to the cytoplasm and cleaved by Dicer to produce a double-stranded siRNA. Each strand is then incorporated into RISC, which locates and cleaves complementary target mRNAs to result in gene suppression.

Upon recognition and binding, a RISC-associated nuclease cleaves the target RNA which is then degraded by cytoplasmic exonucleases (McManus & Sharp 2002). The expression of shRNA enables prolonged gene silencing and is a powerful tool which permits the analysis of loss-of-function phenotypes.

4.2 Results

4.2.1 Subcloning of shRNA B56 δ into pSR

The pMKO.1-GFP retroviral vector containing either no shRNA sequence (pMKO-EV), or sequences targeting PP2A B55 α (shB55 α) or B56 α (shB56 α) were obtained from Addgene Inc. (deposited by Prof. William Hahn), and have been previously verified (Table 2.1) (Chen *et al.* 2004). It was necessary to subclone the shRNA sequence for B56 δ from pSUPER.basic (provided by Prof. Stefan Strack) into the retroviral vector pSUPER.retro.neo+GFP (pSR) (provided by A/Prof. Danilo Perrotti). Both constructs were digested with HindIII/EcoRI and the shRNA insert from pSUPER.basic was ligated into the empty vector backbone of pSR to generate pSR-shB56 δ . Several clones were isolated and successful ligation was confirmed by sequencing. A correct clone was expanded and the purified plasmid was obtained for transfection into the Phoenix retroviral packaging cell line.

4.2.2 Stable knockdown of PP2A regulatory subunits in FDC-P1 WT BCR/ABL cells

To investigate the specific role of PP2A B55 α , B56 α and B56 δ enzyme complexes in BCR/ABL-induced leukaemogenesis, shRNA constructs directed against these subunits were introduced into the FDC-P1 WT BCR/ABL cell line. The bicistronic retroviral vectors pMKO and pSR direct simultaneous expression of the shRNA sequences and GFP. Following retroviral infection, the top 10% of GFP⁺ FDC-P1 cells were isolated [from a heterogeneous population by fluorescence-activated cell sorting \(FACS\)](#) (Figure 4.2). All cell lines were monitored for GFP expression on a routine basis, and were not passaged for longer than 3 weeks. Notably, the degree of GFP intensity differed between each cell line. After one sort, the percentage of GFP⁺ cells increased dramatically in the FDC-P1 WT BCR/ABL pMKO empty vector population, whilst this level of expression was achieved in the shB56 α population after two enrichments (Figure 4.2A and C). The GFP intensity in FDC-P1 WT BCR/ABL

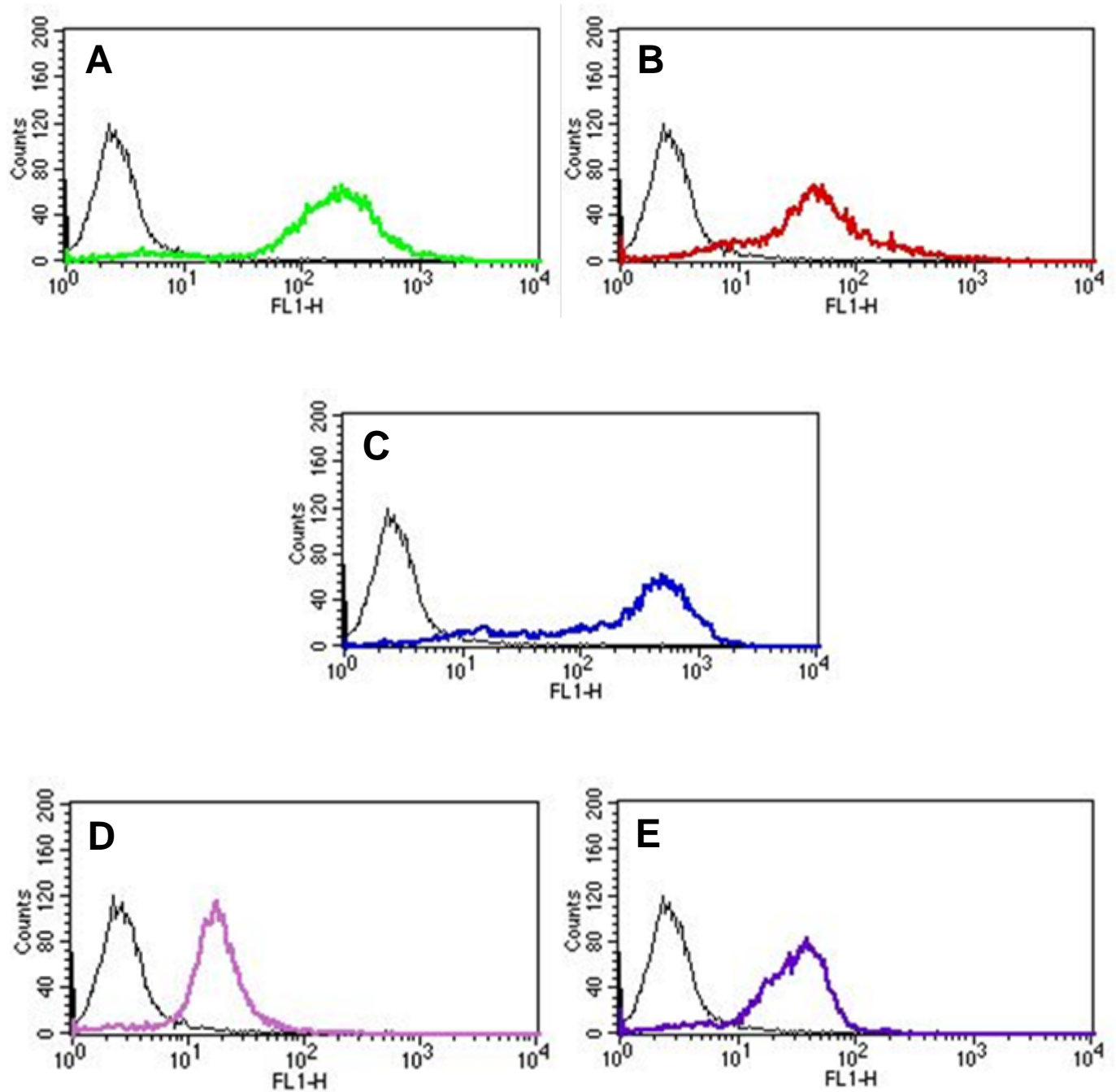


Figure 4.2 Expression of GFP in shRNA-WT BCR/ABL FDC-P1 cell lines

FDC-P1 WT BCR/ABL cells expressing either **A)** pMKO or **D)** pSR empty vectors, or shRNA directed against **B)** B55 α **C)** B56 α and **E)** B56 δ were sorted from a heterogeneous population based on GFP intensity (FL1-H). Flow cytometry plots were obtained from a FACSCalibur. Untransfected FDC-P1 WT BCR/ABL cells were used as a negative control for GFP expression (black line).

shB55 α cells was one log less than pMKO-EV, and further sorting did not improve this (Figure 4.2B). FDC-P1 WT BCR/ABL pSR empty vector and shB56 δ cells displayed similar levels of GFP expression (Figure 4.2D and E).

Downregulation of the individual PP2A B subunits was determined at the gene level by qRT-PCR, and at the protein level by immunoblotting. Compared to FDC-P1 WT BCR/ABL cells transfected with pMKO-EV, the shB55 α and shB56 α sequences resulted in sufficient protein knockdown to 50% and 20% of the corresponding PP2A subunits (Figure 4.3A and B). At the mRNA level, these effects were only observed for the gene of interest, confirming the specificity of target knockdown (Figure 4.4A and B). Suppression of B56 δ protein to ~60% of empty vector levels (Figure 4.3C) was associated with a similar decrease in mRNA expression (Figure 4.4C).

4.2.3 Functional effects of PP2A regulatory subunit knockdown

4.2.3.1 shB56 α restores PP2A activity in FDC-P1 WT BCR/ABL cells

After the shRNA-expressing FDC-P1 WT BCR/ABL cell lines were established, the impact on PP2A phosphatase activity was examined. As expected, FDC-P1 WT BCR/ABL cells expressing the pMKO or pSR control vectors had significantly attenuated PP2A activity compared to FDC-P1 BCR/ABL⁻ cells (Figure 4.5). Interestingly, suppression of PP2A B55 α partly restored this inhibition back to ~80% of normal levels (Figure 4.5). Even more dramatic, the activity of PP2A in FDC-P1 WT BCR/ABL shB56 α cells was indistinguishable from BCR/ABL⁻ controls (Figure 4.5). Notably, downregulation of B56 δ in FDC-P1 WT BCR/ABL cells had no effect on restoring PP2A activity (Figure 4.5). These novel findings indicate that targeting individual PP2A regulatory subunits in BCR/ABL⁺ myeloid progenitors has a differential effect on enzyme activation.

4.2.3.2 shB56 α impairs the proliferation of FDC-P1 WT BCR/ABL cells

Previous studies have shown that restoring PP2A activity by pharmacological activation or overexpression of PP2Ac inhibits the proliferation and survival of BCR/ABL⁺ myeloid progenitors (Neviani *et al.* 2005, Neviani *et al.* 2007). To assess the functional consequences of PP2A reactivation in the shRNA-expressing FDC-P1 WT BCR/ABL cells, a short-term growth assay was performed. Compared to FDC-P1 WT

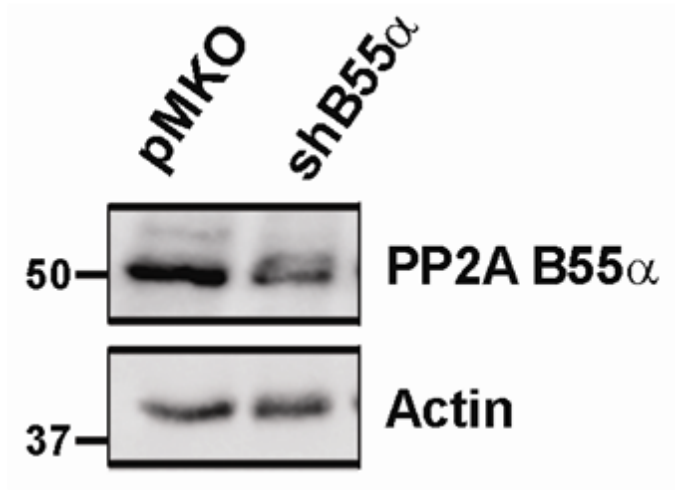
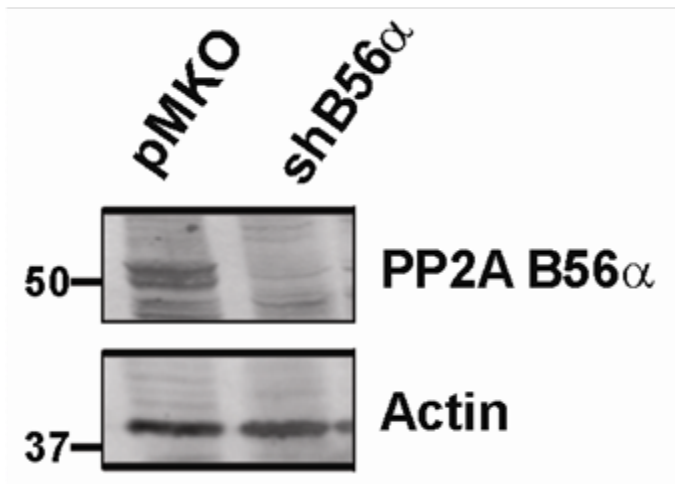
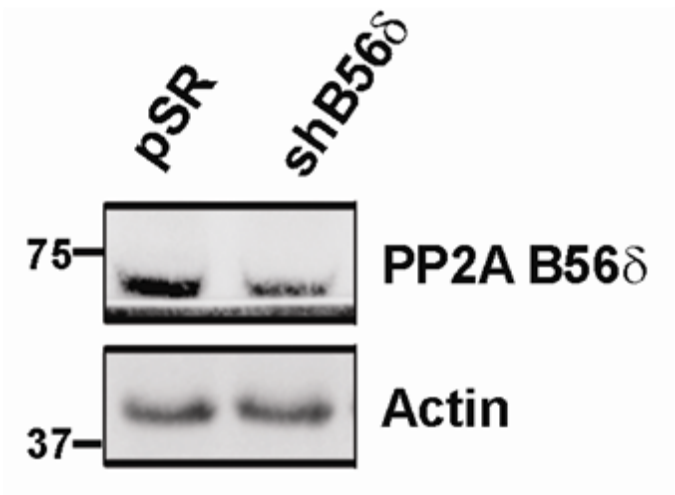
A**B****C**

Figure 4.3 Knockdown of PP2A regulatory subunits in WT BCR/ABL FDC-P1 cells

The expression of A) B55 α B) B56 α or C) B56 δ was assessed in the shRNA-WT BCR/ABL FDC-P1 cell lines. Lysates were subjected to SDS-PAGE and probed for either PP2A B55 α , B56 α or B56 δ . Actin was used as a loading control. Blots are a representative of two independent experiments.

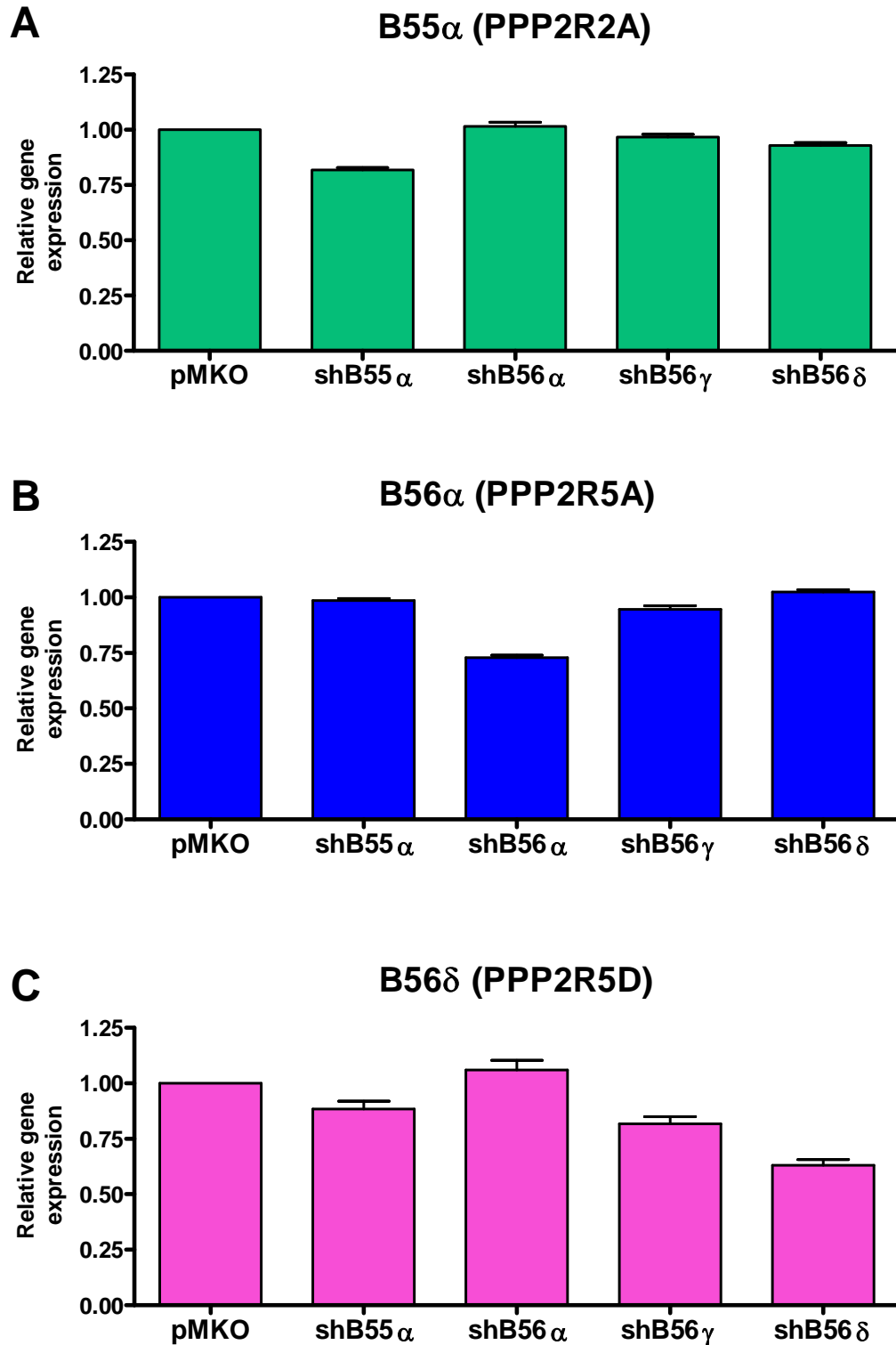


Figure 4.4 mRNA levels of PP2A regulatory subunits in shRNA-WT BCR/ABL FDC-P1 cells

The downregulation of PP2A B55 α , B56 α or B56 δ was confirmed in the shRNA-FDC-P1 WT BCR/ABL cell lines. Total RNA was extracted and qRT-PCR analysis detecting **A**) B55 α (PPP2R2A) **B**) B56 α (PPP2R5A) and **C**) B56 δ (PPP2R5D) was performed. Gene expression is relative to FDC-P1 WT BCR/ABL pMKO empty vector. *Columns*, mean of two independent experiments performed in triplicate; *bars*, SEM.

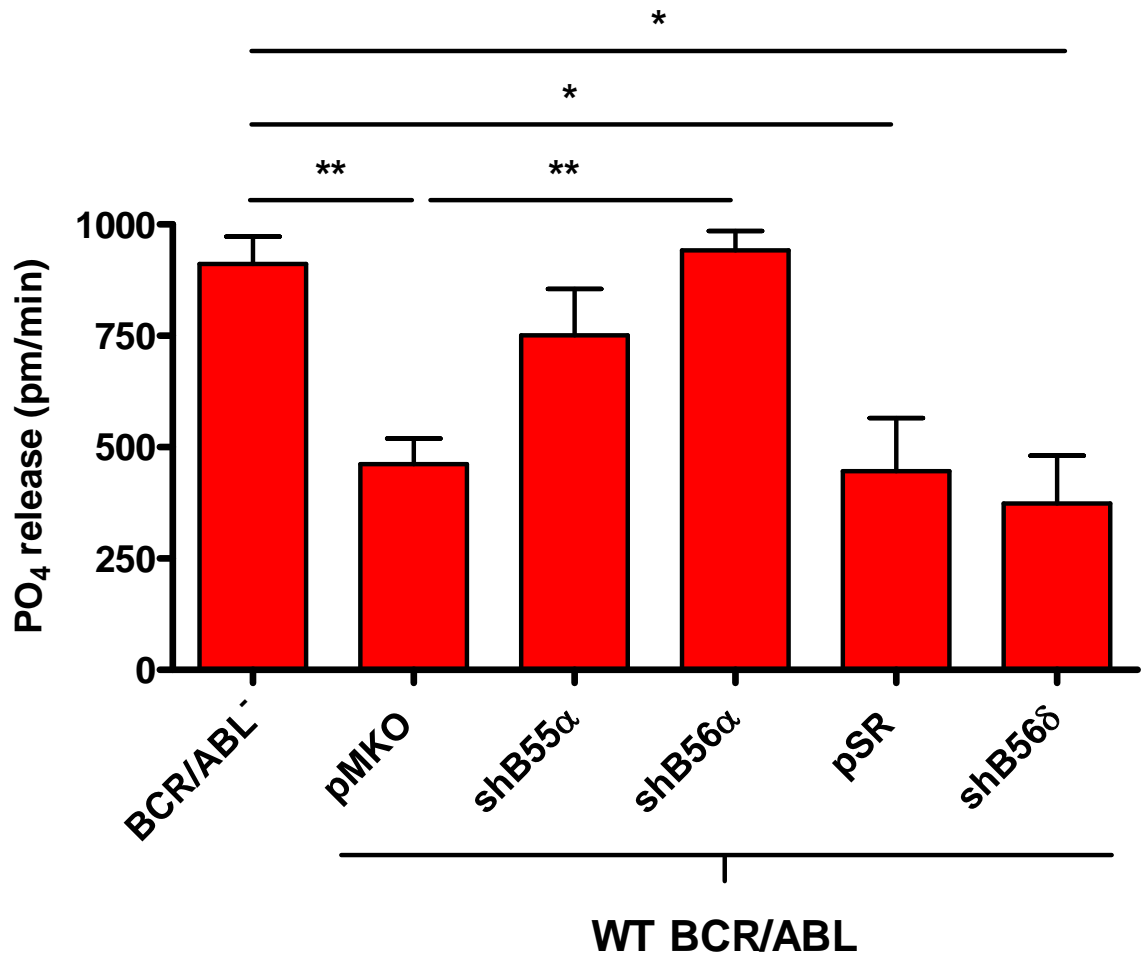


Figure 4.5 PP2A activity in shRNA-WT BCR/ABL FDC-P1 cells

To determine PP2A activity in FDC-P1 cells, the catalytic subunit was immunoprecipitated from whole cell lysates and incubated with a PP2A-specific phospho-peptide. Free phosphate (PO₄) release was measured at an absorbance of 620 nm. Data is presented as the activity of PP2A relative to FDC-P1 BCR/ABL⁻ control cells. *Columns*, mean PO₄ release (pm/min) of three independent experiments performed in duplicate; *bars*, SEM. *p<0.05, **p<0.01, Student's t-test.

BCR/ABL pMKO controls, differences in the growth of FDC-P1 WT BCR/ABL shB55 α cells were not evident until 66 hours, at which time a moderate reduction was noted for the shB55 α population (Figure 4.6). In accordance with a dramatic increase in PP2A activity (Figure 4.5), FDC-P1 WT BCR/ABL shB56 α cells grew at a consistently slower rate compared to pMKO-EV cells (Figure 4.6). An increase in non-viable cells determined by trypan blue exclusion was not observed (data not shown), suggesting that B56 α suppression mainly affects cellular proliferation rather than survival. The growth rate of FDC-P1 WT BCR/ABL cells was not affected by the knockdown of B56 δ (Figure 4.6).

Next, a clonogenic assay was performed. The formation of discrete colonies from individual myeloid progenitors in a semi-solid medium is an excellent indicator of long-term proliferation potential. For this study, 500 cells were plated in methylcellulose and the colonies scored after 7 days (Figure 4.7). FDC-P1 WT BCR/ABL pMKO and pSR controls displayed a cloning efficiency of ~90% and the colonies formed by these cell lines were large and compact, characteristic of an undifferentiated myeloid progenitor phenotype (Figure 4.8 and 4.9) (Piazza *et al.* 2000). The most striking difference in clonogenic potential was observed with B56 α suppression, which resulted in approximately half the number of colonies compared to FDC-P1 WT BCR/ABL pMKO-EV cells (Figure 4.7). In addition, the colonies formed by these cells were dramatically reduced in size (Figure 4.8 and 4.9). No effect on colony number was observed with the other shRNA-expressing FDC-P1 WT BCR/ABL cell lines (shB55 α and shB56 δ) (Figure 4.7). Whilst the cloning efficiency of FDC-P1 WT BCR/ABL shB55 α was similar to pMKO controls, these cells displayed smaller colonies (Figure 4.8 and 4.9); a result which correlates with partially restored PP2A activity and slightly decreased cellular proliferation (Figure 4.5). Interestingly, FDC-P1 WT BCR/ABL shB56 δ cells formed slightly larger colonies compared to FDC-P1 WT BCR/ABL pSR controls (Figure 4.8 and 4.9). Taken together, these findings correlate with the PP2A activity assay data and highlight a general mechanism whereby global activation of PP2A, as seen with shB56 α cells, attenuates BCR/ABL⁺ leukaemogenesis.

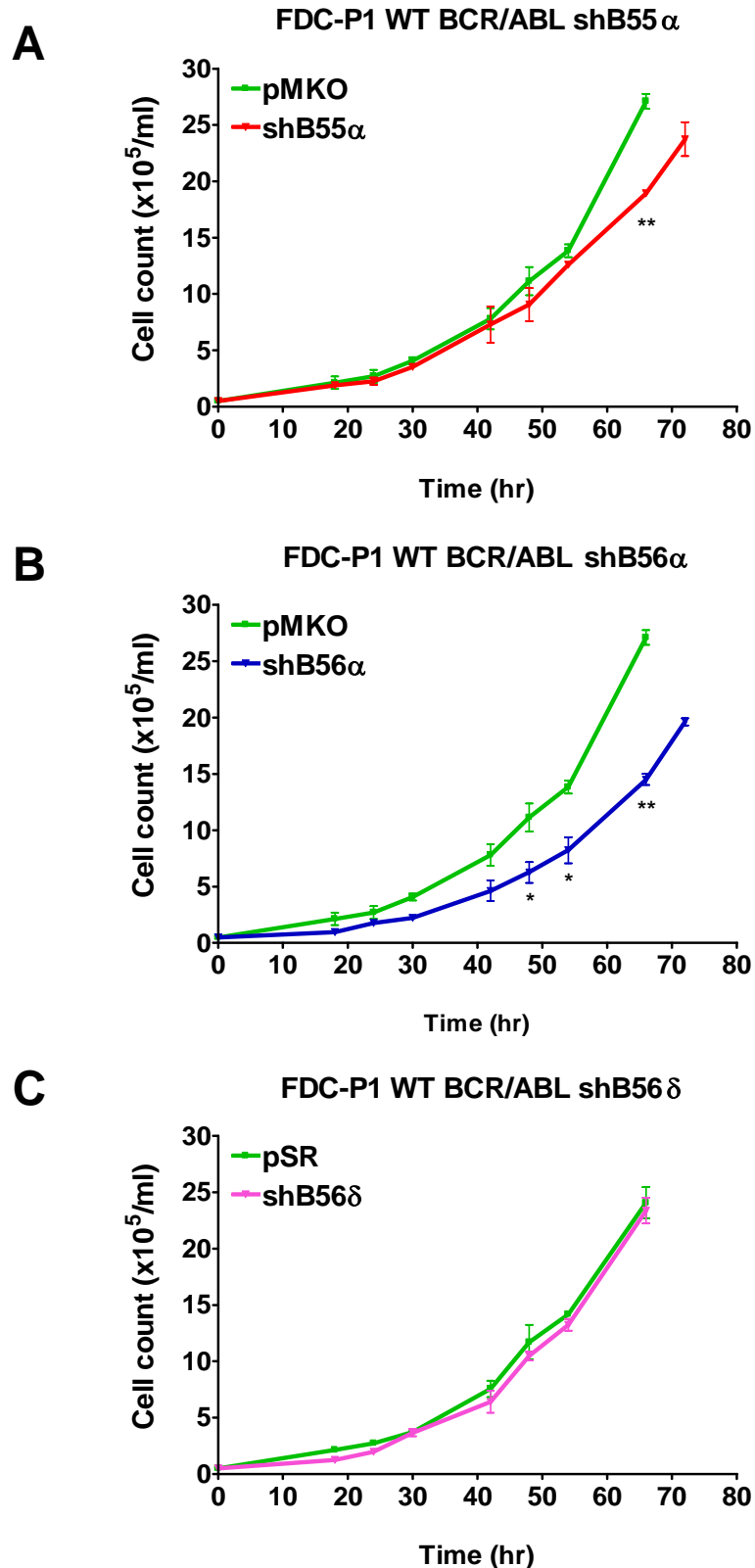


Figure 4.6 Growth rate of shRNA-WT BCR/ABL FDC-P1 cells

FDC-P1 WT BCR/ABL cells expressing either pMKO or pSR empty vectors, or shRNA directed against **A**) B55 α **B**) B56 α or **C**) B56 δ were seeded at 0.5×10^5 /ml and counted every 12 hours using trypan blue to determine viability. *Columns*, mean of three independent experiments performed in duplicate; *bars*, SEM. * $p < 0.05$, ** $p < 0.01$, Student's t-test compared to pMKO.

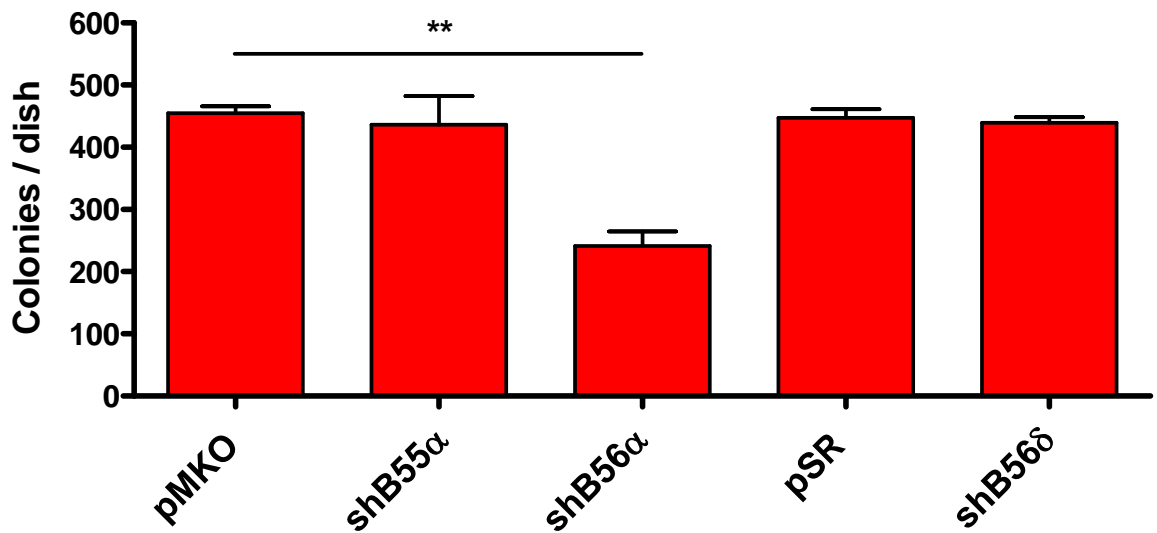


Figure 4.7 Clonogenic potential of shRNA-WT BCR/ABL FDC-P1 cells

For each clonogenic assay, 500 FDC-P1 WT BCR/ABL cells expressing either pMKO or pSR empty vectors, or shRNA directed against B55α, B56α and B56δ were plated in methylcellulose. Colonies were counted after 7 days. *Columns*, mean of three independent experiments performed in triplicate; *bars*, SEM. **p<0.01, Student's t-test compared to pMKO.

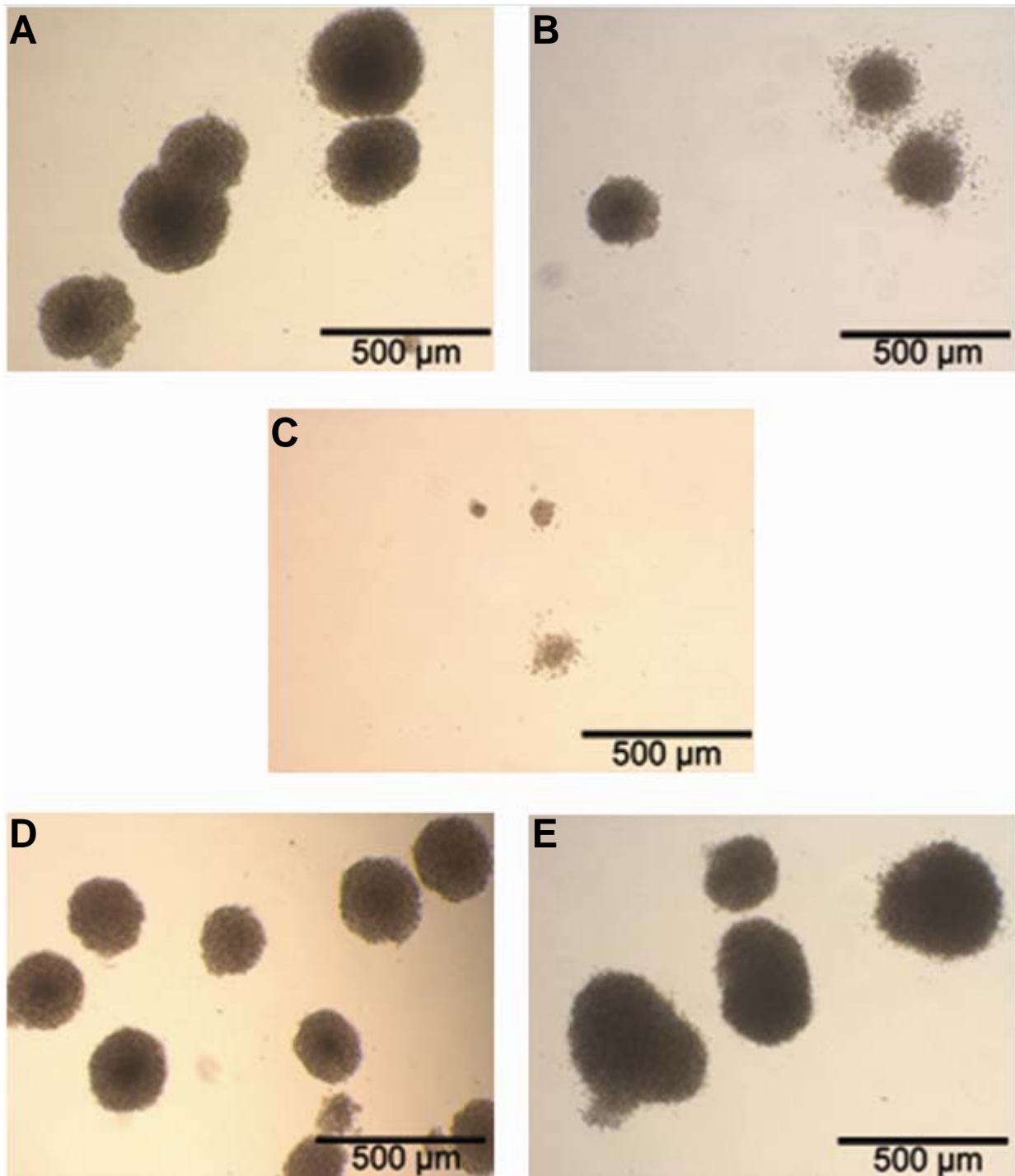


Figure 4.8 Colonies formed by shRNA-WT BCR/ABL FDC-P1 cells

FDC-P1 WT BCR/ABL cells expressing **A**) pMKO **B**) shB55α **C**) shB56α **D**) pSR or **E**) shB56δ were plated in methylcellulose and colonies were inspected (40x magnification) after 7 days using an Olympus microscope (CK40). Photographs were taken with a ColourView II camera and analySIS software.

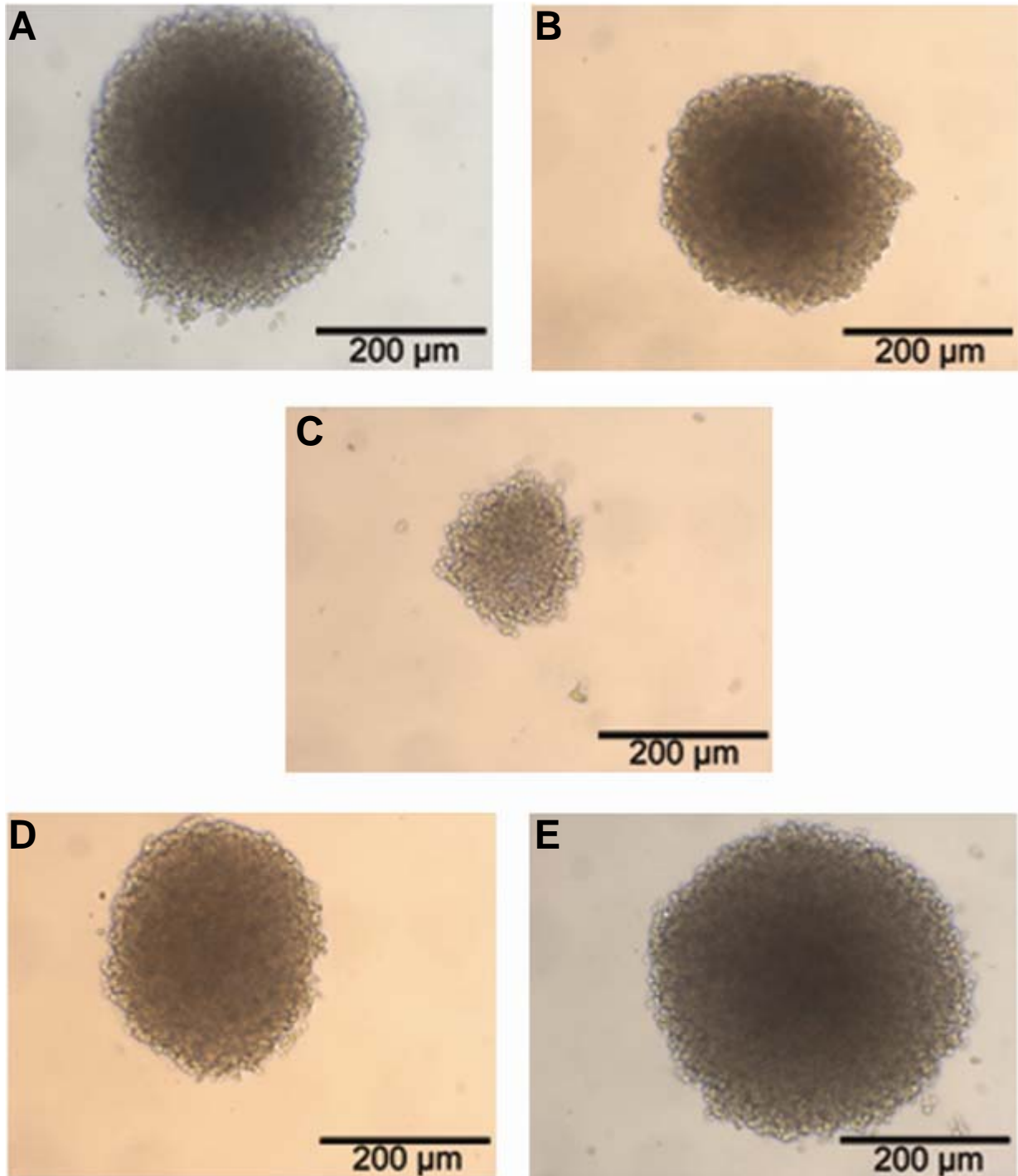


Figure 4.9 Colonies formed by shRNA-WT BCR/ABL FDC-P1 cells at a higher magnification

FDC-P1 WT BCR/ABL cells expressing A) pMKO B) shB55 α C) shB56 α D) pSR or E) shB56 δ were plated in methylcellulose and colonies were inspected (100x magnification) after 7 days using an Olympus microscope (CK40). Photographs were taken with a ColourView II camera and analySIS software.

4.2.3.3 Suppression of B56 α and B56 δ alters the cellular morphology of FDC-P1 WT BCR/ABL cells

The mouse FDC-P1 cell line represents a self-renewing population of myeloid progenitors that are ancestral to monocytes/macrophages and granulocytes (Dexter *et al.* 1980). Under certain experimental conditions FDC-P1 cells can undergo differentiation, which is characterised by changes in morphology such as a large cytoplasm containing vacuoles (Kubota *et al.* 1998, Rohrschneider & Metcalf 1989, Li & Bernard 1992, Piazza *et al.* 2000). To determine whether impaired cell growth of FDC-P1 WT BCR/ABL shB56 α cells was associated with enhanced differentiation, May-Grunwald/Giemsa staining of cytopins was performed (Figure 4.10). FDC-P1 WT BCR/ABL pMKO and pSR control cells, and those expressing shB55 α , displayed typical myeloid progenitor features including a generous nucleus and thin cytoplasm (Figure 4.10 and 4.11). In contrast, a significant proportion of FDC-P1 WT BCR/ABL shB56 α cells contained an enlarged vacuolated cytoplasm (Figure 4.10 and 4.11), which is reportedly a distinguishing feature of partial differentiation towards either the granulocyte or monocyte/macrophage lineage (Piazza *et al.* 2000, Li & Bernard 1992). Interestingly, morphological differences were also observed in the FDC-P1 WT BCR/ABL cells lacking B56 δ . Unique to this population were the presence of cells displaying a prophase appearance and monopolar spindles. These were identified by breakdown of the nuclear envelope and condensed chromosomes that appeared centrally arranged in a cartwheel-like configuration (Figure 4.10 and 4.11) (Horn *et al.* 2007). Even more striking was the detection of extremely large and irregular shaped cells with multiple nuclei (Figure 4.10 and 4.11). These findings suggest that downregulation of B56 δ in FDC-P1 WT BCR/ABL cells may have a dramatic effect on cell cycle regulation to result in defective cytokinesis. All together, the unique morphological changes induced by B56 α and B56 δ suppression in FDC-P1 WT BCR/ABL cells highlights these subunits as potentially important mediators of BCR/ABL⁺ leukaemogenesis.

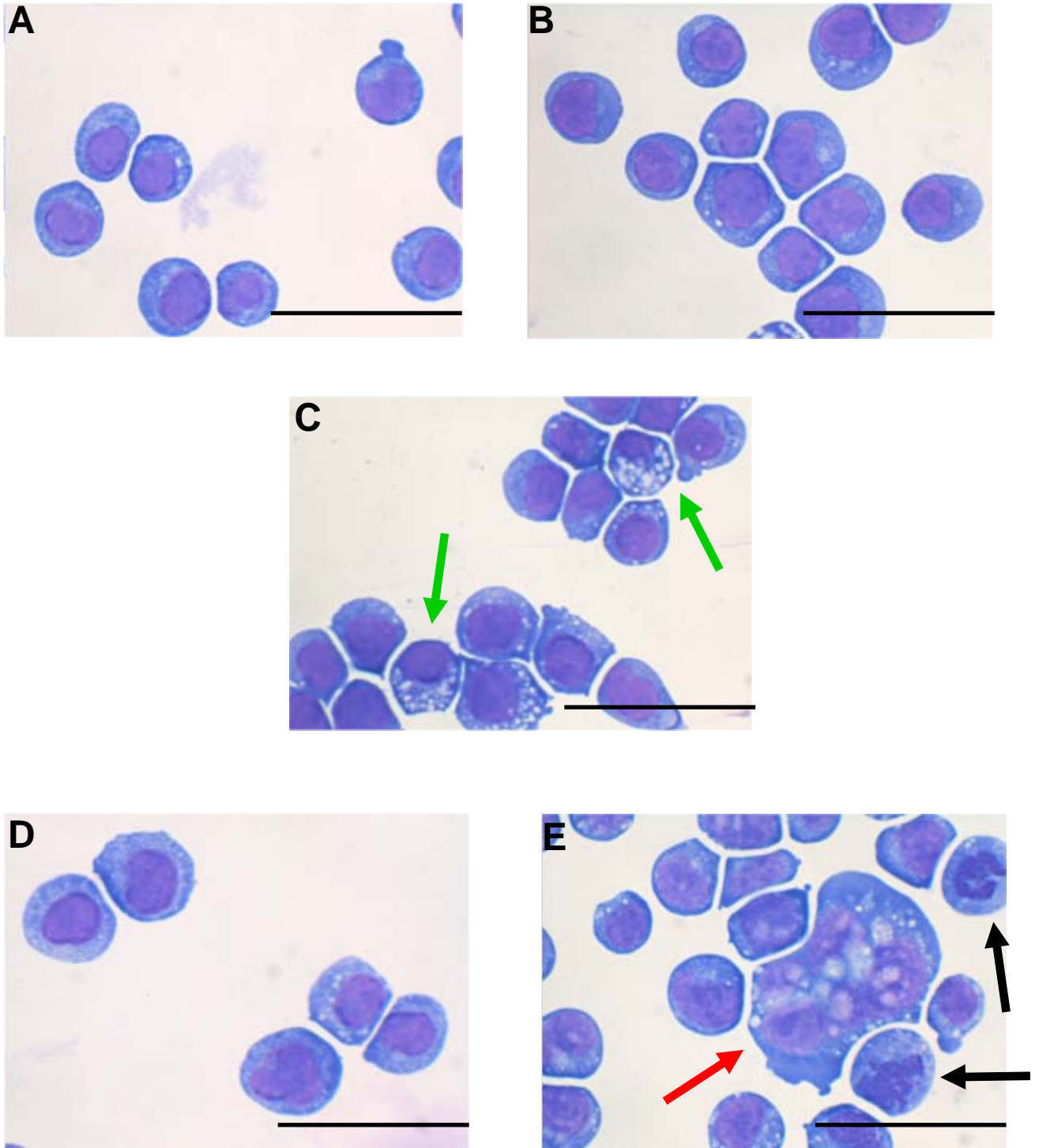


Figure 4.10 Cellular morphology of shRNA-WT BCR/ABL FDC-P1 cells

FDC-P1 WT BCR/ABL cells expressing **A)** pMKO **B)** shB55 α **C)** shB56 α **D)** pSR or **E)** shB56 δ were deposited onto microscope slides by centrifugation and stained with May-Grunwald/Giemsa. Cells were evaluated under 400x magnification on an inverted light microscope (Olympus). Photographs were taken with a ColourView II camera and analySIS software. Normal cells were characterised by a large nucleus to cytoplasm ratio. Arrows indicate cells with an enlarged vacuolated cytoplasm (*green*); monopolar spindles (*black*); or multiple nuclei (*red*). Scale bar, 50 μ m

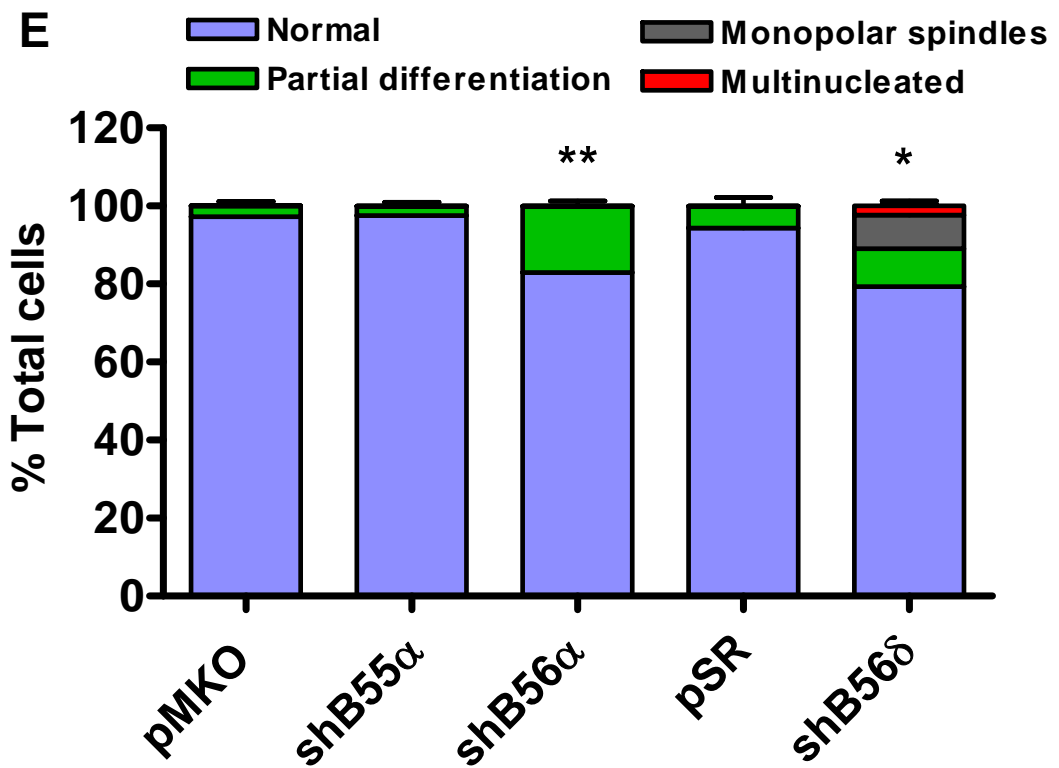
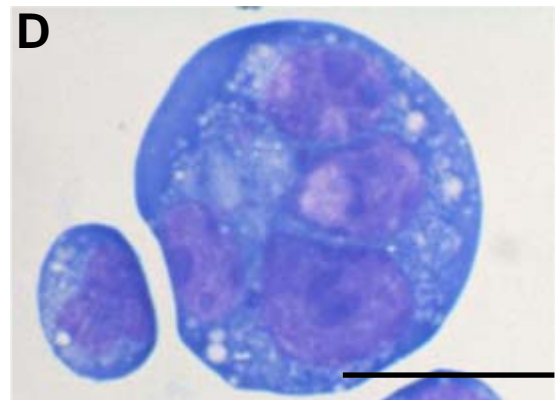
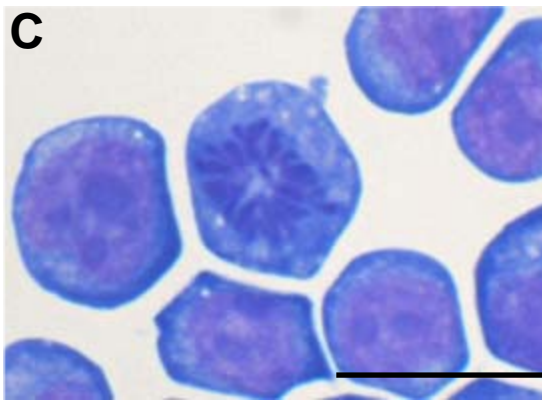
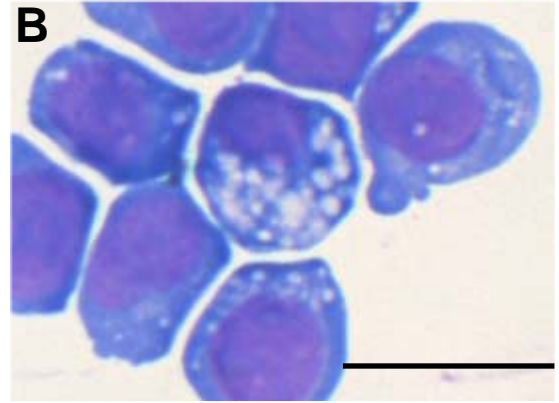
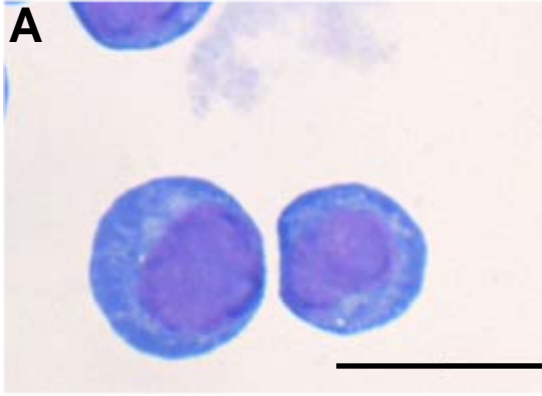


Figure 4.11 Quantitative analysis of the morphological characteristics displayed by shRNA-WT BCR/ABL FDC-P1 cells

FDC-P1 WT BCR/ABL cell lines were scored for characteristics indicative of **A)** normal progenitors (*blue*) **B)** differentiation (*green*) **C)** monopolar spindles (*black*) or **D)** multiple nuclei (*red*). Representative pictures for each feature are shown. **E)** Two independent experiments were performed. 10 pictures were taken at 200x magnification from randomly selected areas of the cytospin, with a total of ~400 cells scored. *Columns*, mean percentage of cells showing each characteristic / total number of cells per view; *bars*, SEM. * $p < 0.05$ for monopolar spindles, ** $p < 0.01$ for partial differentiation. Student's t-test compared to pMKO. *Scale bar*, 25 μm

4.3 Discussion

The results presented in Chapter 3 indicate that the oncogenic kinase activity of BCR/ABL disrupts B subunit binding exchange in myeloid progenitors. Using an shRNA approach, this Chapter investigated the functional importance of specific PP2A complexes and suggests that the increased expression and association of B56 α observed in BCR/ABL⁺ cells (Chapter 3) could contribute to BCR/ABL-mediated leukaemogenesis.

The most evident and consistent finding arising from this body of work is the functional consequence of PP2A B56 α knockdown in FDC-P1 WT BCR/ABL cells. Suppression of this subunit restored PP2A activity back to BCR/ABL⁻ control levels (Figure 4.5), and was associated with significantly reduced proliferation (Figure 4.6), impaired clonogenic potential (Figure 4.7) and altered cellular morphology resembling partial differentiation (Figure 4.10 and 4.11). This data indicates that increased formation of PP2A holoenzymes containing the specific B56 α regulatory subunit is important for BCR/ABL⁺ growth of myeloid progenitors. In agreement with these findings, B56 α has been implicated in the negative regulation of p53, where it forms a complex with Cyclin G and Mdm2 to induce p53 ubiquitination and degradation (Okamoto *et al.* 2002). In this context, PP2A serves as a cellular monitor that maintains p53 in a latent state and prevents apoptosis under normal cellular conditions (Haupt *et al.* 1997). Interestingly, *TP53* is mutated in 25-30% of myeloid CML-BC patients (Feinstein *et al.* 1991), and its loss-of-function contributes to enhanced tumourigenicity (Honda *et al.* 2000) and imatinib-resistance in myeloid precursors (Wendel *et al.* 2006). Therefore, an excess of PP2A-B56 α complexes may deplete functional levels of p53 and augment the development of CML-BC. Conversely, removal of p53-associated B56 α complexes in FDC-P1 WT BCR/ABL shB56 α cells could lead to enhanced p53 function and reduced transformation.

Although the degradation of p53 may explain how B56 α suppression inhibits cell growth, it does not explain how reduced B56 α results in enhanced PP2A activity. As discussed previously (Section 3.3), an abundance of PP2A-B56 α complexes in BCR/ABL⁺ cells may not only potentiate cascades which confer oncogenic signals, but could also deplete the pool of PP2A holoenzymes that normally exert traditional tumour

suppressive function (e.g. B56 γ). As a result, the global increase of PP2A activity observed in the FDC-P1 WT BCR/ABL shB56 α cells may be a reflection of enhanced B56 γ binding to the core PP2A dimer. The differences in PP2A composition between the shRNA-transfected FDC-P1 WT BCR/ABL cell lines and empty vector controls remain undefined and require further investigation. The fact that downregulation of individual PP2A subunits has such a differential effect on restoring PP2A activity in FDC-P1 WT BCR/ABL cells confirms that specific enzyme function is attributable to B subunit abundance and binding (Figure 4.5). This is a novel finding for a myeloid progenitor cell line and suggests that targeting specific PP2A subunits may be an alternate therapeutic strategy for CML patients.

Several reports demonstrate that FDC-P1 cells have the capacity to reversibly differentiate under certain experimental conditions (Kubota et al. 1998, Li & Bernard 1992, Piazza et al. 2000, Rohrschneider & Metcalf 1989). Of note, they do not undergo terminal differentiation but rather progress towards a specific lineage. Expression of the type III RTKs PDGFR or macrophage colony stimulating factor-1 receptor (CSF-1), and subsequent growth in their corresponding ligands, directs differentiation along the monocyte/macrophage pathway (Kubota *et al.* 1998, Rohrschneider & Metcalf 1989). Furthermore, the introduction of fibroblast growth factor receptor into FDC-P1 cells induces an intermediate stage of granulocytic differentiation (Li & Bernard 1992). In agreement with these reports, the stable knockdown of B56 α appears to result in morphological features that resemble partial differentiation (Piazza et al. 2000, Li & Bernard 1992). Whilst this is an interesting observation, it remains possible that these changes indicate cells which are undergoing apoptosis. However, there was no increase in the uptake of trypan blue, or the detection of necrotic cells on the cytospin, suggesting that the FDC-P1 WT BCR/ABL shB56 α cells are viable. Further investigations determining the expression of lineage-specific markers such as Gr-1 and myeloperoxidase for granulocytes, or Mac-1 for monocytes/macrophages, are required to confirm these cells are indeed undergoing differentiation.

In support of the current findings (Figure 4.10), reduced expression of SET has been shown to inhibit the proliferation and induce the *in vitro* differentiation of the poorly differentiated TSU-Pr1 prostate carcinoma cell line (Brody *et al.* 2004). Whilst the activity of PP2A was not determined in this study, it is likely that depletion of SET

enhances enzyme activation and may contribute to the differentiated phenotype observed in these cells. Although speculative at the moment, enhanced differentiation may be the underlying mechanism contributing to the reduced proliferation and impaired clonogenic potential of the FDC-P1 WT BCR/ABL shB56 α cell line. A distinguishing feature of CML-BC is the clonal expansion of differentiation-arrested blast cells that are insensitive to the tyrosine kinase inhibition (Copland *et al.* 2006, Graham *et al.* 2002, Jorgensen *et al.* 2007). Thus, the accumulation of myeloid precursors that lack the ability to form mature granulocytes is a major factor which contributes to the more aggressive and drug-resistant blast crisis phenotype. The ability to partially reverse this phenotype via PP2A manipulation in myeloid progenitors represents an exciting and novel finding.

Taken together, these results identify PP2A B56 α as a positive regulator of BCR/ABL⁺ transformation and contradict several studies which reveal a critical role for B56 α in the negative regulation of certain oncoproteins, including c-Myc and Bcl-2 (Arnold & Sears 2006, Ruvolo *et al.* 2002). In these reports, B56 α functions as a traditional tumour suppressor. Due to the complex regulation and promiscuous nature of the PP2A enzyme, the discovery of opposing roles for B56 α function is not surprising. In the context of c-Myc regulation, PP2A holoenzymes containing the B56 α subunit interact with and induce the ubiquitin-mediated degradation of this potent oncoprotein in human cells. Accordingly, shRNA-mediated knockdown of B56 α results in enhanced c-Myc stabilisation and increased oncogenic potential (Arnold & Sears 2006). The apparent discrepancy between the current study and previous investigations are most likely related to the cellular model studied, as well as differences in the substrates and pathways that are targeted by B56 α in each situation.

The expression of B56 δ is increased in BCR/ABL⁺ myeloid progenitors compared to untransfected cells (Section 3.2.5.2). FDC-P1 WT BCR/ABL cells lacking B56 δ showed no appreciable differences in PP2A activity (Figure 4.5) or proliferation (Figure 4.6 and 4.7); however, a rather interesting finding in regards to cell cycle regulation was observed. Although it is difficult to determine from cytopsin pictures only, the increased frequency of FDC-P1 WT BCR/ABL cells which appear to be in the process of mitosis indicates that knockdown of B56 δ may induce mitotic delay (Figure 4.10 and 4.11). Mitosis is an extremely complex biological process by which a complete copy of the

duplicated genome and cytoplasm is precisely segregated into two daughter cells. To ensure faithful transfer of genomic material, multiple fidelity monitoring checkpoint systems have evolved to prevent cells from dividing in the presence of DNA damage (Figure 4.12). A role for PP2A in cell cycle regulation has long been suspected, with extensive studies in *Saccharomyces cerevisiae* (budding yeast) (Jiang 2006), *Drosophila* (Mayer-Jaekel *et al.* 1993) and *Xenopus* extracts (Margolis *et al.* 2006, Mochida *et al.* 2009) demonstrating its involvement at virtually every stage (De Wulf *et al.* 2009).

Recent evidence supports a unique role for B56 δ in controlling both the entry into and exit from mitosis (Figure 4.12) (Forester *et al.* 2007, Margolis *et al.* 2006). In agreement with the current findings, knockdown of B56 δ in mammalian cells prevents Cyclin B degradation and results in a delayed mitotic exit (Forester *et al.* 2007). Presumably, a transient block in cell cycle progression or defective cytokinesis is responsible for the generation of giant, multinucleated cells (Figure 4.10 and 4.11) (Glotzer 2005). This phenotype is similar to that observed for the Aurora kinase inhibitors, such as ZM447439 (Ditchfield *et al.* 2003) and MK-0457 (VX-680) (Harrington *et al.* 2004). The mechanism by which these inhibitors induce apoptosis is fairly unique and contrasts the classic antimitotic agents (e.g. paclitaxel) in that they do not induce mitotic arrest. Rather, MK-0457 disrupts spindle formation, which causes a slight delay in cell cycle progression (Girdler *et al.* 2006, Tyler *et al.* 2007). Despite the presence of misaligned chromosomes, the drug-treated cells undergo anaphase and exit mitosis prematurely, indicating a compromised spindle assembly checkpoint (Girdler *et al.* 2006). After a period of time, the unsegregated DNA decondenses and the nuclear envelope encloses around an enlarged, multilobed nucleus (Girdler *et al.* 2006). Thus, continued DNA replication in the absence of cell division results in polyploidy (Harrington *et al.* 2004). The increase in colony size observed in the FDC-P1 WT BCR/ABL shB56 δ population (Figure 4.9) is most likely attributable to the presence of large, polyploid cells (Figure 4.10 and 4.11).

Precisely how the suppression of B56 δ could result in mitotic delay and/or defective cytokinesis is unclear. Recent reports implicate a role for PP2A in the regulation of both Aurora A and B function (Horn *et al.* 2007, Sun *et al.* 2008); however, the particular

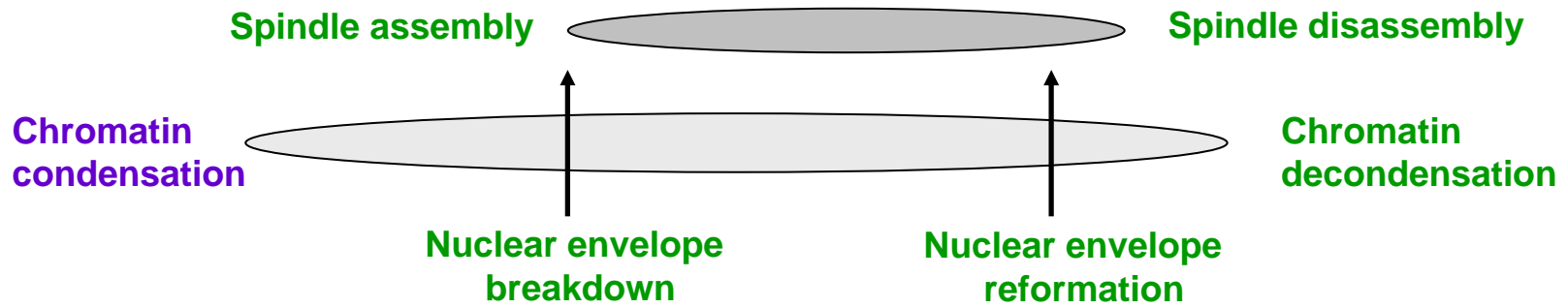
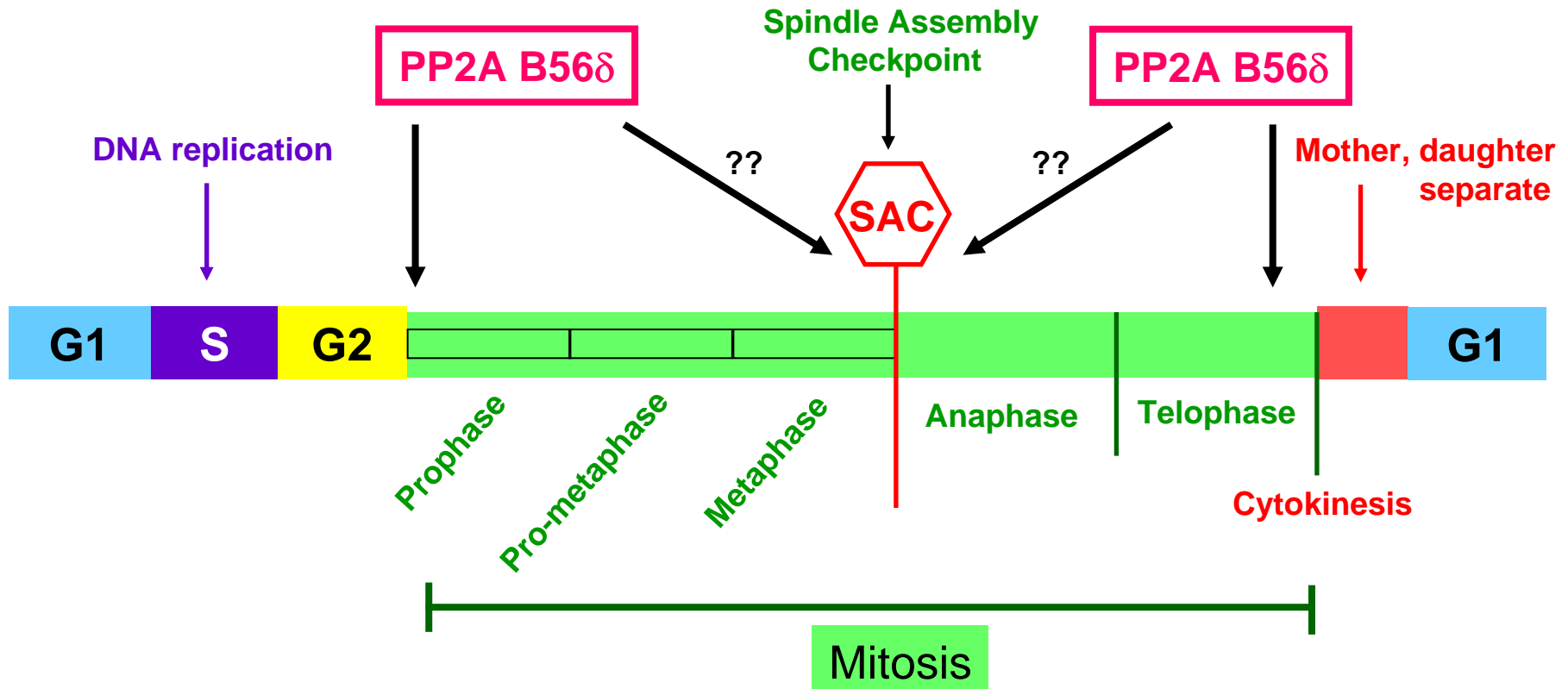


Figure 4.12 Involvement of PP2A B56 δ in cell cycle regulation

Schematic overview of the cell cycle which comprises G1 (blue), S phase (purple), G2 (yellow), mitosis (prophase, pro-metaphase, metaphase, anaphase and telophase; green), and cytokinesis (red). Key events are indicated by arrows and text, which is coloured according to the cell cycle stage that they occur in. Horizontal ellipses depict the appearance of mitotic spindles (dark grey) and condensed chromosomes (light grey). PP2A B56 δ (pink) has been implicated in regulating the entry into and exit from mitosis. Further investigation is required to determine whether it also controls the spindle assembly checkpoint (SAC). Adapted from (De Wulf *et al.* 2009).

PP2A regulatory subunits governing this have not been described. Given that knockdown of B56 δ in FDC-P1 WT BCR/ABL cells resembles aberrant Aurora function (Marumoto *et al.* 2005, Meraldi *et al.* 2002), it is likely that B56 δ is involved in the PP2A-mediated regulation of Aurora kinases during cell cycle progression. Another potential substrate of B56 δ is the Cdc25C phosphatase. At the end of mitosis, B56 δ binds to and inactivates Cdc25C by dephosphorylation of sites critical for its mitotic function. This induces a series of molecular events that results in the proteasome-dependent degradation of Cyclin B (Forester *et al.* 2007), which is required for a timely mitotic exit and proper cell division (Clute & Pines 1999, Glotzer *et al.* 1991).

Myeloid progenitors expressing BCR/ABL have a marked increase in B55 α -containing PP2A complexes (Figure 3.15C). Based on this observation, it was predicted that enhanced binding of B55 α would aberrantly direct the PP2A enzyme to substrates that potentiate the signalling of oncogenic cascades. In support of this, B55 α has been implicated in the positive regulation of numerous pathways that contribute to BCR/ABL⁺ transformation. For example, PP2A B55 α complexes stimulate the MAPK pathway by dephosphorylating KSR-1 and Raf-1 in several mammalian cell models including NIH3T3, COS-1 and HEK293 (Abraham *et al.* 2000, Ory *et al.* 2003, Adams *et al.* 2005, Dougherty *et al.* 2005). Recent investigations demonstrate that B55 α complexes directly dephosphorylate and stabilise the transcription factor, β -catenin (Zhang *et al.* 2009). Loss of β -catenin is associated with reduced self-renewal of the CML stem cell population and importantly, impairs the ability of mice to develop a CML phenotype (Zhao *et al.* 2007, Coluccia *et al.* 2007). Thus, enhanced recruitment of B55 α -containing PP2A complexes, as observed in FDC-P1 WT BCR/ABL cells, could activate MAPK signalling or stabilise β -catenin.

The suppression of PP2A B55 α to approximately 50% of control levels was associated with partial restoration of PP2A activity (Figure 4.5), which resulted in a slight inhibition of cell growth (Figure 4.6) and colony size (Figure 4.9). Given the potential to facilitate BCR/ABL-mediated leukaemogenesis, loss of B55 α in FDC-P1 WT BCR/ABL cells was expected to produce a more profound phenotype. The present analysis was conducted on a polyclonal population, which represents a broad spectrum of cells with various degrees of B55 α expression. If complete knockdown of B55 α

significantly impairs proliferation, these cells may have been outgrown, in which case the loss-of-function phenotype would be masked. The isolation and analysis of individual clones with substantial downregulation of B55 α may prove more effective in determining the role of this subunit in BCR/ABL⁺ leukaemia growth. It should also be noted that WT BCR/ABL cells with knockdown of B56 γ showed no difference in PP2A activity, cell proliferation or clonogenic potential compared to pMKO EV controls (data not shown).

In summary, the novel findings presented in this Chapter identify B56 α and B56 δ as key PP2A subunits important for BCR/ABL-mediated leukaemogenesis (Figure 4.13). This is demonstrated by the fact that removal of B56 α not only enhances the activity of PP2A, but significantly impairs cellular growth, reduces the clonogenic potential and may induce partial differentiation of BCR/ABL⁺ myeloid progenitors. In addition, knockdown of B56 δ appears to perturb cell cycle regulation. This data greatly enhances our knowledge of the biology of PP2A, which can be applicable not only to malignant cells but also to normal cellular function.

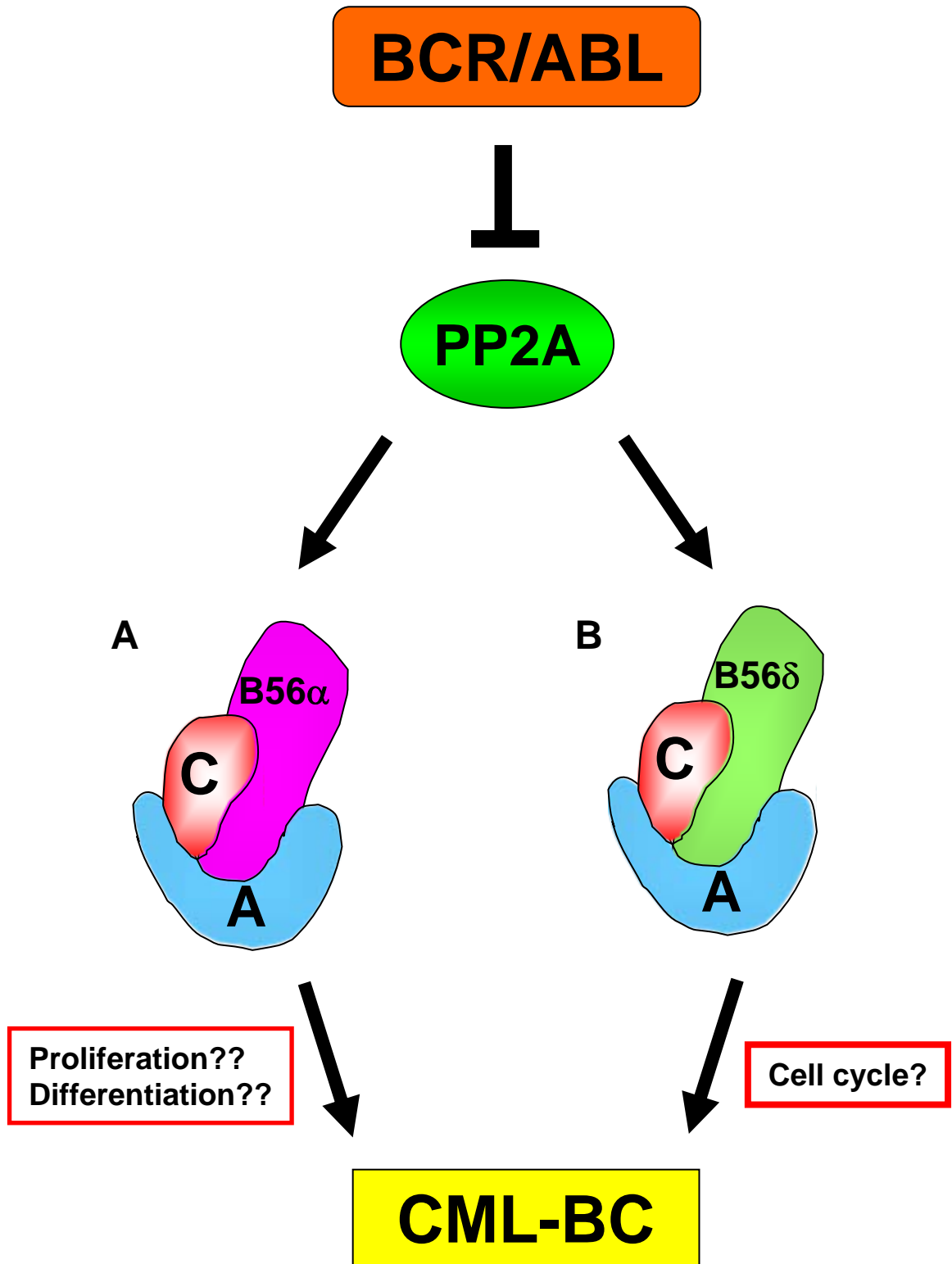


Figure 4.13 Proposed model of PP2A regulation by BCR/ABL in FDC-P1 cells

BCR/ABL may regulate PP2A in myeloid progenitors through two mechanisms. Functional studies from shRNA-expressing WT BCR/ABL FDC-P1 cells indicate that **A)** Enhanced formation of PP2A B56 α complexes may potentiate oncogenic signals through unknown pathways to facilitate proliferation and impair differentiation. **B)** Aberrant regulation of the cell cycle by B56 δ may also contribute to the leukaemic phenotype

CHAPTER 5

INHIBITION OF PP2A BY ONCOGENIC *C-KIT* MUTATIONS

5.1 Introduction

c-KIT is a type 3 RTK that is characterised by 5 extracellular immunoglobulin-like domains and an intracellular split tyrosine kinase domain (Lennartsson *et al.* 2005). Binding of SCF to c-KIT activates multiple signalling pathways that are important for cellular proliferation, differentiation and survival. These include MAPK (Hong *et al.* 2004, Lennartsson *et al.* 1999), PI3K/Akt (Lev *et al.* 1992, Blume-Jensen *et al.* 1998), JAK/STATs (Brizzi *et al.* 1999, Weiler *et al.* 1996) and SFKs (Linnekin *et al.* 1997, Broudy *et al.* 1999, Voytyuk *et al.* 2003). c-KIT is expressed in HSCs, mast cells, germ cells, melanocytes and interstitial cells of Cajal (Ashman 1999). Consistent with this, gain-of-function *c-KIT* mutations have been documented in CBF-AML (Mrozek *et al.* 2008), systemic mastocytosis (Worobec *et al.* 1998), GIST (Hirota *et al.* 1998), testicular seminoma (Kemmer *et al.* 2004) and a subset of melanoma patients (Smalley *et al.* 2009). In GIST samples ~85% of c-KIT aberrations are located in the juxtamembrane domain (JMD; e.g V560G) (Hirota *et al.* 1998), whereas the majority of CBF-AML and systemic mastocytosis patients express kinase domain mutations (e.g. D816V). In most cases, the presence of an activating *c-KIT* mutation is associated with a higher relapse rate and reduced overall survival compared to patients expressing the WT receptor (Mrozek *et al.* 2008).

The c-KIT kinase inhibitor imatinib has shown remarkable success in treating patients with metastatic GIST that harbour JMD *c-KIT* mutations (Demetri *et al.* 2002). In contrast, mutations involving the kinase domain are completely resistant to imatinib inhibition, and as such, c-KIT⁺ CBF-AML and systemic mastocytosis patients are unresponsive to imatinib therapy (Pardanani *et al.* 2003, Piccaluga *et al.* 2007). Recent clinical trials with the second generation tyrosine kinase inhibitor, dasatinib, have also reported disappointing results. In a phase II study, only 2 of 33 patients with systemic mastocytosis showed complete responses to dasatinib treatment, and both tested negative for the D816V *c-KIT* mutation (Verstovsek *et al.* 2008). To improve treatment outcomes for patients with c-KIT⁺ malignancies, a greater understanding of the

signalling cascades activated downstream of c-KIT is required to identify novel therapeutic targets.

BCR/ABL and mutant c-KIT activate similar oncogenic pathways. As BCR/ABL was shown to inhibit PP2A (Neviani *et al.* 2007, Neviani *et al.* 2005) (Chapter 3), it was hypothesised that mutant c-KIT may also inactivate PP2A. Thus the major aims of this Chapter were to determine whether functional inhibition of PP2A is important for c-KIT-driven tumourigenesis, and to investigate whether enhancing the activity of PP2A impairs the *in vitro* growth of myeloid precursors expressing oncogenic c-KIT.

5.2 Results

5.2.1 Mutant c-KIT impairs the activity of PP2A

The FDC-P1 c-KIT⁺ cell model used in this study have been described previously (Frost *et al.* 2002). Briefly, the pRUFneo retroviral vector containing no cDNA (EV), or cDNA encoding the imatinib-sensitive WT c-KIT, the constitutively active imatinib-sensitive JMD V560G c-KIT mutant, or the oncogenic imatinib-resistant kinase domain D816V c-KIT mutant were introduced into the FDC-P1 cell line by retroviral infection using the Ψ2 stable packaging system (Mann *et al.* 1983). Successfully infected cells were initially selected in G418. FDC-P1 cells expressing WT c-KIT were maintained in SCF, whilst the FDC-P1 V560G and D816V c-KIT cells were grown in the absence of factor. The extracellular expression of the c-KIT receptor was routinely monitored by flow cytometry (Figure 5.1) (Frost *et al.* 2002, Roberts *et al.* 2007).

To determine whether oncogenic c-KIT regulates PP2A, the activity associated with PP2Ac immunoprecipitates extracted from FDC-P1 cells was measured. FDC-P1 cells expressing V560G and D816V mutant c-KIT displayed significantly reduced PP2A activity to ~70% of EV control cells (Table 5.1). In contrast, there was no significant difference between EV cells and those expressing the WT c-KIT receptor (Table 5.1). Thus, activating mutations of c-KIT inhibit PP2A activity in myeloid progenitors.

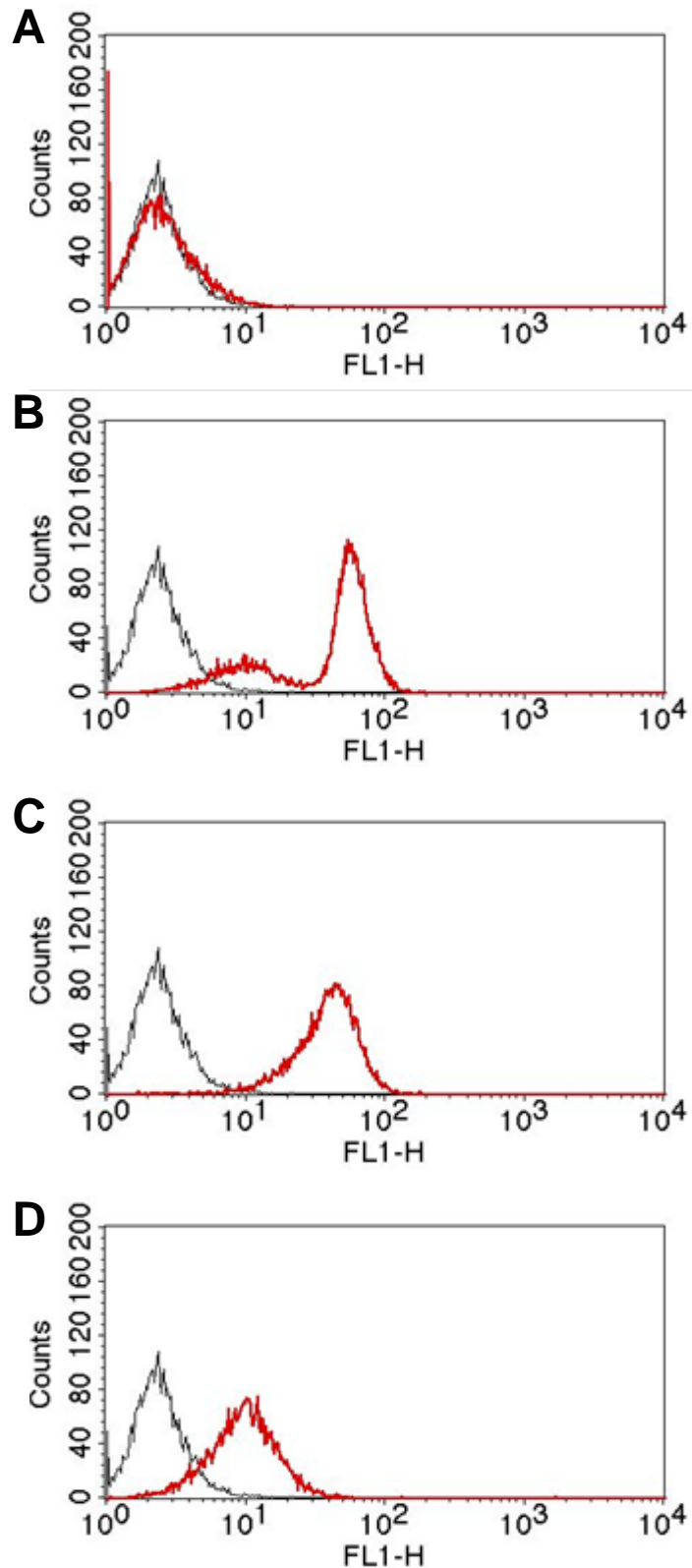


Figure 5.1 Surface expression of c-KIT on FDC-P1 cells

The relative surface expression levels of c-KIT on FDC-P1 cells was determined by immunofluorescent staining and flow cytometric analysis using mAb anti-human c-KIT 1DC3 (red line). An isotype matched negative control mAb IB5 was used to determine background immunofluorescence (black line). **A)** EV **B)** WT c-KIT **C)** V560G c-KIT and **D)** D816V c-KIT.

Table 5.1 Mutant c-KIT impairs PP2A activity

FDC-P1 Cell Line	PO₄ (pm/min)¹	% EV²
EV	810 ± 83	100
WT c-KIT	695 ± 67	88.8
V560G c-KIT	594 ± 98	72.4*
D816V c-KIT	510 ± 62	67.0*

¹PP2Ac was immunoprecipitated from untreated FDC-P1 cells. PP2A activity was determined by incubating the complex with a PP2A-specific phosphopeptide and measuring free phosphate release (PO₄ (pm/min) ± SEM) at an absorbance of 620 nm.

²%EV was calculated by dividing the activity of c-KIT cells by the EV cells.

*p<0.05, n=5, Student's t-test compared to EV.

5.2.2 Mutant c-KIT alters the expression of PP2A subunits

To investigate the mechanisms by which constitutive c-KIT activation inhibits PP2A, levels of the PP2A subunits in all FDC-P1 cell lines were examined by immunoblotting. There was no change in the expression of total or Tyr307-phosphorylated PP2Ac (PP2Ac-p^{Y307}) in FDC-P1 cells expressing WT or mutant c-KIT compared to EV controls (Figure 5.2 and 5.3). Therefore, c-KIT-induced PP2A inhibition is not mediated by reduced expression or phosphorylation of PP2Ac. In contrast, protein expression of the scaffolding subunit (PP2A A) was significantly decreased in FDC-P1 cells expressing both mutant c-KIT receptors, with barely detectable levels present in the FDC-P1 D816V c-KIT cells (Figure 5.2 and 5.3). This identifies a novel mechanism which may contribute to impaired PP2A activity and oncogenic c-KIT-mediated transformation.

Recent evidence demonstrates that aberrant expression of PP2A regulatory subunits in human cells alters the regulation of downstream signalling cascades to potentiate growth and survival signals (Chen *et al.* 2004). In comparison to FDC-P1 EV control cells and those expressing WT c-KIT, the levels of several PP2A B subunits including B55α, B56α, B56γ and B56δ were substantially reduced in the FDC-P1 V560G and D816V mutant c-KIT cells (Figure 5.2 and 5.3). Expression of the B56ε subunit was not affected by c-KIT kinase activity (Figure 5.2 and 5.3). FDC-P1 WT c-KIT cells appeared to express a lower molecular weight isoform of B56γ compared to the EV controls (Figure 5.2 and 5.3). Several splice variants of the B56γ subunit are already

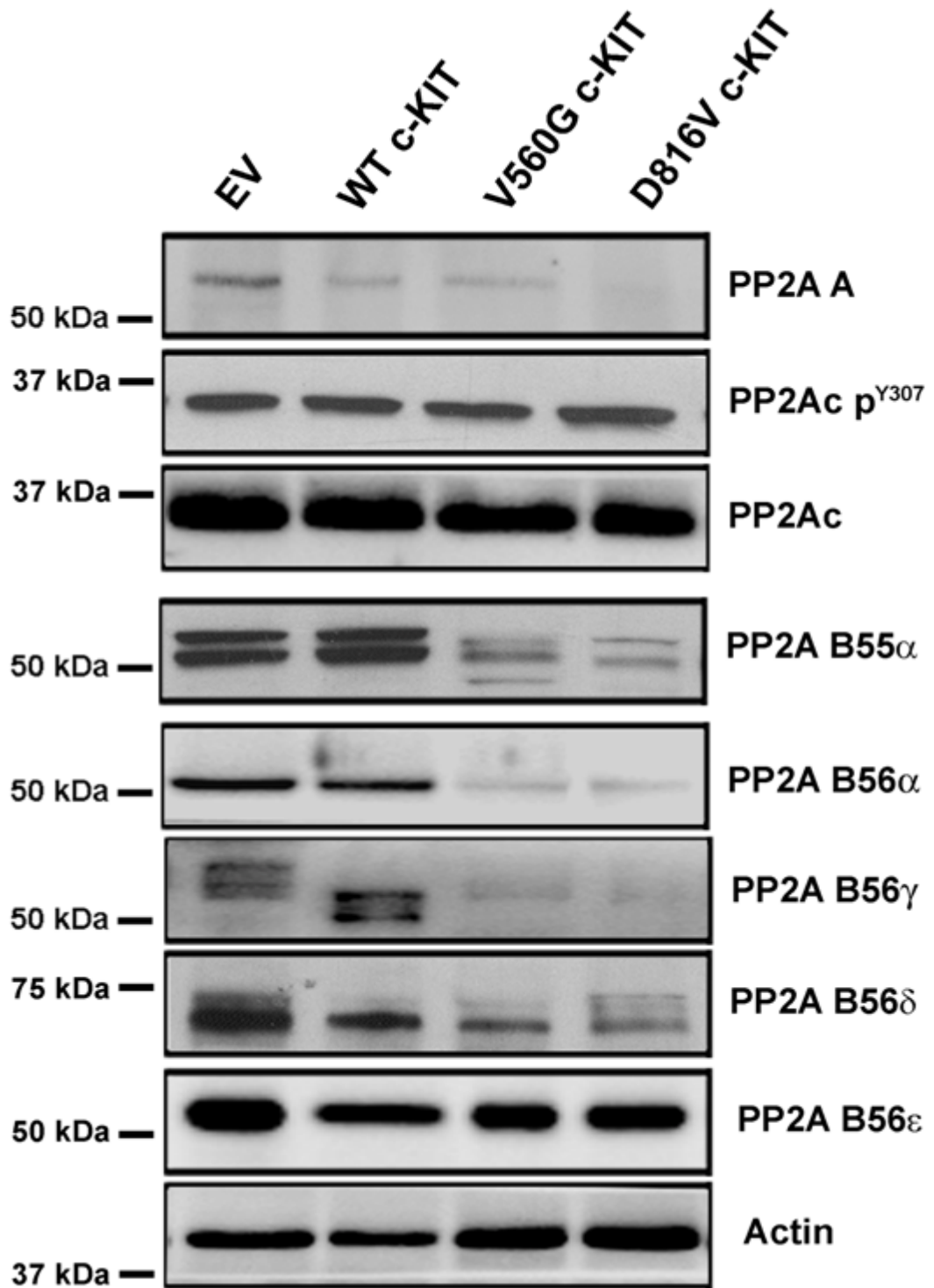


Figure 5.2 Expression of PP2A regulatory subunits in c-KIT⁺ FDC-P1 cells

Untreated FDC-P1 cell lysates were subjected to SDS-PAGE and probed for PP2A A, PP2Ac, PP2Ac p^{Y307}, B55 α , B56 α , B56 γ , B56 δ or B56 ϵ . Actin was used as a loading control. Blots are a representative of three independent experiments.

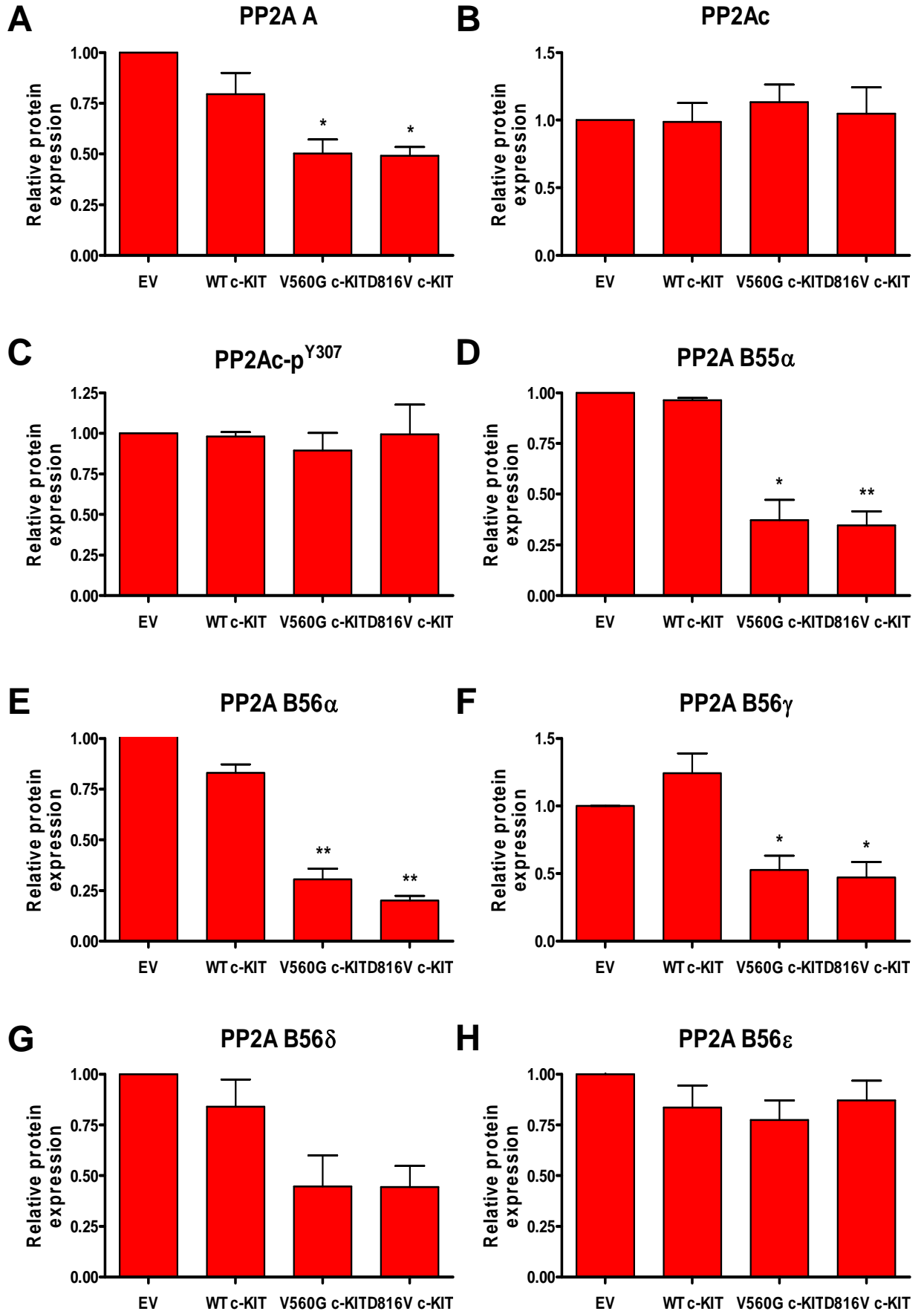


Figure 5.3 Quantitation of PP2A subunits in c-KIT⁺ FDC-P1 cells

Quantitation of **A)** PP2A **B)** PP2Ac **C)** PP2Ac p^{Y307} **D)** B55α **E)** B56α, **F)** B56γ **G)** B56δ and **H)** B56ε protein bands in FDC-P1 c-KIT cells. *Columns*, mean densitometry normalised to actin and relative to EV; *bars*, SEM, n=3. *p<0.05, **p<0.01, Student's t-test compared to EV.

known to exist and this may represent an isoform specifically regulated by WT c-KIT expression (Muneer *et al.* 2002, Martens *et al.* 2004). However, the mechanisms underlying this observation were not investigated further.

5.2.3 Reactivation of PP2A in mutant c-KIT FDC-P1 cells

To determine the biological relevance and potential therapeutic implications of PP2A loss-of-function in mutant c-KIT malignancies, the PP2A pharmacological activator, FTY720, was used (Matsuoka *et al.* 2003, Neviani *et al.* 2007). PP2A activity was enhanced by FTY720 treatment (2.5 μ M; 6 hours) in FDC-P1 cells expressing V560G c-KIT by 1.5-fold, and increased by over 2-fold in FDC-P1 D816V c-KIT cells compared to untreated controls (Figure 5.4). By contrast, minimal effect on PP2A activity was observed in FDC-P1 WT c-KIT cells or EV controls treated with FTY720 (Figure 5.4).

FTY720 is phosphorylated *in vivo* by sphingosine kinase 2 (SphK2) to yield FTY720-P, a structural analogue of sphingosine-1-phosphate (S1P) (Brinkmann *et al.* 2002). FTY720-P binds to S1P-specific G protein-coupled receptors (S1PR) and induces signalling that regulates a variety of cellular processes (Brinkmann & Lynch 2002). To determine whether the enhanced activity of PP2A is dependent on S1PR-mediated signalling, the FDC-P1 cells were incubated with FTY720-P (2.5 μ M; 6 hours). In all cell lines PP2A activity was not increased, providing evidence that the non-phosphorylated version of FTY720 is responsible for PP2A activation (Figure 5.4).

5.2.4 Reactivation of PP2A inhibits the proliferation of mutant c-KIT FDC-P1 cells

The effect of FTY720 on cellular proliferation was examined using a cytotoxicity assay. FDC-P1 cells were treated with increasing concentrations of FTY720 or FTY720-P (0.5–4 μ M) for 48 hours and the ID₅₀ for each cell line was determined. Striking differences in the response to FTY720 were observed between cells expressing activating c-KIT mutants and the WT c-KIT receptor. Specifically, FDC-P1 cells expressing V560G and D816V c-KIT displayed average ID₅₀ values of 2.8 μ M and 2.4 μ M, respectively, whereas SCF-dependent FDC-P1 WT c-KIT cells showed an ID₅₀ of 4.4 μ M (Table 5.2). Furthermore, FDC-P1 cells transformed with EV alone and

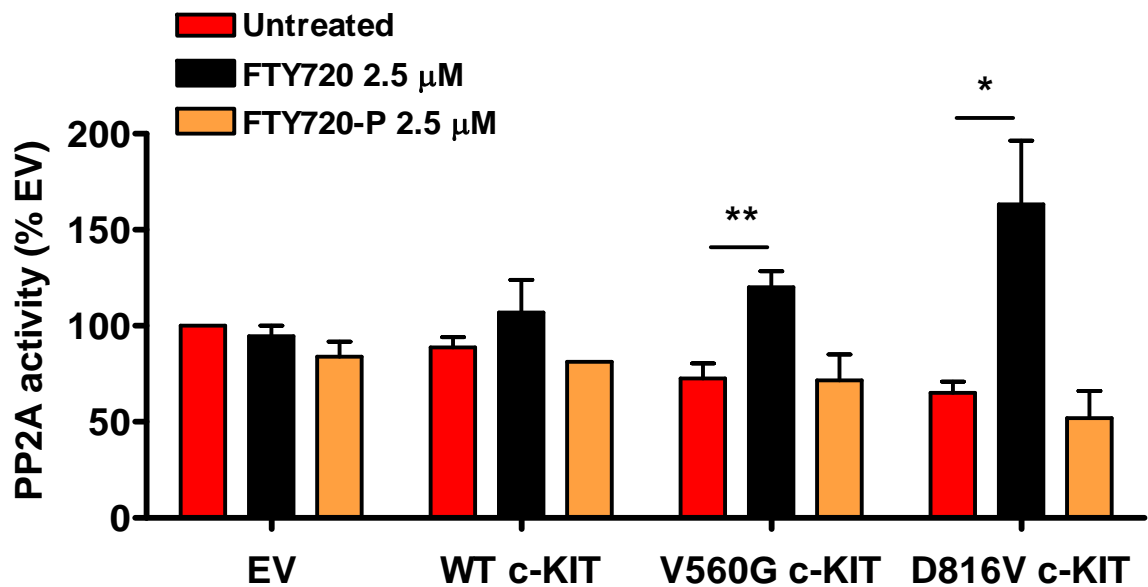


Figure 5.4 Reactivation of PP2A in mutant c-KIT FDC-P1 cells

FDC-P1 cells were treated without or with FTY720 or FTY720-P (2.5 μ M, 6 hours) and PP2Ac was immunoprecipitated from whole cell lysates. PP2A activity was determined by incubating the complex with a PP2A-specific phosphopeptide and measuring free phosphate release at an absorbance of 620 nm. PP2A activity was normalised to untreated FDC-P1 EV controls. *Columns*, mean of PP2A activity (%EV) from three independent experiments performed in duplicate; *bars*, SEM. * $p < 0.05$, ** $p < 0.01$, Student's t-test compared to untreated controls for each cell line.

Table 5.2 Cytotoxicity of PP2A activators in mutant c-KIT FDC-P1 cells

FDC-P1 Cell Line	FTY720 (μM)		Forskolin (μM)		FTY720-P (μM)	
	ID₅₀¹	Sensitivity²	ID₅₀	Sensitivity	ID₅₀	Sensitivity
EV	5.5 + 0.4	1	40.8 + 7.1	1	> 20	N/A
WT c-KIT	4.4 + 0.4	1.25	37.5 + 12.9	1.09	> 20	N/A
V560G c-KIT	2.8 + 0.3	1.96**	19.4 + 6.7	2.10**	> 20	N/A
D816V c-KIT	2.4 + 0.2	2.20**	10.6 + 6.2	3.85**	> 20	N/A

¹ID₅₀ is the concentration (μM) of drug required to kill 50% of cells and was calculated using fit-spline lowess regression of the data shown in Figure 5.5. Data is presented as the mean of at least three independent experiments performed in quadruplicate \pm SEM. ²Sensitivity was determined by dividing the ID₅₀ of the FDC-P1 EV cells by the ID₅₀ of the FDC-P1 c-KIT cell lines. **p<0.01 compared to EV, Student's t-test. N/A, not available.

grown in GM-CSF were considerably more resistant to FTY720 with an ID_{50} of 5.5 μ M (Table 5.2). In this assay, the efficacy of another chemically distinct PP2A activator, forskolin (Neviani et al. 2005, Feschenko *et al.* 2002), was also examined. Consistent with FTY720, FDC-P1 cells expressing V560G and D816V mutant c-KIT were significantly more sensitive to forskolin compared with EV controls (Table 5.2). In addition, incubation with FTY720-P up to 20 μ M had no effect on the growth of any of the FDC-P1 cell lines (Table 5.2). That FTY720 and forskolin have distinct mechanisms of action, yet both activate PP2A, strongly suggests that the cytotoxicity observed in mutant c-KIT FDC-P1 cells is due to enhanced activation of PP2A. Furthermore, this effect is not mediated via S1PR signalling.

5.2.5 Reactivation of PP2A induces apoptosis of mutant c-KIT FDC-P1 cells

The ability of FTY720 to induce apoptosis in c-KIT-expressing myeloid precursors was investigated by staining with the early apoptotic marker, annexin-V. Consistent with the ability to inhibit proliferation, FTY720 (2.5 μ M; 24 hours) markedly increased the percentage of annexin-V positive cells compared to untreated cells in the FDC-P1 V560G c-KIT population (Figure 5.5). FDC-P1 D816V c-KIT cells displayed a heightened response to FTY720 treatment, with ~60% of cells undergoing apoptosis by 24 hours (Figure 5.5). FDC-P1 cells expressing the EV alone or the WT c-KIT receptor showed no increase in annexin-V positive cells at the same concentration of FTY720 at 24 hours (Figure 5.5), or up to 48 hours (data not shown).

Cell cycle analysis of FTY720-treated (2.5 μ M; 36 hours) FDC-P1 V560G c-KIT cells revealed a moderate shift into the sub- G_0 phase, which represents non-viable cells (Figure 5.6). Consistent with the annexin-V data (Figure 5.5), FDC-P1 D816V c-KIT cells were more sensitive to FTY720 treatment with ~60% moving into the sub- G_0 phase at 36 hours (Figure 5.6). By contrast, FDC-P1 EV or WT c-KIT cells remained unaffected by the presence of FTY720 (Figure 5.6). These results demonstrate that myeloid precursors expressing activating *c-KIT* mutations are highly sensitive to PP2A reactivation. Importantly, FTY720 concentrations which have minimal impact on WT c-KIT-dependent proliferation can effectively induce apoptosis in cells expressing constitutively activated c-KIT receptors.

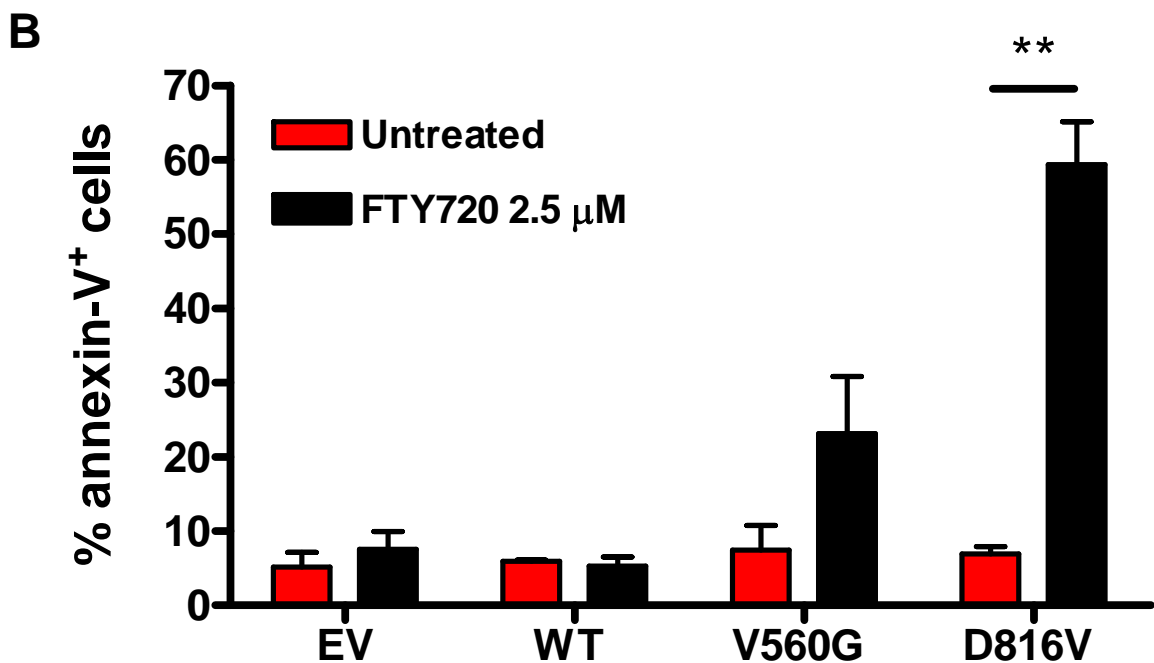
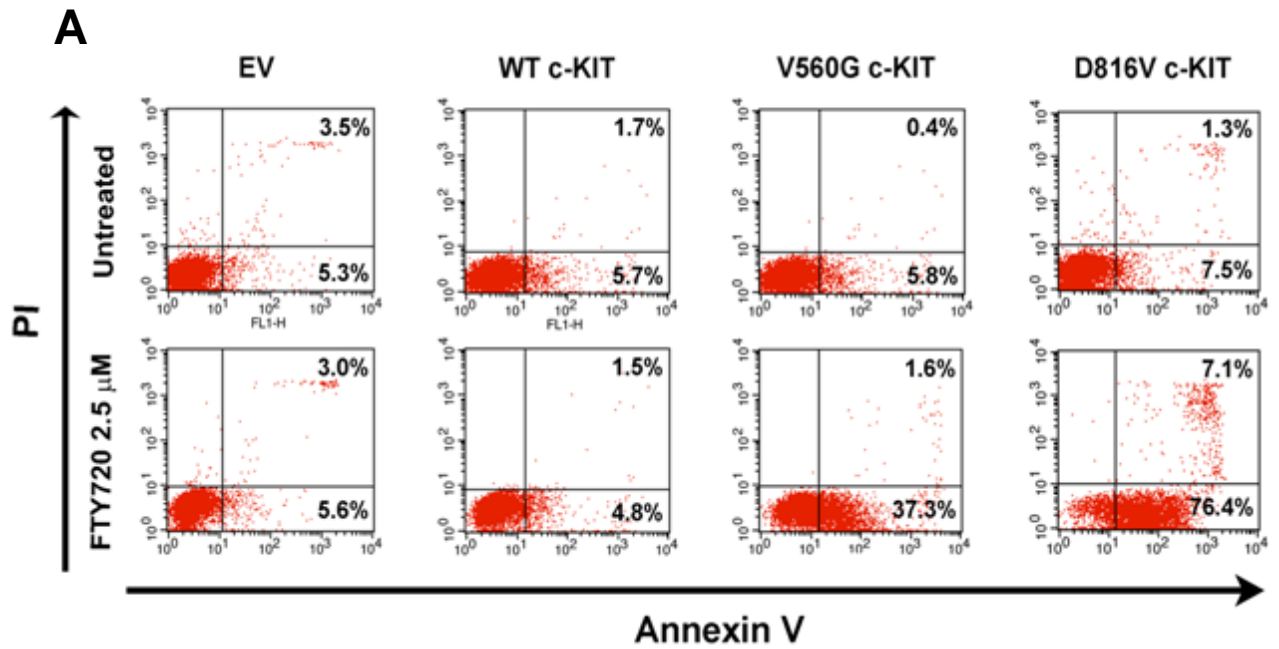


Figure 5.5 Reactivation of PP2A induces apoptosis of mutant c-KIT FDC-P1 cells

A) FDC-P1 cells were incubated in the absence or presence of FTY720 (2.5 μ M, 24 hours). Annexin-V binding was assessed as an early indicator of apoptosis. Propidium iodide (PI) staining indicates necrotic cells. Flow cytometry plots are a representative of four independent experiments. B) Columns, mean percentage of annexin-V⁺ cells; bars, SEM. **p<0.01, Student's t-test compared to untreated controls.

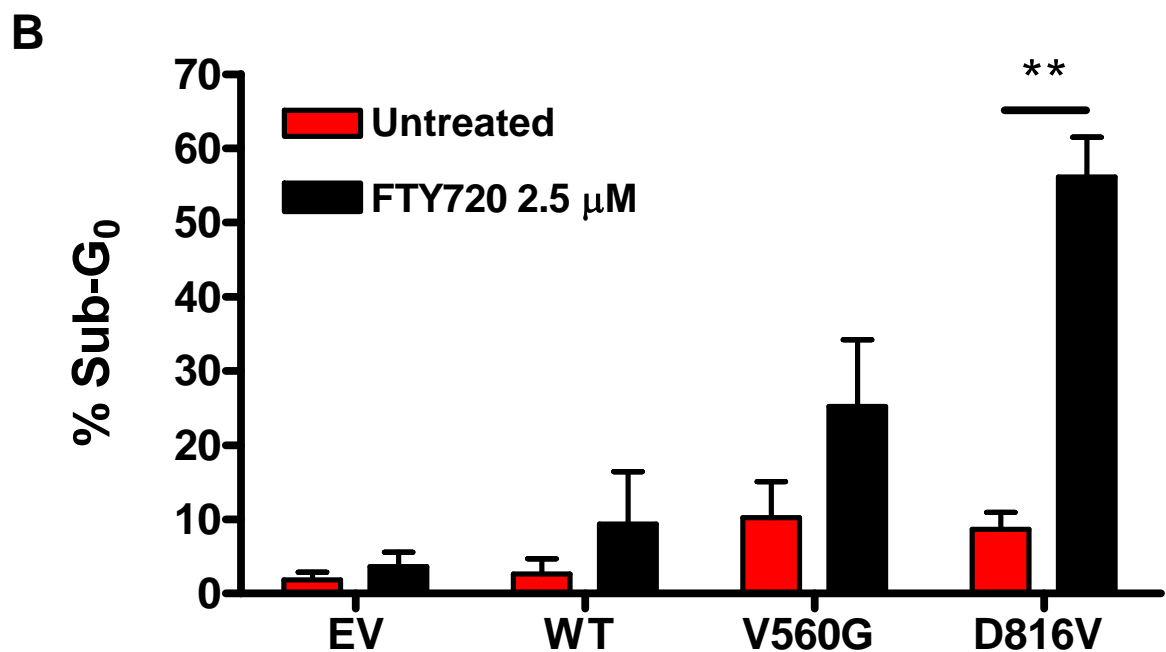
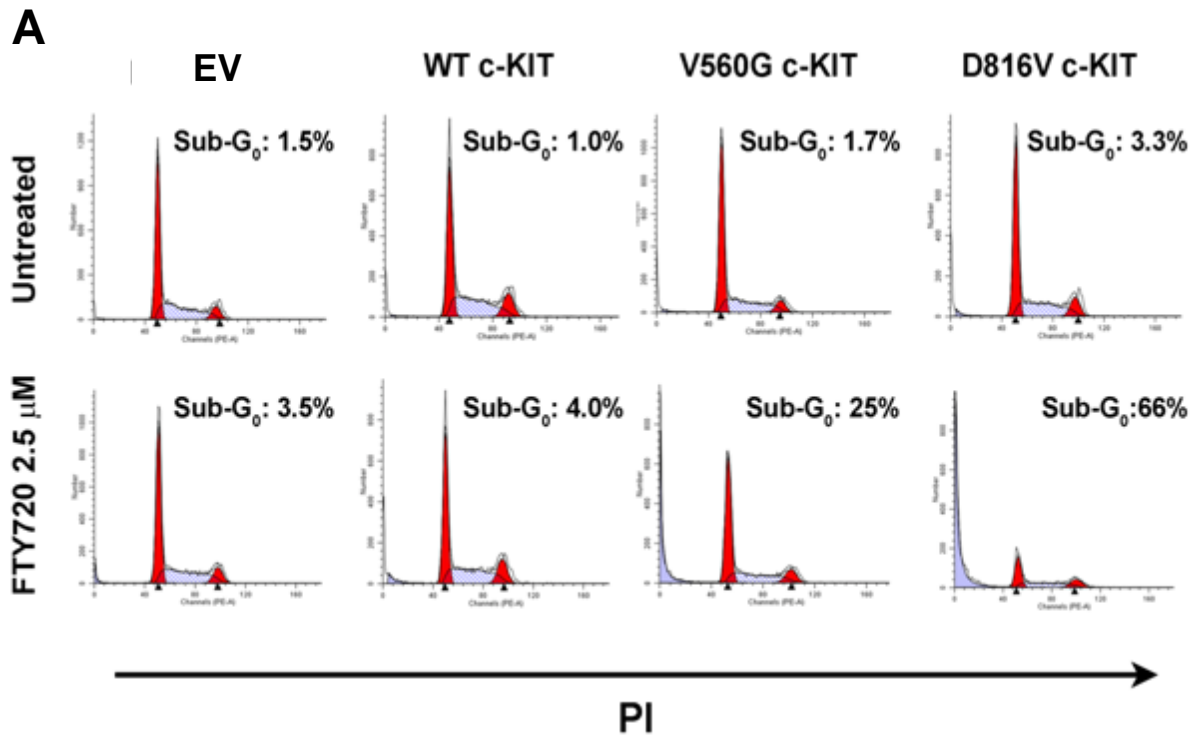


Figure 5.6 Reactivation of PP2A increases the sub-G₀ population of mutant c-KIT FDC-P1 cells

FDC-P1 cells were treated without or with FTY720 (2.5 μM; 36 hours). DNA content was determined by PI staining measured on a FACSCalibur flow cytometer. **A)** Cell cycle distribution was assessed using MODFit software. The sub-G₀ population resides before the first red peak. Plots are a representative of three independent experiments. **B)** Columns, mean percentage of sub-G₀ population; bars, SEM. **p<0.01, Student's t-test compared to untreated controls.

5.2.6 Reactivation of PP2A inhibits the clonogenic potential of mutant c-KIT cells

The effect of FTY720 on the long-term survival of mutant c-KIT-expressing myeloid progenitors was evaluated using a methylcellulose colony formation assay. Importantly, the clonogenic potential of FDC-P1 cells expressing V560G or D816V c-KIT was significantly inhibited to ~50% by 2.5 μ M FTY720 (Figure 5.7). This observation is consistent with the ID₅₀ for these cell lines being approximately 2.5 μ M (Table 5.2). Furthermore, the presence of FTY720 had a dramatic effect on the size of colonies that were formed, with the two mutant c-KIT cell lines displaying markedly smaller colonies than the EV or WT c-KIT cells (Figure 5.8). By contrast, FTY720 treatment only marginally affected the colony forming capability of FDC-P1 WT c-KIT cells and no difference was observed between untreated and FTY720-treated EV controls grown in GM-CSF (Figure 5.7).

To confirm the observed cytotoxic effects were a consequence of PP2A reactivation by FTY720, FDC-P1 D816V c-KIT cells were co-treated with the serine-threonine phosphatase inhibitor, okadaic acid (0.25 nM), at a concentration that specifically inhibits the activity of PP2A only (Cohen *et al.* 1989). Notably, the addition of okadaic acid rescued the colony formation of FTY720-treated cells (Figure 5.9A). Furthermore, the clonogenic potential of FDC-P1 V560G and D816V mutant c-KIT cells treated with FTY720-P (2.5 μ M) resembled that of untreated controls (Figure 5.9B). Together this data further confirms that FTY720 mediates its *in vitro* effects on FDC-P1 mutant c-KIT cells by specifically enhancing PP2A activity, and not via S1PR-mediated signalling.

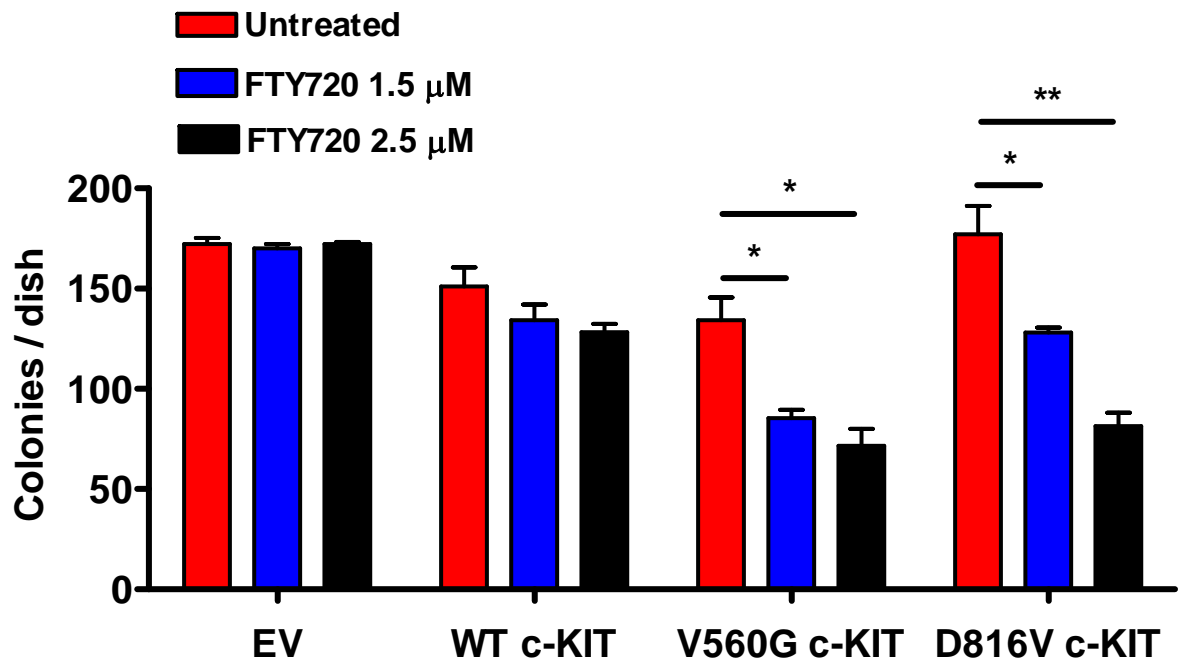


Figure 5.7 Reactivation of PP2A impairs the clonogenic potential of mutant c-KIT FDC-P1 cells

For each assay, 200 FDC-P1 cells were plated without or with FTY720 (1.5 or 2.5 μ M) in methylcellulose and colonies were counted after 7 days. *Columns*, mean of three independent experiments performed in triplicate; *bars*, SEM. * $p < 0.05$, ** $p < 0.01$, Student's t-test compared to untreated controls for each cell line.

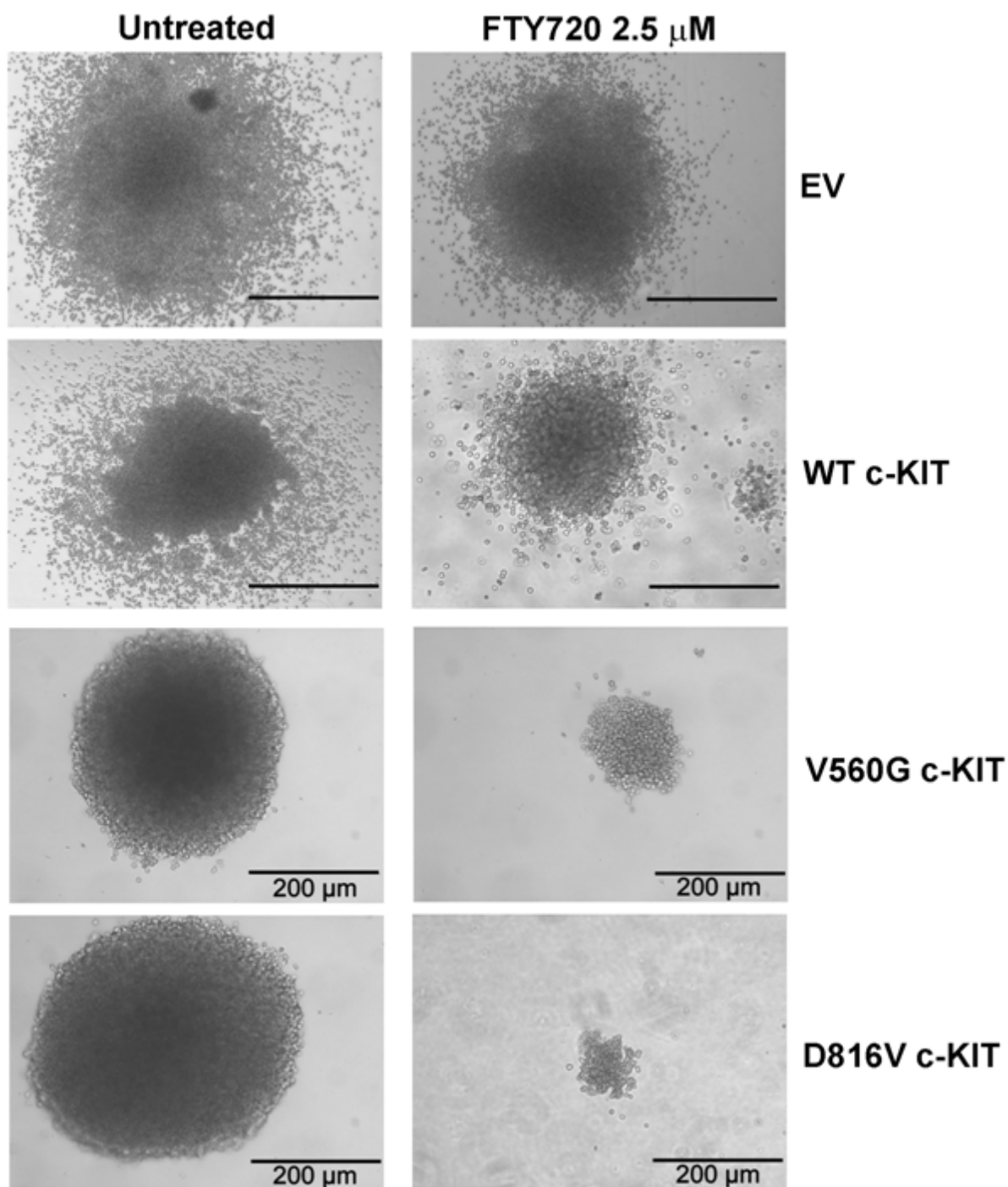


Figure 5.8 Colony formation of FTY720-treated FDC-P1 cells

Untreated and FTY720-treated (2.5 μ M) FDC-P1 colonies were viewed at 100x magnification on a CK40 Olympus microscope. Photographs were taken with a ColourView II camera and analySIS software.

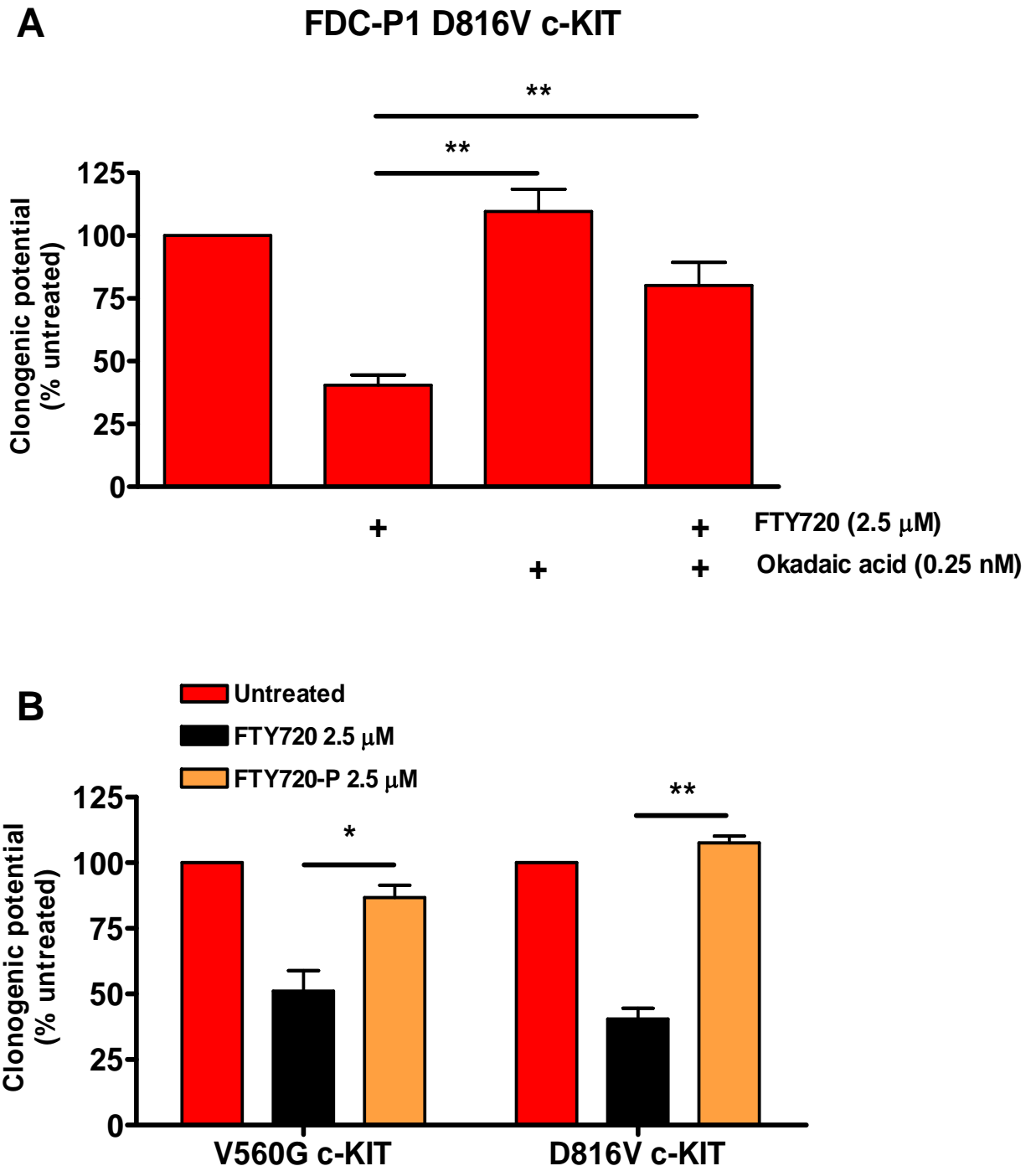


Figure 5.9 Cytotoxic effect of FTY720 on mutant c-KIT FDC-P1 cells requires PP2A reactivation

A) FDC-P1 D816V c-KIT cells were plated in FTY720 (2.5 μ M), okadaic acid (0.25 nM) or FTY720 (2.5 μ M) plus okadaic acid (0.25 nM). **B)** FDC-P1 V560G and D816V c-KIT cells were plated in methylcellulose without or with FTY720 or FTY720-P (2.5 μ M). Colonies were counted after 7 days. Data is presented as percentage of untreated controls for each cell line. *Columns*, mean of three independent experiments performed in triplicate; *bars*, SEM. * $p < 0.05$, ** $p < 0.01$, Student's t-test compared to FTY720-treated for each cell line.

5.2.7 Reactivation of PP2A dephosphorylates c-KIT in FDC-P1 cells

c-KIT activity is regulated by tyrosine phosphorylation (Ashman 1999). Inhibition of c-KIT phosphorylation inactivates the receptor, and hence attenuates the activation of downstream signalling pathways (Linnekin 1999). To determine if PP2A reactivation affects c-KIT phosphorylation, c-KIT was immunoprecipitated from FDC-P1 cells treated without or with FTY720 (2.5 μ M; 6, 12 and 24 hours). Total c-KIT was present as two bands with an apparent molecular weight of 145 and 160 kDa, corresponding to non-glycosylated and glycosylated forms, respectively (Koshimizu *et al.* 1994).

FTY720-induced reactivation of PP2A in both FDC-P1 mutant c-KIT cell lines caused a significant reduction of c-KIT tyrosine phosphorylation at 6 hours (Figure 5.10). In contrast, phosphorylation of the WT c-KIT receptor remained stable at 24 hours, consistent with these cells being less responsive to FTY720 (Figure 5.10). These results suggest that PP2A inhibition is required for sustained c-KIT phosphorylation, and that enhanced activation of PP2A results in c-KIT dephosphorylation.

5.3 Discussion

These findings show for the first time that inhibition of PP2A is required for c-KIT-mediated tumorigenesis. Constitutive activation of c-KIT via the JMD mutation (V560G) or the kinase domain mutation (D816V) inhibits the activity of the tumour suppressor PP2A (Table 5.1). The mechanism of PP2A inhibition is associated with decreased expression of the PP2A structural and regulatory subunits (Figure 5.2). Furthermore, the data indicates that reactivation of PP2A specifically reduces the growth and survival of both imatinib sensitive and -resistant oncogenic c-KIT cells. Thus specific activation of PP2A could provide a unique target for therapeutic intervention in both haematological and solid malignancies expressing mutant c-KIT such as CBF-AML, systemic mastocytosis, GIST, testicular seminoma and melanoma. PP2A inhibition is also crucial for BCR/ABL-mediated leukaemogenesis (Neviani *et al.* 2005) (Chapter 3). Taken together, these results suggest that inactivation of PP2A may be a general mechanism employed by oncogenic tyrosine kinases to induce a tumourigenic phenotype.

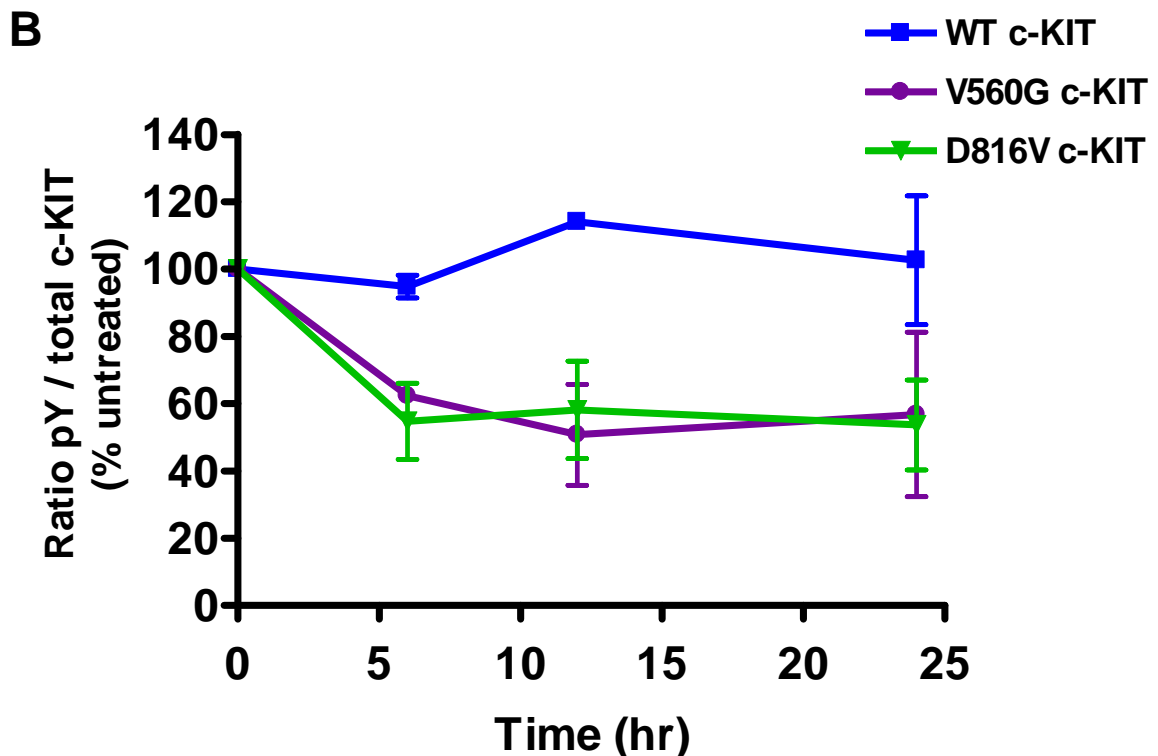
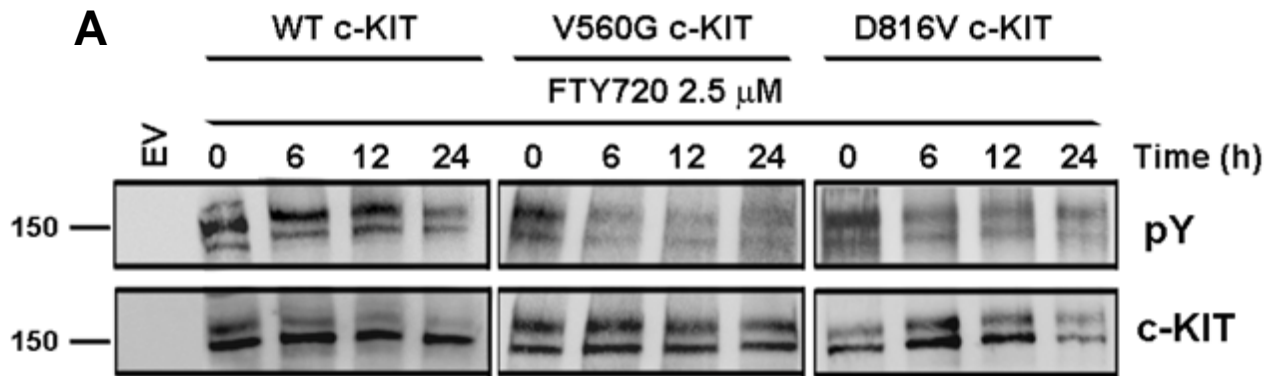


Figure 5.10 Reactivation of PP2A dephosphorylates c-KIT

A) c-KIT was immunoprecipitated from FDC-P1 cells treated without or with FTY720 (2.5 μ M; 6, 12 and 24 hours). Levels of tyrosine phosphorylated (pY) and total c-KIT were determined by immunoblotting with a pY and human c-KIT antibody. Blot is a representative of three independent experiments. **B)** Quantitation of pY c-KIT / total c-KIT levels at each time point relative to untreated controls for each cell line. *Points*, mean of three independent experiments; *bars*, SEM. **NB.** Both the V560G and D816V c-KIT cells are significantly reduced ($p < 0.05$, Student's t-test) compared to WT c-KIT cells at the 6 hour and 12 hour time points, and the D816V cells are significantly reduced ($p < 0.05$) compared to WT c-KIT at the 24 hour point.

Using the pharmacological agent, FTY720, impaired PP2A activity can be restored in myeloid cells expressing mutant c-KIT receptors (Figure 5.4). Importantly, this induces c-KIT dephosphorylation on both imatinib sensitive (V560G) and –resistant (D816V) activating c-KIT mutants (Figure 5.10). The mechanisms underlying this are unclear. As PP2A is a serine/threonine phosphatase, dephosphorylation of c-KIT most likely involves the recruitment of additional proteins that act directly on the receptor. One particular candidate is the tyrosine phosphatase SHP-1, a known negative regulator of c-KIT (Kozlowski *et al.* 1998, Paulson *et al.* 1996). The ubiquitin-dependent degradation of SHP-1 contributes to the transforming potential of the mouse D814Y c-KIT mutant (human homolog of D816) in mast cells (Piao *et al.* 1996). Furthermore, PP2A has been shown to associate with, and activate SHP-1 in FTY720-treated BCR/ABL⁺ myeloid cells, which leads to dephosphorylation and degradation of the oncoprotein (Neviani *et al.* 2005). Thus, restoration of PP2A function by FTY720 may impair the oncogenic potential of mutant c-KIT cells through the activation of SHP-1 and subsequent dephosphorylation of the c-KIT receptor.

Consistent with the inhibition of oncogenic c-KIT, reactivation of PP2A significantly reduced the proliferation (Table 5.2), induced apoptosis (Figure 5.5 and 5.6) and suppressed the clonogenic potential of cells expressing V560G or D816V mutant c-KIT (Figure 5.7 and 5.8). Importantly, at the same concentration of FTY720, these effects were not observed in GM-CSF dependent FDC-P1 EV cells or WT c-KIT cells grown in SCF. This highlights that the growth inhibition observed with FTY720 treatment is dependent on the functional status of PP2A, whereby cells expressing activating *c-KIT* mutations are more sensitive due to impaired PP2A activity. The increased sensitivity of c-KIT mutants compared to WT c-KIT suggests that FTY720 could target malignant cells at low doses without disrupting normal SCF/c-KIT signalling.

FTY720 is a water-soluble, non-toxic drug with high oral bioavailability that is structurally similar to sphingosine and is currently being evaluated as an immunomodulator in phase III trials for multiple sclerosis patients (Brown *et al.* 2007, Takabe *et al.* 2008). FTY720 is phosphorylated by SphK2 and FTY720-P binds to S1PR, which induces internalisation and downregulation of the receptor (Matloubian *et al.* 2004). This traps lymphocytes within secondary lymphoid tissues and is important for its immunomodulatory role (Brinkmann *et al.* 2002). In addition, FTY720 directly

activates purified PP2A dimers and heterotrimers *in vitro* (Matsuoka et al. 2003), and is effective against preclinical models of Ph¹ CML/ALL (Neviani et al. 2007) and B-CLL (Liu *et al.* 2008).

The precise mechanism by which FTY720 enhances PP2A activity remains undefined. It is possible that at high doses FTY720 acts as an intracellular second messenger similar to sphingosine and ceramide, which both induce apoptosis independent of S1PR signalling (Ogretmen & Hannun 2004, Suzuki *et al.* 2004). Recent evidence has shown that direct binding of ceramide to SET restrains the inhibitory effect on PP2A to result in increased PP2A activity (Mukhopadhyay *et al.* 2009). A likely scenario is that FTY720 mimics the actions of ceramide and activates PP2A by removing the endogenous inhibition normally exerted by the SET protein. In addition, ceramide promotes the translocation of PP2A B56 α to the mitochondrial membrane where it dephosphorylates the anti-apoptotic protein, Bcl-2, and enhances cell death (Ruvolo et al. 2002, Ruvolo et al. 1999). Interestingly, oncogenic c-KIT cells showed reduced levels of B56 α (Figure 5.2). Therefore, it is possible that FTY720 may induce apoptosis by enhancing the expression and formation of PP2A-B56 α complexes which direct the enzyme towards Bcl-2.

In agreement with the mechanism whereby FTY720 induces apoptosis of BCR/ABL⁺ cells independently of S1PR signalling (Neviani et al. 2007), the present data also demonstrates that PP2A reactivation does not require FTY720 phosphorylation (Figure 5.4). Furthermore, the cytotoxic effects exerted by FTY720 are specifically mediated by the reactivation of PP2A, as inhibition of FTY720-induced PP2A activation by okadaic acid restores the clonogenic potential of FDC-P1 D816V mutant c-KIT cells (Figure 5.9A). Similar results were observed with FTY720-P, which had no effect on the proliferation (Table 5.2) or survival of myeloid cells expressing oncogenic c-KIT (Figure 5.9B), indicating that PP2A activation is not mediated via S1PR signalling. Consistent with these observations, two chiral analogues of FTY720, AAL151 and AAL149, both induce apoptosis *in vitro* at the same micromolar concentration, but only AAL151 targets and inactivates S1PR at low nanomolar concentrations *in vivo* (Brinkmann et al. 2002, Brinkmann *et al.* 2001).

Incubation with a chemically distinct PP2A activator, forskolin, also impaired mutant c-KIT growth (Table 5.2). Forskolin has traditionally been used as a tool to assess the effects of adenylate cyclase activation; however it was more recently found to activate PP2A (Feschenko et al. 2002). PP2A activation by forskolin is independent of cAMP induction, as 1,9-dideoxyforskolin, an analogue that does not affect cAMP levels, also activates PP2A (Neviani et al. 2005). The hypersensitivity of mutant c-KIT FDC-P1 cells to two distinct PP2A activators strongly indicates that reactivation of PP2A is the essential mechanism of action underlying the observed cytotoxic effects.

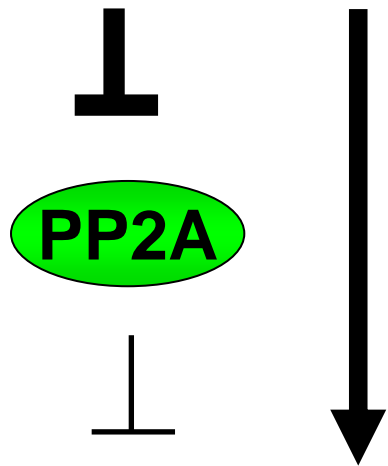
Interestingly, the ability of FTY720 to inhibit oncogenic c-KIT cell growth may be influenced by the particular type of *c-KIT* mutation that is expressed. Overall, cells expressing the aggressive D816V c-KIT mutant displayed heightened sensitivity to FTY720. The mechanisms underlying this increased sensitivity are unclear; however, differences in activation of signalling pathways downstream of the JMD and kinase domain c-KIT mutants are a likely factor. For example, the 85 kDa regulatory subunit of PI3K is constitutively phosphorylated and associated with D816V c-KIT, which is important for its transforming potential (Table 1.3) (Chian *et al.* 2001). PP2A negatively regulates multiple components of important oncogenic pathways including PI3K (Yamada *et al.* 2001), and FTY720 inhibits these pathways through activation of PP2A (Liu et al. 2008, Neviani et al. 2007). Therefore, FTY720-induced PP2A activation in D816V c-KIT cells would simultaneously dephosphorylate c-KIT and inhibit downstream signals to result in reduced growth and survival.

A novel and important finding arising from this body of work is the functional link between oncogenic c-KIT activation and PP2A inhibition (Table 5.1). No study to date has investigated the importance of PP2A regulation in c-KIT-driven transformation. One recent report found that primary AML samples with a high-risk, complex karyotype had significantly reduced PP2A activity compared to those with the CBF-AML translocation t(8;21) (Gallay *et al.* 2009). Notably, the mutation status of c-KIT in these samples was not determined. Studies comparing the activity of PP2A in normal haematopoietic progenitors to CBF-AML samples are required to determine whether the inactivation of PP2A observed in the current FDC-P1 model translates into the clinic.

Regulation of PP2A activity and specificity is complex. Translation of the catalytic subunit is tightly controlled (Janssens & Goris 2001), and indeed, no changes in the total protein expression of PP2Ac in cells with or without c-KIT was found (Figure 5.2 and 5.3). However, expression of the structural and a number of regulatory PP2A subunits were decreased in the mutant c-KIT expressing FDC-P1 cells (Figure 5.2 and 5.3). RNAi knockdown of PP2A A in neuronal cells leads to the proteasomal degradation of B family subunits, with a concomitant loss of total PP2A activity (Strack *et al.* 2004). Furthermore, suppression of PP2A A α or B56 γ using shRNA induces tumourigenicity in the HEK-TER transformation model (Chen *et al.* 2004, Chen *et al.* 2005). Reduced expression of PP2A subunits has also been observed in human gliomas, breast cancers and B-CLL primary samples (Wlodarski *et al.* 2006, Suzuki & Takahashi 2006, Colella *et al.* 2001, Falt *et al.* 2005), as well as lung cancer cell lines (Chen *et al.* 2004). In addition, a dominant negative isoform of B56 γ 1 is associated with increased metastatic potential of the melanoma cell line, BL6 (Ito *et al.* 2000). In the present study, B56 γ is reduced to undetectable levels in both of the mutant c-KIT FDC-P1 cell lines (Figure 5.2 and 5.3). Taken together, downregulation of the structural and regulatory subunits in cells expressing active c-KIT may be one mechanism which could contribute to reduced PP2A activity in these cells. *It is interesting to note that although BCR/ABL and mutant c-KIT both inhibit PP2A activity, BCR/ABL appears to increase PP2A subunit expression, whilst the opposite effect is observed in mutant c-KIT cells. Given the fact that these two oncogenes activate similar downstream signalling pathways, one would hypothesise that they employ a similar mechanism of PP2A regulation. The reason for this apparent discrepancy is currently unknown, and warrants further investigation.*

In summary, the data presented in this Chapter demonstrates for the first time that activating c-KIT receptors inhibit the tumour suppressor, PP2A (Figure 5.11A). Importantly, enhancing the activity of PP2A effectively suppresses the *in vitro* growth of imatinib-sensitive and –resistant oncogenic c-KIT cells (Figure 5.11B). This study, together with those related to the interplay between PP2A and BCR/ABL (Neviani *et al.* 2007) (Chapters 3 and 4), indicate that functional inactivation of PP2A may represent a key step in the induction and maintenance of leukaemias and, perhaps, other solid tumours characterised by the aberrant activation of oncogenic tyrosine kinases.

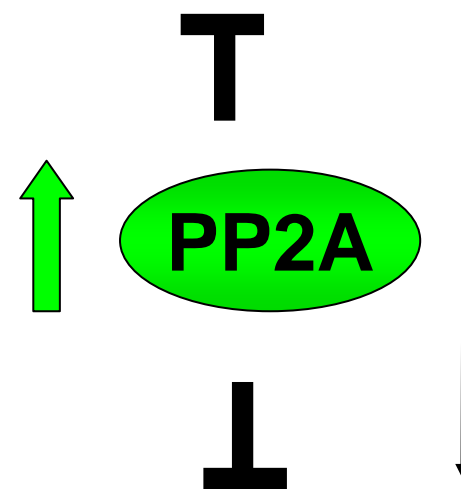
A Mutant c-KIT



Signalling pathways

TUMOURIGENESIS

B Mutant c-KIT



Signalling pathways

TUMOURIGENESIS

Reactivate PP2A



e.g. FTY720

Figure 5.11 Regulation of PP2A by mutant c-KIT and reactivation with FTY720

A) Activating oncogenic c-KIT receptors in myeloid progenitors impair PP2A activity, which contributes to the tumourigenic phenotype. **B)** Reactivation of PP2A with FTY720 inactivates the oncogenic tyrosine kinase itself, and is predicted to inhibit downstream signalling pathways to reduce mutant c-KIT-driven tumour growth.

CHAPTER 6

FTY720 INHIBITS MUTANT c-KIT TUMOUR GROWTH *IN VIVO*

6.1 Introduction

Oncogenic mutations of the receptor tyrosine kinase c-KIT play an important role in the pathogenesis of several malignancies including CBF-AML, systemic mastocytosis and GIST. Whilst JMD mutations commonly detected in GIST are sensitive to imatinib (e.g V560G), the kinase domain mutations frequently encountered in CBF-AML and systemic mastocytosis (e.g D816V) are unresponsive to targeted inhibition (Frost *et al.* 2002). It is likely that successful treatment of c-KIT-driven cancers may require alternative strategies which simultaneously target c-KIT and its oncogenic signalling pathways via mechanisms different to those employed by traditional inhibitors. Using FDC-P1 mouse myeloid cells expressing imatinib-sensitive (V560G) or –resistant (D816V) mutant c-KIT, the findings from Chapter 5 demonstrate that inhibition of PP2A is required for c-KIT-mediated tumourigenesis. As such, enhancing the tumour suppressive activity of PP2A is an attractive therapeutic strategy for these malignancies.

Several studies have demonstrated the antiproliferative agents, forskolin and ceramide, both mediate cell death through the activation of PP2A (Dobrowsky *et al.* 1993, Feschenko *et al.* 2002, Hannun & Obeid 2002). More recently, enhanced activity of PP2A was discovered as an underlying mechanism by which the sphingosine analogue, FTY720, induces apoptosis of Jurkat cells (Matsuoka *et al.* 2003). Furthermore, FTY720 has demonstrated promising results against *in vitro* and *in vivo* models of imatinib-resistant Ph¹ CML/ALL (Neviani *et al.* 2007) and B-CLL (Liu *et al.* 2008). Importantly, no cytotoxic effects were observed with long-term FTY720 treatment, highlighting its specificity for leukaemia cells. Results obtained from the present study indicate that the pharmacological reactivation of PP2A by FTY720 inhibits c-KIT-mediated growth and survival of myeloid progenitors, as demonstrated by reduced proliferation, enhanced apoptosis and impaired clonogenicity of FDC-P1 mutant c-KIT cells (Chapter 5). In addition, FTY720 also impairs the oncogenic activation of c-KIT itself. All together these results indicate that the reactivation of PP2A may be a novel treatment strategy for mutant c-KIT⁺ cancers. Thus this Chapter aimed to assess the

preclinical efficacy of FTY720 in an *in vivo* model of V560G and D816V c-KIT tumour growth.

6.2 Results

6.2.1 Establishing an *in vivo* model for FDC-P1 c-KIT tumour growth

To evaluate the therapeutic potential of reactivating PP2A in oncogenic c-KIT cells, it was necessary to establish a mouse model for c-KIT⁺ tumour growth. FDC-P1 cells were originally isolated from DBA/2J mice (Dexter *et al.* 1980), and as such, this strain was used to develop a syngeneic model for the growth of tumours formed by FDC-P1 cells expressing either the V560G or D816V mutant c-KIT (Cullinane *et al.* 2005). Cells expressing WT c-KIT do not form tumours in mice and therefore could not be included as a negative control (Ferrao *et al.* 1997). A preliminary study was conducted to investigate the tumour kinetics and determine the optimal cell number required for tumour growth. The mice were randomised into groups of 4 that received s.c. injections of either 2.5 or 5 x 10⁶ FDC-P1 cells on both flanks. Developing tumours were visibly inspected and palpated daily until day 18, when the volumes were accurately measured with callipers. At this point the tumours grew at a rapid rate, with most mice reaching the ~2100 mm³ limit and being sacrificed by day 23. No differences were observed between the growth rate of tumours formed by 2.5 or 5 x 10⁶ cells (Figure 6.1). For both cell lines, the take rate for the higher dose was 100%, whilst 3 out of 4 mice developed tumours in the lower group. Based on this observation, 5 x 10⁶ cells/tumour site was chosen as an optimal cell number to inject. The body weight of the mice remained stable for the first 14 days, at which point a gradual increase correlated with tumour development (Figure 6.1).

6.2.2 Evaluating the toxicity of FTY720 in DBA/2J mice

Numerous preclinical models have demonstrated the safety of FTY720 treatment, with no adverse events being reported following long term administration up to 10 mg/Kg/day (Neviani *et al.* 2007, Liu *et al.* 2008). However, an initial toxicity study was required to determine the maximum tolerable dose for FTY720 in the DBA/2J strain. The mice were randomised into three groups of 4 with the first group receiving daily saline i.p. injections, whilst the other two groups were administered daily i.p. injections

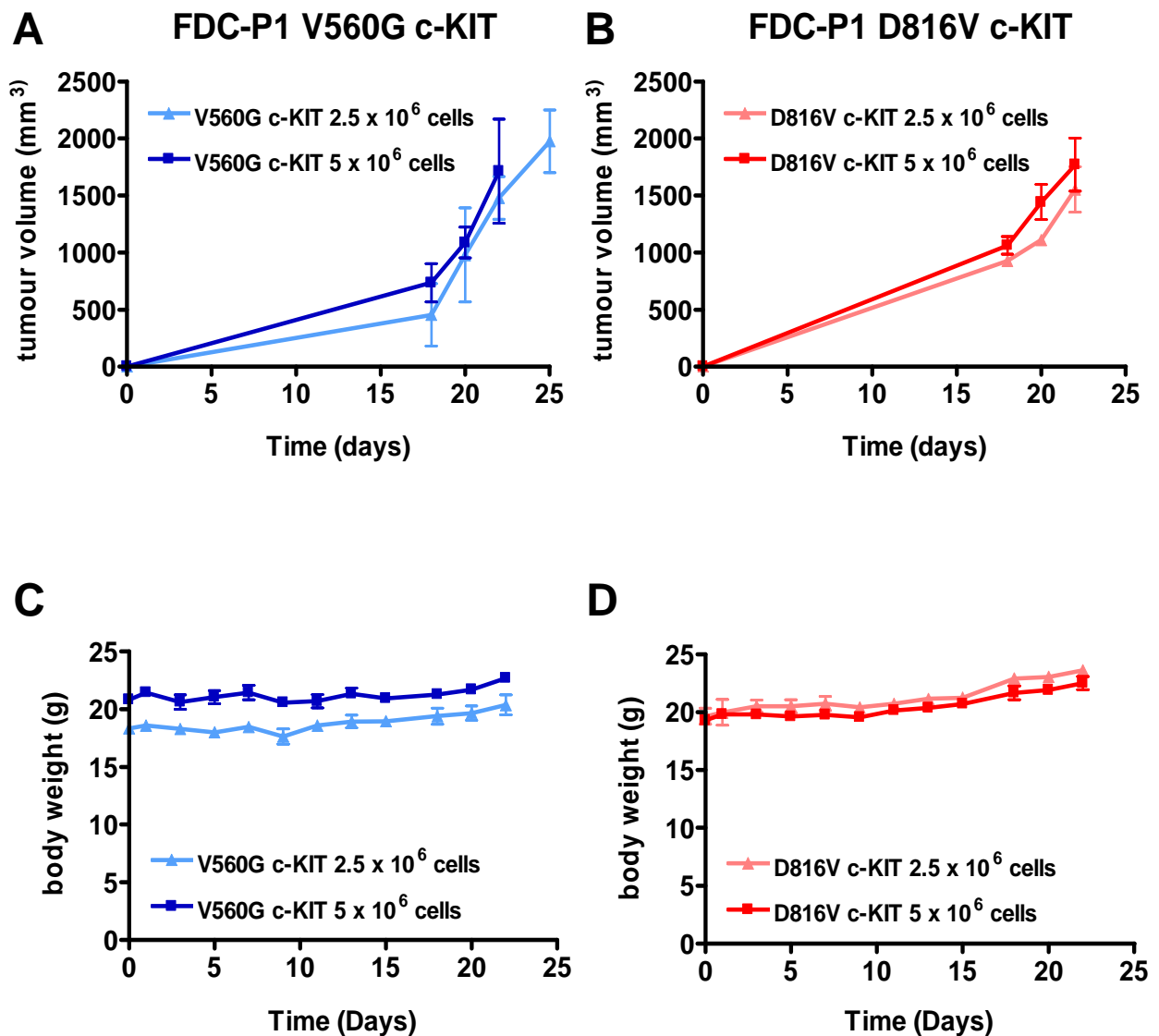


Figure 6.1 Preliminary studies of FDC-P1 V560G and D816V c-KIT tumour growth
 DBA/2J mice were randomised into groups of 4. FDC-P1 cells expressing V560G or D816V c-KIT were s.c. inoculated into both flanks (2.5 or 5 x 10⁶ cells/site). **A)** and **B)** Tumour volume was determined by calliper measurement using the formula: $tumour\ volume = 0.5 \times length\ (mm) \times width^2\ (mm)$. *Points*, mean tumour volume (mm³) from 4 mice; *bars*, SEM. **C)** and **D)** Mice were weighed every second day to monitor for toxic side effects. *Points*, mean body weight (g) from 4 mice; *bars*, SEM.

of 5 or 10 mg/Kg FTY720. An initial decline in animal weight after the first two FTY720 treatments was observed. However, this stabilised at day 5 of treatment, and the mice continued to gain weight until they were sacrificed at day 23 (Figure 6.2). No further signs of acute or delayed toxicity were noted. Haematological data revealed no difference in the number of red blood cells compared to saline controls. FTY720 (10 mg/Kg/day) resulted in significantly reduced white blood cell counts and splenic weight (Table 6.1). As FTY720 is an immunomodulator and induces reversible lymphopaenia in animal models and humans, this finding was expected (Pinschewer *et al.* 2000, Budde *et al.* 2002, Chiba *et al.* 1998, Skerjanec *et al.* 2005). No other toxic side effects were noted (Table 6.1). Based on these observations, 10 mg/Kg/day FTY720 was the dose chosen for the subsequent treatment studies.

6.2.3 FTY720 delays mutant c-KIT tumour growth

Next, the efficacy of FTY720 against established tumours expressing either the V560G or D816V mutant c-KIT was evaluated in the syngeneic mouse model. FDC-P1 cells (5×10^6) were s.c. injected into the left and right flanks of DBA/2J mice. Once the tumours reached $\sim 200 \text{ mm}^3$ on day 5, the control mice received daily administration of saline [(i.p. or oral gavage (p.o.)]. Mice bearing V560G c-KIT tumours received daily doses of FTY720 (10 mg/Kg) via i.p. injection, whilst two routes of administration were tested on mice harbouring D816V c-KIT tumours (i.p and p.o.). Imatinib treatment (50 mg/Kg/day p.o.) was also performed on a minimal number of mice as a positive control for this model.

Compared to saline-treated mice, the growth of V560G c-KIT tumours was marginally suppressed by FTY720 (Figure 6.3). Consistent with *in vitro* results (Chapter 5), administration of FTY720 significantly delayed the growth of tumours expressing D816V c-KIT (Figure 6.3). This effect was observed up to 23 days post-tumour injection. No significant difference was seen between i.p. and oral dosing of FTY720 against D816V c-KIT⁺ tumours (Figure 6.3). As expected, imatinib was extremely effective at suppressing the growth of V560G c-KIT tumours, but had no effect on tumours harbouring the D816V mutant (Figure 6.4).

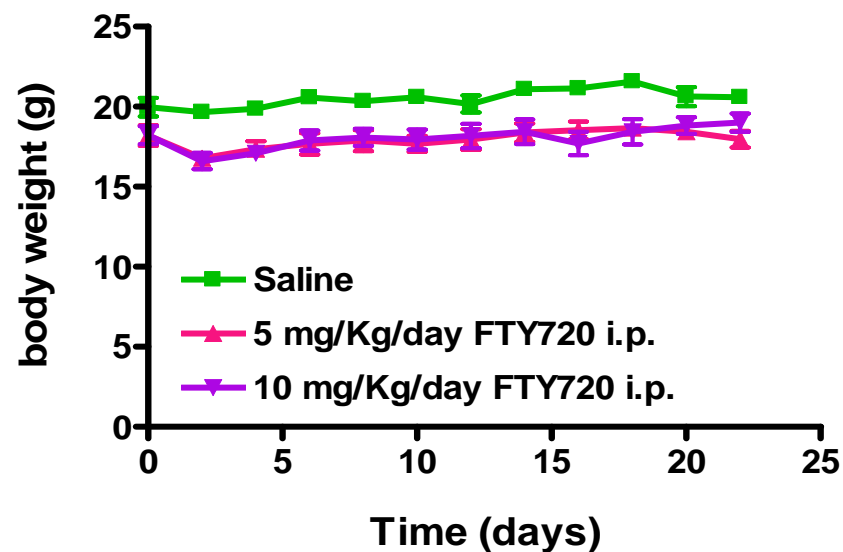


Figure 6.2 Safe administration of FTY720 in DBA/2J mice

Mice were randomised into groups of 4 that received daily i.p. injections of either saline, 5 or 10 mg/Kg/day FTY720. Body weights were monitored every second day. *Points*, mean body weight (g) from 4 mice; *bars*, SEM.

Table 6.1 Toxicity data for FTY720 treatment

Treatment ¹	Spleen (mg)	Liver (mg)	Kidney (mg)	RBC (x10 ¹² /dL)	WBC (x10 ⁸ /dL)
Saline	89 ± 8	1135 ± 48	269 ± 5	1.3 ± 0.02	5.2 ± 1.2
5 mg/Kg FTY720	73 ± 4	1035 ± 61	250 ± 15	1.2 ± 0.05	3.0 ± 0.2
10 mg/Kg FTY720	56 ± 7*	1040 ± 20	243 ± 7	1.3 ± 0.03	1.9 ± 0.3*

¹On day 23 all mice were sacrificed. The organs were weighed and the red and white blood cells (RBC/WBC) were counted. Data is presented as mean ± SEM, n=4. *p<0.05, Student's t-test compared to saline-treated.

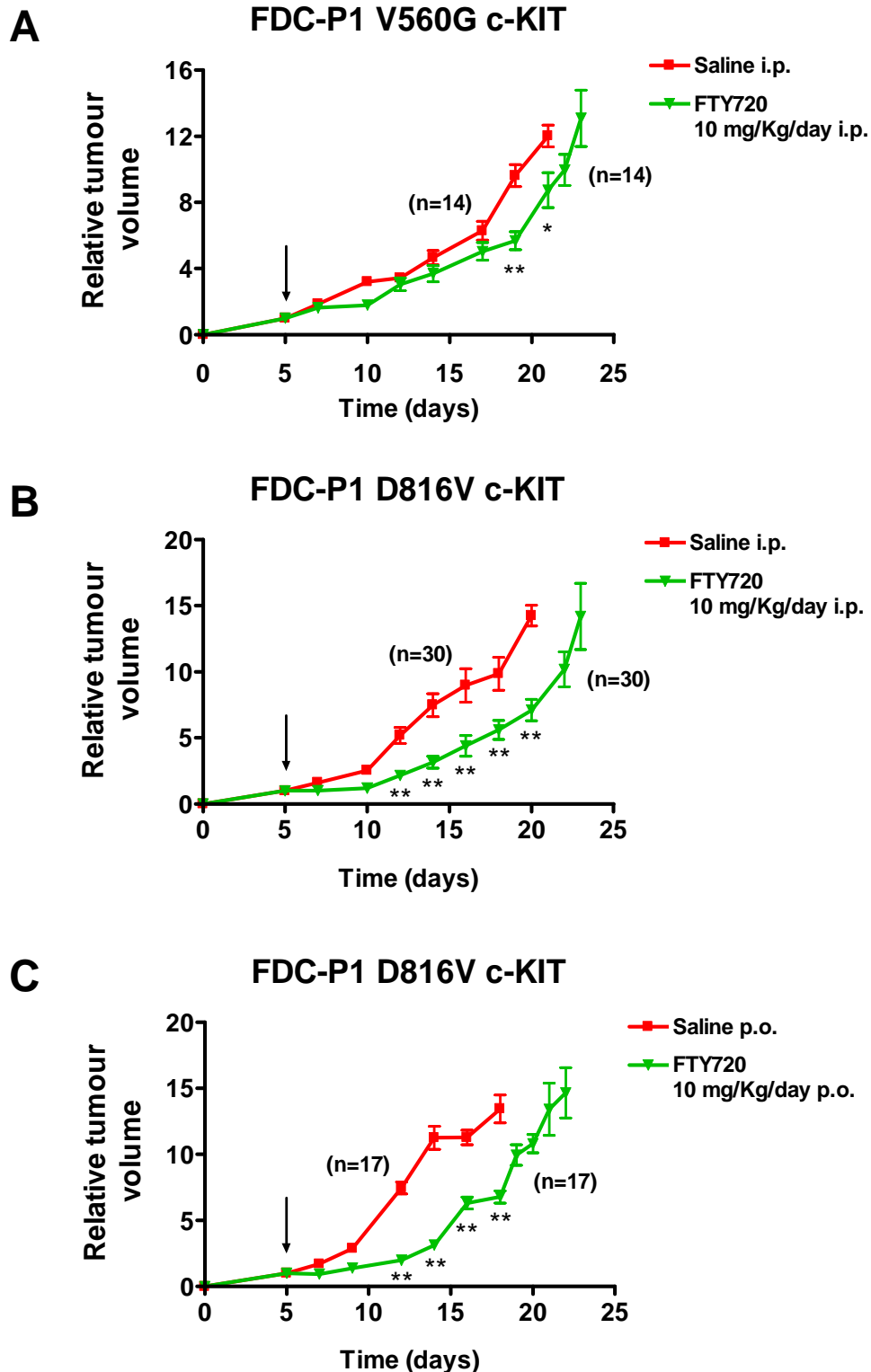


Figure 6.3 FTY720 delays mutant c-KIT tumour growth

FDC-P1 cells expressing A) V560G or B) and C) D816V c-KIT were s.c. inoculated into both flanks of DBA/2J mice (5×10^6 cells/site). Treatment started day 5 post-tumour injection with daily administration (i.p. or p.o.) of either saline or 10 mg/Kg FTY720 (arrows). Relative tumour volume was calculated by dividing the tumour volume on any given day by the tumour volume at start of treatment (day 5). Points, mean of individual mice; bars, SEM. * $p < 0.05$, ** $p < 0.01$, Student's t-test compared to saline-treated.

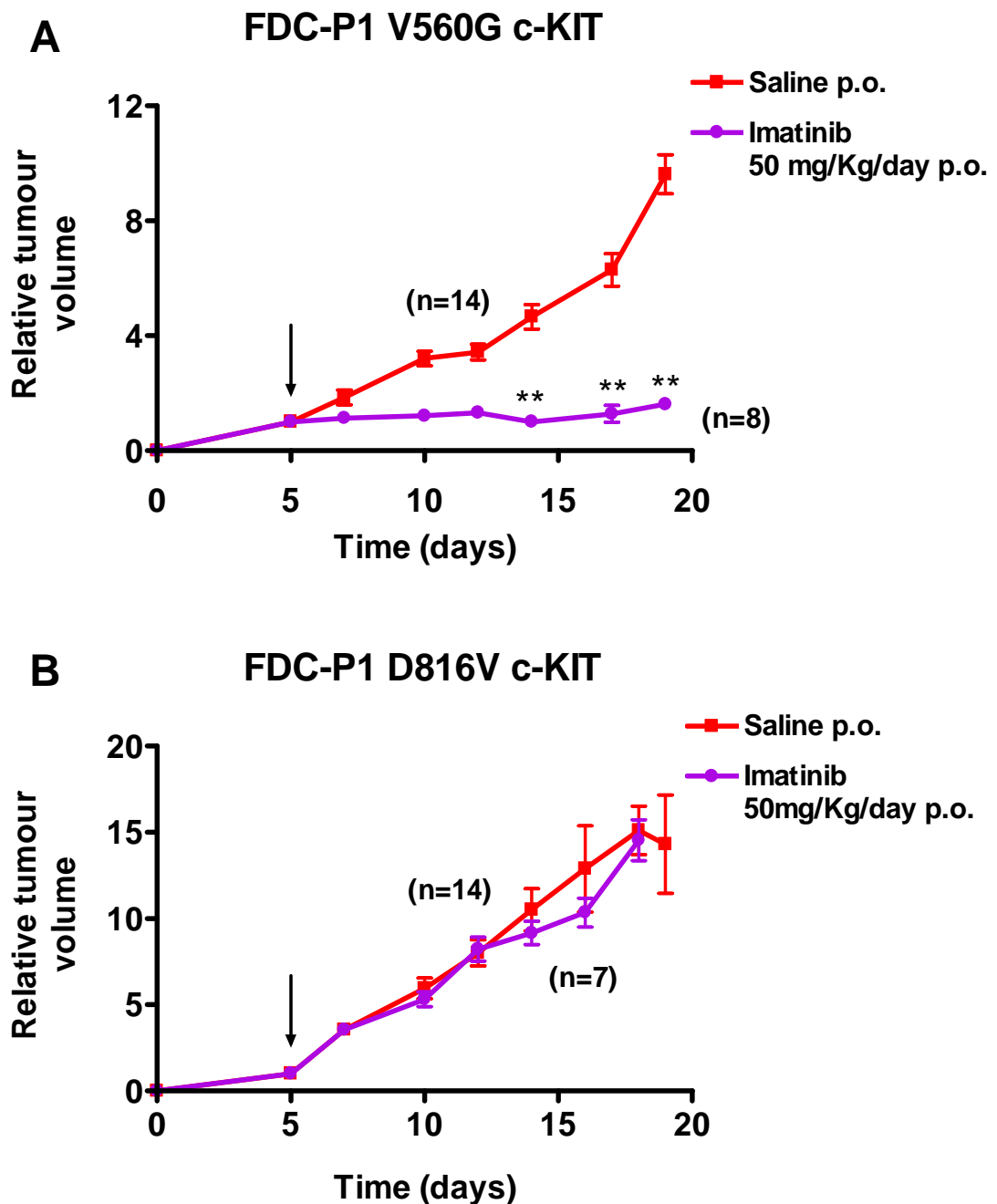


Figure 6.4 Effect of imatinib on mutant c-KIT tumour growth

FDC-P1 cells expressing **A)** V560G or **B)** D816V c-KIT were s.c. inoculated into both flanks of DBA/2J mice (5×10^6 cells/site). Treatment started day 5 post-tumour injection with daily p.o. administration of saline or 50 mg/Kg imatinib (*arrows*). Relative tumour volume was calculated by dividing the tumour volume on any given day by the tumour volume at start of treatment (day 5). *Points*, mean of individual mice; *bars*, SEM. ** $p < 0.01$, Student's t-test compared to saline-treated.

It was noted that tumours expressing the D816V *c-KIT* mutation grew at a faster rate than those harbouring V560G c-KIT. As the kinase domain mutation elicits stronger receptor activation (Mol *et al.* 2003) and demonstrates a more transformed phenotype compared to the JMD mutation, this result was not surprising (Lam *et al.* 1999).

6.2.4 FTY720 improves the survival of mice bearing mutant c-KIT tumours

When the total tumour volume exceeded $\sim 2100 \text{ mm}^3$, the mice were sacrificed. The estimated probabilities for survival were calculated using the Kaplan-Meier method, and the log-rank test was used to determine the differences among survival distributions. For mice harbouring V560G c-KIT tumours, the median survival for FTY720-treated mice was 24 days, a modest increase from 21 days for saline-treated mice (Figure 6.5). Similarly, for tumours expressing D816V c-KIT, FTY720 significantly prolonged the survival of mice from 18 to 22 days (Figure 6.5). Consistent with the tumour growth data, all mice bearing V560G c-KIT tumours and receiving imatinib were still alive up until day 40. In contrast, the survival curve for mice harbouring D816V c-KIT tumours resembled saline-treated controls (Figure 6.6). This highlights the effectiveness of FTY720 compared to imatinib for the treatment of D816V c-KIT malignancies.

6.2.5 FTY720 prevents the infiltration of D816V c-KIT cells into secondary organs

At day 14, a subset of mice from each group were sacrificed, with the tumours evaluated and weighed. Compared to saline-treated mice, FTY720 significantly reduced the tumour mass in both the V560G c-KIT and D816V c-KIT groups (Figure 6.7). Accordingly, an increase in TUNEL staining, which detects cells undergoing apoptosis, was observed in tumours treated with FTY720 compared to saline-treated controls (Figure 6.8 and 6.9).

The D816V c-KIT tumours grew at a faster rate than those expressing V560G c-KIT (Figure 6.3). Consistent with this observation, saline-treated mice from the D816V c-KIT group developed splenomegaly by day 14, as indicated by an increase in splenic weight compared to age-matched controls (Figure 6.10). Importantly, the spleen size of

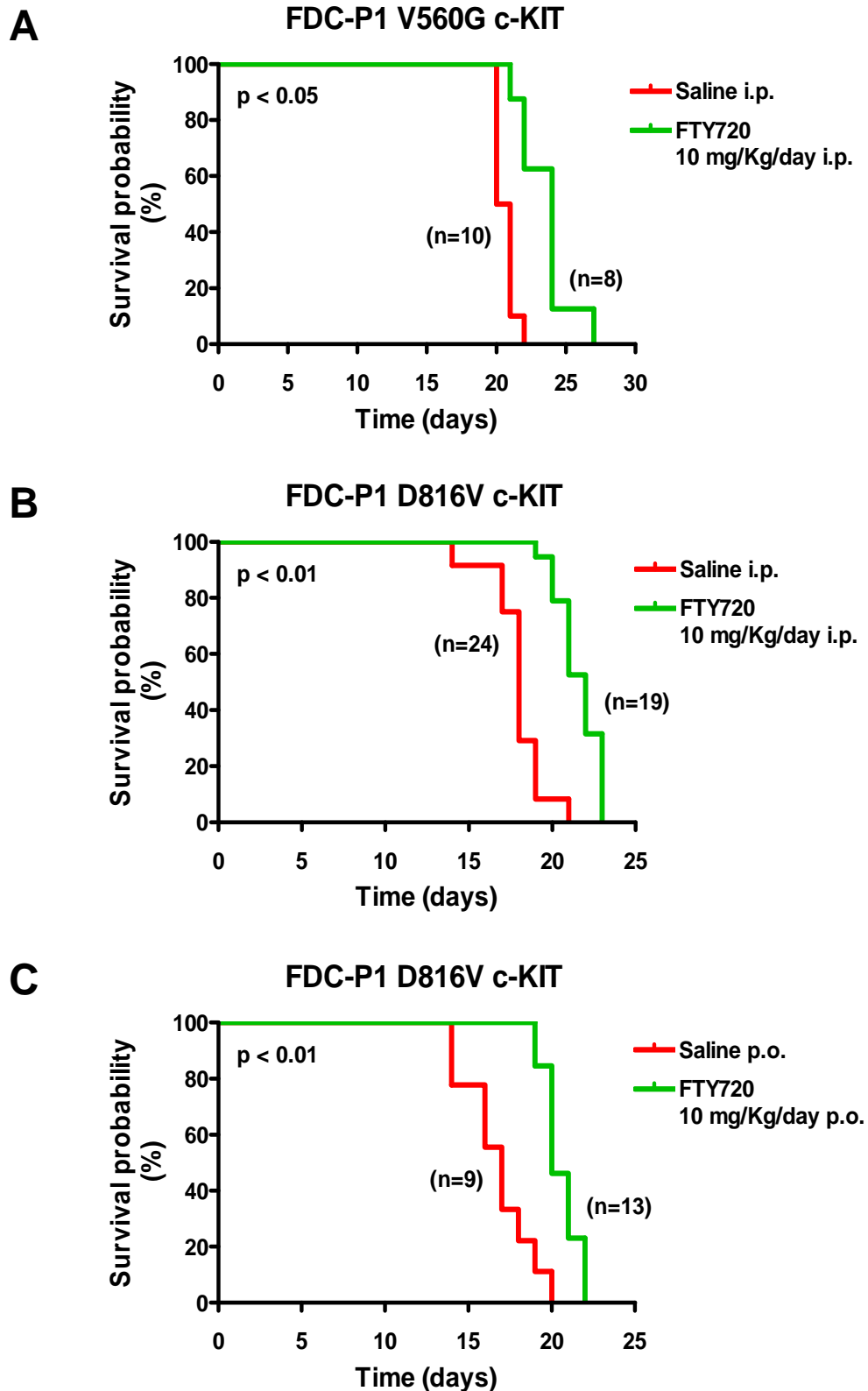


Figure 6.5 FTY720 improves the survival of mice bearing mutant c-KIT tumours FDC-P1 cells expressing A) V560G or B) and C) D816V c-KIT were s.c. inoculated into both flanks of DBA/2J mice (5×10^6 cells/site). Treatment started day 5 post-tumour injection with daily administration (i.p. or p.o.) of either saline or 10 mg/Kg FTY720. The estimated probabilities for survival were calculated using the Kaplan-Meier method, and the log-rank test was used to determine the differences among survival distributions.

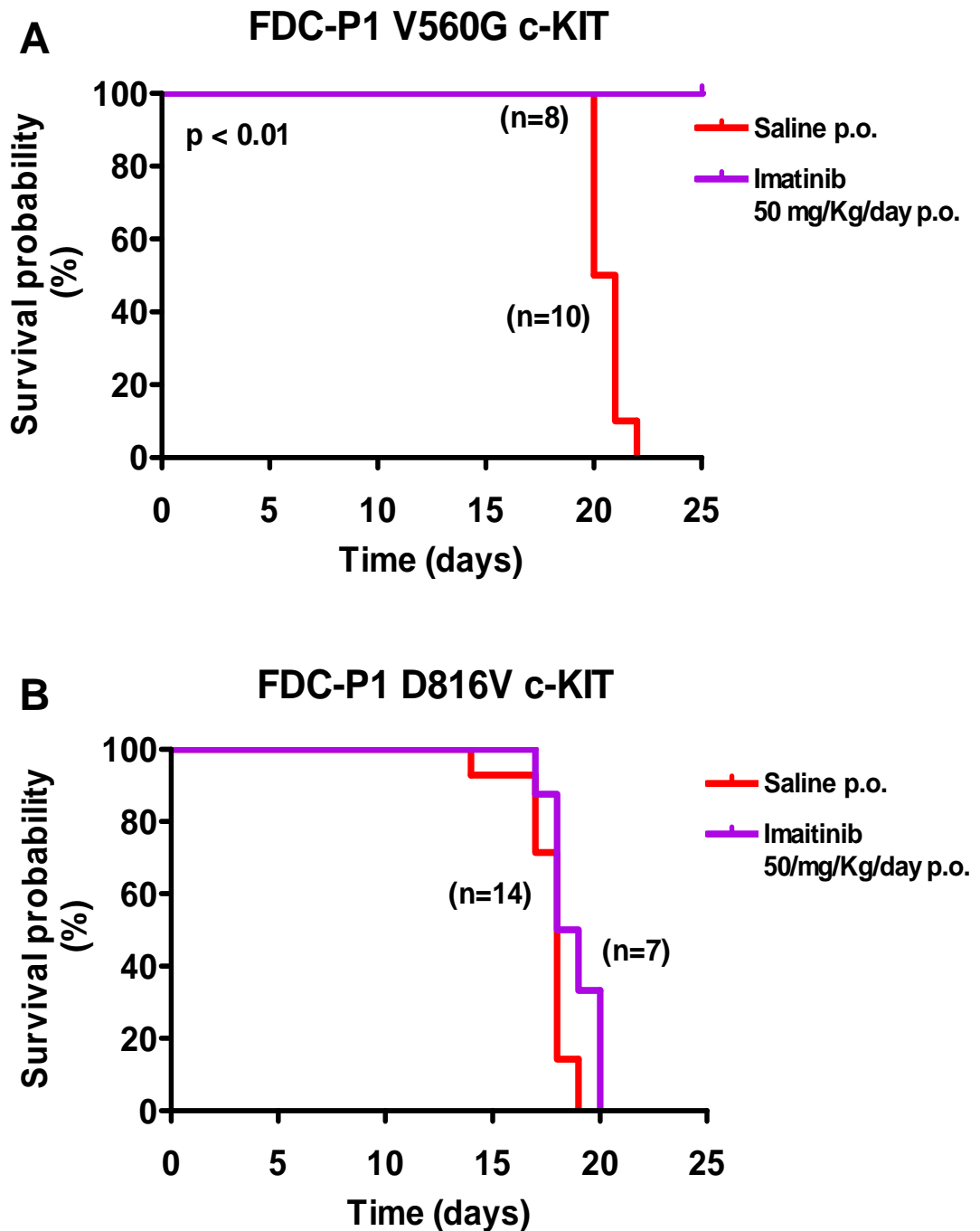


Figure 6.6 Effect of imatinib on the survival of mice bearing mutant c-KIT tumours

FDC-P1 cells expressing **A)** V560G or **B)** D816V c-KIT were s.c. inoculated into both flanks of DBA/2J mice (5×10^6 cells/site). Treatment started day 5 post-tumour injection with daily p.o. administration of saline or 50 mg/Kg FTY720. The estimated probabilities for survival were calculated using the Kaplan-Meier method, and the log-rank test was used to determine the differences among survival distributions.

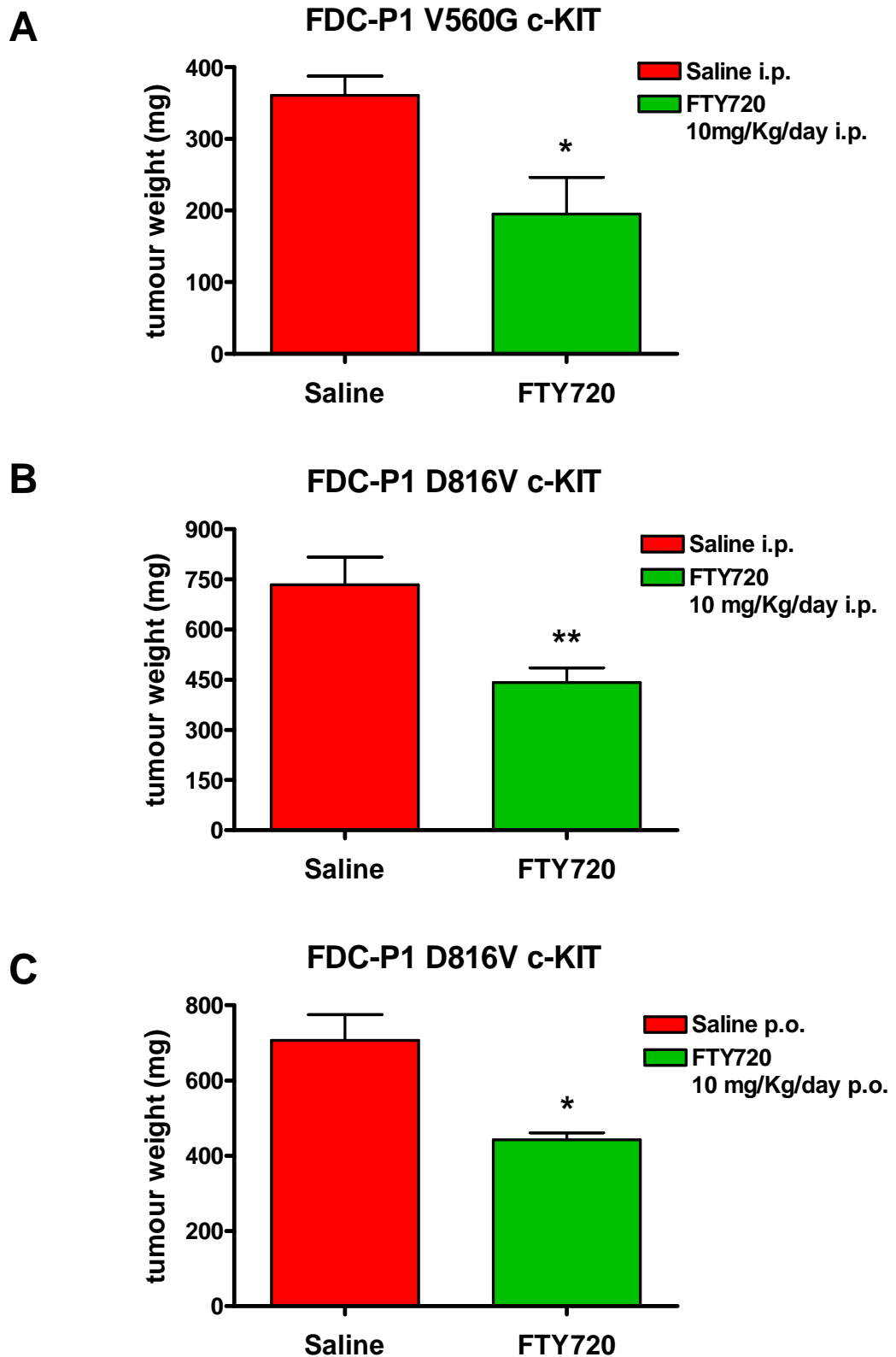


Figure 6.7 FTY720 reduces mutant c-KIT tumour burden at day 14
 FDC-P1 cells expressing A) V560G or B) and C) D816V c-KIT were s.c. inoculated into both flanks of DBA/2J mice (5×10^6 cells/site). Treatment started day 5 post-tumour injection with daily administration (i.p. or p.o.) of either saline or 10 mg/Kg FTY720. At day 14, a subset of mice were sacrificed and the tumour mass was recorded. *Columns*, mean tumour weight (mg); *bars*, SEM. * $p < 0.05$, $n = 6$; ** $p < 0.01$, $n = 12$, Student's t-test FTY720-treated compared to saline.

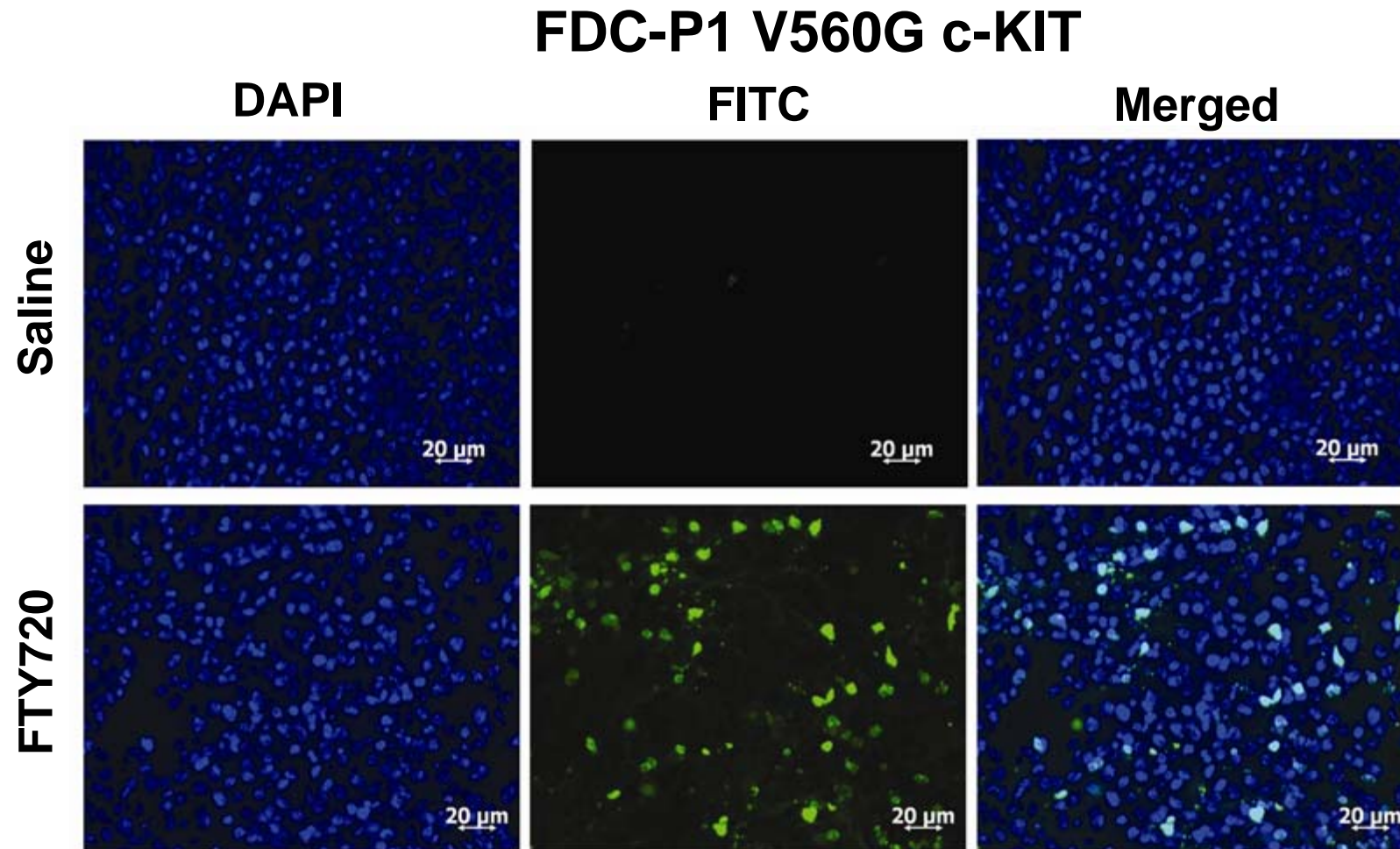


Figure 6.8 FTY720 induces apoptosis in FDC-P1 V560G c-KIT tumours at day 14

Apoptotic death within FDC-P1 V560G c-KIT tumour tissue harvested at day 14 from saline and FTY720 (10/mg/Kg/day)-treated mice was assessed by TUNEL staining detected by FITC. Images were acquired at 400x magnification on DAPI (blue) and FITC (green) channels with an Axioplan 2 imaging system and merged with Axio Vision v4.7 software.

FDC-P1 D816V c-KIT

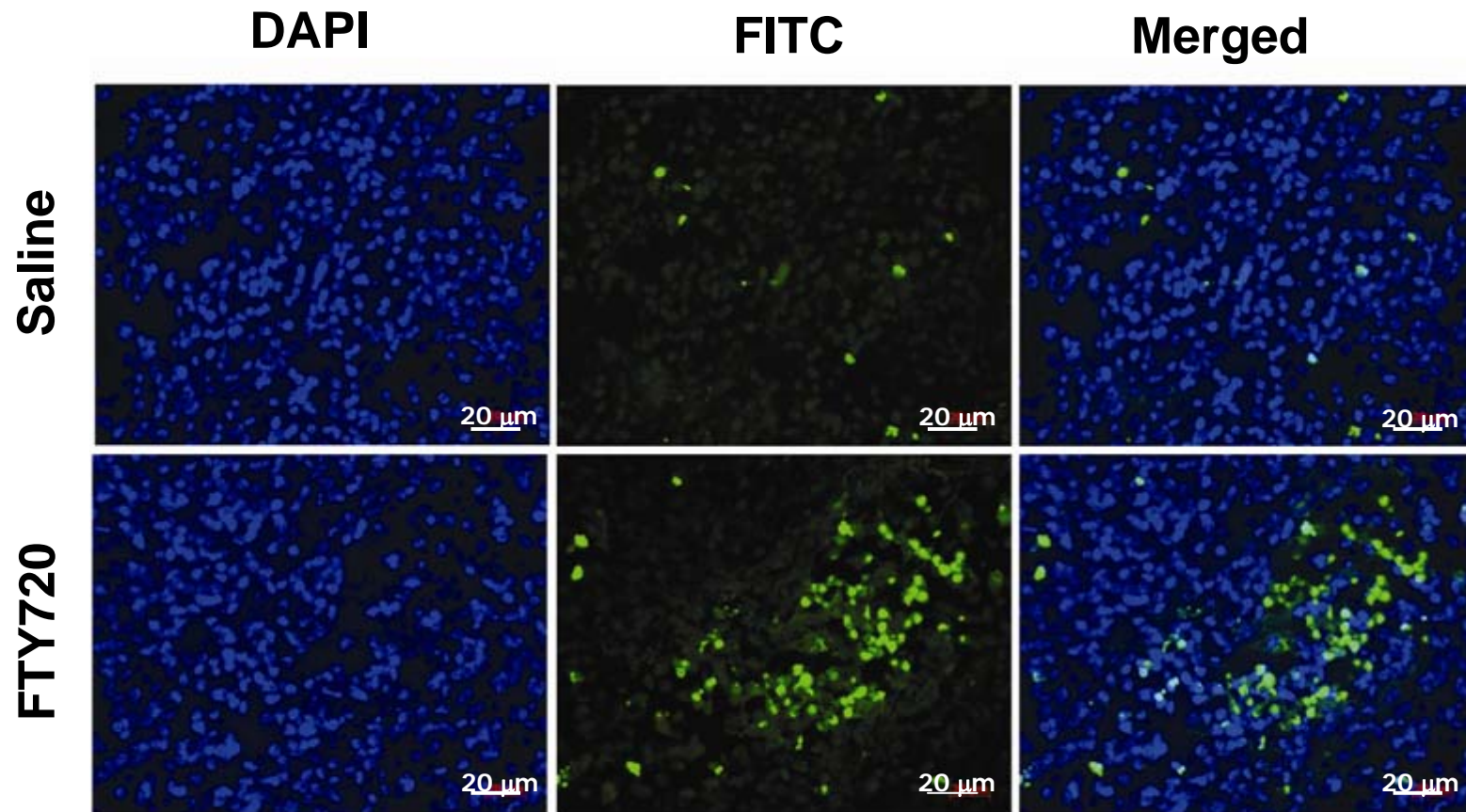


Figure 6.9 FTY720 induces apoptosis in FDC-P1 D816Vc-KIT tumours at day 14

Apoptotic death within FDC-P1 D816V c-KIT tumour tissue harvested at day 14 from saline and FTY720 (10/mg/Kg/day)-treated mice was assessed by TUNEL staining as detected by FITC. Images were acquired at 400x magnification on DAPI (blue) and FITC (green) channels with an Axioplan 2 imaging system and merged with Axio Vision v4.7 software.

FDC-P1 D816V c-KIT

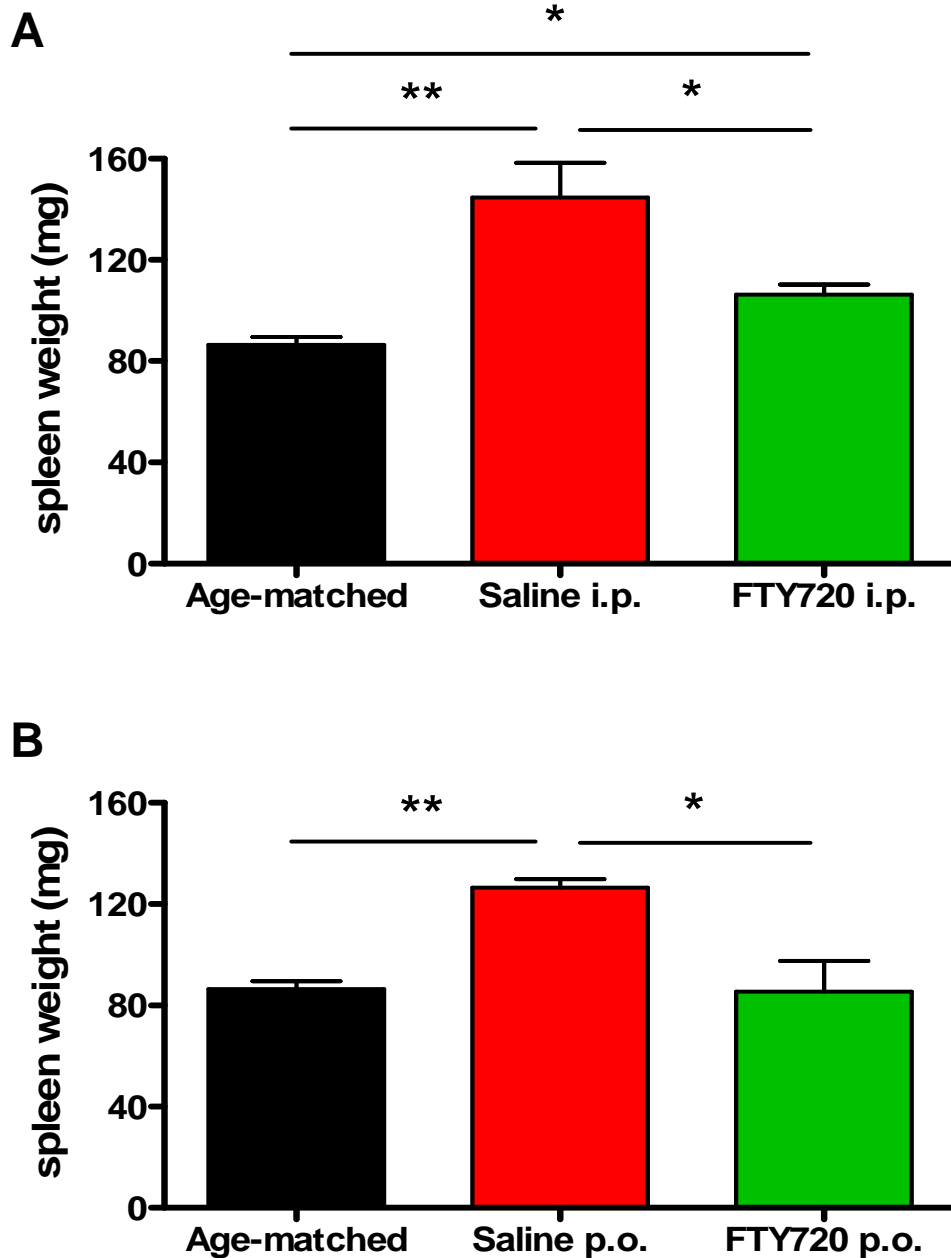


Figure 6.10 FTY720 reduces the splenic weight of mice bearing FDC-P1 D816V c-KIT tumours

FDC-P1 cells expressing D816V c-KIT were s.c. inoculated into both flanks of DBA/2J mice (5×10^6 cells/site). Treatment started day 5 post-tumour injection with daily administration of saline and 10 mg/Kg FTY720 either **A**) i.p. or **B**) oral. At day 14, a subset of mice were sacrificed and the spleen mass was recorded. *Columns*, mean spleen weight (mg); *bars*, SEM. * $p < 0.05$, ** $p < 0.01$, Student's t-test. Age-matched, $n=17$; saline i.p., $n=6$; FTY720 i.p., $n=6$; saline p.o., $n=3$; FTY720 p.o., $n=3$.

FTY720-treated mice was significantly lower than saline-treated controls (Figure 6.10). Immunohistochemical staining confirmed the extensive infiltration of c-KIT⁺ tumour cells from the primary site of s.c. injection into the spleen, with a disruption of splenic architecture and intense c-KIT positive staining observed in saline-treated mice only (Figure 6.11). Importantly, the histopathology of FTY720-treated mice resembled that of age-matched controls and the presence of c-KIT⁺ cells was almost non-detectable (Figure 6.11). Similar results were observed in the bone marrow, indicating that FTY720 treatment delays the migration of D816V c-KIT tumour cells into secondary lymphoid organs (Figure 6.12). It should be noted that no splenomegaly (Figure 6.13) or c-KIT positive staining was observed at day 14 in mice injected with V560G c-KIT cells (Figure 6.14).

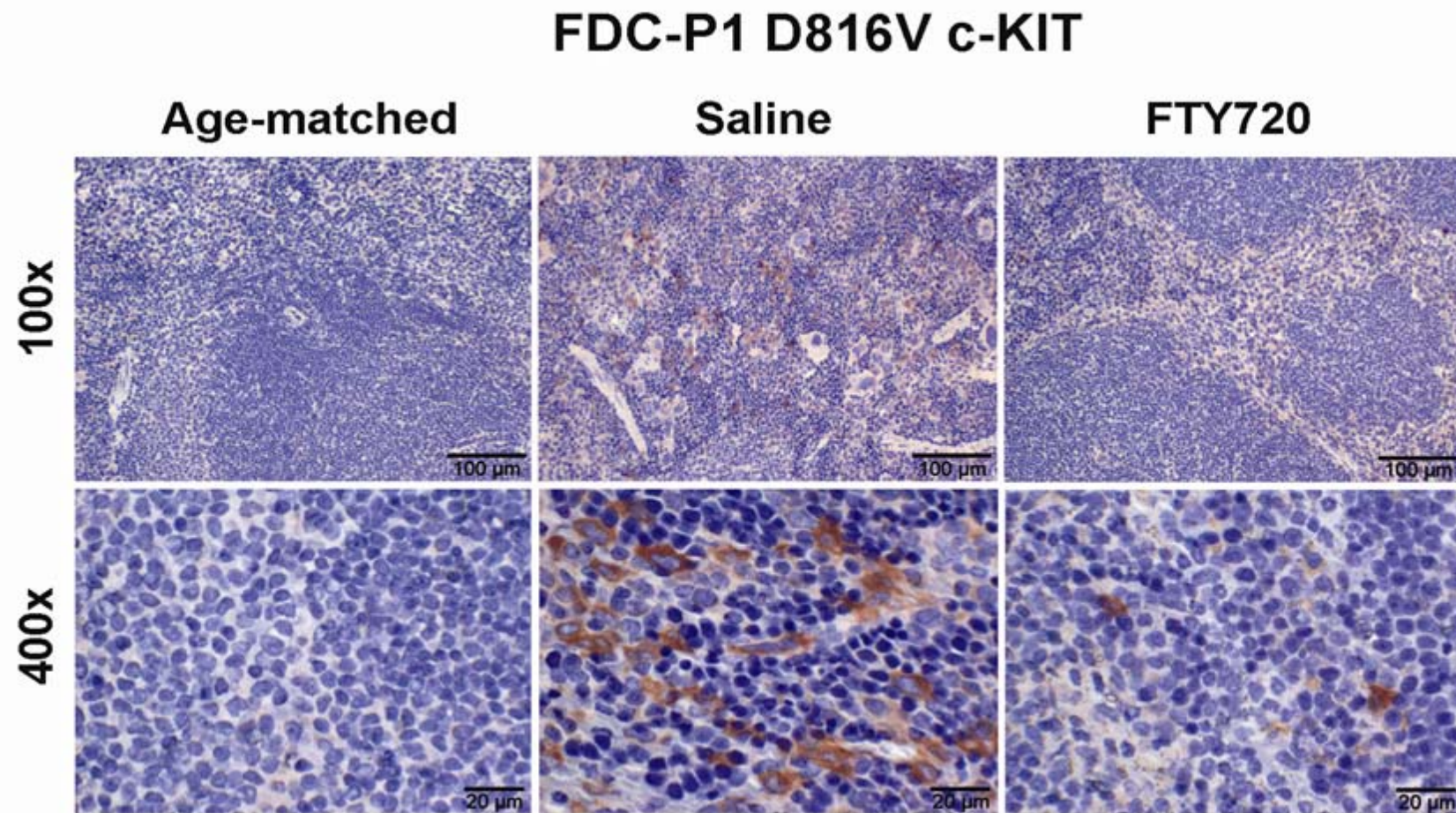


Figure 6.11 FTY720 prevents the infiltration of FDC-P1 D816V c-KIT cells into the spleen

Immunohistochemical staining for human c-KIT was carried out on 4 μ m tissue sections from formalin-fixed, paraffin-embedded spleens harvested at day 14. Positive staining was detected using DAB (red) as the chromogen. Sections were evaluated under 100x or 400x magnification on an inverted light microscope and pictures were taken with a ColorView II camera and analySIS software.

FDC-P1 D816V c-KIT

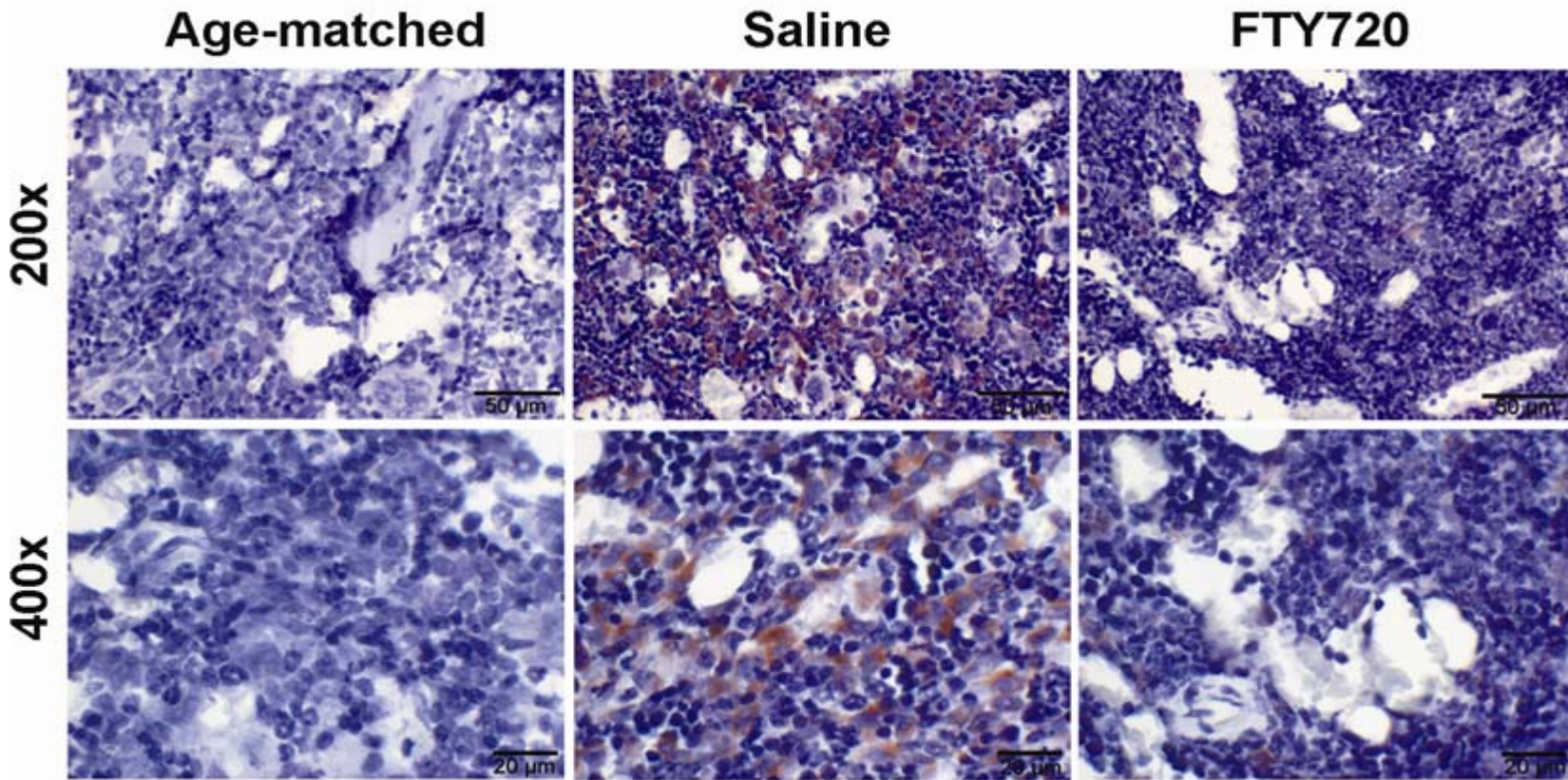


Figure 6.12 FTY720 prevents the infiltration of FDC-P1 D816V c-KIT cells into the bone marrow

Immunohistochemical staining for human c-KIT was carried out on 4 μm sections from formalin-fixed, paraffin-embedded bone marrow harvested at day 14. Positive staining was detected using DAB (red) as the chromogen. Sections were evaluated under 200x or 400x magnification on an inverted light microscope and pictures were taken with a ColorView II camera and analySIS software.

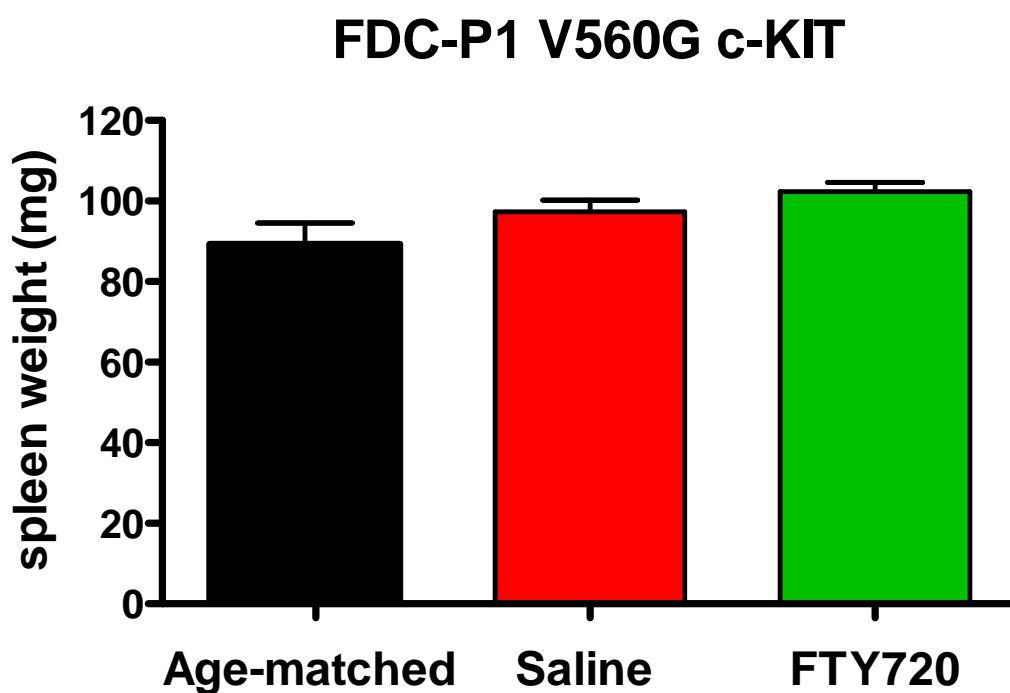


Figure 6.13 Mice bearing V560G c-KIT tumours do not develop splenomegaly
A) FDC-P1 cells expressing V560G were s.c. inoculated into both flanks of DBA/2J mice (5×10^6 cells/site). Treatment started day 5 post-tumour injection with daily i.p. injections of saline or 10 mg/Kg FTY720. At day 14, a subset of mice were sacrificed and the spleen mass was recorded. *Columns*, mean spleen weight (mg); *bars*, SEM. Age-matched, n=17; saline i.p., n=3; FTY720 i.p., n=3.

FDC-P1 V560G c-KIT

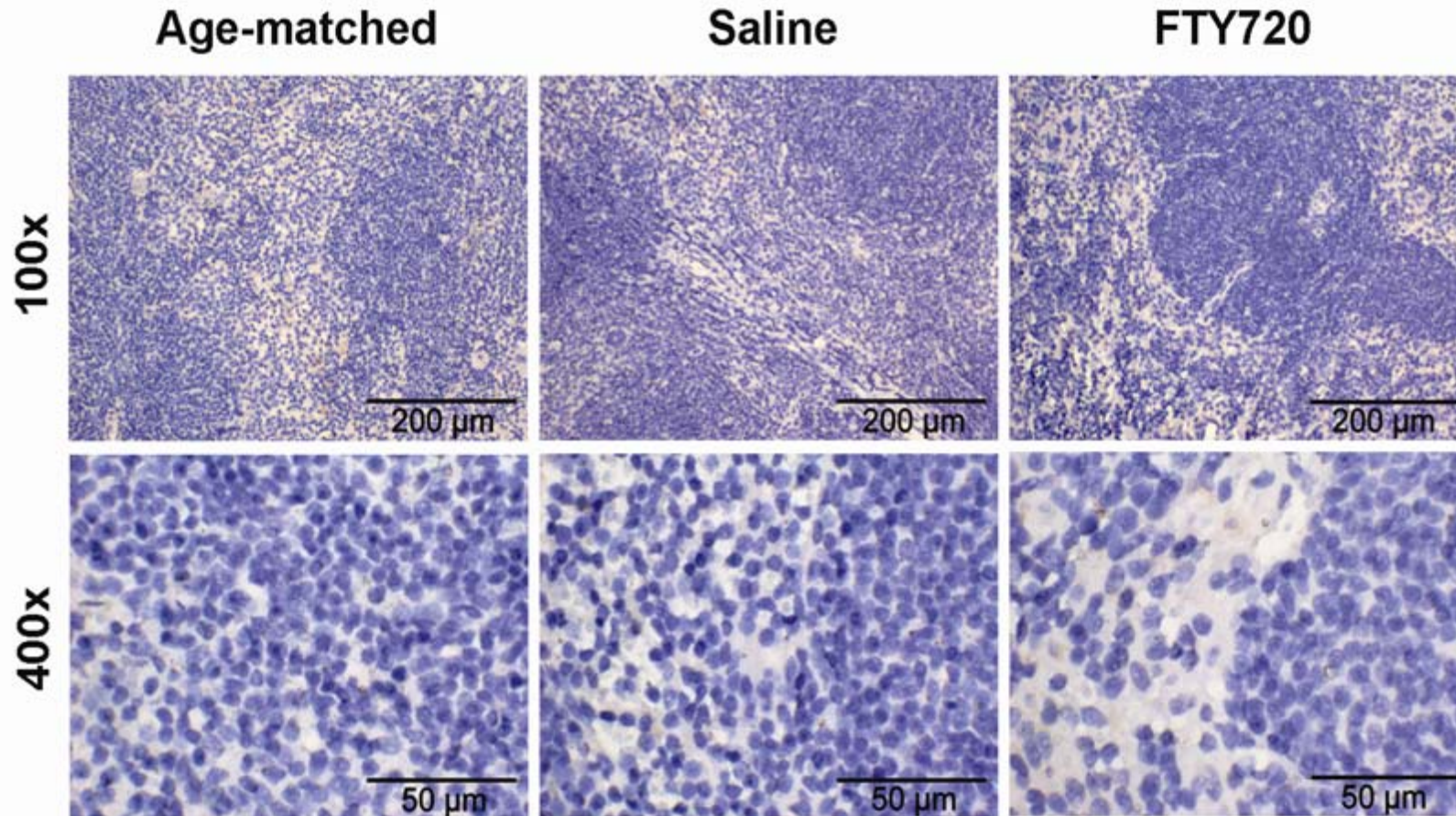


Figure 6.14 Absence of V560G c-KIT cells in the spleen

Immunohistochemical staining for human c-KIT was carried out on 4 mm sections from formalin-fixed, paraffin-embedded spleen harvested at day 14. Positive staining was detected using DAB (red) as the chromogen. Sections were evaluated under 100x or 400x magnification on an inverted light microscope and pictures were taken with a ColorView II camera and analySIS software.

6.3 Discussion

Given the lack of effective treatments available for c-KIT⁺ patients who are unresponsive to current tyrosine kinase inhibitors, it is important to explore the possibility of whether molecules that have been developed for other diseases might serve to inhibit drug-resistant c-KIT⁺ malignancies. The identification of leads among compounds that are already being tested in the clinic may expedite the development of therapeutic strategies for overcoming resistance. The fact that FTY720 demonstrates a favourable safety profile in humans (Budde *et al.* 2002, Skerjanec *et al.* 2005, Kovarik *et al.* 2004b, Tedesco-Silva *et al.* 2005) and is effective against oncogenic c-KIT⁺ cells *in vitro* (Chapter 5), warranted further investigation of this compound as an alternative therapeutic strategy for c-KIT⁺ cancers.

The results presented in this Chapter provide evidence that tumours harbouring oncogenic *c-KIT* mutations are sensitive to FTY720 treatment. Daily administration of FTY720 significantly delayed the growth of c-KIT⁺ tumours via induction of apoptosis at the cellular level (Figure 6.3, 6.8 and 6.9). The observed reduction in tumour mass resulted in prolonged survival of FTY720-treated mice compared to saline-treated controls (Figure 6.5). Furthermore, FTY720 prevented the infiltration of FDC-P1 D816V c-KIT tumour cells into secondary lymphoid organs such as the spleen and bone marrow (Figure 6.11 and 6.12).

FTY720 is considered promising for the treatment of multiple sclerosis (Kappos *et al.* 2006, O'Connor *et al.* 2009). Two phase III trials are currently being conducted, with recent reports showing obvious benefits for patients receiving FTY720 over the standard of care (Cohen *et al.* 2009). Importantly, FTY720 is non-toxic and demonstrates an excellent tolerability profile in humans. Consistent with its role as an immunomodulator, FTY720 transiently reduces peripheral lymphocytes, with numbers generally returning to normal levels four weeks after the cessation of treatment (Budde *et al.* 2002, Skerjanec *et al.* 2005, Tedesco-Silva *et al.* 2005, Kovarik *et al.* 2004a). Indeed these effects were confirmed in the present study, with a dose-dependent decrease in white blood cell numbers observed with daily administration of FTY720 in DBA/2J mice (Table 6.1).

High micromolar concentrations of FTY720 have been shown to effectively inhibit the growth of several haematological malignancies including promyelocytic leukaemia (Shinomiya *et al.* 1997), T-cell leukaemia (Nagahara *et al.* 2000) and multiple myeloma (Yasui *et al.* 2005). More recently FTY720 has demonstrated remarkable therapeutic efficacy against *in vivo* models of Ph¹ CML/ALL and B-CLL (Liu *et al.* 2008, Neviani *et al.* 2007). It has also proven beneficial against solid tumours including breast (Azuma *et al.* 2002), prostate (Chua *et al.* 2005, Permpongkosol *et al.* 2002), glioma (Sonoda *et al.* 2001) and hepatocellular carcinoma (Hung *et al.* 2008, Lee *et al.* 2004); although the exact mechanisms by which FTY720 delays solid tumour growth have not been fully defined. Whilst FTY720 induces apoptosis in these models with an ID₅₀ ranging between 5–18 µM, its inhibitory effects against oncogenic c-KIT kinase activity occurs at a lower concentration (2.5 µM) (Table 5.2). The heightened sensitivity of mutant c-KIT tumours to FTY720 highlights the potential of targeting malignant cells at doses that do not impair the viability of normal haematopoietic function (Kahan 2004).

To date, no studies have reported the specific administration of FTY720 to DBA/2J mice. Therefore a preliminary study was conducted to evaluate the toxicity and determine the maximum tolerable dose of FTY720 in this model. The dosing schedule was based on prior reports indicating that short-term (20-35 days) administration of 10 mg/Kg/day FTY720 *i.p.* severely impacts tumour growth without causing toxicity (Lee *et al.* 2004, Azuma *et al.* 2002). Furthermore, long-term treatment (>100 days) at doses up to 10mg/Kg/day does not affect haematopoietic or non-haematopoietic tissue function (Kim *et al.* 2003, Liu *et al.* 2008, Neviani *et al.* 2007). In contrast, the administration of higher doses (15-20 mg/Kg/day) to rodents for 4 to 6 months is lethal, with the major cause of death resulting from pulmonary smooth muscle hypertrophy/hyperplasia with bronchoconstriction (Kahan 2004).

Whilst a majority of the preclinical studies administer FTY720 via *i.p.* injection, oral administration is the primary route in humans. Clinical trials investigating the pharmacokinetics of daily FTY720 dosing report several unique properties. Firstly, FTY720 exhibits a prolonged absorption phase, which can be explained by its ability to be absorbed over the whole length of the gastrointestinal tract (Budde *et al.* 2002). In addition, FTY720 has a long elimination half-life, and as a result, minimal fluctuations of plasma concentration are detected over the dosing interval period. This observation

justifies the daily administration of FTY720 in the current DBA/2J model (Budde et al. 2002, Kovarik *et al.* 2004a). All together, the pharmacokinetic profile of FTY720 confers high bioavailability between 60 to 90%, with maximal plasma concentrations attained within 12 to 24 hours and a steady state reached in 4 weeks (Skerjanec et al. 2005, Kahan *et al.* 2003). To more closely resemble the clinical setting and allow a direct comparison between two different routes of FTY720 administration, both i.p. injection and oral gavage were included in this study. It should be noted that although the oral administration appears to be more effective against the D816V c-KIT tumours (Figure 6.3), this is actually due to initial differences in tumour kinetics between the saline-treated groups, where orally-treated mice showed a faster growth rate compared to the i.p. injected group. Accordingly, no improvement in survival between the two routes of FTY720 administration was observed (Figure 6.5).

A recent clinical study has shown that oral administration of FTY720 results in enhanced lymphopaenia compared with intravenous injection (Kovarik *et al.* 2007). Given that FTY720-P is responsible for retarding lymphocyte mobilisation, these findings suggest that a proportion of FTY720 is phosphorylated in the liver, where there is an abundance of SphK2 (Liu *et al.* 2000). Consequently, the potent depletion of lymphocytes observed with oral dosing is most likely due to increased plasma levels of the active FTY720-P. In the current study, no appreciable difference in mutant c-KIT tumour growth was observed between the i.p. and oral dosing regimens of FTY720 (Figure 6.3 and 6.5). This provides supporting evidence that the non-phosphorylated version of FTY720 is responsible for the inhibitory effects observed on c-KIT⁺ tumour growth. As only the non-phosphorylated FTY720 activates PP2A, this strongly suggests that the observed reduction in tumour growth is due to PP2A reactivation rather than inhibition of **S1PR** signalling. Measurement of PP2A activity in the tumours is required to confirm this. It is also important to investigate the extent of c-KIT inhibition within the FTY720-treated tumours. Importantly, these results indicate that the oral administration of FTY720 is a valid dosing regime, as a similar proportion of unphosphorylated FTY720 must be reaching the target tumour cells to induce apoptosis.

It is widely accepted that D816V c-KIT tumours are completely unresponsive to imatinib treatment, and indeed the present data also confirms this (Figure 6.4 and 6.6). Dasatinib binds to the active confirmation of the c-KIT receptor and is effective against

D816V c-KIT⁺ patient-derived mast cells *in vitro* (Shah et al. 2006). However, these results have not translated into the clinic, with limited efficacy observed in c-KIT⁺ AML and systemic mastocytosis patients (Purtill *et al.* 2008, Rondoni *et al.* 2007, Verstovsek et al. 2008). While the precise mechanisms responsible for this observation are unclear, it is likely that concentrations which effectively inhibit D816V c-KIT activity in preclinical models are not therapeutically achievable in patients. To combat this issue of drug resistance, several small molecules have been developed and tested against D816V c-KIT. These include the FLT3 inhibitors midostaurin (Gotlib *et al.* 2005) and tandutinib (Corbin *et al.* 2004), and the novel c-KIT kinase inhibitors EXEL-0862 (Pan *et al.* 2007) and AP23464 (Corbin *et al.* 2005). In regards to the use of midostaurin (formerly PKC412), one case study reported a transient clinical response in a D816V c-KIT⁺ mast cell leukaemia patient (Gotlib et al. 2005). Whilst a marked decrease in peripheral mast cells was observed, in a similar observation to phase II trials in FLT3⁺ AML (Stone *et al.* 2005), there was minimal reduction in the burden of mast cells and leukaemic blasts within the bone marrow. These findings suggest that the bone marrow microenvironment may secrete unidentified factors which render the cells insensitive to midostaurin treatment (Gotlib et al. 2005). The quinazoline-based inhibitor tandutinib (formerly MLN518) (Corbin et al. 2004), and the novel kinase inhibitor EXEL-0862 (Pan et al. 2007), effectively inhibit the growth of D816V c-KIT cells *in vitro*; although their *in vivo* activity has not been investigated. Lastly, whilst studies examining the therapeutic potential of the c-KIT inhibitor AP23464 against tumours formed by the mouse mastocytoma cell line, P815, showed reduced c-KIT phosphorylation levels, no significant decrease in tumour size was recorded (Corbin *et al.* 2005).

Taken together, the development of small molecules which effectively bind to, and inhibit, kinase domain c-KIT mutants has proven extremely difficult. Thus, successful treatment of these cancers will most likely require alternate strategies that simultaneously target the oncogenic receptor as well as its downstream signalling cascades. The data presented in this Chapter strongly supports the hypothesis that FTY720-induced reactivation of PP2A is an effective therapeutic approach for the treatment of mutant c-KIT⁺ patients who are unresponsive to current tyrosine kinase inhibitors. In addition, these findings identify a novel treatment strategy which may be effective against other cancers characterised by functional loss of PP2A activity.

CHAPTER 7

CONCLUSIONS AND FUTURE DIRECTIONS

The ability to balance a complex network of signal transduction pathways is imperative for maintaining normal cellular homeostasis. A key mechanism governing signal activation is protein phosphorylation, which is controlled by the balanced activities of protein kinases and phosphatases. Genetic or regulatory alterations of specific tyrosine kinases can result in the aberrant activation of oncogenic pathways that induce cell growth and inhibit apoptosis, thus facilitating a tumourigenic phenotype. Indeed, numerous oncogenic tyrosine kinases have been implicated in the pathogenesis of human malignancies. A selection of these include BCR/ABL in CML (Ben-Neriah *et al.* 1986), c-KIT and FLT3 in AML (Mrozek *et al.* 2008, Meshinchi & Appelbaum 2009), and epidermal growth factor receptor (EGFR) in non-small-cell lung cancer (Hirsch *et al.* 2009).

The advent of targeted therapies for specific malignancies, such as imatinib for CML, resulted in a surge of optimism in the field of oncology. Despite the general positive response of chronic phase CML patients to imatinib treatment, a small proportion are unresponsive to targeted inhibition (Druker *et al.* 2006). Furthermore, a serious problem that emerges with time is the development of resistance, which occurs primarily through the outgrowth of subclones bearing mutations in the target kinase that interfere with drug binding (Gorre *et al.* 2001, Shah & Sawyers 2003). Initially reported in CML, this mechanism is broadly applicable to other cancers, such as c-KIT in GIST (Antonescu *et al.* 2005). In addition, a range of mutations in FLT3 confer resistance to midostaurin (Weisberg *et al.* 2009), and certain mutations within the EGFR are unresponsive to gefitinib (Gazdar 2009). Second-generation compounds (e.g. dasatinib), are effective against some imatinib-resistant mutations; however, the issue of drug resistance continues to exist (Soverini *et al.* 2007). Furthermore, tyrosine kinase inhibitors described to date do not effectively kill the leukaemic stem cells (Copland *et al.* 2006, Graham *et al.* 2002, Jorgensen *et al.* 2007). Therefore, the investigation of signalling pathways regulated by oncogenic tyrosine kinases may identify novel treatment approaches directed against rational therapeutic targets. One promising candidate is the potential tumour suppressor, PP2A.

Using mouse myeloid progenitor cells, the results presented in Chapters 3 and 4 of this thesis highlight that PP2A is indeed regulated by active BCR/ABL. A detailed investigation of individual PP2A holoenzyme components showed, for the first time, increased expression and association of the structural and specific regulatory subunits in BCR/ABL⁺ myeloid progenitors. Mechanistically, an abundance of these subunits favours the assembly of PP2A holoenzymes containing B55 α and B56 α (Figure 7.1A), with simultaneous displacement of PP2A-B56 γ complexes that normally exert negative regulation (Figure 7.1B). Whilst enhanced expression is not regulated at the mRNA level, the precise mechanisms governing these effects remain undefined. One possibility is that BCR/ABL inhibits the ubiquitin-mediated degradation of PP2A subunits and increases protein stability. To detect dysfunctional ubiquitin machinery, FDC-P1 cells treated with a proteasome inhibitor, such as MG132, would show enrichment of the polyubiquitinated PP2A subunit in the empty vector controls but not in the BCR/ABL⁺ cells. A further investigation could include the immunoprecipitation of ubiquitin-containing complexes and subsequent probing for the specific PP2A subunit of interest, which would be faint or undetectable in FDC-P1 cells expressing BCR/ABL.

Although the increased formation of PP2A complexes that potentiate oncogenic signalling (e.g. B55 α and B56 α) may explain how elevated subunit expression contributes to BCR/ABL-leukaemogenesis, it does not explain the observed reduction in PP2A activity. This could arise from technical considerations associated with the experimental protocol. The phosphatase assay measures free phosphate that is cleaved by isolated PP2Ac immunoprecipitates, and is indicative of global PP2A activity. As the regulatory subunit plays a key role in determining PP2A activation, one improvement of this assay would be to isolate the individual B subunits from the FDC-P1 cell lines, and determine the associated PP2A activity. Another experiment could be to isolate specific PP2A heterotrimers from BCR/ABL⁺ cells and assess the *in vitro* dephosphorylation of known PP2A substrates such as Ras, β -catenin and p53. In addition to directing substrate specificity, the B subunit also targets the PP2A holoenzyme to distinct locations within the cell. Using immunofluorescence staining to assess differences in subcellular distribution of specific complexes may further define the underlying mechanisms by which PP2A function is perturbed in BCR/ABL⁺ myeloid progenitors.

To investigate which subunits are functionally important for BCR/ABL-mediated leukaemogenesis, individual PP2A regulatory subunits were targeted with shRNA sequences in FDC-P1 WT BCR/ABL cells, and the loss-of-function phenotype was examined. These studies identified B56 α as a key PP2A subunit that contributes to BCR/ABL⁺ leukaemia growth. This was demonstrated by the fact that downregulation of B56 α not only restored PP2A activity, but significantly inhibited cellular proliferation, and reduced the clonogenic potential of BCR/ABL⁺ cells. Future studies examining the tumour growth rate of shB56 α WT BCR/ABL FDC-P1 cells compared to empty vector controls in an *in vivo* model will further highlight the importance of B56 α in facilitating the leukaemic phenotype. Preliminary observations based on cellular morphology indicate that knockdown of B56 α may also induce partial differentiation, although this requires confirmation by analysis of lineage-specific markers and ruling out the induction of apoptosis. A characteristic feature of CML-BC is the expansion of myeloid or lymphoid precursors that facilitate the rapidly fatal blast crisis phenotype, and are also insensitive to tyrosine kinase inhibition (Copland *et al.* 2006, Graham *et al.* 2002, Jorgensen *et al.* 2007). The potential to partially reverse this phenotype via PP2A manipulation, specifically by downregulation of B56 α , represents an exciting and novel finding.

[A notable consequence of enhanced B56 \$\alpha\$ association in the FDC-P1 cells expressing BCR/ABL may be the displacement of B56 \$\gamma\$ from the core PP2A dimer.](#) Several lines of evidence support the involvement of B56 γ in mediating the tumour suppressive function of PP2A in mammalian cells (Westermarck & Hahn 2008). Overexpression of this subunit in the FDC-P1 BCR/ABL myeloid progenitors will elucidate whether depletion of PP2A-B56 γ complexes contributes to the leukaemic phenotype in these cells. Furthermore, in the shB56 α WT BCR/ABL FDC-P1 cells, a reasonable prediction is that the restoration of PP2A activity is a reflection of increased B56 γ binding and function. Future studies aimed at isolating the catalytic subunit from these cells and determining the proportion of bound regulatory subunits will confirm whether suppression of B56 α leads to enhanced formation of PP2A complexes containing B56 γ .

Interestingly, the knockdown of PP2A B56 δ in FDC-P1 WT BCR/ABL cells was associated with an increased proportion of cells which appeared to be undergoing mitotic delay. Another striking observation was the presence of large, irregular shaped

cells containing multiple nuclei, which indicates defective cytokinesis. Although speculative at the moment, these findings suggest that B56 δ may be an important regulator of the cell cycle in BCR/ABL⁺ myeloid progenitors (Figure 7.1C). Recent evidence demonstrates a specific role for B56 δ in controlling the entry into and exit from mitosis (Forester *et al.* 2007, Margolis *et al.* 2006). A detailed analysis of the downstream molecules targeted by PP2A B56 δ will not only shed light on the importance of this enzyme in cell cycle regulation, but will also determine its relevance in the pathogenesis of BCR/ABL⁺ CML. It is predicted that continued DNA synthesis without cytokinesis would have catastrophic effects on cell survival (Gizatullin *et al.* 2006, Harrington *et al.* 2004). Whether or not the polyploid cells in the shB56 δ WT BCR/ABL FDC-P1 population eventually undergo apoptosis remains unknown, and would be an interesting avenue of future investigation. Of note, the morphological changes observed in these cells resemble the phenotype previously reported for Aurora kinase inhibition in colon and pancreatic cancer (Harrington *et al.* 2004). This suggests that targeting individual PP2A subunits is a valid approach for the development of novel CML therapies.

Collectively, the results presented in Chapters 3 and 4 provide new insight into the biology of PP2A, and begin to uncover the precise mechanisms by which BCR/ABL induces transformation via PP2A in myeloid cell lines. An important next step would be to investigate the molecular regulation of PP2A in CML patient samples. Interestingly, preliminary analysis of CD34⁺ progenitors isolated from patients who have responded favourably to imatinib, show a dose-dependent reduction of PP2Ac-p^{Y307} upon exposure to imatinib in culture. In contrast, imatinib-resistant CD34⁺ blasts show considerably higher levels of PP2Ac-p^{Y307} with imatinib treatment up to 5 μ M (Appendix Figure 1). Since increased phosphorylation transiently inactivates the PP2A enzyme (Chen *et al.* 2004), this preliminary data supports the findings that inhibition of BCR/ABL reactivates PP2A in imatinib-sensitive cells only.

In addition to CD34⁺ CML-BC myeloid progenitors, PP2A inhibition has also been demonstrated in Ph¹ ALL patient samples. Importantly, reactivation of PP2A with FTY720 impairs the growth of these cells *in vitro* (Neviani *et al.* 2007). From a clinical perspective, *de novo* Ph¹ ALL resembles CML lymphoid blast crisis, and generally presents as a more aggressive disease that responds poorly to tyrosine kinase inhibition

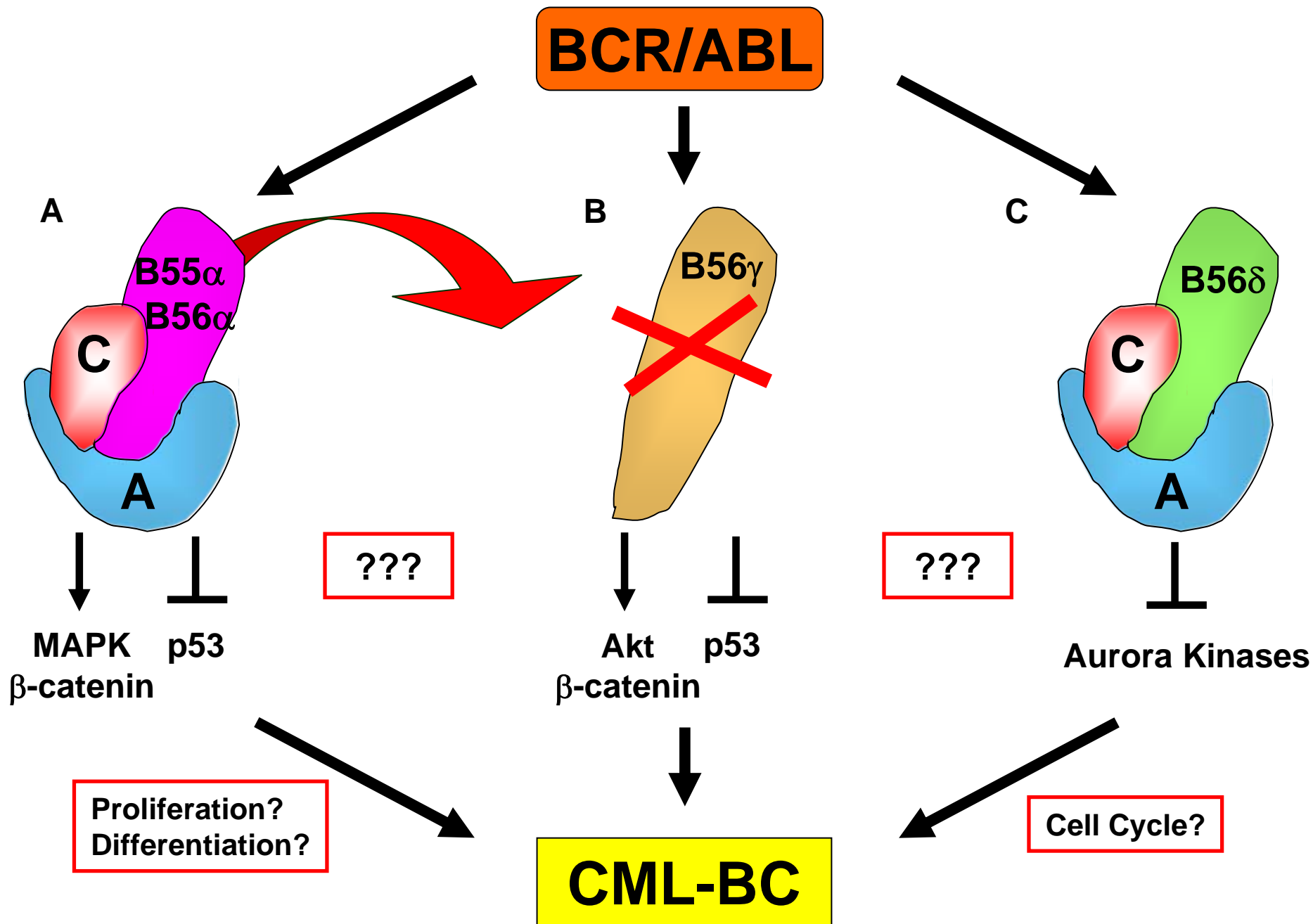


Figure 7.1 Proposed model of PP2A regulation by BCR/ABL in myeloid progenitors

BCR/ABL alters PP2A function through a variety of mechanisms (Chapters 3 and 4).

A) BCR/ABL enhances the formation of PP2A complexes containing B55 α , which may induce the activation of certain pathways such as MAPK and Wnt/ β -catenin. In addition, an abundance of PP2A holoenzymes containing B56 α could inhibit p53. Together these effects appear to contribute to enhanced proliferation and impaired differentiation of myeloid cells. Functional studies with knockdown of B56 α identify this subunit as a key player in BCR/ABL-mediated leukaemogenesis. **B)** The simultaneous displacement of PP2A B56 γ from the core AC dimer in BCR/ABL⁺ cells may also result in aberrant regulation of Akt, β -catenin and p53. **C)** PP2A B56 δ appears to be important for cell cycle regulation BCR/ABL⁺ cells, with a potential target being Aurora kinases.

(Wong & Witte 2004). Administration of dasatinib typically induces significant haematological and cytogenetic responses that are rapidly lost despite persistent treatment, suggesting that additional aberrations downstream from the kinase contribute to the more aggressive phenotype and to the reduced therapeutic response (Mullighan *et al.* 2008). Furthermore, the underlying mechanisms governing the development of lymphoid, as opposed to myeloid blast crisis are poorly understood. Given that PP2A is functionally inactivated in Ph¹ ALL (Neviani *et al.* 2007), it would be interesting to investigate its regulation by BCR/ABL in lymphoid cell lines.

In this body of work, the regulation of PP2A was also extended to another oncogenic tyrosine kinase, c-KIT. The data presented in Chapter 5 demonstrates for the first time that constitutively active c-KIT receptors (V560G and D816V) inhibit the activity of PP2A in myeloid progenitors, and this contributes to the tumourigenic phenotype (Figure 7.2A). Activating mutations in c-KIT are associated with a variety of cancers, including GISTs, AML, testicular seminomas and melanoma. Thus these novel findings may have wide applicability to a range of human malignancies. An important follow up would be to investigate the activation status of PP2A in primary mutant c-KIT⁺ patient samples.

In contrast to BCR/ABL, oncogenic c-KIT cells displayed reduced expression of the PP2A structural and several regulatory subunits (B55 α , B56 α , B56 γ and B56 δ) (Figure 7.2A). Subsequent investigations in our laboratory indicate that these changes are not regulated at the transcriptional level (A.M. Smith, N.M. Verrills, personal communication); thus the precise mechanisms governing this effect remain to be determined. Overexpressing the individual PP2A subunits in oncogenic c-KIT cells and determining the functional effects on cell growth will further define their importance in c-KIT-mediated tumourigenesis. Indeed, preliminary studies in our laboratory have shown that overexpression of the PP2A A subunit in D816V c-KIT FDC-P1 cells inhibits factor-independent growth (N.M. Verrills, personal communication). In support of the current findings, previous reports on human glioma, breast cancer and B-CLL primary samples also suggest that depletion of PP2A components contributes to tumourigenic transformation (Wlodarski *et al.* 2006, Suzuki & Takahashi 2006, Colella *et al.* 2001, Falt *et al.* 2005). Furthermore, somatic alterations of the gene encoding PP2A A β (PPP2R1B) have been detected in up to 15% of colon, lung and breast cancers

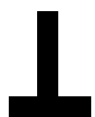
(Calin *et al.* 2000, Takagi *et al.* 2000, Tamaki *et al.* 2004, Wang *et al.* 1998). Mutations of the more abundant PP2A A α subunit have also been observed, albeit at a lower frequency (Calin *et al.* 2000). The cancer-associated A α and A β mutants display altered PP2A holoenzyme assembly that correlates with PP2A inhibition (Chen *et al.* 2005, Ruediger *et al.* 2001a, Ruediger *et al.* 2001b, Sablina *et al.* 2007). In addition, reduced expression and inhibition of PP2A activity contributes to the less-differentiated invasive phenotype associated with estrogen receptor negative breast cancer (Keen *et al.* 2004, Keen *et al.* 2005).

Importantly, reactivation of PP2A with FTY720 significantly inhibited proliferation, induced apoptosis and suppressed the clonogenic potential of imatinib-sensitive (V560G) and –resistant (D816V) FDC-P1 cells *in vitro* (Figure 7.2B). The molecular mechanisms by which FTY720 enhances the activity of PP2A remain undefined. Although it is known to directly activate purified PP2A dimers and trimers *in vitro* (Matsuoka *et al.* 2003), further investigation is required to elucidate the precise interactions with PP2A in myeloid progenitors expressing oncogenic c-KIT. Another interesting follow up would be to determine the sensitivity of individual PP2A complexes to FTY720-induced PP2A activation (Figure 7.2B). Notably, the cytotoxic effects of FTY720 are dependent on the functional status of PP2A whereby mutant c-KIT cells, but not empty vector controls or WT c-KIT cells grown in SCF, are sensitive to low concentrations of FTY720, presumably due to their altered PP2A complexes and markedly reduced PP2A activity.

The promising *in vitro* findings obtained with FTY720 were translated into an *in vivo* model, where the daily administration of FTY720 significantly delayed the growth of mutant c-KIT⁺ tumours. Furthermore, FTY720 prevented the infiltration of D816V c-KIT tumour cells into secondary lymphoid organs. As a consequence, the survival of FTY720-treated mice was significantly improved compared to saline-treated controls. Notably, the administration of FTY720 did not completely cure the mice. This observation is most likely attributable to the particular type of *in vivo* model that was used. Specifically, the D816V c-KIT⁺ subcutaneous tumours were very aggressive, with the first saline-treated mouse reaching its designated cull volume by day 14. Given this rapid tumour burden, it is likely that insufficient levels of FTY720 were reaching the tumour. As a result, the cells located within the middle would be protected from

A

Mutant c-KIT

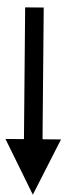


PP2A

Activity

B55 α
B56 α ,
 γ , δ

Expression



TUMOURIGENESIS

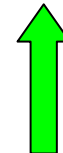
Reactivate PP2A



e.g. FTY720

B

Mutant c-KIT



PP2A

Activity

B55 α
B56 α ,
 γ , δ

Expression
???



TUMOURIGENESIS

Figure 7.2 Summary of PP2A regulation by oncogenic c-KIT in myeloid progenitors

A) Decreased expression of the PP2A structural subunit and specific regulatory subunits (B55 α , B56 α , B56 γ and B56 δ) by mutant c-KIT is associated with reduced PP2A activity. Together, these effects are essential for c-KIT-mediated tumorigenesis (Chapter 5).

B) Reactivation of PP2A, for example with FTY720, inhibits the oncogenic c-KIT receptor itself and impairs the *in vitro* and *in vivo* growth of imatinib-sensitive and –resistant c-KIT FDC-P1 cells (Chapters 5 and 6). The effect of FTY720 on PP2A regulatory subunit expression and holoenzyme composition is unknown.

FTY720-induced PP2A reactivation, and therefore continue to proliferate in the presence of drug. These results could be improved by performing a tail vein injection of the mutant c-KIT FDC-P1 cells and establishing a systemic model which more closely resembles a myeloproliferative disease. Indeed, 50% of T315I BCR/ABL⁺ mice displaying systemic CML-like disease were still alive after 27 weeks of daily treatment with 10 mg/Kg FTY720, whereas all of the saline-treated mice were sacrificed by week 5 (Neviani et al. 2007). Therefore, future studies will most likely show enhanced therapeutic efficacy of FTY720 in a D816V c-KIT leukaemia model in comparison to the current subcutaneous model.

Based on previous results with BCR/ABL⁺ myeloid progenitors (Neviani et al. 2007), it was predicted that reactivation of PP2A by FTY720 induced apoptosis in mutant c-KIT cells through inactivation of the oncogenic receptor itself, and simultaneous inhibition of downstream signalling pathways. Indeed, FTY720-induced apoptosis was observed in the c-KIT mutants both *in vitro* and *in vivo*. Importantly, FTY720 treatment markedly reduced the phosphorylation of mutant c-KIT receptors, whilst having no effect on WT c-KIT. This is an exciting finding as small molecules which are designed to specifically bind to, and inhibit, c-KIT are completely ineffective against the kinase domain mutants. In addition, preliminary results from our laboratory indicate that reactivation of PP2A with FTY720 dephosphorylates the anti-apoptotic protein, BAD, in cells expressing D816V mutant c-KIT compared to WT c-KIT (A.M. Smith, N.M. Verrills, personal communication). Following on from this, a detailed analysis of other pathways, such as PI3K/Akt and STAT5, will reveal the complete effect of FTY720 on oncogenic cascade inhibition.

Currently no effective treatments are available for the inhibition of activating kinase domain *c-KIT* mutations. As such, there is a strong need for the development of improved therapeutic options for drug-resistant patients. The results obtained in this study demonstrate that myeloid precursors expressing D816V c-KIT are highly sensitive to reactivation of PP2A by FTY720. In addition to its use as a monotherapy, another therapeutic application for FTY720 may be the combination with a second-generation tyrosine kinase inhibitor, such as dasatinib. Although this compound inhibits D816V c-KIT receptors *in vitro*, it has proven largely ineffective in the clinic. However, the simultaneous administration of dasatinib with FTY720 may result in an additive or

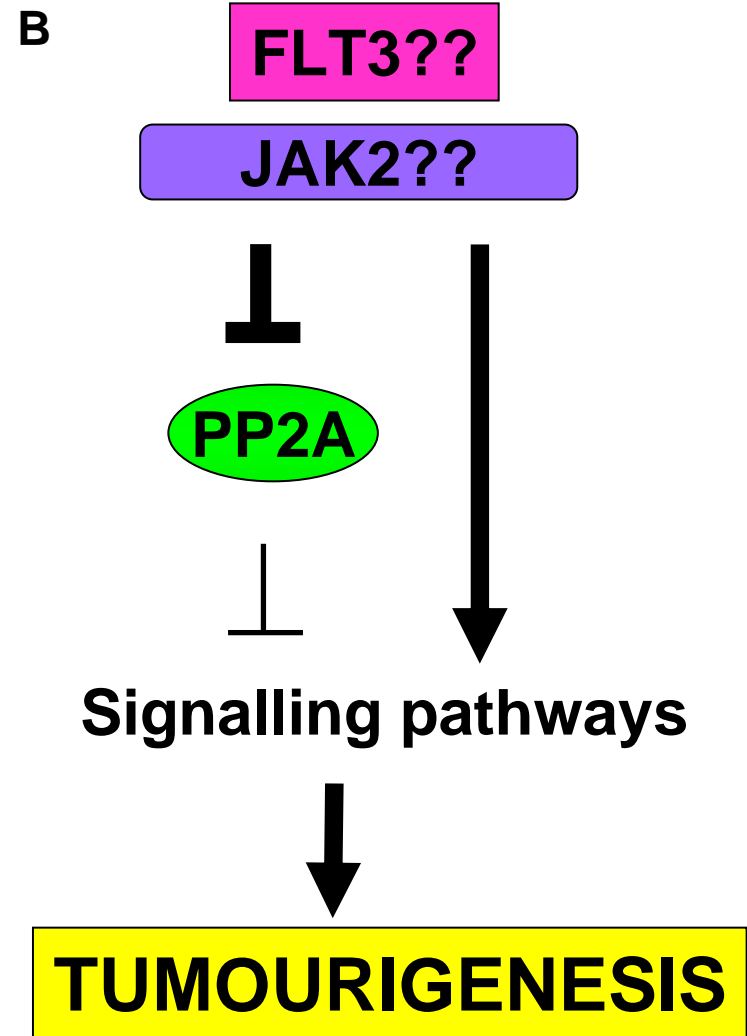
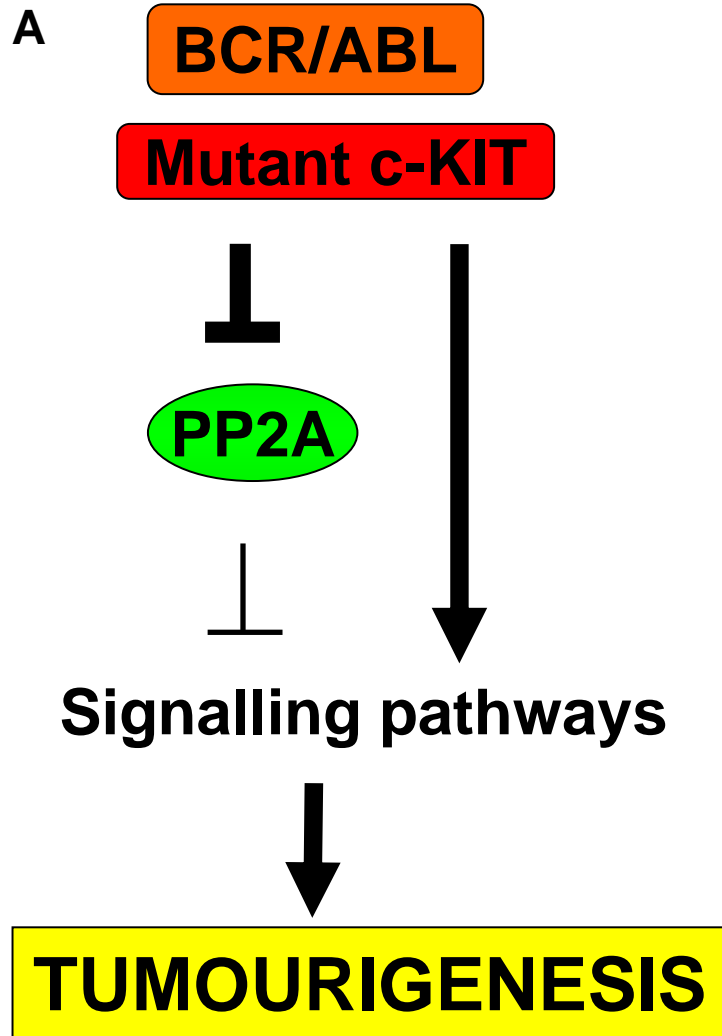
synergistic effect. This hypothesis is based on the observation that reactivation of PP2A not only inhibits oncogenic pathways downstream of the D816V c-KIT receptor, but effectively inactivates the kinase itself. Therefore, the combination of both compounds may reduce the concentration of dasatinib required for targeted inhibition of c-KIT mutants *in vivo*. Preliminary data from cytotoxicity assays indicate that the addition of FTY720 and dasatinib markedly reduces the viability of cells incubated with either drug alone, indicating at least an additive effect (Appendix Figure 2). Further investigation into the effect of different concentration ratios, in addition to testing these combinations *in vivo*, will validate their potential use in the clinic.

In support of the findings that enhanced PP2A activity specifically induces apoptosis of mutant c-KIT cells, several studies have recently confirmed PP2A activation as a powerful therapeutic approach in a range of human malignancies. For example, α -tocopheryl succinate has been shown to mediate its antitumour effects against LNCaP prostate cancer cells through a complex network of signalling pathways that are mediated by the activation of PP2A (Huang *et al.* 2009). Furthermore, the antiproliferative effects of the dithiolethione compound, ACS-1, in aggressive human lung and breast cancer cell lines is attributed to a dose-dependent increase in PP2A activity, which inhibits Akt signalling and results in reduced c-myc expression (Switzer *et al.* 2009). Lastly, impaired PP2A activity in MDA-MB-231 breast cancer cells can be restored with adiponectin-activated AMPK, and inhibits invasiveness in an *in vivo* metastasis model (Kim *et al.* 2009). It would be interesting to compare the efficacy of FTY720-induced PP2A reactivation in these cancer models, and conversely, to test these compounds in the BCR/ABL and mutant c-KIT-expressing FDC-P1 cells.

Taken together, the data presented in this thesis demonstrates that two very different oncogenic tyrosine kinases both require inhibition of PP2A activity and altered PP2A subunit expression for tumorigenicity. This suggests that functional inhibition of PP2A may be a common mechanism of tyrosine kinase driven tumour growth. In support of this, increased phosphorylation of PP2Ac, which generally reduces PP2A activity (Chen *et al.* 1992), has been reported in HER-2⁺ breast tumour specimens compared to normal breast tissue. Furthermore, elevated levels of PP2Ac-p^{Y307} significantly correlate with tumour progression (Wong *et al.* 2009). The HER-2 kinase is often overexpressed or amplified in breast cancer, and its activation contributes to tumour progression by

increasing proliferation as well as promoting metastasis and invasion (Freudenberg *et al.* 2009). The study by Wong *et al.*, identifies another important link between an activating tyrosine kinase and the regulation of a phosphatase in malignant disease. In addition to this, stimulation of Rat-1 fibroblasts or A431 epithelial cells with EGF also impairs the activity of PP2A and facilitates signalling through the MAPK pathway (Belcher *et al.* 2005, Ugi *et al.* 2002). Future investigation into the regulation of PP2A by mutated and constitutively active kinases such as FLT3 in AML (Meshinchi & Appelbaum 2009), EGFR in non-small-cell lung cancer (Hirsch *et al.* 2009) and JAK2 in myeloproliferative disorders (Levine & Gilliland 2008) will reveal whether PP2A inhibition contributes to the transforming potential of oncogenic tyrosine kinases (Figure 7.3).

In summary, this body of work highlights the complex regulation of PP2A by the oncogenic tyrosine kinases, BCR/ABL and c-KIT. Identifying the specific PP2A holoenzymes that are perturbed in cancers characterised by aberrant kinase activation substantially contributes to our understanding of cancer cell signalling and of PP2A biology. Importantly, these PP2A subunits may provide novel therapeutic targets to form the basis of improved cancer therapies. The heightened sensitivity of D816V c-KIT cells to FTY720, in conjunction with low toxicity, supports the translational application of PP2A-activating agents for the treatment of drug-resistant c-KIT⁺ patients. Taken together, the data suggests that functional inactivation of PP2A may represent a general mechanism employed by constitutively active kinases to facilitate tumour growth. As such, the reactivation of PP2A is a valid and powerful therapeutic strategy which may be applicable to a wide range of human malignancies.



APPENDIX 1 – BUFFERS AND STOCK SOLUTIONS

DNA loading buffer: 50% glycerol, 1 mM EDTA, 0.4% bromophenol Blue, 0.4% xylene cyanol

FACS fixative: 2% (w/v) glucose, 1% formaldehyde, 0.02% sodium azide in PBS

10% formic acid in 10% NBF (1L): 100 ml 90% formic acid, 900 ml 10% NBF

Freezing mix: 30% FCS, 20% DMSO and 50% Roswell Park Memorial Institute medium. The solution was filter sterilized through a 0.22 µm filter and stored at -20°C.

Inoue Transformation Buffer: 55 mM MnCl₂, 15 mM CaCl₂, 250 mM KCl and 10 mM PIPES was made up to 30 ml with milli-Q water. The solution was filter sterilized through a 0.45 µm filter and stored at 4°C.

IP lysis buffer: 1% NP40, 150 mM NaCl, 50 mM Tris pH 8.0) supplemented with 20 µl/ml protease inhibitor cocktail (Sigma).

LB Medium (1L): 10 g Bacto tryptone, 5 g Bacto yeast extract, 10 g NaCl, pH 7.0. The solution was sterilized by autoclaving and if required, ampicillin was added at a final concentration of 100 µg/ml.

LB Agar Plates: 15 g Bacto-agar was added to LB medium prior to autoclaving. The solution was allowed to cool and if required, ampicillin was added at a final concentration of 100 µg/ml. Plates were poured under aseptic conditions, dried and stored at 4°C.

10% NBF (1L): 100 ml 40% formalin (aqueous solution of formaldehyde), 4 g sodium dihydrogen orthophosphate (monohydrate), 6.5 g disodium hydrogen orthophosphate (anhydrous)

PBA: 0.1% BSA and 0.1% sodium azide in PBS.

PBS: 0.138 M NaCl, 0.0027 M KCl pH 7.4.

PBT: 1% BSA, 0.1% Tween-20 made up in PBS

Polyacrylamide Separating Gel (12%): 50 ml 30% acrylamide, 12.5 ml 1.5 M Tris pH 8.8 (375 mM), 500 μ l 10% SDS (0.1%), 16.75 ml milli-Q water, 50 μ l/10 ml 10% ammonium persulphate, 5 μ l/10 ml TEMED.

Polyacrylamide Stacking Gel (4%): 3.3 ml 30% acrylamide, 6.3 ml 0.5 M Tris pH 6.8 (375 mM), 250 μ l 10% SDS (0.1%), 15 ml milli-Q water, 100 μ l/10 ml 10% APS and 10 μ l/10 ml TEMED.

PP2A Activity Assay Lysis Buffer: 20 mM imidazole-HCL, 2 mM EDTA, 2 mM EDTA

pNPP Ser/Thr Assay Buffer: 50 mM Tris pH 7.0, 100 μ M CaCl₂

RBC lysis buffer: 320 mM sucrose, 5 mM MgCl₂, 10% Triton X-100, 10 mM Tris-HCl pH 7.8

RIPA Buffer: 1% NP40, 150mM NaCl, 50mM Tris pH 7.5, 0.1% SDS, 0.25% sodium deoxycholate) supplemented with 20 μ l/ml protease inhibitor cocktail (Sigma).

Modified RIPA Buffer: 1% NP40, 50 mM Tris pH 7.6, 150 mM NaCl, 1 mM EDTA, 0.25% Na deoxycholate, 0.05% SDS supplemented with 5 mM sodium fluoride, 5 mM sodium vanadate, 1 mM phenylmethyl sulphonyl fluoride (PMSF) and 20 μ l/ml protease inhibitor cocktail (Sigma).

RNA Lysis Buffer: 4M guanidium thiocyanate, 25 mM Na citrate pH 7.0, 0.5% sarkosyl, β -mercaptoethanol, made up in DEPC-treated water and stored in the dark.

Stripping Buffer: 0.2M glycine, 100 mM β -mercaptoethanol, pH 2.6. Store at 4°C. Preheat aliquots to 55°C and do 3x 20 minute incubations followed by 3x 10 minutes TBS-T washes.

5x SDS loading buffer: 60 mM Tris pH 6.8, 25% glycerol, 2% SDS, 375 mM DTT, 0.1% bromophenol blue

50x TAE (1L): 0.5 M EDTA pH 8.0, 57.1 ml glacial acetic acid, 242 g Tris base.

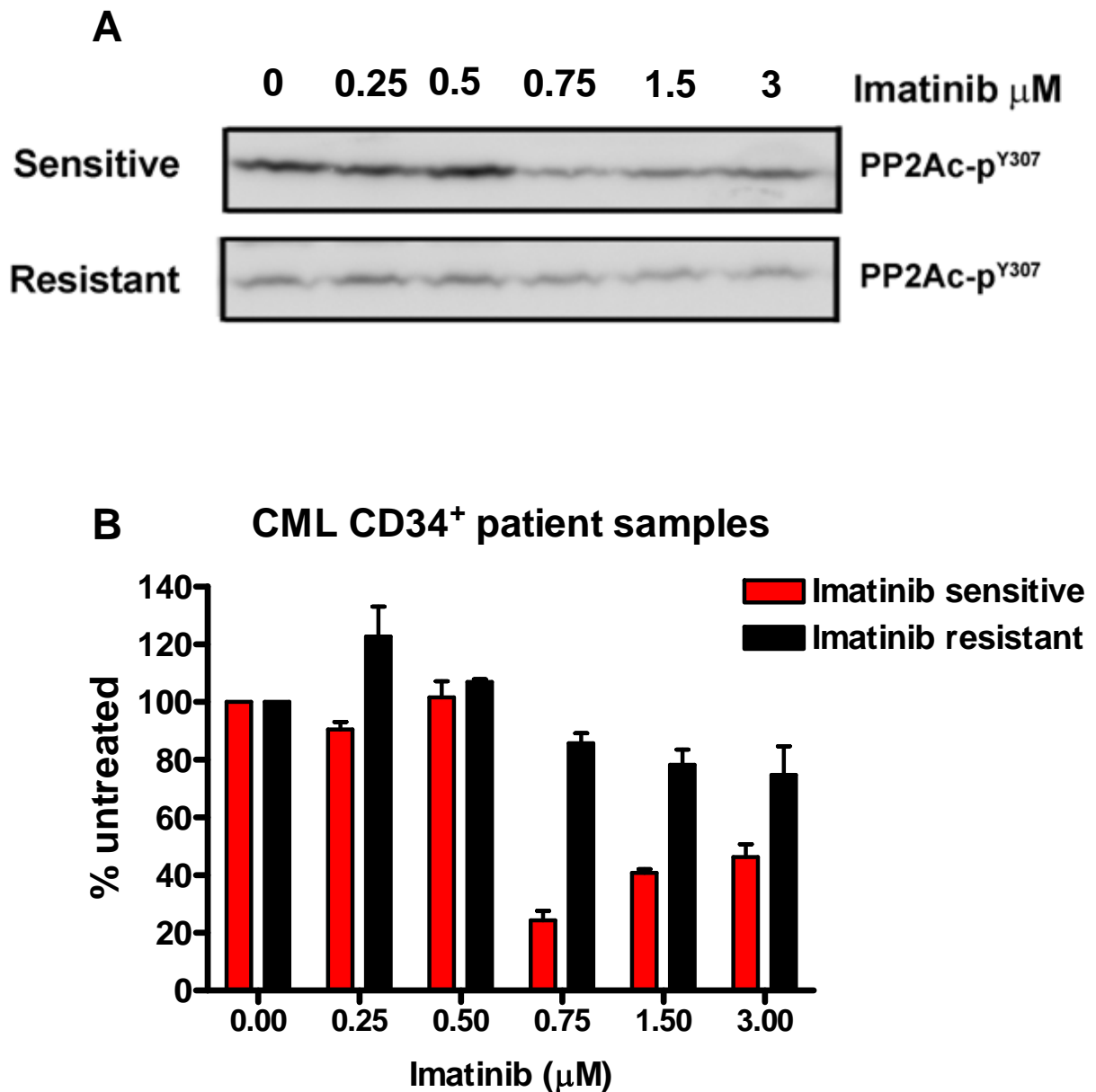
10x TBS (2L): 200 ml 1M Tris pH 8.0, 175.3 g NaCl

1x TBS-T (2L): 1 mM Tris pH 8.0, 150 mM NaCl, 0.1% Tween-20

1x Transfer Buffer (2L): 200 ml 10x western solution, 400 ml methanol

10x Western Solution (1L): 30.3 g Tris base, 144 g glycine

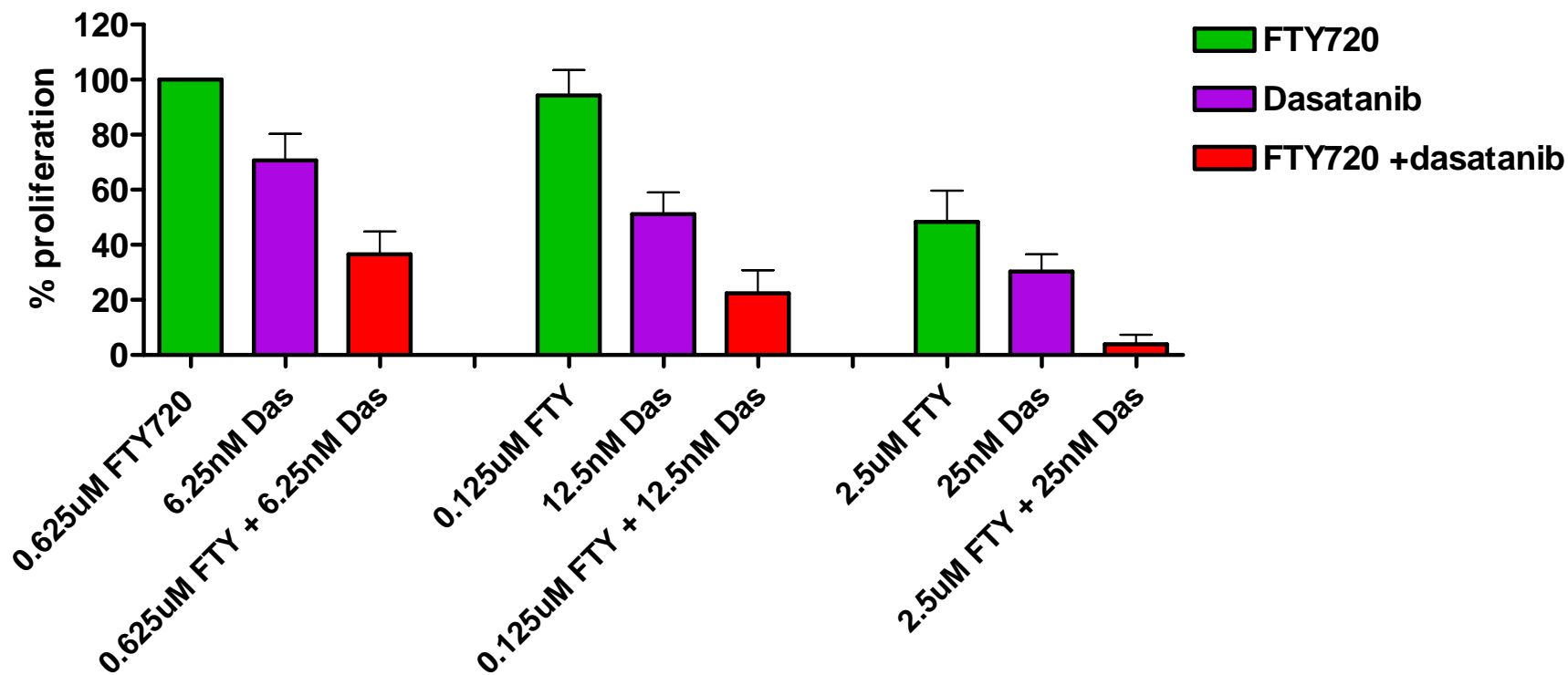
1x Western Solution (1L): 100 ml 10x western solution, 5 ml 20% SDS



Appendix Figure 1 Expression of PP2Ac-p^{Y307} in CD34⁺ CML primary samples

A) Membranes were obtained from Prof Timothy Hughes at IMVS. CD34⁺ cells were isolated from imatinib-sensitive or -resistant CML-CP patients then treated *in vitro* with increasing concentrations of imatinib (0-3 μM) for 2 hours. For each sample, 2×10^6 cells were lysed and the lysates were prepared in 1x sample buffer, subjected to SDS-PAGE, then transferred onto PVDF membranes and initially probed for CrkL. These steps were performed by lab personnel at IMVS. At the University of Newcastle, the dried blots were briefly rehydrated in 100% methanol then stripped and visualised with ECL to confirm complete removal of the CrkL signal. The membranes were blocked and probed for PP2Ac-p^{Y307} as described in Section 2.6.2.

B) Quantitation of two independent blots from two imatinib-sensitive or -resistant patients. *Columns*, percentage of mean densitometry normalised to untreated controls; *bars*, SEM.



Appendix Figure 2 Combined effects of FTY720 and dasatinib on D816V c-KIT FDC-P1 cell growth

A cytotoxicity assay was performed on FDC-P1 D816V c-KIT cells with the indicated concentrations of FTY720 (μM), dasatinib (nM) or FTY720 (μM) and dasatinib (nM) together. *Columns*, mean cell viability normalised to 0.625 μM FTY720. Three independent assays were performed in quadruplicate; *bars*, SEM.

REFERENCES

- Aberle, H., Bauer, A., Stappert, J., Kispert, A. and Kemler, R. (1997) beta-catenin is a target for the ubiquitin-proteasome pathway. *The EMBO journal*, **16**, 3797-3804.
- Abraham, D., Podar, K., Pacher, M. et al. (2000) Raf-1-associated protein phosphatase 2A as a positive regulator of kinase activation. *J Biol Chem*, **275**, 22300-22304.
- Abrams, T. J., Lee, L. B., Murray, L. J., Pryer, N. K. and Cherrington, J. M. (2003) SU11248 inhibits KIT and platelet-derived growth factor receptor beta in preclinical models of human small cell lung cancer. *Mol Cancer Ther*, **2**, 471-478.
- Adachi, Y., Pavlakis, G. N. and Copeland, T. D. (1994) Identification and characterization of SET, a nuclear phosphoprotein encoded by the translocation break point in acute undifferentiated leukemia. *J Biol Chem*, **269**, 2258-2262.
- Adams, D. G., Coffee, R. L., Jr., Zhang, H., Pelech, S., Strack, S. and Wadzinski, B. E. (2005) Positive regulation of Raf1-MEK1/2-ERK1/2 signaling by protein serine/threonine phosphatase 2A holoenzymes. *J Biol Chem*, **280**, 42644-42654.
- Adler, H. T., Nallaseth, F. S., Walter, G. and Tkachuk, D. C. (1997) HRX leukemic fusion proteins form a heterocomplex with the leukemia-associated protein SET and protein phosphatase 2A. *J Biol Chem*, **272**, 28407-28414.
- Agarwal, K. C. and Parks, R. E., Jr. (1983) Forskolin: a potential antimetastatic agent. *Int J Cancer*, **32**, 801-804.
- Ahuja, H., Bar-Eli, M., Advani, S. H., Benchimol, S. and Cline, M. J. (1989) Alterations in the p53 gene and the clonal evolution of the blast crisis of chronic myelocytic leukemia. *Proc Natl Acad Sci U S A*, **86**, 6783-6787.
- Aichberger, K. J., Gleixner, K. V., Mirkina, I. et al. (2009) Identification of pro-apoptotic Bim as a tumor suppressor in neoplastic mast cells: role of KIT D816V and effects of various targeted drugs. *Blood*.
- Albert, R., Hinterding, K., Brinkmann, V. et al. (2005) Novel immunomodulator FTY720 is phosphorylated in rats and humans to form a single stereoisomer. Identification, chemical proof, and biological characterization of the biologically active species and its enantiomer. *J Med Chem*, **48**, 5373-5377.
- Alessi, D. R., Gomez, N., Moorhead, G., Lewis, T., Keyse, S. M. and Cohen, P. (1995) Inactivation of p42 MAP kinase by protein phosphatase 2A and a protein tyrosine phosphatase, but not CL100, in various cell lines. *Curr Biol*, **5**, 283-295.
- Alfonso, Q.-C., Fabio Pires De Souza, S., Hagop, K., Susan, O. B., Stefan, F., Ahmed, A., Gautam, B. and Jorge, C. (2009) Dynamics and management of cytopenias associated with dasatinib therapy in patients with chronic myeloid leukemia in chronic phase after imatinib failure. *Cancer*, **9999**, NA.
- Andrabi, S., Gjoerup, O. V., Kean, J. A., Roberts, T. M. and Schaffhausen, B. (2007) Protein phosphatase 2A regulates life and death decisions via Akt in a context-dependent manner. *Proc Natl Acad Sci U S A*, **104**, 19011-19016.
- Antonescu, C. R., Besmer, P., Guo, T. et al. (2005) Acquired resistance to imatinib in gastrointestinal stromal tumor occurs through secondary gene mutation. *Clin Cancer Res*, **11**, 4182-4190.
- Antonescu, C. R., Viale, A., Sarran, L. et al. (2004) Gene expression in gastrointestinal stromal tumors is distinguished by KIT genotype and anatomic site. *Clin Cancer Res*, **10**, 3282-3290.

-
- Appelbaum, F. R., Kopecky, K. J., Tallman, M. S. et al. (2006) The clinical spectrum of adult acute myeloid leukaemia associated with core binding factor translocations. *Br J Haematol*, **135**, 165-173.
- Apperley, J. F., Cortes, J. E., Kim, D. W. et al. (2009) Dasatinib in the Treatment of Chronic Myeloid Leukemia in Accelerated Phase After Imatinib Failure: The START A Trial. *J Clin Oncol*.
- Arino, J., Woon, C. W., Brautigan, D. L., Miller, T. B., Jr. and Johnson, G. L. (1988) Human liver phosphatase 2A: cDNA and amino acid sequence of two catalytic subunit isotypes. *Proc Natl Acad Sci U S A*, **85**, 4252-4256.
- Arnold, H. K. and Sears, R. C. (2006) Protein phosphatase 2A regulatory subunit B56alpha associates with c-myc and negatively regulates c-myc accumulation. *Molecular and cellular biology*, **26**, 2832-2844.
- Ashida, A., Takata, M., Murata, H., Kido, K. and Saida, T. (2009) Pathological activation of KIT in metastatic tumors of acral and mucosal melanomas. *Int J Cancer*, **124**, 862-868.
- Ashman, L. K. (1999) The biology of stem cell factor and its receptor C-kit. *Int J Biochem Cell Biol*, **31**, 1037-1051.
- Asou, H., Tashiro, S., Hamamoto, K., Otsuji, A., Kita, K. and Kamada, N. (1991) Establishment of a human acute myeloid leukemia cell line (Kasumi-1) with 8;21 chromosome translocation. *Blood*, **77**, 2031-2036.
- Aylett, G., Cole, S., Caruana, G. and Ashman, L. K. (1995) Specificity and functional effects of MAb to c-Kit protein. In: *Leucocyte Typing V - White Cell Differentiation Antigens*. Oxford University Press.
- Azuma, H., Takahara, S., Ichimaru, N. et al. (2002) Marked prevention of tumor growth and metastasis by a novel immunosuppressive agent, FTY720, in mouse breast cancer models. *Cancer research*, **62**, 1410-1419.
- Baharians, Z. and Schonthal, A. H. (1998) Autoregulation of protein phosphatase type 2A expression. *J Biol Chem*, **273**, 19019-19024.
- Bajpai, R., Makhijani, K., Rao, P. R. and Shashidhara, L. S. (2004) Drosophila Twins regulates Armadillo levels in response to Wg/Wnt signal. *Development (Cambridge, England)*, **131**, 1007-1016.
- Beghini, A., Cairoli, R., Morra, E. and Larizza, L. (1998) In vivo differentiation of mast cells from acute myeloid leukemia blasts carrying a novel activating ligand-independent C-kit mutation. *Blood Cells Mol Dis*, **24**, 262-270.
- Beghini, A., Magnani, I., Ripamonti, C. B. and Larizza, L. (2002) Amplification of a novel c-Kit activating mutation Asn(822)-Lys in the Kasumi-1 cell line: a t(8;21)-Kit mutant model for acute myeloid leukemia. *Hematol J*, **3**, 157-163.
- Beghini, A., Peterlongo, P., Ripamonti, C. B., Larizza, L., Cairoli, R., Morra, E. and Mecucci, C. (2000) C-kit mutations in core binding factor leukemias. *Blood*, **95**, 726-727.
- Belcher, S. M., Le, H. H., Spurling, L. and Wong, J. K. (2005) Rapid estrogenic regulation of extracellular signal-regulated kinase 1/2 signaling in cerebellar granule cells involves a G protein- and protein kinase A-dependent mechanism and intracellular activation of protein phosphatase 2A. *Endocrinology*, **146**, 5397-5406.
- Ben-Neriah, Y., Daley, G. Q., Mes-Masson, A. M., Witte, O. N. and Baltimore, D. (1986) The chronic myelogenous leukemia-specific P210 protein is the product of the bcr/abl hybrid gene. *Science*, **233**, 212-214.

-
- Bene, M. C., Bernier, M., Casasnovas, R. O. et al. (1998) The reliability and specificity of c-kit for the diagnosis of acute myeloid leukemias and undifferentiated leukemias. The European Group for the Immunological Classification of Leukemias (EGIL). *Blood*, **92**, 596-599.
- Besmer, P., Murphy, J. E., George, P. C. et al. (1986) A new acute transforming feline retrovirus and relationship of its oncogene v-kit with the protein kinase gene family. *Nature*, **320**, 415-421.
- Bhatia, R., Holtz, M., Niu, N., Gray, R., Snyder, D. S., Sawyers, C. L., Arber, D. A., Slovak, M. L. and Forman, S. J. (2003) Persistence of malignant hematopoietic progenitors in chronic myelogenous leukemia patients in complete cytogenetic remission following imatinib mesylate treatment. *Blood*, **101**, 4701-4707.
- Bialojan, C. and Takai, A. (1988) Inhibitory effect of a marine-sponge toxin, okadaic acid, on protein phosphatases. Specificity and kinetics. *Biochem J*, **256**, 283-290.
- Bloomfield, C. D., Lawrence, D., Byrd, J. C. et al. (1998) Frequency of Prolonged Remission Duration after High-Dose Cytarabine Intensification in Acute Myeloid Leukemia Varies by Cytogenetic Subtype. *Cancer research*, **58**, 4173-4179.
- Blume-Jensen, P., Janknecht, R. and Hunter, T. (1998) The kit receptor promotes cell survival via activation of PI 3-kinase and subsequent Akt-mediated phosphorylation of Bad on Ser136. *Curr Biol*, **8**, 779-782.
- Blume-Jensen, P., Wernstedt, C., Heldin, C. H. and Ronnstrand, L. (1995) Identification of the major phosphorylation sites for protein kinase C in kit/stem cell factor receptor in vitro and in intact cells. *J Biol Chem*, **270**, 14192-14200.
- Boissel, N., Leroy, H., Brethon, B. et al. (2006) Incidence and prognostic impact of c-Kit, FLT3, and Ras gene mutations in core binding factor acute myeloid leukemia (CBF-AML). *Leukemia*, **20**, 965-970.
- Borgatti, P., Martelli, A. M., Tabellini, G., Bellacosa, A., Capitani, S. and Neri, L. M. (2003) Threonine 308 phosphorylated form of Akt translocates to the nucleus of PC12 cells under nerve growth factor stimulation and associates with the nuclear matrix protein nucleolin. *Journal of cellular physiology*, **196**, 79-88.
- Boyar, M. S. and Taub, R. N. (2007) New strategies for treating GIST when imatinib fails. *Cancer Invest*, **25**, 328-335.
- Bradeen, H. A., Eide, C. A., O'Hare, T., Johnson, K. J., Willis, S. G., Lee, F. Y., Druker, B. J. and Deininger, M. W. (2006) Comparison of imatinib mesylate, dasatinib (BMS-354825), and nilotinib (AMN107) in an N-ethyl-N-nitrosourea (ENU)-based mutagenesis screen: high efficacy of drug combinations. *Blood*, **108**, 2332-2338.
- Brinkmann, V., Davis, M. D., Heise, C. E. et al. (2002) The immune modulator FTY720 targets sphingosine 1-phosphate receptors. *J Biol Chem*, **277**, 21453-21457.
- Brinkmann, V. and Lynch, K. R. (2002) FTY720: targeting G-protein-coupled receptors for sphingosine 1-phosphate in transplantation and autoimmunity. *Current opinion in immunology*, **14**, 569-575.
- Brinkmann, V., Wilt, C., Kristofic, C., Nikolova, Z., Hof, R. P., Chen, S., Albert, R. and Cottens, S. (2001) FTY720: dissection of membrane receptor-operated, stereospecific effects on cell migration from receptor-independent antiproliferative and apoptotic effects. *Transplantation proceedings*, **33**, 3078-3080.

-
- Brizzi, M. F., Dentelli, P., Rosso, A., Yarden, Y. and Pegoraro, L. (1999) STAT protein recruitment and activation in c-Kit deletion mutants. *J Biol Chem*, **274**, 16965-16972.
- Brody, J. R., Kadkol, S. S., Hauer, M. C., Rajaii, F., Lee, J. and Pasternack, G. R. (2004) pp32 reduction induces differentiation of TSU-Pr1 cells. *The American journal of pathology*, **164**, 273-283.
- Broudy, V. C., Lin, N. L., Liles, W. C., Corey, S. J., O'Laughlin, B., Mou, S. and Linnekin, D. (1999) Signaling via Src family kinases is required for normal internalization of the receptor c-Kit. *Blood*, **94**, 1979-1986.
- Brown, B. A., Kantesaria, P. P. and McDevitt, L. M. (2007) Fingolimod: a novel immunosuppressant for multiple sclerosis. *Ann Pharmacother*, **41**, 1660-1668.
- Bryant, J. C., Westphal, R. S. and Wadzinski, B. E. (1999) Methylated C-terminal leucine residue of PP2A catalytic subunit is important for binding of regulatory Balph subunit. *Biochem J*, **339 (Pt 2)**, 241-246.
- Buchdunger, E., Cioffi, C. L., Law, N., Stover, D., Ohno-Jones, S., Druker, B. J. and Lydon, N. B. (2000) Abl protein-tyrosine kinase inhibitor STI571 inhibits in vitro signal transduction mediated by c-kit and platelet-derived growth factor receptors. *The Journal of pharmacology and experimental therapeutics*, **295**, 139-145.
- Buchdunger, E., Zimmermann, J., Mett, H., Meyer, T., Muller, M., Druker, B. J. and Lydon, N. B. (1996) Inhibition of the Abl protein-tyrosine kinase in vitro and in vivo by a 2-phenylaminopyrimidine derivative. *Cancer research*, **56**, 100-104.
- Budde, K., Schmouder, R. L., Brunkhorst, R. et al. (2002) First human trial of FTY720, a novel immunomodulator, in stable renal transplant patients. *J Am Soc Nephrol*, **13**, 1073-1083.
- Byrd, J. C., Dodge, R. K., Carroll, A. et al. (1999) Patients With t(8;21)(q22;q22) and Acute Myeloid Leukemia Have Superior Failure-Free and Overall Survival When Repetitive Cycles of High-Dose Cytarabine Are Administered. *J Clin Oncol*, **17**, 3767-3775.
- Byrd, J. C., Mrozek, K., Dodge, R. K. et al. (2002) Pretreatment cytogenetic abnormalities are predictive of induction success, cumulative incidence of relapse, and overall survival in adult patients with de novo acute myeloid leukemia: results from Cancer and Leukemia Group B (CALGB 8461). *Blood*, **100**, 4325-4336.
- Byrd, J. C., Ruppert, A. S., Mrozek, K. et al. (2004) Repetitive Cycles of High-Dose Cytarabine Benefit Patients With Acute Myeloid Leukemia and inv(16)(p13q22) or t(16;16)(p13;q22): Results from CALGB 8461. *J Clin Oncol*, **22**, 1087-1094.
- Cairolì, R., Beghini, A., Morello, E., Grillo, G., Montillo, M., Larizza, L. and Morra, E. (2005) Imatinib mesylate in the treatment of Core Binding Factor leukemias with KIT mutations. A report of three cases. *Leukemia research*, **29**, 397-400.
- Calabretta, B. and Perrotti, D. (2004) The biology of CML blast crisis. *Blood*, **103**, 4010-4022.
- Calin, G. A., di Iasio, M. G., Caprini, E. et al. (2000) Low frequency of alterations of the alpha (PPP2R1A) and beta (PPP2R1B) isoforms of the subunit A of the serine-threonine phosphatase 2A in human neoplasms. *Oncogene*, **19**, 1191-1195.
- Cammenga, J., Horn, S., Bergholz, U., Sommer, G., Besmer, P., Fiedler, W. and Stocking, C. (2005) Extracellular KIT receptor mutants, commonly found in core binding factor AML, are constitutively active and respond to imatinib mesylate. *Blood*, **106**, 3958-3961.

-
- Care, R. S., Valk, P. J., Goodeve, A. C. et al. (2003) Incidence and prognosis of c-KIT and FLT3 mutations in core binding factor (CBF) acute myeloid leukaemias. *Br J Haematol*, **121**, 775-777.
- Carlson, S. G., Eng, E., Kim, E. G., Perlman, E. J., Copeland, T. D. and Ballermann, B. J. (1998) Expression of SET, an inhibitor of protein phosphatase 2A, in renal development and Wilms' tumor. *J Am Soc Nephrol*, **9**, 1873-1880.
- Carpten, J. D., Faber, A. L., Horn, C. et al. (2007) A transforming mutation in the pleckstrin homology domain of AKT1 in cancer. *Nature*, **448**, 439-444.
- Casteran, N., De Sepulveda, P., Beslu, N., Aoubala, M., Letard, S., Lecocq, E., Rottapel, R. and Dubreuil, P. (2003) Signal transduction by several KIT juxtamembrane domain mutations. *Oncogene*, **22**, 4710-4722.
- Castilla, L. H., Garrett, L., Adya, N. et al. (1999) The fusion gene Cbfb-MYH11 blocks myeloid differentiation and predisposes mice to acute myelomonocytic leukaemia. *Nat Genet*, **23**, 144-146.
- Chalfant, C. E., Kishikawa, K., Mumby, M. C., Kamibayashi, C., Bielawska, A. and Hannun, Y. A. (1999) Long chain ceramides activate protein phosphatase-1 and protein phosphatase-2A. Activation is stereospecific and regulated by phosphatidic acid. *J Biol Chem*, **274**, 20313-20317.
- Chalfant, C. E., Szulc, Z., Roddy, P., Bielawska, A. and Hannun, Y. A. (2004) The structural requirements for ceramide activation of serine-threonine protein phosphatases. *Journal of lipid research*, **45**, 496-506.
- Chan, L. C., Karhi, K. K., Rayter, S. I. et al. (1987) A novel abl protein expressed in Philadelphia chromosome positive acute lymphoblastic leukaemia. *Nature*, **325**, 635-637.
- Chan, P. M., Ilangumaran, S., La Rose, J., Chakrabarty, A. and Rottapel, R. (2003) Autoinhibition of the kit receptor tyrosine kinase by the cytosolic juxtamembrane region. *Molecular and cellular biology*, **23**, 3067-3078.
- Chen, H., Isozaki, K., Kinoshita, K., Ohashi, A., Shinomura, Y., Matsuzawa, Y., Kitamura, Y. and Hirota, S. (2003) Imatinib inhibits various types of activating mutant kit found in gastrointestinal stromal tumors. *Int J Cancer*, **105**, 130-135.
- Chen, J., Martin, B. L. and Brautigan, D. L. (1992) Regulation of protein serine-threonine phosphatase type-2A by tyrosine phosphorylation. *Science*, **257**, 1261-1264.
- Chen, J., Parsons, S. and Brautigan, D. L. (1994) Tyrosine phosphorylation of protein phosphatase 2A in response to growth stimulation and v-src transformation of fibroblasts. *J Biol Chem*, **269**, 7957-7962.
- Chen, J., Peterson, R. T. and Schreiber, S. L. (1998) [alpha]4 Associates with Protein Phosphatases 2A, 4, and 6. *Biochemical and biophysical research communications*, **247**, 827-832.
- Chen, L. L., Trent, J. C., Wu, E. F. et al. (2004a) A missense mutation in KIT kinase domain 1 correlates with imatinib resistance in gastrointestinal stromal tumors. *Cancer research*, **64**, 5913-5919.
- Chen, W., Arroyo, J. D., Timmons, J. C., Possemato, R. and Hahn, W. C. (2005) Cancer-associated PP2A Aalpha subunits induce functional haploinsufficiency and tumorigenicity. *Cancer research*, **65**, 8183-8192.
- Chen, W., Possemato, R., Campbell, K. T., Plattner, C. A., Pallas, D. C. and Hahn, W. C. (2004b) Identification of specific PP2A complexes involved in human cell transformation. *Cancer Cell*, **5**, 127-136.

-
- Chen, Y., Xu, Y., Bao, Q., Xing, Y., Li, Z., Lin, Z., Stock, J. B., Jeffrey, P. D. and Shi, Y. (2007) Structural and biochemical insights into the regulation of protein phosphatase 2A by small t antigen of SV40. *Nat Struct Mol Biol*, **14**, 527-534.
- Chevallier, P., Hunault-Berger, M., Larosa, F., Dauriac, C., Garand, R. and Harousseau, J. L. (2009) A phase II trial of high-dose imatinib mesylate for relapsed or refractory c-kit positive and Bcr-Abl negative acute myeloid leukaemia: the AFR-15 trial. *Leukemia research*, **33**, 1124-1126.
- Chian, R., Young, S., Danilkovitch-Miagkova, A., Ronnstrand, L., Leonard, E., Ferrao, P., Ashman, L. and Linnekin, D. (2001) Phosphatidylinositol 3 kinase contributes to the transformation of hematopoietic cells by the D816V c-Kit mutant. *Blood*, **98**, 1365-1373.
- Chiba, K., Yanagawa, Y., Masubuchi, Y., Kataoka, H., Kawaguchi, T., Ohtsuki, M. and Hoshino, Y. (1998) FTY720, a novel immunosuppressant, induces sequestration of circulating mature lymphocytes by acceleration of lymphocyte homing in rats. I. FTY720 selectively decreases the number of circulating mature lymphocytes by acceleration of lymphocyte homing. *J Immunol*, **160**, 5037-5044.
- Cho, U. S., Morrone, S., Sablina, A. A., Arroyo, J. D., Hahn, W. C. and Xu, W. (2007) Structural basis of PP2A inhibition by small t antigen. *PLoS Biol*, **5**, e202.
- Cho, U. S. and Xu, W. (2007) Crystal structure of a protein phosphatase 2A heterotrimeric holoenzyme. *Nature*, **445**, 53-57.
- Chua, C. W., Lee, D. T., Ling, M. T., Zhou, C., Man, K., Ho, J., Chan, F. L., Wang, X. and Wong, Y. C. (2005) FTY720, a fungus metabolite, inhibits in vivo growth of androgen-independent prostate cancer. *Int J Cancer*, **117**, 1039-1048.
- Clute, P. and Pines, J. (1999) Temporal and spatial control of cyclin B1 destruction in metaphase. *Nature cell biology*, **1**, 82-87.
- Cohen, J., Pelletier, J., Kappos, L. et al. (2009) Oral Fingolimod (FTY720) Versus Interferon Beta-1a in Relapsing/Remitting Multiple Sclerosis: Results from a Phase III Study (TRANSFORMS). In: *American Academy of Neurology*. Seattle.
- Cohen, P., Klumpp, S. and Schelling, D. L. (1989) An improved procedure for identifying and quantitating protein phosphatases in mammalian tissues. *FEBS Lett*, **250**, 596-600.
- Colella, S., Ohgaki, H., Ruediger, R., Yang, F., Nakamura, M., Fujisawa, H., Kleihues, P. and Walter, G. (2001) Reduced expression of the Aalpha subunit of protein phosphatase 2A in human gliomas in the absence of mutations in the Aalpha and Abeta subunit genes. *Int J Cancer*, **93**, 798-804.
- Coluccia, A. M. L., Vacca, A., Dunach, M., Mologni, L., Redaelli, S., Bustos, V. H., Benati, D., Pinna, L. A. and Gambacorti-Passerini, C. (2007) Bcr-Abl stabilizes [beta]-catenin in chronic myeloid leukemia through its tyrosine phosphorylation. *The EMBO journal*, **26**, 1456-1466.
- Copland, M., Hamilton, A., Elrick, L. J., Baird, J. W., Allan, E. K., Jordanides, N., Barow, M., Mountford, J. C. and Holyoake, T. L. (2006) Dasatinib (BMS-354825) targets an earlier progenitor population than imatinib in primary CML but does not eliminate the quiescent fraction. *Blood*, **107**, 4532-4539.
- Corbin, A. S., Demehri, S., Griswold, I. J. et al. (2005) In vitro and in vivo activity of ATP-based kinase inhibitors AP23464 and AP23848 against activation-loop mutants of Kit. *Blood*, **106**, 227-234.
- Corbin, A. S., Griswold, I. J., La Rosee, P., Yee, K. W. H., Heinrich, M. C., Reimer, C. L., Druker, B. J. and Deininger, M. W. N. (2004) Sensitivity of oncogenic KIT mutants to the kinase inhibitors MLN518 and PD180970. *Blood*, **104**, 3754-3757.

-
- Corless, C. L., Fletcher, J. A. and Heinrich, M. C. (2004) Biology of gastrointestinal stromal tumors. *J Clin Oncol*, **22**, 3813-3825.
- Cortes, J., Giles, F., O'Brien, S. et al. (2003) Results of imatinib mesylate therapy in patients with refractory or recurrent acute myeloid leukemia, high-risk myelodysplastic syndrome, and myeloproliferative disorders. *Cancer*, **97**, 2760-2766.
- Cortes, J., O'Brien, S. and Kantarjian, H. (2004) Discontinuation of imatinib therapy after achieving a molecular response. *Blood*, **104**, 2204-2205.
- Cortes, J., Rousselot, P., Kim, D. W. et al. (2007) Dasatinib induces complete hematologic and cytogenetic responses in patients with imatinib-resistant or -intolerant chronic myeloid leukemia in blast crisis. *Blood*, **109**, 3207-3213.
- Cortez, D., Kadlec, L. and Pendergast, A. M. (1995) Structural and signaling requirements for BCR-ABL-mediated transformation and inhibition of apoptosis. *Molecular and cellular biology*, **15**, 5531-5541.
- Creyghton, M. P., Roel, G., Eichhorn, P. J., Hijmans, E. M., Maurer, I., Destree, O. and Bernards, R. (2005) PR72, a novel regulator of Wnt signaling required for Naked cuticle function. *Genes Dev*, **19**, 376-386.
- Creyghton, M. P., Roel, G., Eichhorn, P. J., Vredeveld, L. C., Destree, O. and Bernards, R. (2006) PR130 is a modulator of the Wnt-signaling cascade that counters repression of the antagonist Naked cuticle. *Proc Natl Acad Sci U S A*, **103**, 5397-5402.
- Cullinane, C., Dorow, D. S., Kansara, M., Conus, N., Binns, D., Hicks, R. J., Ashman, L. K., McArthur, G. A. and Thomas, D. M. (2005) An in vivo tumor model exploiting metabolic response as a biomarker for targeted drug development. *Cancer research*, **65**, 9633-9636.
- Cully, M., You, H., Levine, A. J. and Mak, T. W. (2006) Beyond PTEN mutations: the PI3K pathway as an integrator of multiple inputs during tumorigenesis. *Nat Rev Cancer*, **6**, 184-192.
- Curtin, J. A., Busam, K., Pinkel, D. and Bastian, B. C. (2006) Somatic activation of KIT in distinct subtypes of melanoma. *J Clin Oncol*, **24**, 4340-4346.
- Cyster, J. G. (2005) Chemokines, sphingosine-1-phosphate, and cell migration in secondary lymphoid organs. *Annu Rev Immunol*, **23**, 127-159.
- Dagher, R., Cohen, M., Williams, G. et al. (2002) Approval summary: imatinib mesylate in the treatment of metastatic and/or unresectable malignant gastrointestinal stromal tumors. *Clin Cancer Res*, **8**, 3034-3038.
- Daley, G. Q. and Baltimore, D. (1988) Transformation of an interleukin 3-dependent hematopoietic cell line by the chronic myelogenous leukemia-specific P210bcr/abl protein. *Proc Natl Acad Sci U S A*, **85**, 9312-9316.
- Datta, K., Bellacosa, A., Chan, T. O. and Tsichlis, P. N. (1996) Akt is a direct target of the phosphatidylinositol 3-kinase. Activation by growth factors, v-src and v-Har-ras, in Sf9 and mammalian cells. *J Biol Chem*, **271**, 30835-30839.
- Dayyani, F., Wang, J., Yeh, J.-R. J., Ahn, E.-Y., Tobey, E., Zhang, D.-E., Bernstein, I. D., Peterson, R. T. and Sweetser, D. A. (2008) Loss of TLE1 and TLE4 from the del(9q) commonly deleted region in AML cooperates with AML1-ETO to affect myeloid cell proliferation and survival. *Blood*, **111**, 4338-4347.
- De Wulf, P., Montani, F. and Visintin, R. (2009) Protein phosphatases take the mitotic stage. *Current opinion in cell biology*.
- Debiec-Rychter, M., Cools, J., Dumez, H. et al. (2005) Mechanisms of resistance to imatinib mesylate in gastrointestinal stromal tumors and activity of the PKC412 inhibitor against imatinib-resistant mutants. *Gastroenterology*, **128**, 270-279.

-
- Deichmann, M., Polychronidis, M., Wacker, J., Thome, M. and Naher, H. (2001) The protein phosphatase 2A subunit Bgamma gene is identified to be differentially expressed in malignant melanomas by subtractive suppression hybridization. *Melanoma Res*, **11**, 577-585.
- Deininger, M., Buchdunger, E. and Druker, B. J. (2005) The development of imatinib as a therapeutic agent for chronic myeloid leukemia. *Blood*, **105**, 2640-2653.
- Demetri, G. D., Heinrich, M. C., Fletcher, J. A. et al. (2009) Molecular Target Modulation, Imaging, and Clinical Evaluation of Gastrointestinal Stromal Tumor Patients Treated with Sunitinib Malate after Imatinib Failure. *Clinical Cancer Research*, **15**, 5902-5909.
- Demetri, G. D., van Oosterom, A. T., Garrett, C. R. et al. (2006) Efficacy and safety of sunitinib in patients with advanced gastrointestinal stromal tumour after failure of imatinib: a randomised controlled trial. *Lancet*, **368**, 1329-1338.
- Demetri, G. D., von Mehren, M., Blanke, C. D. et al. (2002) Efficacy and safety of imatinib mesylate in advanced gastrointestinal stromal tumors. *N Engl J Med*, **347**, 472-480.
- Dexter, T. M., Garland, J., Scott, D., Scolnick, E. and Metcalf, D. (1980) Growth of factor-dependent hemopoietic precursor cell lines. *J Exp Med*, **152**, 1036-1047.
- Ditchfield, C., Johnson, V. L., Tighe, A., Ellston, R., Haworth, C., Johnson, T., Mortlock, A., Keen, N. and Taylor, S. S. (2003) Aurora B couples chromosome alignment with anaphase by targeting BubR1, Mad2, and Cenp-E to kinetochores. *The Journal of cell biology*, **161**, 267-280.
- Dobrowsky, R. T., Kamibayashi, C., Mumby, M. C. and Hannun, Y. A. (1993) Ceramide activates heterotrimeric protein phosphatase 2A. *J Biol Chem*, **268**, 15523-15530.
- Dohoney, K. M., Guillermin, C., Whiteford, C., Elbi, C., Lambert, P. F., Hager, G. L. and Brady, J. N. (2004) Phosphorylation of p53 at serine 37 is important for transcriptional activity and regulation in response to DNA damage. *Oncogene*, **23**, 49-57.
- Dougherty, M. K., Muller, J., Ritt, D. A. et al. (2005) Regulation of Raf-1 by direct feedback phosphorylation. *Mol Cell*, **17**, 215-224.
- Downing, J. R. (2003) The core-binding factor leukemias: lessons learned from murine models. *Curr Opin Genet Dev*, **13**, 48-54.
- Downing, J. R., Head, D. R., Curcio-Brint, A. M. et al. (1993) An AML1/ETO fusion transcript is consistently detected by RNA-based polymerase chain reaction in acute myelogenous leukemia containing the (8;21)(q22;q22) translocation. *Blood*, **81**, 2860-2865.
- Druker, B. J., Guilhot, F., O'Brien, S. G. et al. (2006) Five-year follow-up of patients receiving imatinib for chronic myeloid leukemia. *N Engl J Med*, **355**, 2408-2417.
- Druker, B. J., Sawyers, C. L., Kantarjian, H., Resta, D. J., Reese, S. F., Ford, J. M., Capdeville, R. and Talpaz, M. (2001a) Activity of a specific inhibitor of the BCR-ABL tyrosine kinase in the blast crisis of chronic myeloid leukemia and acute lymphoblastic leukemia with the Philadelphia chromosome. *N Engl J Med*, **344**, 1038-1042.
- Druker, B. J., Talpaz, M., Resta, D. J. et al. (2001b) Efficacy and safety of a specific inhibitor of the BCR-ABL tyrosine kinase in chronic myeloid leukemia. *N Engl J Med*, **344**, 1031-1037.

-
- Druker, B. J., Tamura, S., Buchdunger, E., Ohno, S., Segal, G. M., Fanning, S., Zimmermann, J. and Lydon, N. B. (1996) Effects of a selective inhibitor of the Abl tyrosine kinase on the growth of Bcr-Abl positive cells. *Nature medicine*, **2**, 561-566.
- Duensing, A., Heinrich, M. C., Fletcher, C. D. and Fletcher, J. A. (2004) Biology of gastrointestinal stromal tumors: KIT mutations and beyond. *Cancer Invest*, **22**, 106-116.
- Dunwell, T. L., Hesson, L. B., Pavlova, T. et al. (2009) Epigenetic analysis of childhood acute lymphoblastic leukemia. *Epigenetics*, **4**, 185-193.
- Eastman, Q. and Grosschedl, R. (1999) Regulation of LEF-1/TCF transcription factors by Wnt and other signals. *Current opinion in cell biology*, **11**, 233-240.
- Eichhorn, P. J., Creighton, M. P. and Bernards, R. (2009) Protein phosphatase 2A regulatory subunits and cancer. *Biochim Biophys Acta*, **1795**, 1-15.
- el Bawab, S., Mao, C., Obeid, L. M. and Hannun, Y. A. (2002) Ceramidases in the regulation of ceramide levels and function. *Sub-cellular biochemistry*, **36**, 187-205.
- Elmaagacli, A. H., Beelen, D. W., Opalka, B., Seeber, S. and Schaefer, U. W. (2000) The amount of BCR-ABL fusion transcripts detected by the real-time quantitative polymerase chain reaction method in patients with Philadelphia chromosome positive chronic myeloid leukemia correlates with the disease stage. *Ann Hematol*, **79**, 424-431.
- Faderl, S., Talpaz, M., Estrov, Z., O'Brien, S., Kurzrock, R. and Kantarjian, H. M. (1999) The biology of chronic myeloid leukemia. *N Engl J Med*, **341**, 164-172.
- Faivre, S., Demetri, G., Sargent, W. and Raymond, E. (2007) Molecular basis for sunitinib efficacy and future clinical development. *Nat Rev Drug Discov*, **6**, 734-745.
- Falt, S., Merup, M., Gahrton, G., Lambert, B. and Wennborg, A. (2005) Identification of progression markers in B-CLL by gene expression profiling. *Experimental hematology*, **33**, 883-893.
- Feinstein, E., Cimino, G., Gale, R. P. et al. (1991) p53 in chronic myelogenous leukemia in acute phase. *Proc Natl Acad Sci U S A*, **88**, 6293-6297.
- Ferrao, P., Gonda, T. J. and Ashman, L. K. (1997) Expression of constitutively activated human c-Kit in Myb transformed early myeloid cells leads to factor independence, histiocytic differentiation, and tumorigenicity. *Blood*, **90**, 4539-4552.
- Feschenko, M. S., Stevenson, E., Nairn, A. C. and Sweadner, K. J. (2002) A novel cAMP-stimulated pathway in protein phosphatase 2A activation. *The Journal of pharmacology and experimental therapeutics*, **302**, 111-118.
- Fletcher, C. D., Berman, J. J., Corless, C. et al. (2002) Diagnosis of gastrointestinal stromal tumors: A consensus approach. *Hum Pathol*, **33**, 459-465.
- Forester, C. M., Maddox, J., Louis, J. V., Goris, J. and Virshup, D. M. (2007) Control of mitotic exit by PP2A regulation of Cdc25C and Cdk1. *Proc Natl Acad Sci U S A*, **104**, 19867-19872.
- Fornierod, M., Boer, J., van Baal, S. et al. (1995) Relocation of the carboxyterminal part of CAN from the nuclear envelope to the nucleus as a result of leukemia-specific chromosome rearrangements. *Oncogene*, **10**, 1739-1748.
- Foster, R., Griffith, R., Ferrao, P. and Ashman, L. (2004) Molecular basis of the constitutive activity and STI571 resistance of Asp816Val mutant KIT receptor tyrosine kinase. *J Mol Graph Model*, **23**, 139-152.

-
- Francia, G., Poulson, R., Hanby, A. M., Mitchell, S. D., Williams, G., McKee, P. and Hart, I. R. (1999) Identification by differential display of a protein phosphatase-2A regulatory subunit preferentially expressed in malignant melanoma cells. *Int J Cancer*, **82**, 709-713.
- Freudenberg, J. A., Wang, Q., Katsumata, M., Drebin, J., Nagatomo, I. and Greene, M. I. (2009) The role of HER2 in early breast cancer metastasis and the origins of resistance to HER2-targeted therapies. *Experimental and Molecular Pathology*, **87**, 1-11.
- Frost, M. J., Ferrao, P. T., Hughes, T. P. and Ashman, L. K. (2002) Juxtamembrane mutant V560GKit is more sensitive to Imatinib (STI571) compared with wild-type c-kit whereas the kinase domain mutant D816VKit is resistant. *Mol Cancer Ther*, **1**, 1115-1124.
- Fujiki, H. and Suganuma, M. (2009) Carcinogenic aspects of protein phosphatase 1 and 2A inhibitors. *Prog Mol Subcell Biol*, **46**, 221-254.
- Fujita, T., Inoue, K., Yamamoto, S., Ikumoto, T., Sasaki, S., Toyama, R., Chiba, K., Hoshino, Y. and Okumoto, T. (1994) Fungal metabolites. Part 11. A potent immunosuppressive activity found in *Isaria sinclairii* metabolite. *The Journal of antibiotics*, **47**, 208-215.
- Galadari, S., Kishikawa, K., Kamibayashi, C., Mumby, M. C. and Hannun, Y. A. (1998) Purification and characterization of ceramide-activated protein phosphatases. *Biochemistry*, **37**, 11232-11238.
- Gallay, N., Dos Santos, C., Cuzin, L. et al. (2009) The level of AKT phosphorylation on threonine 308 but not on serine 473 is associated with high-risk cytogenetics and predicts poor overall survival in acute myeloid leukaemia. *Leukemia*, **23**, 1029-1038.
- Garg, R. J., Kantarjian, H., O'Brien, S., Quintas-Cardama, A., Faderl, S., Estrov, Z. and Cortes, J. (2009) The use of nilotinib or dasatinib after failure to two prior tyrosine kinase inhibitors (TKI): long-term follow-up. *Blood*.
- Gari, M., Goodeve, A., Wilson, G., Winship, P., Langabeer, S., Linch, D., Vandenberghe, E., Peake, I. and Reilly, J. (1999) c-kit proto-oncogene exon 8 in-frame deletion plus insertion mutations in acute myeloid leukaemia. *Br J Haematol*, **105**, 894-900.
- Gazdar, A. F. (2009) Activating and resistance mutations of EGFR in non-small-cell lung cancer: role in clinical response to EGFR tyrosine kinase inhibitors. *Oncogene*, **28**, S24-S31.
- Giles, F. J., Larson, R., Le Coutre, P., Baccarani, M., Tavorath, R., Alland, L., Kantarjian, H. M., Hughes, T. and Ottmann, O. (2006) A phase II study of AMN107, a novel inhibitor of Bcr-Abl, administered to imatinib-resistant or intolerant patients (pts) with Ph+ chronic myelogenous leukemia (CML) in blast crisis (BC) or relapsed/refractory Ph+ acute lymphoblastic leukemia (ALL). *ASCO Meeting Abstracts*, **24**, 6536-.
- Girdler, F., Gascoigne, K. E., Evers, P. A., Hartmuth, S., Crafter, C., Foote, K. M., Keen, N. J. and Taylor, S. S. (2006) Validating Aurora B as an anti-cancer drug target. *J Cell Sci*, **119**, 3664-3675.
- Gizatullin, F., Yao, Y., Kung, V., Harding, M. W., Loda, M. and Shapiro, G. I. (2006) The Aurora Kinase Inhibitor VX-680 Induces Endoreduplication and Apoptosis Preferentially in Cells with Compromised p53-Dependent Postmitotic Checkpoint Function. *Cancer research*, **66**, 7668-7677.
- Glotzer, M. (2005) The Molecular Requirements for Cytokinesis. *Science*, **307**, 1735-1739.

-
- Glotzer, M., Murray, A. W. and Kirschner, M. W. (1991) Cyclin is degraded by the ubiquitin pathway. *Nature*, **349**, 132-138.
- Goodman, V. L., Rock, E. P., Dagher, R. et al. (2007) Approval summary: sunitinib for the treatment of imatinib refractory or intolerant gastrointestinal stromal tumors and advanced renal cell carcinoma. *Clin Cancer Res*, **13**, 1367-1373.
- Goris, J. and Merlevede, W. (1988) Isolation of an active form of the ATP + Mg²⁺-dependent protein phosphatase stimulated by the deinhibitor protein and by p-nitrophenyl phosphate. *Biochem J*, **254**, 501-507.
- Gorre, M. E., Mohammed, M., Ellwood, K., Hsu, N., Paquette, R., Rao, P. N. and Sawyers, C. L. (2001) Clinical resistance to STI-571 cancer therapy caused by BCR-ABL gene mutation or amplification. *Science*, **293**, 876-880.
- Gotlib, J., Berube, C., Growney, J. D. et al. (2005) Activity of the tyrosine kinase inhibitor PKC412 in a patient with mast cell leukemia with the D816V KIT mutation. *Blood*, **106**, 2865-2870.
- Gotz, J., Probst, A., Ehler, E., Hemmings, B. and Kues, W. (1998) Delayed embryonic lethality in mice lacking protein phosphatase 2A catalytic subunit Calpha. *Proc Natl Acad Sci U S A*, **95**, 12370-12375.
- Gotz, J., Probst, A., Mistl, C., Nitsch, R. M. and Ehler, E. (2000) Distinct role of protein phosphatase 2A subunit Calpha in the regulation of E-cadherin and beta-catenin during development. *Mech Dev*, **93**, 83-93.
- Graham, S. M., Jorgensen, H. G., Allan, E., Pearson, C., Alcorn, M. J., Richmond, L. and Holyoake, T. L. (2002) Primitive, quiescent, Philadelphia-positive stem cells from patients with chronic myeloid leukemia are insensitive to STI571 in vitro. *Blood*, **99**, 319-325.
- Graler, M. H. and Goetzl, E. J. (2004) The immunosuppressant FTY720 down-regulates sphingosine 1-phosphate G-protein-coupled receptors. *Faseb J*, **18**, 551-553.
- Greenberger, J. S., Sakakeeny, M. A., Humphries, R. K., Eaves, C. J. and Eckner, R. J. (1983) Demonstration of permanent factor-dependent multipotential (erythroid/neutrophil/basophil) hematopoietic progenitor cell lines. *Proc Natl Acad Sci U S A*, **80**, 2931-2935.
- Griswold, I. J., MacPartlin, M., Bumm, T. et al. (2006) Kinase domain mutants of Bcr-Abl exhibit altered transformation potency, kinase activity, and substrate utilization, irrespective of sensitivity to imatinib. *Molecular and cellular biology*, **26**, 6082-6093.
- Groves, M. R., Hanlon, N., Turowski, P., Hemmings, B. A. and Barford, D. (1999) The structure of the protein phosphatase 2A PR65/A subunit reveals the conformation of its 15 tandemly repeated HEAT motifs. *Cell*, **96**, 99-110.
- Guergnon, J., Dessauge, F., Dominguez, V. et al. (2006) Use of Penetrating Peptides Interacting with PP1/PP2A Proteins As a General Approach for a Drug Phosphatase Technology. *Mol Pharmacol*, **69**, 1115-1124.
- Guilhot, F., Apperley, J., Kim, D. W. et al. (2007) Dasatinib induces significant hematologic and cytogenetic responses in patients with imatinib-resistant or -intolerant chronic myeloid leukemia in accelerated phase. *Blood*, **109**, 4143-4150.
- Guo, C. Y., Brautigan, D. L. and Lerner, J. M. (2002) ATM-dependent dissociation of B55 regulatory subunit from nuclear PP2A in response to ionizing radiation. *J Biol Chem*, **277**, 4839-4844.
- Gutzkow, K. B., Naderi, S. and Blomhoff, H. K. (2002) Forskolin-mediated G1 arrest in acute lymphoblastic leukaemia cells: phosphorylated pRB sequesters E2Fs. *J Cell Sci*, **115**, 1073-1082.

-
- Hahn, W. C., Counter, C. M., Lundberg, A. S., Beijersbergen, R. L., Brooks, M. W. and Weinberg, R. A. (1999) Creation of human tumour cells with defined genetic elements. *Nature*, **400**, 464-468.
- Hahn, W. C., Dessain, S. K., Brooks, M. W., King, J. E., Elenbaas, B., Sabatini, D. M., DeCaprio, J. A. and Weinberg, R. A. (2002) Enumeration of the simian virus 40 early region elements necessary for human cell transformation. *Molecular and cellular biology*, **22**, 2111-2123.
- Hannun, Y. A. and Obeid, L. M. (2002) The Ceramide-centric universe of lipid-mediated cell regulation: stress encounters of the lipid kind. *J Biol Chem*, **277**, 25847-25850.
- Hapel, A. J., Warren, H. S. and Hume, D. A. (1984) Different colony-stimulating factors are detected by the "interleukin-3"-dependent cell lines FDC-PI and 32D cl-23. *Blood*, **64**, 786-790.
- Hariharan, I. K., Adams, J. M. and Cory, S. (1988) bcr-abl oncogene renders myeloid cell line factor independent: potential autocrine mechanism in chronic myeloid leukemia. *Oncogene research*, **3**, 387-399.
- Harrington, E. A., Bebbington, D., Moore, J. et al. (2004) VX-680, a potent and selective small-molecule inhibitor of the Aurora kinases, suppresses tumor growth in vivo. *Nature medicine*, **10**, 262-267.
- Haupt, Y., Maya, R., Kazaz, A. and Oren, M. (1997) Mdm2 promotes the rapid degradation of p53. *Nature*, **387**, 296-299.
- Haystead, T. A., Sim, A. T., Carling, D., Honnor, R. C., Tsukitani, Y., Cohen, P. and Hardie, D. G. (1989) Effects of the tumour promoter okadaic acid on intracellular protein phosphorylation and metabolism. *Nature*, **337**, 78-81.
- Heidel, F., Cortes, J., Rucker, F. G. et al. (2007) Results of a multicenter phase II trial for older patients with c-Kit-positive acute myeloid leukemia (AML) and high-risk myelodysplastic syndrome (HR-MDS) using low-dose Ara-C and Imatinib. *Cancer*, **109**, 907-914.
- Heinrich, M. C., Corless, C. L., Demetri, G. D. et al. (2003) Kinase mutations and imatinib response in patients with metastatic gastrointestinal stromal tumor. *J Clin Oncol*, **21**, 4342-4349.
- Heinrich, M. C., Corless, C. L., Liegl, B. et al. (2007) Mechanisms of sunitinib malate (SU) resistance in gastrointestinal stromal tumors (GISTs). *ASCO Meeting Abstracts*, **25**, 10006-.
- Heinrich, M. C., Griffith, D. J., Druker, B. J., Wait, C. L., Ott, K. A. and Zigler, A. J. (2000) Inhibition of c-kit receptor tyrosine kinase activity by STI 571, a selective tyrosine kinase inhibitor. *Blood*, **96**, 925-932.
- Heinrich, M. C., Maki, R. G., Corless, C. L. et al. (2008) Primary and secondary kinase genotypes correlate with the biological and clinical activity of sunitinib in imatinib-resistant gastrointestinal stromal tumor. *J Clin Oncol*, **26**, 5352-5359.
- Hemmings, B. A., Adams-Pearson, C., Maurer, F., Muller, P., Goris, J., Merlevede, W., Hofsteenge, J. and Stone, S. R. (1990) alpha- and beta-forms of the 65-kDa subunit of protein phosphatase 2A have a similar 39 amino acid repeating structure. *Biochemistry*, **29**, 3166-3173.
- Hendrix, P., Mayer-Jackel, R. E., Cron, P., Goris, J., Hofsteenge, J., Merlevede, W. and Hemmings, B. A. (1993) Structure and expression of a 72-kDa regulatory subunit of protein phosphatase 2A. Evidence for different size forms produced by alternative splicing. *J Biol Chem*, **268**, 15267-15276.

-
- Hennessy, B., Giles, F., Cortes, J. et al. (2004) Management of patients with systemic mastocytosis: review of M. D. Anderson Cancer Center experience. *American journal of hematology*, **77**, 209-214.
- Heriche, J. K., Lebrin, F., Rabilloud, T., Leroy, D., Chambaz, E. M. and Goldberg, Y. (1997) Regulation of protein phosphatase 2A by direct interaction with casein kinase 2alpha. *Science*, **276**, 952-955.
- Hernandez, S. E., Krishnaswami, M., Miller, A. L. and Koleske, A. J. (2004) How do Abl family kinases regulate cell shape and movement? *Trends in cell biology*, **14**, 36-44.
- Higuchi, M., O'Brien, D., Kumaravelu, P., Lenny, N., Yeoh, E. J. and Downing, J. R. (2002) Expression of a conditional AML1-ETO oncogene bypasses embryonic lethality and establishes a murine model of human t(8;21) acute myeloid leukemia. *Cancer Cell*, **1**, 63-74.
- Hirota, S., Isozaki, K., Moriyama, Y. et al. (1998) Gain-of-function mutations of c-kit in human gastrointestinal stromal tumors. *Science*, **279**, 577-580.
- Hirsch, F. R., Varella-Garcia, M. and Cappuzzo, F. (2009) Predictive value of EGFR and HER2 overexpression in advanced non-small-cell lung cancer. *Oncogene*, **28 Suppl 1**, S32-37.
- Hochhaus, A., Kantarjian, H. M., Baccarani, M. et al. (2007) Dasatinib induces notable hematologic and cytogenetic responses in chronic-phase chronic myeloid leukemia after failure of imatinib therapy. *Blood*, **109**, 2303-2309.
- Honda, H., Ushijima, T., Wakazono, K., Oda, H., Tanaka, Y., Aizawa, S., Ishikawa, T., Yazaki, Y. and Hirai, H. (2000) Acquired loss of p53 induces blastic transformation in p210(bcr/abl)-expressing hematopoietic cells: a transgenic study for blast crisis of human CML. *Blood*, **95**, 1144-1150.
- Hong, L., Munugalavadla, V. and Kapur, R. (2004) c-Kit-mediated overlapping and unique functional and biochemical outcomes via diverse signaling pathways. *Molecular and cellular biology*, **24**, 1401-1410.
- Hopkins, T. G., Marples, M. and Stark, D. (2008) Sunitinib in the management of gastrointestinal stromal tumours (GISTs). *Eur J Surg Oncol*, **34**, 844-850.
- Horn, V., Thelu, J., Garcia, A., Albiges-Rizo, C., Block, M. R. and Viallet, L. (2007) Functional interaction of aurora-A and PP2A during mitosis. *Mol Biol Cell*, **18**, 1233-1241.
- Hsu, W., Zeng, L. and Costantini, F. (1999) Identification of a domain of Axin that binds to the serine/threonine protein phosphatase 2A and a self-binding domain. *J Biol Chem*, **274**, 3439-3445.
- Hu, Z., Pan, X.-F., Wu, F.-Q. et al. (2009) Synergy between Proteasome Inhibitors and Imatinib Mesylate in Chronic Myeloid Leukemia. *PLoS ONE*, **4**, e6257.
- Huang, P.-H., Wang, D., Chuang, H.-C., Wei, S., Kulp, S. K. and Chen, C.-S. (2009) {alpha}-Tocopheryl succinate and derivatives mediate the transcriptional repression of androgen receptor in prostate cancer cells by targeting the PP2A-JNK-Sp1-signaling axis. *Carcinogenesis*, **30**, 1125-1131.
- Hughes, T., Saglio, G., Branford, S. et al. (2009) Impact of baseline BCR-ABL mutations on response to nilotinib in patients with chronic myeloid leukemia in chronic phase. *J Clin Oncol*, **27**, 4204-4210.
- Hughes, T. P., Kaeda, J., Branford, S. et al. (2003) Frequency of major molecular responses to imatinib or interferon alfa plus cytarabine in newly diagnosed chronic myeloid leukemia. *N Engl J Med*, **349**, 1423-1432.

-
- Hung, J. H., Lu, Y. S., Wang, Y. C. et al. (2008) FTY720 induces apoptosis in hepatocellular carcinoma cells through activation of protein kinase C delta signaling. *Cancer research*, **68**, 1204-1212.
- Ikeda, H., Kanakura, Y., Tamaki, T. et al. (1991) Expression and functional role of the proto-oncogene c-kit in acute myeloblastic leukemia cells. *Blood*, **78**, 2962-2968.
- Ikeda, S., Kishida, S., Yamamoto, H., Murai, H., Koyama, S. and Kikuchi, A. (1998) Axin, a negative regulator of the Wnt signaling pathway, forms a complex with GSK-3beta and beta-catenin and promotes GSK-3beta-dependent phosphorylation of beta-catenin. *The EMBO journal*, **17**, 1371-1384.
- Inui, S., Sanjo, H., Maeda, K., Yamamoto, H., Miyamoto, E. and Sakaguchi, N. (1998) Ig receptor binding protein 1 (alpha4) is associated with a rapamycin-sensitive signal transduction in lymphocytes through direct binding to the catalytic subunit of protein phosphatase 2A. *Blood*, **92**, 539-546.
- Ito, A., Kataoka, T. R., Watanabe, M., Nishiyama, K., Mazaki, Y., Sabe, H., Kitamura, Y. and Nojima, H. (2000) A truncated isoform of the PP2A B56 subunit promotes cell motility through paxillin phosphorylation. *The EMBO journal*, **19**, 562-571.
- Ito, A., Koma, Y., Watabe, K., Nagano, T., Endo, Y., Nojima, H. and Kitamura, Y. (2003) A truncated isoform of the protein phosphatase 2A B56gamma regulatory subunit may promote genetic instability and cause tumor progression. *The American journal of pathology*, **162**, 81-91.
- Ivaska, J., Nissinen, L., Immonen, N., Eriksson, J. E., Kahari, V. M. and Heino, J. (2002) Integrin alpha 2 beta 1 promotes activation of protein phosphatase 2A and dephosphorylation of Akt and glycogen synthase kinase 3 beta. *Molecular and cellular biology*, **22**, 1352-1359.
- Janssens, V. and Goris, J. (2001) Protein phosphatase 2A: a highly regulated family of serine/threonine phosphatases implicated in cell growth and signalling. *Biochem J*, **353**, 417-439.
- Janssens, V., Jordens, J., Stevens, I., Van Hoof, C., Martens, E., De Smedt, H., Engelborghs, Y., Waelkens, E. and Goris, J. (2003) Identification and functional analysis of two Ca²⁺-binding EF-hand motifs in the B⁵⁶/PR72 subunit of protein phosphatase 2A. *J Biol Chem*, **278**, 10697-10706.
- Janssens, V., Longin, S. and Goris, J. (2008) PP2A holoenzyme assembly: in cauda venenum (the sting is in the tail). *Trends in Biochemical Sciences*, **33**, 113-121.
- Jaumot, M. and Hancock, J. F. (2001) Protein phosphatases 1 and 2A promote Raf-1 activation by regulating 14-3-3 interactions. *Oncogene*, **20**, 3949-3958.
- Jiang, Y. (2006) Regulation of the cell cycle by protein phosphatase 2A in *Saccharomyces cerevisiae*. *Microbiology and Molecular Biology Reviews*, **70**, 440-+.
- Jiao, B., Wu, C.-F., Liang, Y. et al. (2009) AML1-ETO9a is correlated with C-KIT overexpression/mutations and indicates poor disease outcome in t(8;21) acute myeloid leukemia-M2.
- Jordens, J., Janssens, V., Longin, S. et al. (2006) The protein phosphatase 2A phosphatase activator is a novel peptidyl-prolyl cis/trans-isomerase. *J Biol Chem*, **281**, 6349-6357.
- Jorgensen, H. G., Allan, E. K., Jordanides, N. E., Mountford, J. C. and Holyoake, T. L. (2007) Nilotinib exerts equipotent antiproliferative effects to imatinib and does not induce apoptosis in CD34+ CML cells. *Blood*, **109**, 4016-4019.

-
- Junttila, M. R., Puustinen, P., Niemela, M. et al. (2007) CIP2A inhibits PP2A in human malignancies. *Cell*, **130**, 51-62.
- Kahan, B. D. (2004) FTY720: from bench to bedside. *Transplantation proceedings*, **36**, 531S-543S.
- Kahan, B. D., Karlix, J. L., Ferguson, R. M., Leichtman, A. B., Mulgaonkar, S., Gonwa, T. A., Skerjanec, A., Schmouder, R. L. and Chodoff, L. (2003) Pharmacodynamics, pharmacokinetics, and safety of multiple doses of FTY720 in stable renal transplant patients: a multicenter, randomized, placebo-controlled, phase I study. *Transplantation*, **76**, 1079-1084.
- Kajiguchi, T., Lee, S., Lee, M. J., Trepel, J. B. and Neckers, L. (2008) KIT regulates tyrosine phosphorylation and nuclear localization of beta-catenin in mast cell leukemia. *Leukemia research*, **32**, 761-770.
- Kalla, C., Scheuermann, M. O., Kube, I., Schlotter, M., Mertens, D., Dohner, H., Stilgenbauer, S. and Lichter, P. (2007) Analysis of 11q22-q23 deletion target genes in B-cell chronic lymphocytic leukaemia: evidence for a pathogenic role of NPAT, CUL5, and PPP2R1B. *Eur J Cancer*, **43**, 1328-1335.
- Kantarjian, H., Cortes, J., Kim, D. W. et al. (2009a) Phase 3 study of dasatinib 140 mg once daily versus 70 mg twice daily in patients with chronic myeloid leukemia in accelerated phase resistant or intolerant to imatinib: 15-month median follow-up. *Blood*, **113**, 6322-6329.
- Kantarjian, H., Giles, F., Wunderle, L. et al. (2006) Nilotinib in imatinib-resistant CML and Philadelphia chromosome-positive ALL. *N Engl J Med*, **354**, 2542-2551.
- Kantarjian, H., Pasquini, R., Hamerschlak, N. et al. (2007a) Dasatinib or high-dose imatinib for chronic-phase chronic myeloid leukemia after failure of first-line imatinib: a randomized phase 2 trial. *Blood*, **109**, 5143-5150.
- Kantarjian, H., Pasquini, R., Levy, V. et al. (2009b) Dasatinib or high-dose imatinib for chronic-phase chronic myeloid leukemia resistant to imatinib at a dose of 400 to 600 milligrams daily: two-year follow-up of a randomized phase 2 study (START-R). *Cancer*, **115**, 4136-4147.
- Kantarjian, H., Sawyers, C., Hochhaus, A. et al. (2002a) Hematologic and cytogenetic responses to imatinib mesylate in chronic myelogenous leukemia. *N Engl J Med*, **346**, 645-652.
- Kantarjian, H. M., Cortes, J., O'Brien, S. et al. (2002b) Imatinib mesylate (STI571) therapy for Philadelphia chromosome-positive chronic myelogenous leukemia in blast phase. *Blood*, **99**, 3547-3553.
- Kantarjian, H. M., Dixon, D., Keating, M. J., Talpaz, M., Walters, R. S., McCredie, K. B. and Freireich, E. J. (1988) Characteristics of accelerated disease in chronic myelogenous leukemia. *Cancer*, **61**, 1441-1446.
- Kantarjian, H. M., Giles, F., Gattermann, N. et al. (2007b) Nilotinib (formerly AMN107), a highly selective BCR-ABL tyrosine kinase inhibitor, is effective in patients with Philadelphia chromosome-positive chronic myelogenous leukemia in chronic phase following imatinib resistance and intolerance. *Blood*, **110**, 3540-3546.
- Kantarjian, H. M., Giles, F., Quintas-Cardama, A. and Cortes, J. (2007c) Important Therapeutic Targets in Chronic Myelogenous Leukemia. *Clin Cancer Res*, **13**, 1089-1097.
- Kantarjian, H. M., Keating, M. J., Talpaz, M., Walters, R. S., Smith, T. L., Cork, A., McCredie, K. B. and Freireich, E. J. (1987) Chronic myelogenous leukemia in blast crisis. Analysis of 242 patients. *Am J Med*, **83**, 445-454.

-
- Kao, G., Tuck, S., Baillie, D. and Sundaram, M. V. (2004) C. elegans SUR-6/PR55 cooperates with LET-92/protein phosphatase 2A and promotes Raf activity independently of inhibitory Akt phosphorylation sites. *Development (Cambridge, England)*, **131**, 755-765.
- Kappos, L., Antel, J., Comi, G. et al. (2006) Oral fingolimod (FTY720) for relapsing multiple sclerosis. *N Engl J Med*, **355**, 1124-1140.
- Keen, J. C. and Davidson, N. E. (2003) The biology of breast carcinoma. *Cancer*, **97**, 825-833.
- Keen, J. C., Garrett-Mayer, E., Pettit, C., Mack, K. M., Manning, J., Herman, J. G. and Davidson, N. E. (2004) Epigenetic regulation of protein phosphatase 2A (PP2A), lymphotactin (XCL1) and estrogen receptor alpha (ER) expression in human breast cancer cells. *Cancer Biol Ther*, **3**, 1304-1312.
- Keen, J. C., Zhou, Q., Park, B. H., Pettit, C., Mack, K. M., Blair, B., Brenner, K. and Davidson, N. E. (2005) Protein Phosphatase 2A Regulates Estrogen Receptor α (ER) Expression through Modulation of ER mRNA Stability. *Journal of Biological Chemistry*, **280**, 29519-29524.
- Kemmer, K., Corless, C. L., Fletcher, J. A. et al. (2004) KIT mutations are common in testicular seminomas. *The American journal of pathology*, **164**, 305-313.
- Khanna, A., Bockelman, C., Hemmes, A. et al. (2009) MYC-Dependent Regulation and Prognostic Role of CIP2A in Gastric Cancer. *J. Natl. Cancer Inst.*, **101**, 793-805.
- Khew-Goodall, Y. and Hemmings, B. A. (1988) Tissue-specific expression of mRNAs encoding alpha- and beta-catalytic subunits of protein phosphatase 2A. *FEBS Lett*, **238**, 265-268.
- Kim, K.-y., Baek, A., Hwang, J.-E. et al. (2009) Adiponectin-Activated AMPK Stimulates Dephosphorylation of AKT through Protein Phosphatase 2A Activation. *Cancer research*, **69**, 4018-4026.
- Kim, Y. M., Sachs, T., Asavaroengchai, W., Bronson, R. and Sykes, M. (2003) Graft-versus-host disease can be separated from graft-versus-lymphoma effects by control of lymphocyte trafficking with FTY720. *J Clin Invest*, **111**, 659-669.
- Kindler, T., Breitenbuecher, F., Marx, A. et al. (2004) Efficacy and safety of imatinib in adult patients with c-kit-positive acute myeloid leukemia. *Blood*, **103**, 3644-3654.
- Kiuchi, M., Adachi, K., Tomatsu, A. et al. (2005) Asymmetric synthesis and biological evaluation of the enantiomeric isomers of the immunosuppressive FTY720-phosphate. *Bioorganic & medicinal chemistry*, **13**, 425-432.
- Klippel, A., Escobedo, J. A., Hirano, M. and Williams, L. T. (1994) The interaction of small domains between the subunits of phosphatidylinositol 3-kinase determines enzyme activity. *Molecular and cellular biology*, **14**, 2675-2685.
- Koma, Y. I., Ito, A., Watabe, K., Kimura, S. H. and Kitamura, Y. (2004) A truncated isoform of the PP2A B56gamma regulatory subunit reduces irradiation-induced Mdm2 phosphorylation and could contribute to metastatic melanoma cell radioresistance. *Histology and histopathology*, **19**, 391-400.
- Kong, M., Fox, C. J., Mu, J., Solt, L., Xu, A., Cinalli, R. M., Birnbaum, M. J., Lindsten, T. and Thompson, C. B. (2004) The PP2A-associated protein alpha4 is an essential inhibitor of apoptosis. *Science*, **306**, 695-698.
- Konopka, J. B. and Witte, O. N. (1985) Detection of c-abl tyrosine kinase activity in vitro permits direct comparison of normal and altered abl gene products. *Molecular and cellular biology*, **5**, 3116-3123.

-
- Koshimizu, U., Tsujimura, T., Isozaki, K., Nomura, S., Furitsu, T., Kanakura, Y., Kitamura, Y. and Nishimune, Y. (1994) Wn mutation of c-kit receptor affects its post-translational processing and extracellular expression. *Oncogene*, **9**, 157-162.
- Kovarik, J. M., Hartmann, S., Bartlett, M., Riviere, G. J., Neddermann, D., Wang, Y., Port, A. and Schmouder, R. L. (2007) Oral-intravenous crossover study of fingolimod pharmacokinetics, lymphocyte responses and cardiac effects. *Biopharmaceutics & drug disposition*, **28**, 97-104.
- Kovarik, J. M., Schmouder, R., Barilla, D., Riviere, G. J., Wang, Y. and Hunt, T. (2004a) Multiple-dose FTY720: tolerability, pharmacokinetics, and lymphocyte responses in healthy subjects. *Journal of clinical pharmacology*, **44**, 532-537.
- Kovarik, J. M., Schmouder, R., Barilla, D., Wang, Y. and Kraus, G. (2004b) Single-dose FTY720 pharmacokinetics, food effect, and pharmacological responses in healthy subjects. *British journal of clinical pharmacology*, **57**, 586-591.
- Kozlowski, M., Larose, L., Lee, F., Le, D. M., Rottapel, R. and Siminovitch, K. A. (1998) SHP-1 binds and negatively modulates the c-Kit receptor by interaction with tyrosine 569 in the c-Kit juxtamembrane domain. *Molecular and cellular biology*, **18**, 2089-2099.
- Kubicek, M., Pacher, M., Abraham, D., Podar, K., Eulitz, M. and Baccarini, M. (2002) Dephosphorylation of Ser-259 regulates Raf-1 membrane association. *J Biol Chem*, **277**, 7913-7919.
- Kubota, Y., Angelotti, T., Niederfellner, G., Herbst, R. and Ullrich, A. (1998) Activation of phosphatidylinositol 3-kinase is necessary for differentiation of FDC-P1 cells following stimulation of type III receptor tyrosine kinases. *Cell Growth Differ*, **9**, 247-256.
- Kuo, Y. C., Huang, K. Y., Yang, C. H., Yang, Y. S., Lee, W. Y. and Chiang, C. W. (2008) Regulation of phosphorylation of Thr-308 of Akt, cell proliferation, and survival by the B55alpha regulatory subunit targeting of the protein phosphatase 2A holoenzyme to Akt. *J Biol Chem*, **283**, 1882-1892.
- Lam, L. P., Chow, R. Y. and Berger, S. A. (1999) A transforming mutation enhances the activity of the c-Kit soluble tyrosine kinase domain. *Biochem J*, **338** (Pt 1), 131-138.
- Law, B. and Rossie, S. (1995) The dimeric and catalytic subunit forms of protein phosphatase 2A from rat brain are stimulated by C2-ceramide. *J Biol Chem*, **270**, 12808-12813.
- le Coutre, P., Ottmann, O. G., Giles, F. et al. (2008) Nilotinib (formerly AMN107), a highly selective BCR-ABL tyrosine kinase inhibitor, is active in patients with imatinib-resistant or -intolerant accelerated-phase chronic myelogenous leukemia. *Blood*, **111**, 1834-1839.
- Lechward, K., Awotunde, O. S., Swiatek, W. and Muszynska, G. (2001) Protein phosphatase 2A: variety of forms and diversity of functions. *Acta Biochim Pol*, **48**, 921-933.
- Lee, J. C., Hapel, A. J. and Ihle, J. N. (1982) Constitutive production of a unique lymphokine (IL 3) by the WEHI-3 cell line. *J Immunol*, **128**, 2393-2398.
- Lee, T. K., Man, K., Ho, J. W. et al. (2004) FTY720 induces apoptosis of human hepatoma cell lines through PI3-K-mediated Akt dephosphorylation. *Carcinogenesis*, **25**, 2397-2405.

-
- Lennartsson, J., Blume-Jensen, P., Hermanson, M., Ponten, E., Carlberg, M. and Ronnstrand, L. (1999) Phosphorylation of Shc by Src family kinases is necessary for stem cell factor receptor/c-kit mediated activation of the Ras/MAP kinase pathway and c-fos induction. *Oncogene*, **18**, 5546-5553.
- Lennartsson, J., Jelacic, T., Linnekin, D. and Shivakrupa, R. (2005) Normal and oncogenic forms of the receptor tyrosine kinase kit. *Stem Cells*, **23**, 16-43.
- Leoni, L. M., Shih, H. C., Deng, L., Tuey, C., Walter, G., Carson, D. A. and Cottam, H. B. (1998) Modulation of ceramide-activated protein phosphatase 2A activity by low molecular weight aromatic compounds. *Biochemical pharmacology*, **55**, 1105-1111.
- Letourneux, C., Rocher, G. and Porteu, F. (2006) B56-containing PP2A dephosphorylate ERK and their activity is controlled by the early gene IEX-1 and ERK. *The EMBO journal*, **25**, 727-738.
- Leulliot, N., Quevillon-Cheruel, S., Sorel, I. et al. (2004) Structure of protein phosphatase methyltransferase 1 (PPM1), a leucine carboxyl methyltransferase involved in the regulation of protein phosphatase 2A activity. *J Biol Chem*, **279**, 8351-8358.
- Leulliot, N., Vicentini, G., Jordens, J., Quevillon-Cheruel, S., Schiltz, M., Barford, D., van Tilbeurgh, H. and Goris, J. (2006) Crystal structure of the PP2A phosphatase activator: implications for its PP2A-specific PPIase activity. *Mol Cell*, **23**, 413-424.
- Lev, S., Givol, D. and Yarden, Y. (1992) Interkinase domain of kit contains the binding site for phosphatidylinositol 3' kinase. *Proc Natl Acad Sci U S A*, **89**, 678-682.
- Levine, R. L. and Gilliland, D. G. (2008) Myeloproliferative disorders. *Blood*, **112**, 2190-2198.
- Li, H. H., Cai, X., Shouse, G. P., Piluso, L. G. and Liu, X. (2007) A specific PP2A regulatory subunit, B56gamma, mediates DNA damage-induced dephosphorylation of p53 at Thr55. *The EMBO journal*, **26**, 402-411.
- Li, M. and Bernard, O. (1992) FDC-P1 myeloid cells engineered to express fibroblast growth factor receptor 1 proliferate and differentiate in the presence of fibroblast growth factor and heparin. *Proceedings of the National Academy of Sciences of the United States of America*, **89**, 3315-3319.
- Li, M., Guo, H. and Damuni, Z. (1995) Purification and characterization of two potent heat-stable protein inhibitors of protein phosphatase 2A from bovine kidney. *Biochemistry*, **34**, 1988-1996.
- Li, M., Makkinje, A. and Damuni, Z. (1996) The myeloid leukemia-associated protein SET is a potent inhibitor of protein phosphatase 2A. *J Biol Chem*, **271**, 11059-11062.
- Li, W., Ge, Z., Liu, C., Liu, Z., Bjorkholm, M., Jia, J. and Xu, D. (2008) CIP2A Is Overexpressed in Gastric Cancer and Its Depletion Leads to Impaired Clonogenicity, Senescence, or Differentiation of Tumor Cells. *Clin Cancer Res*, **14**, 3722-3728.
- Li, X., Scuderi, A., Letsou, A. and Virshup, D. M. (2002) B56-associated protein phosphatase 2A is required for survival and protects from apoptosis in *Drosophila melanogaster*. *Molecular and cellular biology*, **22**, 3674-3684.
- Li, X. and Virshup, D. M. (2002) Two conserved domains in regulatory B subunits mediate binding to the A subunit of protein phosphatase 2A. *Eur J Biochem*, **269**, 546-552.

-
- Li, X., Yost, H. J., Virshup, D. M. and Seeling, J. M. (2001) Protein phosphatase 2A and its B56 regulatory subunit inhibit Wnt signaling in *Xenopus*. *The EMBO journal*, **20**, 4122-4131.
- Lin, X. H., Walter, J., Scheidtmann, K., Ohst, K., Newport, J. and Walter, G. (1998) Protein phosphatase 2A is required for the initiation of chromosomal DNA replication. *Proc Natl Acad Sci U S A*, **95**, 14693-14698.
- Linnekin, D. (1999) Early signaling pathways activated by c-Kit in hematopoietic cells. *Int J Biochem Cell Biol*, **31**, 1053-1074.
- Linnekin, D., DeBerry, C. S. and Mou, S. (1997) Lyn associates with the juxtamembrane region of c-Kit and is activated by stem cell factor in hematopoietic cell lines and normal progenitor cells. *J Biol Chem*, **272**, 27450-27455.
- Liu, H., Sugiura, M., Nava, V. E., Edsall, L. C., Kono, K., Poulton, S., Milstien, S., Kohama, T. and Spiegel, S. (2000) Molecular cloning and functional characterization of a novel mammalian sphingosine kinase type 2 isoform. *J Biol Chem*, **275**, 19513-19520.
- Liu, P., Tarle, S. A., Hajra, A., Claxton, D. F., Marlton, P., Freedman, M., Siciliano, M. J. and Collins, F. S. (1993) Fusion between transcription factor CBF beta/PEBP2 beta and a myosin heavy chain in acute myeloid leukemia. *Science*, **261**, 1041-1044.
- Liu, Q., Zhao, X., Frizzera, F. et al. (2008) FTY720 demonstrates promising preclinical activity for chronic lymphocytic leukemia and lymphoblastic leukemia/lymphoma. *Blood*, **111**, 275-284.
- Logrono, R., Jones, D. V., Faruqi, S. and Bhutani, M. S. (2004) Recent advances in cell biology, diagnosis, and therapy of gastrointestinal stromal tumor (GIST). *Cancer Biol Ther*, **3**, 251-258.
- Longin, S., Jordens, J., Martens, E. et al. (2004) An inactive protein phosphatase 2A population is associated with methylesterase and can be re-activated by the phosphotyrosyl phosphatase activator. *Biochem J*, **380**, 111-119.
- Longin, S., Zwaenepoel, K., Louis, J. V., Dilworth, S., Goris, J. and Janssens, V. (2007) Selection of protein phosphatase 2A regulatory subunits is mediated by the C-terminus of the catalytic subunit. *J Biol Chem*.
- Longley, B. J., Jr., Metcalfe, D. D., Tharp, M., Wang, X., Tyrrell, L., Lu, S. Z., Heitjan, D. and Ma, Y. (1999) Activating and dominant inactivating c-KIT catalytic domain mutations in distinct clinical forms of human mastocytosis. *Proc Natl Acad Sci U S A*, **96**, 1609-1614.
- Loughrey, M. B., Waring, P. M., Dobrovic, A., Demetri, G., Kovalenko, S. and McArthur, G. (2006) Polyclonal resistance in gastrointestinal stromal tumor treated with sequential kinase inhibitors. *Clin Cancer Res*, **12**, 6205-6206; author reply 6206-6207.
- Lozzio, C. B. and Lozzio, B. B. (1975) Human chronic myelogenous leukemia cell-line with positive Philadelphia chromosome. *Blood*, **45**, 321-334.
- Lugo, T. G., Pendergast, A. M., Muller, A. J. and Witte, O. N. (1990) Tyrosine kinase activity and transformation potency of bcr-abl oncogene products. *Science*, **247**, 1079-1082.
- Luo, J., Manning, B. D. and Cantley, L. C. (2003) Targeting the PI3K-Akt pathway in human cancer: rationale and promise. *Cancer Cell*, **4**, 257-262.

-
- Ma, Y., Zeng, S., Metcalfe, D. D., Akin, C., Dimitrijevic, S., Butterfield, J. H., McMahon, G. and Longley, B. J. (2002) The c-KIT mutation causing human mastocytosis is resistant to STI571 and other KIT kinase inhibitors; kinases with enzymatic site mutations show different inhibitor sensitivity profiles than wild-type kinases and those with regulatory-type mutations. *Blood*, **99**, 1741-1744.
- MacKintosh, C., Beattie, K. A., Klumpp, S., Cohen, P. and Codd, G. A. (1990) Cyanobacterial microcystin-LR is a potent and specific inhibitor of protein phosphatases 1 and 2A from both mammals and higher plants. *FEBS Lett*, **264**, 187-192.
- Magenta, A., Fasanaro, P., Romani, S., Di Stefano, V., Capogrossi, M. C. and Martelli, F. (2008) Protein phosphatase 2A subunit PR70 interacts with pRb and mediates its dephosphorylation. *Molecular and cellular biology*, **28**, 873-882.
- Magnusdottir, A., Stenmark, P., Flodin, S., Nyman, T., Kotenyova, T., Graslund, S., Ogg, D. and Nordlund, P. (2009) The structure of the PP2A regulatory subunit B56 gamma: the remaining piece of the PP2A jigsaw puzzle. *Proteins*, **74**, 212-221.
- Maki, R. G., Fletcher, J. A., Heinrich, M. C. et al. (2005) Results from a continuation trial of SU11248 in patients (pts) with imatinib (IM)-resistant gastrointestinal stromal tumor (GIST). *ASCO Meeting Abstracts*, **23**, 9011-.
- Malagola, M., Martinelli, G., Rondoni, M. et al. (2005) Imatinib mesylate in the treatment of c-kit-positive acute myeloid leukemia: is this the real target? *Blood*, **105**, 904-905.
- Mandala, S., Hajdu, R., Bergstrom, J. et al. (2002) Alteration of lymphocyte trafficking by sphingosine-1-phosphate receptor agonists. *Science*, **296**, 346-349.
- Mann, R., Mulligan, R. C. and Baltimore, D. (1983) Construction of a retrovirus packaging mutant and its use to produce helper-free defective retrovirus. *Cell*, **33**, 153-159.
- Manning, B. D. and Cantley, L. C. (2007) AKT/PKB signaling: navigating downstream. *Cell*, **129**, 1261-1274.
- Marcucci, G., Mrozek, K., Ruppert, A. S. et al. (2005) Prognostic Factors and Outcome of Core Binding Factor Acute Myeloid Leukemia Patients With t(8;21) Differ From Those of Patients With inv(16): A Cancer and Leukemia Group B Study. *J Clin Oncol*, **23**, 5705-5717.
- Margolis, S. S., Perry, J. A., Forester, C. M. et al. (2006) Role for the PP2A/B56delta phosphatase in regulating 14-3-3 release from Cdc25 to control mitosis. *Cell*, **127**, 759-773.
- Markovaj, J., Trnkovaj, Z., Michkovaj, P., Maaloufovaj, J., Staraj, J., Cetkovskaj, P. and Schwarz, J. . (2009) Monitoring of minimal residual disease in patients with core binding factor acute myeloid leukemia and the impact of C-KIT, FLT3, and JAK2 mutations on clinical outcome. *Leukemia and Lymphoma*.
- Marsh, A., Healey, S., Lewis, A. et al. (2006) Mutation analysis of five candidate genes in familial breast cancer. *Breast Cancer Res Treat*.
- Martens, E., Stevens, I., Janssens, V., Vermeesch, J., Gotz, J., Goris, J. and Van Hoof, C. (2004) Genomic organisation, chromosomal localisation tissue distribution and developmental regulation of the PR61/B' regulatory subunits of protein phosphatase 2A in mice. *Journal of molecular biology*, **336**, 971-986.
- Marumoto, T., Zhang, D. and Saya, H. (2005) Aurora-A - a guardian of poles. *Nat Rev Cancer*, **5**, 42-50.

-
- Masson, K., Heiss, E., Band, H. and Ronnstrand, L. (2006) Direct binding of Cbl to Tyr568 and Tyr936 of the stem cell factor receptor/c-Kit is required for ligand-induced ubiquitination, internalization and degradation. *Biochem J*, **399**, 59-67.
- Masson, K. and Ronnstrand, L. (2009) Oncogenic signaling from the hematopoietic growth factor receptors c-Kit and Flt3. *Cell Signal*, **21**, 1717-1726.
- Matloubian, M., Lo, C. G., Cinamon, G., Lesneski, M. J., Xu, Y., Brinkmann, V., Allende, M. L., Proia, R. L. and Cyster, J. G. (2004) Lymphocyte egress from thymus and peripheral lymphoid organs is dependent on S1P receptor 1. *Nature*, **427**, 355-360.
- Matsuoka, Y., Nagahara, Y., Ikekita, M. and Shinomiya, T. (2003) A novel immunosuppressive agent FTY720 induced Akt dephosphorylation in leukemia cells. *Br J Pharmacol*, **138**, 1303-1312.
- Mayer-Jaekel, R. E., Ohkura, H., Gomes, R., Sunkel, C. E., Baumgartner, S., Hemmings, B. A. and Glover, D. M. (1993) The 55 kd regulatory subunit of Drosophila protein phosphatase 2A is required for anaphase. *Cell*, **72**, 621-633.
- Mayer, R. E., Hendrix, P., Cron, P., Matthies, R., Stone, S. R., Goris, J., Merlevede, W., Hofsteenge, J. and Hemmings, B. A. (1991) Structure of the 55-kDa regulatory subunit of protein phosphatase 2A: evidence for a neuronal-specific isoform. *Biochemistry*, **30**, 3589-3597.
- McCright, B., Rivers, A. M., Audlin, S. and Virshup, D. M. (1996) The B56 family of protein phosphatase 2A (PP2A) regulatory subunits encodes differentiation-induced phosphoproteins that target PP2A to both nucleus and cytoplasm. *J Biol Chem*, **271**, 22081-22089.
- McCright, B. and Virshup, D. M. (1995) Identification of a new family of protein phosphatase 2A regulatory subunits. *J Biol Chem*, **270**, 26123-26128.
- McManus, M. T. and Sharp, P. A. (2002) Gene silencing in mammals by small interfering RNAs. *Nature reviews*, **3**, 737-747.
- Meraldi, P., Honda, R. and Nigg, E. A. (2002) Aurora-A overexpression reveals tetraploidization as a major route to centrosome amplification in p53^{-/-} cells. *The EMBO journal*, **21**, 483-492.
- Meshinchi, S. and Appelbaum, F. R. (2009) Structural and Functional Alterations of FLT3 in Acute Myeloid Leukemia. *Clinical Cancer Research*, **15**, 4263-4269.
- Miller, J. R., Hocking, A. M., Brown, J. D. and Moon, R. T. (1999) Mechanism and function of signal transduction by the Wnt/beta-catenin and Wnt/Ca²⁺ pathways. *Oncogene*, **18**, 7860-7872.
- Mochida, S., Ikeo, S., Gannon, J. and Hunt, T. (2009) Regulated activity of PP2A-B55 delta is crucial for controlling entry into and exit from mitosis in Xenopus egg extracts. *Embo Journal*, **28**, 2777-2785.
- Mol, C. D., Dougan, D. R., Schneider, T. R. et al. (2004) Structural basis for the autoinhibition and STI-571 inhibition of c-Kit tyrosine kinase. *J Biol Chem*, **279**, 31655-31663.
- Mrozek, K., Marcucci, G., Paschka, P. and Bloomfield, C. D. (2008) Advances in molecular genetics and treatment of core-binding factor acute myeloid leukemia. *Curr Opin Oncol*, **20**, 711-718.
- Mukhopadhyay, A., Saddoughi, S. A., Song, P. et al. (2009) Direct interaction between the inhibitor 2 and ceramide via sphingolipid-protein binding is involved in the regulation of protein phosphatase 2A activity and signaling. *FASEB J.*, **23**, 751-763.

-
- Muller, A. M., Duque, J., Shizuru, J. A. and Lubbert, M. (2008) Complementing mutations in core binding factor leukemias: from mouse models to clinical applications. *Oncogene*, **27**, 5759-5773.
- Mullighan, C. G., Williams, R. T., Downing, J. R. and Sherr, C. J. (2008) Failure of CDKN2A/B (INK4A/B-ARF)-mediated tumor suppression and resistance to targeted therapy in acute lymphoblastic leukemia induced by BCR-ABL. *Genes Dev*, **22**, 1411-1415.
- Muneer, S., Ramalingam, V., Wyatt, R., Schultz, R. A., Minna, J. D. and Kamibayashi, C. (2002) Genomic organization and mapping of the gene encoding the PP2A B56gamma regulatory subunit. *Genomics*, **79**, 344-348.
- Murata, K., Wu, J. and Brautigan, D. L. (1997) B cell receptor-associated protein alpha4 displays rapamycin-sensitive binding directly to the catalytic subunit of protein phosphatase 2A. *Proc Natl Acad Sci U S A*, **94**, 10624-10629.
- Nagahara, Y., Ikekita, M. and Shinomiya, T. (2000) Immunosuppressant FTY720 induces apoptosis by direct induction of permeability transition and release of cytochrome c from mitochondria. *J Immunol*, **165**, 3250-3259.
- Nesbit, C. E., Tersak, J. M. and Prochownik, E. V. (1999) MYC oncogenes and human neoplastic disease. *Oncogene*, **18**, 3004-3016.
- Neviani, P., Santhanam, R., Oaks, J. J. et al. (2007) FTY720, a new alternative for treating blast crisis chronic myelogenous leukemia and Philadelphia chromosome-positive acute lymphocytic leukemia. *J Clin Invest*, **117**, 2408-2421.
- Neviani, P., Santhanam, R., Trotta, R. et al. (2005) The tumor suppressor PP2A is functionally inactivated in blast crisis CML through the inhibitory activity of the BCR/ABL-regulated SET protein. *Cancer Cell*, **8**, 355-368.
- Nieborowska-Skorska, M., Wasik, M. A., Slupianek, A., Salomoni, P., Kitamura, T., Calabretta, B. and Skorski, T. (1999) Signal transducer and activator of transcription (STAT)5 activation by BCR/ABL is dependent on intact Src homology (SH)3 and SH2 domains of BCR/ABL and is required for leukemogenesis. *J Exp Med*, **189**, 1229-1242.
- Ning, Z. Q., Li, J. and Arceci, R. J. (2001a) Signal transducer and activator of transcription 3 activation is required for Asp(816) mutant c-Kit-mediated cytokine-independent survival and proliferation in human leukemia cells. *Blood*, **97**, 3559-3567.
- Ning, Z. Q., Li, J., McGuinness, M. and Arceci, R. J. (2001b) STAT3 activation is required for Asp(816) mutant c-Kit induced tumorigenicity. *Oncogene*, **20**, 4528-4536.
- Nishida, K., Yoshida, Y., Itoh, M. et al. (1999) Gab-family adapter proteins act downstream of cytokine and growth factor receptors and T- and B-cell antigen receptors. *Blood*, **93**, 1809-1816.
- Nowell, P. C. and Hungerford, D. A. (1960) Chromosome studies on normal and leukemic human leukocytes. *J Natl Cancer Inst*, **25**, 85-109.
- Nunbhakdi-Craig, V., Schuechner, S., Sontag, J. M., Montgomery, L., Pallas, D. C., Juno, C., Mudrak, I., Ogris, E. and Sontag, E. (2007) Expression of protein phosphatase 2A mutants and silencing of the regulatory B alpha subunit induce a selective loss of acetylated and detyrosinated microtubules. *J Neurochem*, **101**, 959-971.
- O'Brien, S. G., Guilhot, F., Larson, R. A. et al. (2003) Imatinib compared with interferon and low-dose cytarabine for newly diagnosed chronic-phase chronic myeloid leukemia. *N Engl J Med*, **348**, 994-1004.

-
- O'Connor, P., Comi, G., Montalban, X., Antel, J., Radue, E. W., de Vera, A., Pohlmann, H. and Kappos, L. (2009) Oral fingolimod (FTY720) in multiple sclerosis: two-year results of a phase II extension study. *Neurology*, **72**, 73-79.
- O'Farrell, A. M., Abrams, T. J., Yuen, H. A. et al. (2003) SU11248 is a novel FLT3 tyrosine kinase inhibitor with potent activity in vitro and in vivo. *Blood*, **101**, 3597-3605.
- O'Hare, T., Walters, D. K., Stoffregen, E. P. et al. (2005) In vitro activity of Bcr-Abl inhibitors AMN107 and BMS-354825 against clinically relevant imatinib-resistant Abl kinase domain mutants. *Cancer research*, **65**, 4500-4505.
- Ogretmen, B. and Hannun, Y. A. (2004) Biologically active sphingolipids in cancer pathogenesis and treatment. *Nat Rev Cancer*, **4**, 604-616.
- Ogris, E., Du, X., Nelson, K. C., Mak, E. K., Yu, X. X., Lane, W. S. and Pallas, D. C. (1999) A protein phosphatase methylesterase (PME-1) is one of several novel proteins stably associating with two inactive mutants of protein phosphatase 2A. *J Biol Chem*, **274**, 14382-14391.
- Ogris, E., Gibson, D. M. and Pallas, D. C. (1997) Protein phosphatase 2A subunit assembly: the catalytic subunit carboxy terminus is important for binding cellular B subunit but not polyomavirus middle tumor antigen. *Oncogene*, **15**, 911-917.
- Okamoto, K., Kamibayashi, C., Serrano, M., Prives, C., Mumby, M. C. and Beach, D. (1996) p53-dependent association between cyclin G and the B' subunit of protein phosphatase 2A. *Molecular and cellular biology*, **16**, 6593-6602.
- Okamoto, K., Li, H., Jensen, M. R., Zhang, T., Taya, Y., Thorgeirsson, S. S. and Prives, C. (2002) Cyclin G recruits PP2A to dephosphorylate Mdm2. *Mol Cell*, **9**, 761-771.
- Okazaki, T., Bell, R. M. and Hannun, Y. A. (1989) Sphingomyelin turnover induced by vitamin D3 in HL-60 cells. Role in cell differentiation. *J Biol Chem*, **264**, 19076-19080.
- Ory, S., Zhou, M., Conrads, T. P., Veenstra, T. D. and Morrison, D. K. (2003) Protein phosphatase 2A positively regulates Ras signaling by dephosphorylating KSR1 and Raf-1 on critical 14-3-3 binding sites. *Curr Biol*, **13**, 1356-1364.
- Osborne, C. K., Yochmowitz, M. G., Knight, W. A., 3rd and McGuire, W. L. (1980) The value of estrogen and progesterone receptors in the treatment of breast cancer. *Cancer*, **46**, 2884-2888.
- Pallas, D. C., Shahrik, L. K., Martin, B. L., Jaspers, S., Miller, T. B., Brautigan, D. L. and Roberts, T. M. (1990) Polyoma small and middle T antigens and SV40 small t antigen form stable complexes with protein phosphatase 2A. *Cell*, **60**, 167-176.
- Pan, J., Quintas-Cardama, A., Kantarjian, H. M. et al. (2007) EXEL-0862, a novel tyrosine kinase inhibitor, induces apoptosis in vitro and ex vivo in human mast cells expressing the KIT D816V mutation. *Blood*, **109**, 315-322.
- Pardanani, A., Elliott, M., Reeder, T., Li, C. Y., Baxter, E. J., Cross, N. C. and Tefferi, A. (2003) Imatinib for systemic mast-cell disease. *Lancet*, **362**, 535-536.
- Paschka, P., Marcucci, G., Ruppert, A. S. et al. (2006) Adverse prognostic significance of KIT mutations in adult acute myeloid leukemia with inv(16) and t(8;21): a Cancer and Leukemia Group B Study. *J Clin Oncol*, **24**, 3904-3911.
- Paulson, R. F., Vesely, S., Siminovitch, K. A. and Bernstein, A. (1996) Signalling by the W/Kit receptor tyrosine kinase is negatively regulated in vivo by the protein tyrosine phosphatase Shp1. *Nat Genet*, **13**, 309-315.

-
- Pear, W. S., Miller, J. P., Xu, L. et al. (1998) Efficient and rapid induction of a chronic myelogenous leukemia-like myeloproliferative disease in mice receiving P210 bcr/abl-transduced bone marrow. *Blood*, **92**, 3780-3792.
- Pear, W. S., Nolan, G. P., Scott, M. L. and Baltimore, D. (1993) Production of high-titer helper-free retroviruses by transient transfection. *Proc Natl Acad Sci U S A*, **90**, 8392-8396.
- Pearson, G., Robinson, F., Beers Gibson, T., Xu, B. E., Karandikar, M., Berman, K. and Cobb, M. H. (2001) Mitogen-activated protein (MAP) kinase pathways: regulation and physiological functions. *Endocr Rev*, **22**, 153-183.
- Permpongkosol, S., Wang, J. D., Takahara, S., Matsumiya, K., Nonomura, N., Nishimura, K., Tsujimura, A., Kongkanand, A. and Okuyama, A. (2002) Anticarcinogenic effect of FTY720 in human prostate carcinoma DU145 cells: modulation of mitogenic signaling, FAK, cell-cycle entry and apoptosis. *Int J Cancer*, **98**, 167-172.
- Perrotti, D. and Neviani, P. (2008) Protein phosphatase 2A (PP2A), a drugable tumor suppressor in Ph1(+) leukemias. *Cancer Metastasis Rev*.
- Perrotti, D., Cesi, V., Trotta, R. et al. (2002) BCR-ABL suppresses C/EBPalpha expression through inhibitory action of hnRNP E2. *Nat Genet*, **30**, 48-58.
- Perrotti, D., Iervolino, A., Cesi, V., Cirinna, M., Lombardini, S., Grassilli, E., Bonatti, S., Claudio, P. P. and Calabretta, B. (2000) BCR-ABL Prevents c-Jun-Mediated and Proteasome-Dependent FUS (TLS) Proteolysis through a Protein Kinase Cbeta II-Dependent Pathway. *Mol. Cell. Biol.*, **20**, 6159-6169.
- Peters, D. G., Hoover, R. R., Gerlach, M. J., Koh, E. Y., Zhang, H., Choe, K., Kirschmeier, P., Bishop, W. R. and Daley, G. Q. (2001) Activity of the farnesyl protein transferase inhibitor SCH66336 against BCR/ABL-induced murine leukemia and primary cells from patients with chronic myeloid leukemia. *Blood*, **97**, 1404-1412.
- Peterson, L. F., Boyapati, A., Ahn, E.-Y., Biggs, J. R., Okumura, A. J., Lo, M.-C., Yan, M. and Zhang, D.-E. (2007) Acute myeloid leukemia with the 8q22;21q22 translocation: secondary mutational events and alternative t(8;21) transcripts. *Blood*, **110**, 799-805.
- Piao, X., Paulson, R., van der Geer, P., Pawson, T. and Bernstein, A. (1996) Oncogenic mutation in the Kit receptor tyrosine kinase alters substrate specificity and induces degradation of the protein tyrosine phosphatase SHP-1. *Proc Natl Acad Sci U S A*, **93**, 14665-14669.
- Piazza, F., Valens, J., Lagasse, E. and Schindler, C. (2000) Myeloid differentiation of FdCP1 cells is dependent on Stat5 processing. *Blood*, **96**, 1358-1365.
- Piccaluga, P. P., Malagola, M., Rondoni, M. et al. (2007) Imatinib mesylate in the treatment of newly diagnosed or refractory/resistant c-KIT positive acute myeloid leukemia. Results of an Italian Multicentric Phase II Study. *Haematologica*, **92**, 1721-1722.
- Pinschewer, D. D., Ochsenbein, A. F., Odermatt, B., Brinkmann, V., Hengartner, H. and Zinkernagel, R. M. (2000) FTY720 Immunosuppression Impairs Effector T Cell Peripheral Homing Without Affecting Induction, Expansion, and Memory. *J Immunol*, **164**, 5761-5770.
- Prickett, T. D. and Brautigan, D. L. (2004) Overlapping binding sites in protein phosphatase 2A for association with regulatory A and alpha-4 (mTap42) subunits. *J Biol Chem*, **279**, 38912-38920.

-
- Purtill, D., Cooney, J., Sinniah, R., Carnley, B., Cull, G., Augustson, B. and Cannell, P. (2008) Dasatinib therapy for systemic mastocytosis: four cases. *Eur J Haematol*, **80**, 456-458.
- Qiu, F. H., Ray, P., Brown, K., Barker, P. E., Jhanwar, S., Ruddle, F. H. and Besmer, P. (1988) Primary structure of c-kit: relationship with the CSF-1/PDGF receptor kinase family--oncogenic activation of v-kit involves deletion of extracellular domain and C terminus. *The EMBO journal*, **7**, 1003-1011.
- Rane, S. G. and Reddy, E. P. (2002) JAKs, STATs and Src kinases in hematopoiesis. *Oncogene*, **21**, 3334-3358.
- Ratcliffe, M. J., Itoh, K. and Sokol, S. Y. (2000) A positive role for the PP2A catalytic subunit in Wnt signal transduction. *J Biol Chem*, **275**, 35680-35683.
- Rayner, J. R. and Gonda, T. J. (1994) A simple and efficient procedure for generating stable expression libraries by cDNA cloning in a retroviral vector. *Molecular and cellular biology*, **14**, 880-887.
- Ren, R. (2005) Mechanisms of BCR-ABL in the pathogenesis of chronic myelogenous leukaemia. *Nat Rev Cancer*, **5**, 172-183.
- Resjo, S., Goransson, O., Harndahl, L., Zolnierowicz, S., Manganiello, V. and Degerman, E. (2002) Protein phosphatase 2A is the main phosphatase involved in the regulation of protein kinase B in rat adipocytes. *Cell Signal*, **14**, 231-238.
- Reya, T. and Clevers, H. (2005) Wnt signalling in stem cells and cancer. *Nature*, **434**, 843-850.
- Rivera, R. S., Nagatsuka, H., Gunduz, M. et al. (2008) C-kit protein expression correlated with activating mutations in KIT gene in oral mucosal melanoma. *Virchows Arch*, **452**, 27-32.
- Roberts, K. G., Odell, A. F., Byrnes, E. M., Baleato, R. M., Griffith, R., Lyons, A. B. and Ashman, L. K. (2007) Resistance to c-KIT kinase inhibitors conferred by V654A mutation. *Mol Cancer Ther*, **6**, 1159-1166.
- Rodriguez-Viciano, P., Collins, C. and Fried, M. (2006) Polyoma and SV40 proteins differentially regulate PP2A to activate distinct cellular signaling pathways involved in growth control. *Proc Natl Acad Sci U S A*, **103**, 19290-19295.
- Roeder, I., Horn, M., Glauche, I., Hochhaus, A., Mueller, M. C. and Loeffler, M. (2006) Dynamic modeling of imatinib-treated chronic myeloid leukemia: functional insights and clinical implications. *Nature medicine*, **12**, 1181-1184.
- Rohrschneider, L. R. and Metcalf, D. (1989) Induction of macrophage colony-stimulating factor-dependent growth and differentiation after introduction of the murine c-fms gene into FDC-P1 cells. *Molecular and cellular biology*, **9**, 5081-5092.
- Rondoni, M., Paolini, S., Colarossi, S. et al. (2007) Response to Dasatinib in Patients with Aggressive Systemic Mastocytosis with D816V Kit Mutation. *ASH Annual Meeting Abstracts*, **110**, 3562-.
- Roumiantsev, S., Shah, N. P., Gorre, M. E., Nicoll, J., Brasher, B. B., Sawyers, C. L. and Van Etten, R. A. (2002) Clinical resistance to the kinase inhibitor STI-571 in chronic myeloid leukemia by mutation of Tyr-253 in the Abl kinase domain P-loop. *Proc Natl Acad Sci U S A*, **99**, 10700-10705.
- Ruediger, R., Pham, H. T. and Walter, G. (2001a) Alterations in protein phosphatase 2A subunit interaction in human carcinomas of the lung and colon with mutations in the A beta subunit gene. *Oncogene*, **20**, 1892-1899.
- Ruediger, R., Pham, H. T. and Walter, G. (2001b) Disruption of protein phosphatase 2A subunit interaction in human cancers with mutations in the A alpha subunit gene. *Oncogene*, **20**, 10-15.

-
- Ruvolo, P. P., Clark, W., Mumby, M., Gao, F. and May, W. S. (2002) A functional role for the B56 alpha-subunit of protein phosphatase 2A in ceramide-mediated regulation of Bcl2 phosphorylation status and function. *J Biol Chem*, **277**, 22847-22852.
- Ruvolo, P. P., Deng, X., Ito, T., Carr, B. K. and May, W. S. (1999) Ceramide induces Bcl2 dephosphorylation via a mechanism involving mitochondrial PP2A. *J Biol Chem*, **274**, 20296-20300.
- Sablina, A. A., Chen, W., Arroyo, J. D., Corral, L., Hector, M., Bulmer, S. E., DeCaprio, J. A. and Hahn, W. C. (2007) The tumor suppressor PP2A Abeta regulates the RalA GTPase. *Cell*, **129**, 969-982.
- Sacchi, S., Kantarjian, H. M., O'Brien, S. et al. (1999) Chronic myelogenous leukemia in nonlymphoid blastic phase: analysis of the results of first salvage therapy with three different treatment approaches for 162 patients. *Cancer*, **86**, 2632-2641.
- Sarbassov, D. D., Guertin, D. A., Ali, S. M. and Sabatini, D. M. (2005) Phosphorylation and regulation of Akt/PKB by the rictor-mTOR complex. *Science*, **307**, 1098-1101.
- Savage, D. G., Szydlo, R. M. and Goldman, J. M. (1997) Clinical features at diagnosis in 430 patients with chronic myeloid leukaemia seen at a referral centre over a 16-year period. *Br J Haematol*, **96**, 111-116.
- Sawyers, C. L., Hochhaus, A., Feldman, E. et al. (2002) Imatinib induces hematologic and cytogenetic responses in patients with chronic myelogenous leukemia in myeloid blast crisis: results of a phase II study. *Blood*, **99**, 3530-3539.
- Sawyers, C. L., McLaughlin, J. and Witte, O. N. (1995) Genetic requirement for Ras in the transformation of fibroblasts and hematopoietic cells by the Bcr-Abl oncogene. *J Exp Med*, **181**, 307-313.
- Saydam, G., Aydin, H. H., Sahin, F., Selvi, N., Oktem, G., Terzioglu, E., Buyukkececi, F. and Omay, S. B. (2003) Involvement of protein phosphatase 2A in interferon-alpha-2b-induced apoptosis in K562 human chronic myelogenous leukaemia cells. *Leukemia research*, **27**, 709-717.
- Schaeffer, H. J. and Weber, M. J. (1999) Mitogen-activated protein kinases: specific messages from ubiquitous messengers. *Molecular and cellular biology*, **19**, 2435-2444.
- Schessl, C., Rawat, V. P. S., Cusan, M. et al. (2005) The AML1-ETO fusion gene and the FLT3 length mutation collaborate in inducing acute leukemia in mice. *The Journal of Clinical Investigation*, **115**, 2159-2168.
- Schindler, T., Bornmann, W., Pellicena, P., Miller, W. T., Clarkson, B. and Kuriyan, J. (2000) Structural mechanism for STI-571 inhibition of abelson tyrosine kinase. *Science*, **289**, 1938-1942.
- Schittenhelm, M. M., Shiraga, S., Schroeder, A. et al. (2006) Dasatinib (BMS-354825), a Dual SRC/ABL Kinase Inhibitor, Inhibits the Kinase Activity of Wild-Type, Juxtamembrane, and Activation Loop Mutant KIT Isoforms Associated with Human Malignancies. *Cancer research*, **66**, 473-481.
- Schlenk, R. F., Benner, A., Krauter, J. et al. (2004) Individual Patient Data-Based Meta-Analysis of Patients Aged 16 to 60 Years With Core Binding Factor Acute Myeloid Leukemia: A Survey of the German Acute Myeloid Leukemia Intergroup. *J Clin Oncol*, **22**, 3741-3750.
- Schmidt-Arras, D., Bohmer, S. A., Koch, S. et al. (2009) Anchoring of FLT3 in the endoplasmic reticulum alters signaling quality. *Blood*, **113**, 3568-3576.

-
- Schnittger, S., Kohl, T. M., Haferlach, T., Kern, W., Hiddemann, W., Spiekermann, K. and Schoch, C. (2006) KIT-D816 mutations in AML1-ETO-positive AML are associated with impaired event-free and overall survival. *Blood*, **107**, 1791-1799.
- Schweiger, S. and Schneider, R. (2003) The MID1/PP2A complex: a key to the pathogenesis of Opitz BBB/G syndrome. *Bioessays*, **25**, 356-366.
- Seamon, K. and Daly, J. W. (1981) Activation of adenylate cyclase by the diterpene forskolin does not require the guanine nucleotide regulatory protein. *J Biol Chem*, **256**, 9799-9801.
- Seamon, K. B., Padgett, W. and Daly, J. W. (1981) Forskolin: unique diterpene activator of adenylate cyclase in membranes and in intact cells. *Proc Natl Acad Sci U S A*, **78**, 3363-3367.
- Sears, R., Nuckolls, F., Haura, E., Taya, Y., Tamai, K. and Nevins, J. R. (2000) Multiple Ras-dependent phosphorylation pathways regulate Myc protein stability. *Genes Dev*, **14**, 2501-2514.
- Seeling, J. M., Miller, J. R., Gil, R., Moon, R. T., White, R. and Virshup, D. M. (1999) Regulation of beta-catenin signaling by the B56 subunit of protein phosphatase 2A. *Science*, **283**, 2089-2091.
- Shah, N. P., Lee, F. Y., Luo, R., Jiang, Y., Donker, M. and Akin, C. (2006) Dasatinib (BMS-354825) inhibits KITD816V, an imatinib-resistant activating mutation that triggers neoplastic growth in most patients with systemic mastocytosis. *Blood*, **108**, 286-291.
- Shah, N. P. and Sawyers, C. L. (2003) Mechanisms of resistance to STI571 in Philadelphia chromosome-associated leukemias. *Oncogene*, **22**, 7389-7395.
- Shah, N. P., Tran, C., Lee, F. Y., Chen, P., Norris, D. and Sawyers, C. L. (2004) Overriding imatinib resistance with a novel ABL kinase inhibitor. *Science*, **305**, 399-401.
- Shimada, A., Taki, T., Tabuchi, K., Tawa, A., Horibe, K., Tsuchida, M., Hanada, R., Tsukimoto, I. and Hayashi, Y. (2006) KIT mutations, and not FLT3 internal tandem duplication, are strongly associated with a poor prognosis in pediatric acute myeloid leukemia with t(8;21): a study of the Japanese Childhood AML Cooperative Study Group. *Blood*, **107**, 1806-1809.
- Shinomiya, T., Li, X. K., Amemiya, H. and Suzuki, S. (1997) An immunosuppressive agent, FTY720, increases intracellular concentration of calcium ion and induces apoptosis in HL-60. *Immunology*, **91**, 594-600.
- Shivakrupa, R., Bernstein, A., Watring, N. and Linnekin, D. (2003) Phosphatidylinositol 3'-kinase is required for growth of mast cells expressing the kit catalytic domain mutant. *Cancer research*, **63**, 4412-4419.
- Shouse, G. P., Cai, X. and Liu, X. (2008) Serine 15 phosphorylation of p53 directs its interaction with B56gamma and the tumor suppressor activity of B56gamma-specific protein phosphatase 2A. *Molecular and cellular biology*, **28**, 448-456.
- Shuai, K., Halpern, J., ten Hoeve, J., Rao, X. and Sawyers, C. L. (1996) Constitutive activation of STAT5 by the BCR-ABL oncogene in chronic myelogenous leukemia. *Oncogene*, **13**, 247-254.
- Sill, H., Goldman, J. M. and Cross, N. C. (1995) Homozygous deletions of the p16 tumor-suppressor gene are associated with lymphoid transformation of chronic myeloid leukemia. *Blood*, **85**, 2013-2016.
- Silver, R. T., Talpaz, M., Sawyers, C. L. et al. (2004) Four Years of Follow-Up of 1027 Patients with Late Chronic Phase (L-CP), Accelerated Phase (AP), or Blast Crisis (BC) Chronic Myeloid Leukemia (CML) Treated with Imatinib in Three Large Phase II Trials. *ASH Annual Meeting Abstracts*, **104**, 23-.

-
- Silverstein, A. M., Barrow, C. A., Davis, A. J. and Mumby, M. C. (2002) Actions of PP2A on the MAP kinase pathway and apoptosis are mediated by distinct regulatory subunits. *Proc Natl Acad Sci U S A*, **99**, 4221-4226.
- Skaggs, B. J., Gorre, M. E., Ryzkin, A. et al. (2006) Phosphorylation of the ATP-binding loop directs oncogenicity of drug-resistant BCR-ABL mutants. *Proc Natl Acad Sci U S A*, **103**, 19466-19471.
- Skerjanec, A., Tedesco, H., Neumayer, H.-H., Cole, E., Budde, K., Hsu, C.-H. and Schmouder, R. (2005) FTY720, a novel immunomodulator in de novo kidney transplant patients: pharmacokinetics and exposure-response relationship. In: *Journal of clinical pharmacology*, Vol. 45, pp. 1268(1211).
- Skorski, T., Bellacosa, A., Nieborowska-Skorska, M. et al. (1997) Transformation of hematopoietic cells by BCR/ABL requires activation of a PI-3k/Akt-dependent pathway. *The EMBO journal*, **16**, 6151-6161.
- Skorski, T., Kanakaraj, P., Nieborowska-Skorska, M., Ratajczak, M. Z., Wen, S. C., Zon, G., Gewirtz, A. M., Perussia, B. and Calabretta, B. (1995) Phosphatidylinositol-3 kinase activity is regulated by BCR/ABL and is required for the growth of Philadelphia chromosome-positive cells. *Blood*, **86**, 726-736.
- Smalley, K. S. M., Contractor, R., Nguyen, T. K. et al. (2008) Identification of a Novel Subgroup of Melanomas with KIT/Cyclin-Dependent Kinase-4 Overexpression. *Cancer research*, **68**, 5743-5752.
- Smalley, K. S. M., Nathanson, K. L. and Flaherty, K. T. (2009) Genetic Subgrouping of Melanoma Reveals New Opportunities for Targeted Therapy. *Cancer research*, **69**, 3241-3244.
- Sneed, T. B., Kantarjian, H. M., Talpaz, M. et al. (2004) The significance of myelosuppression during therapy with imatinib mesylate in patients with chronic myelogenous leukemia in chronic phase. *Cancer*, **100**, 116-121.
- Sonoda, Y., Yamamoto, D., Sakurai, S., Hasegawa, M., Aizu-Yokota, E., Momoi, T. and Kasahara, T. (2001) FTY720, a novel immunosuppressive agent, induces apoptosis in human glioma cells. *Biochemical and biophysical research communications*, **281**, 282-288.
- Sontag, E. (2001) Protein phosphatase 2A: the Trojan Horse of cellular signaling. *Cell Signal*, **13**, 7-16.
- Sontag, E., Fedorov, S., Kamibayashi, C., Robbins, D., Cobb, M. and Mumby, M. (1993) The interaction of SV40 small tumor antigen with protein phosphatase 2A stimulates the map kinase pathway and induces cell proliferation. *Cell*, **75**, 887-897.
- Soo Hoo, L., Zhang, J. Y. and Chan, E. K. (2002) Cloning and characterization of a novel 90 kDa 'companion' auto-antigen of p62 overexpressed in cancer. *Oncogene*, **21**, 5006-5015.
- Soverini, S., Colarossi, S., Gnani, A. et al. (2007) Resistance to dasatinib in Philadelphia-positive leukemia patients and the presence or the selection of mutations at residues 315 and 317 in the BCR-ABL kinase domain. *Haematologica*, **92**, 401-404.
- Soverini, S., Gnani, A., Colarossi, S. et al. (2009) Philadelphia-positive patients who already harbor imatinib-resistant Bcr-Abl kinase domain mutations have a higher likelihood of developing additional mutations associated with resistance to second- or third-line tyrosine kinase inhibitors. *Blood*, **114**, 2168-2171.
- Soverini, S., Martinelli, G., Rosti, G. et al. (2005) ABL mutations in late chronic phase chronic myeloid leukemia patients with up-front cytogenetic resistance to

-
- imatinib are associated with a greater likelihood of progression to blast crisis and shorter survival: a study by the GIMEMA Working Party on Chronic Myeloid Leukemia. *J Clin Oncol*, **23**, 4100-4109.
- Speck, N. A. and Gilliland, D. G. (2002) Core-binding factors in haematopoiesis and leukaemia. *Nat Rev Cancer*, **2**, 502-513.
- Steelman, L. S., Pohnert, S. C., Shelton, J. G., Franklin, R. A., Bertrand, F. E. and McCubrey, J. A. (2004) JAK/STAT, Raf/MEK/ERK, PI3K/Akt and BCR-ABL in cell cycle progression and leukemogenesis. *Leukemia*, **18**, 189-218.
- Stevens, I., Janssens, V., Martens, E., Dilworth, S., Goris, J. and Van Hoof, C. (2003) Identification and characterization of B"-subunits of protein phosphatase 2 A in *Xenopus laevis* oocytes and adult tissues. *Eur J Biochem*, **270**, 376-387.
- Stone, R. M., DeAngelo, D. J., Klimek, V. et al. (2005) Patients with acute myeloid leukemia and an activating mutation in FLT3 respond to a small-molecule FLT3 tyrosine kinase inhibitor, PKC412. *Blood*, **105**, 54-60.
- Strack, S., Chang, D., Zaucha, J. A., Colbran, R. J. and Wadzinski, B. E. (1999) Cloning and characterization of B delta, a novel regulatory subunit of protein phosphatase 2A. *FEBS Lett*, **460**, 462-466.
- Strack, S., Cribbs, J. T. and Gomez, L. (2004) Critical role for protein phosphatase 2A heterotrimers in mammalian cell survival. *J Biol Chem*, **279**, 47732-47739.
- Suganuma, M., Fujiki, H., Suguri, H. et al. (1988) Okadaic acid: an additional non-phorbol-12-tetradecanoate-13-acetate-type tumor promoter. *Proc Natl Acad Sci U S A*, **85**, 1768-1771.
- Sun, J., Pedersen, M., Bengtsson, S. and Ronnstrand, L. (2007) Grb2 mediates negative regulation of stem cell factor receptor/c-Kit signaling by recruitment of Cbl. *Experimental cell research*, **313**, 3935-3942.
- Sun, J., Pedersen, M. and Ronnstrand, L. (2008a) Gab2 is involved in differential phosphoinositide 3-kinase signaling by two splice forms of c-Kit. *J Biol Chem*, **283**, 27444-27451.
- Sun, J., Pedersen, M. and Ronnstrand, L. (2009) The D816V Mutation of c-Kit Circumvents a Requirement for Src Family Kinases in c-Kit Signal Transduction. *J. Biol. Chem.*, **284**, 11039-11047.
- Sun, L., Gao, J., Dong, X. et al. (2008b) EB1 promotes Aurora-B kinase activity through blocking its inactivation by protein phosphatase 2A. *Proc Natl Acad Sci U S A*, **105**, 7153-7158.
- Sun, L., Liang, C., Shirazian, S. et al. (2003) Discovery of 5-[5-fluoro-2-oxo-1,2-dihydroindol-(3Z)-ylidenemethyl]-2,4- dimethyl-1H-pyrrole-3-carboxylic acid (2-diethylaminoethyl)amide, a novel tyrosine kinase inhibitor targeting vascular endothelial and platelet-derived growth factor receptor tyrosine kinase. *J Med Chem*, **46**, 1116-1119.
- Suzuki, E., Handa, K., Toledo, M. S. and Hakomori, S. (2004) Sphingosine-dependent apoptosis: a unified concept based on multiple mechanisms operating in concert. *Proc Natl Acad Sci U S A*, **101**, 14788-14793.
- Suzuki, K. and Takahashi, K. (2003) Reduced expression of the regulatory A subunit of serine/threonine protein phosphatase 2A in human breast cancer MCF-7 cells. *International journal of oncology*, **23**, 1263-1268.
- Suzuki, K. and Takahashi, K. (2006) Induction of E-cadherin endocytosis by loss of protein phosphatase 2A expression in human breast cancers. *Biochemical and biophysical research communications*, **349**, 255-260.
- Switzer, C. H., Ridnour, L. A., Cheng, R. Y. S., Sparatore, A., Del Soldato, P., Moody, T. W., Vitek, M. P., Roberts, D. D. and Wink, D. A. (2009) Dithiolethione

-
- compounds inhibit Akt signaling in human breast and lung cancer cells by increasing PP2A activity. *Oncogene*.
- Taetle, R. and Li-en, S. (1984) Further studies on mechanisms of abnormal prostaglandin response by chronic myelogenous leukaemia granulocyte/macrophage progenitors. *Leukemia research*, **8**, 833-842.
- Takabe, K., Paugh, S. W., Milstien, S. and Spiegel, S. (2008) "Inside-Out" Signaling of Sphingosine-1-Phosphate: Therapeutic Targets. *Pharmacol Rev*, **60**, 181-195.
- Takagi, Y., Futamura, M., Yamaguchi, K., Aoki, S., Takahashi, T. and Saji, S. (2000) Alterations of the PPP2R1B gene located at 11q23 in human colorectal cancers. *Gut*, **47**, 268-271.
- Talpaz, M., Shah, N. P., Kantarjian, H. et al. (2006) Dasatinib in imatinib-resistant Philadelphia chromosome-positive leukemias. *N Engl J Med*, **354**, 2531-2541.
- Tamaki, M., Goi, T., Hirono, Y., Katayama, K. and Yamaguchi, A. (2004) PPP2R1B gene alterations inhibit interaction of PP2A-Abeta and PP2A-C proteins in colorectal cancers. *Oncol Rep*, **11**, 655-659.
- Tamborini, E., Bonadiman, L., Greco, A. et al. (2004) A new mutation in the KIT ATP pocket causes acquired resistance to imatinib in a gastrointestinal stromal tumor patient. *Gastroenterology*, **127**, 294-299.
- Taniguchi, M., Nishida, T., Hirota, S., Isozaki, K., Ito, T., Nomura, T., Matsuda, H. and Kitamura, Y. (1999) Effect of c-kit mutation on prognosis of gastrointestinal stromal tumors. *Cancer research*, **59**, 4297-4300.
- Tedesco-Silva, H., Mourad, G., Kahan, B. D. et al. (2005) FTY720, a novel immunomodulator: efficacy and safety results from the first phase 2A study in de novo renal transplantation. *Transplantation*, **79**, 1553-1560.
- Tefferi, A. and Vardiman, J. W. (2008) Classification and diagnosis of myeloproliferative neoplasms: the 2008 World Health Organization criteria and point-of-care diagnostic algorithms. *Leukemia*, **22**, 14-22.
- ten Hoeve, J., Arlinghaus, R. B., Guo, J. Q., Heisterkamp, N. and Groffen, J. (1994) Tyrosine phosphorylation of CRKL in Philadelphia+ leukemia. *Blood*, **84**, 1731-1736.
- Therasse, P., Arbuck, S. G., Eisenhauer, E. A. et al. (2000) New Guidelines to Evaluate the Response to Treatment in Solid Tumors. *J. Natl. Cancer Inst.*, **92**, 205-216.
- Thomas, S. M. and Brugge, J. S. (1997) Cellular functions regulated by Src family kinases. *Annual review of cell and developmental biology*, **13**, 513-609.
- Thommes, K., Lennartsson, J., Carlberg, M. and Ronnstrand, L. (1999) Identification of Tyr-703 and Tyr-936 as the primary association sites for Grb2 and Grb7 in the c-Kit/stem cell factor receptor. *Biochem J*, **341** (Pt 1), 211-216.
- Tickenbrock, L., Hehn, S., Sargin, B., Evers, G., Ng, P. R., Choudhary, C., Berdel, W. E., Muller-Tidow, C. and Serve, H. (2008) Activation of Wnt signaling in cKit-ITD mediated transformation and imatinib sensitivity in acute myeloid leukemia. *International journal of hematology*, **88**, 174-180.
- Tokarski, J. S., Newitt, J. A., Chang, C. Y. et al. (2006) The structure of Dasatinib (BMS-354825) bound to activated ABL kinase domain elucidates its inhibitory activity against imatinib-resistant ABL mutants. *Cancer research*, **66**, 5790-5797.
- Trockenbacher, A., Suckow, V., Foerster, J., Winter, J., Krauss, S., Ropers, H. H., Schneider, R. and Schweiger, S. (2001) MID1, mutated in Opitz syndrome, encodes an ubiquitin ligase that targets phosphatase 2A for degradation. *Nat Genet*, **29**, 287-294.

-
- Tsujimura, T., Hashimoto, K., Kitayama, H. et al. (1999) Activating mutation in the catalytic domain of c-kit elicits hematopoietic transformation by receptor self-association not at the ligand-induced dimerization site. *Blood*, **93**, 1319-1329.
- Tyler, R. K., Shpiro, N., Marquez, R. and Eyers, P. A. (2007) VX-680 inhibits Aurora A and Aurora B kinase activity in human cells. *Cell cycle (Georgetown, Tex)*, **6**, 2846-2854.
- Ugi, S., Imamura, T., Ricketts, W. and Olefsky, J. M. (2002) Protein phosphatase 2A forms a molecular complex with Shc and regulates Shc tyrosine phosphorylation and downstream mitogenic signaling. *Molecular and cellular biology*, **22**, 2375-2387.
- Valent, P., Akin, C., Sperr, W. R. et al. (2005) Mastocytosis: pathology, genetics, and current options for therapy. *Leukemia & lymphoma*, **46**, 35-48.
- Van Glabbeke, M., Verweij, J., Casali, P. G. et al. (2005) Initial and late resistance to imatinib in advanced gastrointestinal stromal tumors are predicted by different prognostic factors: a European Organisation for Research and Treatment of Cancer-Italian Sarcoma Group-Australasian Gastrointestinal Trials Group study. *J Clin Oncol*, **23**, 5795-5804.
- van Oosterom, A. T., Judson, I., Verweij, J. et al. (2001) Safety and efficacy of imatinib (STI571) in metastatic gastrointestinal stromal tumours: a phase I study. *Lancet*, **358**, 1421-1423.
- Vanderwinden, J. M., Wang, D., Paternotte, N., Mignon, S., Isozaki, K. and Erneux, C. (2006) Differences in signaling pathways and expression level of the phosphoinositide phosphatase SHIP1 between two oncogenic mutants of the receptor tyrosine kinase KIT. *Cell Signal*, **18**, 661-669.
- Vanhaesebroeck, B. and Alessi, D. R. (2000) The PI3K-PDK1 connection: more than just a road to PKB. *Biochem J*, **346 Pt 3**, 561-576.
- Vega-Ruiz, A., Cortes, J. E., Sever, M., Manshouri, T., Quintas-Cardama, A., Luthra, R., Kantarjian, H. M. and Verstovsek, S. (2009) Phase II study of imatinib mesylate as therapy for patients with systemic mastocytosis. *Leukemia research*, **33**, 1481-1484.
- Verrills, N. M., Po'uha, S. T., Liu, M. L., Liaw, T. Y., Larsen, M. R., Ivery, M. T., Marshall, G. M., Gunning, P. W. and Kavallaris, M. (2006) Alterations in gamma-actin and tubulin-targeted drug resistance in childhood leukemia. *J Natl Cancer Inst*, **98**, 1363-1374.
- Verstovsek, S., Akin, C., Manshouri, T. et al. (2006) Effects of AMN107, a novel aminopyrimidine tyrosine kinase inhibitor, on human mast cells bearing wild-type or mutated codon 816 c-kit. *Leukemia research*, **30**, 1365-1370.
- Verstovsek, S., Tefferi, A., Cortes, J. et al. (2008) Phase II Study of Dasatinib in Philadelphia Chromosome-Negative Acute and Chronic Myeloid Diseases, Including Systemic Mastocytosis. *Clin Cancer Res*, **14**, 3906-3915.
- Verweij, J., Casali, P. G., Zalcberg, J. et al. (2004) Progression-free survival in gastrointestinal stromal tumours with high-dose imatinib: randomised trial. *Lancet*, **364**, 1127-1134.
- Virshup, D. M. (2000) Protein phosphatase 2A: a panoply of enzymes. *Current opinion in cell biology*, **12**, 180-185.
- Vogelstein, B., Lane, D. and Levine, A. J. (2000) Surfing the p53 network. *Nature*, **408**, 307-310.
- von Bubnoff, N., Manley, P. W., Mestan, J., Sanger, J., Peschel, C. and Duyster, J. (2006) Bcr-Abl resistance screening predicts a limited spectrum of point

-
- mutations to be associated with clinical resistance to the Abl kinase inhibitor nilotinib (AMN107). *Blood*, **108**, 1328-1333.
- Weiler, S. R., Mou, S., DeBerry, C. S., Keller, J. R., Ruscetti, F. W., Ferris, D. K., Longo, D. L. and Linnekin, D. (1996) JAK2 is associated with the c-kit proto-oncogene product and is phosphorylated in response to stem cell factor. *Blood*, **87**, 3688-3693.
- Weisberg, E., Manley, P., Mestan, J., Cowan-Jacob, S., Ray, A. and Griffin, J. D. (2006) AMN107 (nilotinib): a novel and selective inhibitor of BCR-ABL. *Br J Cancer*, **94**, 1765-1769.
- Weisberg, E., Manley, P. W., Breitenstein, W. et al. (2005) Characterization of AMN107, a selective inhibitor of native and mutant Bcr-Abl. *Cancer Cell*, **7**, 129-141.
- Weisberg, E., Rosemary, B., Qingsong, L., Richard, S., Nathanael, G. and James, D. G. (2009) FLT3 inhibition and mechanisms of drug resistance in mutant FLT3-positive AML. *Drug resistance updates : reviews and commentaries in antimicrobial and anticancer chemotherapy*, **12**, 81-89.
- Wendel, H. G., de Stanchina, E., Cepero, E. et al. (2006) Loss of p53 impedes the antileukemic response to BCR-ABL inhibition. *Proc Natl Acad Sci U S A*, **103**, 7444-7449.
- Wera, S., Fernandez, A., Lamb, N. J., Turowski, P., Hemmings-Mieszczak, M., Mayer-Jaekel, R. E. and Hemmings, B. A. (1995) Deregulation of translational control of the 65-kDa regulatory subunit (PR65 alpha) of protein phosphatase 2A leads to multinucleated cells. *J Biol Chem*, **270**, 21374-21381.
- Westermarck, J. and Hahn, W. C. (2008) Multiple pathways regulated by the tumor suppressor PP2A in transformation. *Trends Mol Med*, **14**, 152-160.
- Wetzler, M., Talpaz, M., Van Etten, R. A., Hirsh-Ginsberg, C., Beran, M. and Kurzrock, R. (1993) Subcellular localization of Bcr, Abl, and Bcr-Abl proteins in normal and leukemic cells and correlation of expression with myeloid differentiation. *J Clin Invest*, **92**, 1925-1939.
- Wheeler, D. L., Iida, M. and Dunn, E. F. (2009) The Role of Src in Solid Tumors. *Oncologist*, **14**, 667-678.
- Widmann, C., Gibson, S., Jarpe, M. B. and Johnson, G. L. (1999) Mitogen-activated protein kinase: conservation of a three-kinase module from yeast to human. *Physiol Rev*, **79**, 143-180.
- Willert, K., Logan, C. Y., Arora, A., Fish, M. and Nusse, R. (1999) A Drosophila Axin homolog, Daxin, inhibits Wnt signaling. *Development (Cambridge, England)*, **126**, 4165-4173.
- Williams, R. T., Roussel, M. F. and Sherr, C. J. (2006) Arf gene loss enhances oncogenicity and limits imatinib response in mouse models of Bcr-Abl-induced acute lymphoblastic leukemia. *Proc Natl Acad Sci U S A*, **103**, 6688-6693.
- Wlodarski, P., Grajkowska, W., Lojek, M., Rainko, K. and Jozwiak, J. (2006) Activation of Akt and Erk pathways in medulloblastoma. *Folia Neuropathol*, **44**, 214-220.
- Wong, L. L., Chang, C. F., Koay, E. S. and Zhang, D. (2009) Tyrosine phosphorylation of PP2A is regulated by HER-2 signalling and correlates with breast cancer progression. *International journal of oncology*, **34**, 1291-1301.
- Wong, S. and Witte, O. N. (2004) The BCR-ABL story: bench to bedside and back. *Annu Rev Immunol*, **22**, 247-306.
- Woodring, P. J., Hunter, T. and Wang, J. Y. (2003) Regulation of F-actin-dependent processes by the Abl family of tyrosine kinases. *J Cell Sci*, **116**, 2613-2626.

-
- Worobec, A. S., Semere, T., Nagata, H. and Metcalfe, D. D. (1998) Clinical correlates of the presence of the Asp816Val c-kit mutation in the peripheral blood mononuclear cells of patients with mastocytosis. *Cancer*, **83**, 2120-2129.
- Xiang, Z., Kreisel, F., Cain, J., Colson, A. and Tomasson, M. H. (2007) Neoplasia driven by mutant c-KIT is mediated by intracellular, not plasma membrane, receptor signaling. *Molecular and cellular biology*, **27**, 267-282.
- Xing, Y., Xu, Y., Chen, Y. et al. (2006) Structure of Protein Phosphatase 2A Core Enzyme Bound to Tumor-Inducing Toxins. *Cell*, **127**, 341-353.
- Xu, Y., Xing, Y., Chen, Y. et al. (2006) Structure of the protein phosphatase 2A holoenzyme. *Cell*, **127**, 1239-1251.
- Yamada, T., Katagiri, H., Asano, T., Inukai, K., Tsuru, M., Kodama, T., Kikuchi, M. and Oka, Y. (2001) 3-phosphoinositide-dependent protein kinase 1, an Akt1 kinase, is involved in dephosphorylation of Thr-308 of Akt1 in Chinese hamster ovary cells. *J Biol Chem*, **276**, 5339-5345.
- Yamamoto, H., Hinoi, T., Michiue, T. et al. (2001) Inhibition of the Wnt signaling pathway by the PR61 subunit of protein phosphatase 2A. *J Biol Chem*, **276**, 26875-26882.
- Yan, Z., Fedorov, S. A., Mumby, M. C. and Williams, R. S. (2000) PR48, a novel regulatory subunit of protein phosphatase 2A, interacts with Cdc6 and modulates DNA replication in human cells. *Molecular and cellular biology*, **20**, 1021-1029.
- Yang, J., Wu, J., Tan, C. and Klein, P. S. (2003) PP2A:B56epsilon is required for Wnt/beta-catenin signaling during embryonic development. *Development (Cambridge, England)*, **130**, 5569-5578.
- Yarden, Y., Kuang, W. J., Yang-Feng, T. et al. (1987) Human proto-oncogene c-kit: a new cell surface receptor tyrosine kinase for an unidentified ligand. *The EMBO journal*, **6**, 3341-3351.
- Yasui, H., Hideshima, T., Raje, N. et al. (2005) FTY720 induces apoptosis in multiple myeloma cells and overcomes drug resistance. *Cancer research*, **65**, 7478-7484.
- Yeh, E., Cunningham, M., Arnold, H. et al. (2004) A signalling pathway controlling c-Myc degradation that impacts oncogenic transformation of human cells. *Nature cell biology*, **6**, 308-318.
- Yeh, L. S., Hsieh, Y. Y., Chang, J. G., Chang, W. W., Chang, C. C. and Tsai, F. J. (2007) Mutation analysis of the tumor suppressor gene PPP2R1B in human cervical cancer. *Int J Gynecol Cancer*, **17**, 868-871.
- Yu, J., Boyapati, A. and Rundell, K. (2001) Critical role for SV40 small-t antigen in human cell transformation. *Virology*, **290**, 192-198.
- Yuan, H., Veldman, T., Rundell, K. and Schlegel, R. (2002) Simian virus 40 small tumor antigen activates AKT and telomerase and induces anchorage-independent growth of human epithelial cells. *J Virol*, **76**, 10685-10691.
- Yuan, Y., Zhou, L., Miyamoto, T. et al. (2001) AML1-ETO expression is directly involved in the development of acute myeloid leukemia in the presence of additional mutations. *Proceedings of the National Academy of Sciences of the United States of America*, **98**, 10398-10403.
- Zemann, B., Kinzel, B., Muller, M., Reuschel, R., Mechtcheriakova, D., Urtz, N., Bornancin, F., Baumruker, T. and Billich, A. (2006) Sphingosine kinase type 2 is essential for lymphopenia induced by the immunomodulatory drug FTY720. *Blood*, **107**, 1454-1458.
- Zhang, W., Yang, J., Liu, Y., Chen, X., Yu, T., Jia, J. and Liu, C. (2009) PR55alpha, a regulatory subunit of PP2A, specifically regulates PP2A-mediated beta-catenin dephosphorylation. *J. Biol. Chem.*, M109.013698.

-
- Zhang, X. and Ren, R. (1998) Bcr-Abl efficiently induces a myeloproliferative disease and production of excess interleukin-3 and granulocyte-macrophage colony-stimulating factor in mice: a novel model for chronic myelogenous leukemia. *Blood*, **92**, 3829-3840.
- Zhao, C., Blum, J., Chen, A., Kwon, H. Y., Jung, S. H., Cook, J. M., Lagoo, A. and Reya, T. (2007) Loss of beta-catenin impairs the renewal of normal and CML stem cells in vivo. *Cancer Cell*, **12**, 528-541.
- Zhao, J. J., Gjoerup, O. V., Subramanian, R. R., Cheng, Y., Chen, W., Roberts, T. M. and Hahn, W. C. (2003) Human mammary epithelial cell transformation through the activation of phosphatidylinositol 3-kinase. *Cancer Cell*, **3**, 483-495.
- Zhou, B., Wang, Z. X., Zhao, Y., Brautigan, D. L. and Zhang, Z. Y. (2002) The specificity of extracellular signal-regulated kinase 2 dephosphorylation by protein phosphatases. *J Biol Chem*, **277**, 31818-31825.
- Zhou, J., Pham, H. T., Ruediger, R. and Walter, G. (2003a) Characterization of the Aalpha and Abeta subunit isoforms of protein phosphatase 2A: differences in expression, subunit interaction, and evolution. *Biochem J*, **369**, 387-398.
- Zhou, J., Pham, H. T. and Walter, G. (2003b) The formation and activity of PP2A holoenzymes do not depend on the isoform of the catalytic subunit. *J Biol Chem*, **278**, 8617-8622.
- Zolnierowicz, S., Csontos, C., Bondor, J., Verin, A., Mumby, M. C. and DePaoli-Roach, A. A. (1994) Diversity in the regulatory B-subunits of protein phosphatase 2A: identification of a novel isoform highly expressed in brain. *Biochemistry*, **33**, 11858-11867.